THE CLAUSTRUM: CHARTING A WAY FORWARD FOR THE BRAIN'S MOST MYSTERIOUS NUCLEUS

EDITED BY: Ariel Y. Deutch and Brian N. Mathur
PUBLISHED IN: Frontiers in Systems Neuroscience

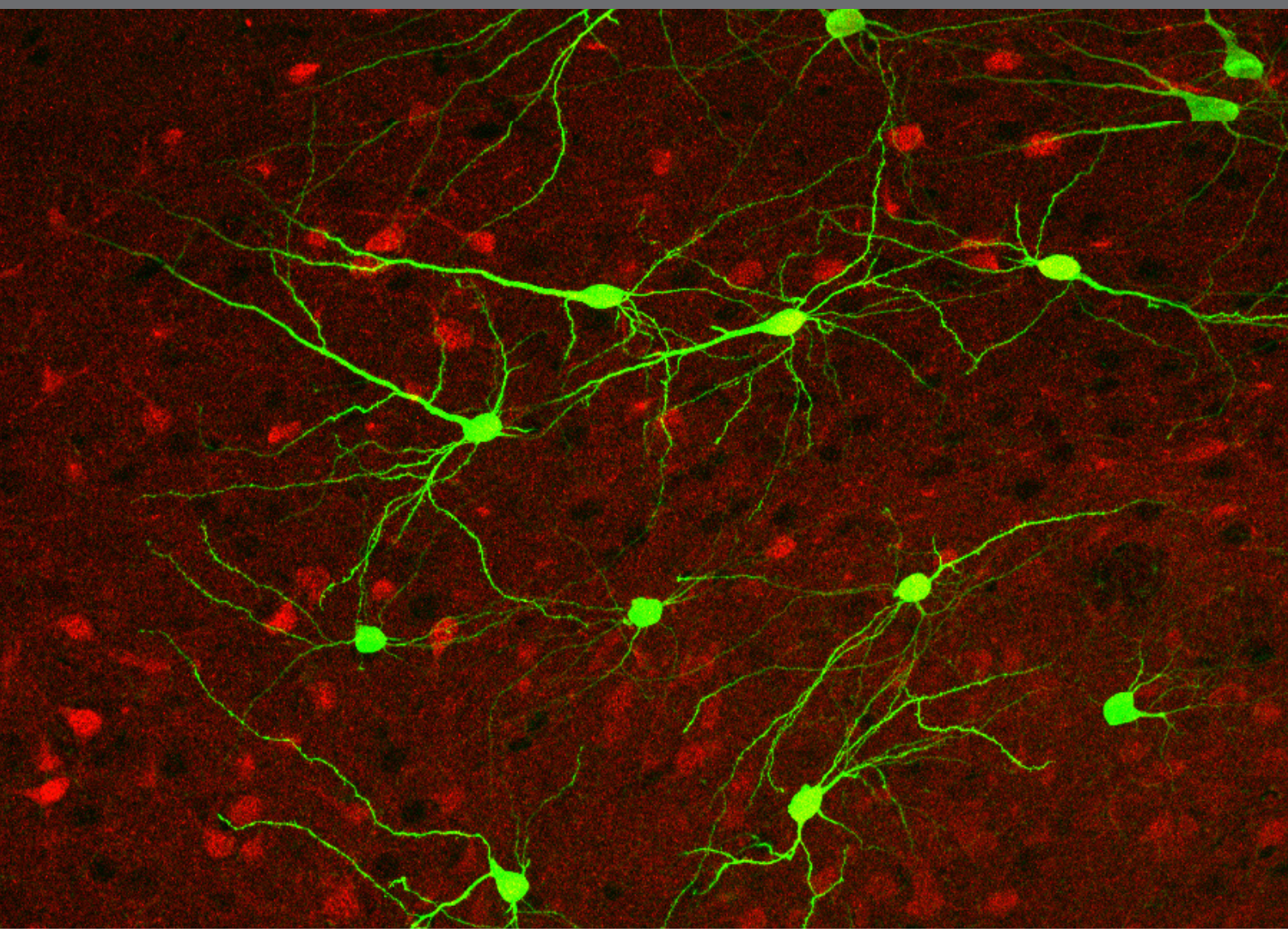

frontiers Research Topics

frontiers

ISSN 1664-8714
ISBN 978-2-88919-542-8
DOI 10.3389/978-2-88919-542-8

About Frontiers

Frontiers is more than just an open-access publisher of scholarly articles: it is a pioneering approach to the world of academia, radically improving the way scholarly research is managed. The grand vision of Frontiers is a world where all people have an equal opportunity to seek, share and generate knowledge. Frontiers provides immediate and permanent online open access to all its publications, but this alone is not enough to realize our grand goals.

Frontiers Journal Series

The Frontiers Journal Series is a multi-tier and interdisciplinary set of open-access, online journals, promising a paradigm shift from the current review, selection and dissemination processes in academic publishing. All Frontiers journals are driven by researchers for researchers; therefore, they constitute a service to the scholarly community. At the same time, the Frontiers Journal Series operates on a revolutionary invention, the tiered publishing system, initially addressing specific communities of scholars, and gradually climbing up to broader public understanding, thus serving the interests of the lay society, too.

Dedication to Quality

Each Frontiers article is a landmark of the highest quality, thanks to genuinely collaborative interactions between authors and review editors, who include some of the world's best academicians. Research must be certified by peers before entering a stream of knowledge that may eventually reach the public - and shape society; therefore, Frontiers only applies the most rigorous and unbiased reviews.

Frontiers revolutionizes research publishing by freely delivering the most outstanding research, evaluated with no bias from both the academic and social point of view.

By applying the most advanced information technologies, Frontiers is catapulting scholarly publishing into a new generation.

What are Frontiers Research Topics?

Frontiers Research Topics are very popular trademarks of the Frontiers Journals Series: they are collections of at least ten articles, all centered on a particular subject. With their unique mix of varied contributions from Original Research to Review Articles, Frontiers Research Topics unify the most influential researchers, the latest key findings and historical advances in a hot research area! Find out more on how to host your own Frontiers Research Topic or contribute to one as an author by contacting the Frontiers Editorial Office: **researchtopics@frontiersin.org**

THE CLAUSTRUM: CHARTING A WAY FORWARD FOR THE BRAIN'S MOST MYSTERIOUS NUCLEUS

Topic Editors:
Ariel Y. Deutch, Vanderbilt University Medical Center, USA
Brian N. Mathur, University of Maryland School of Medicine, USA

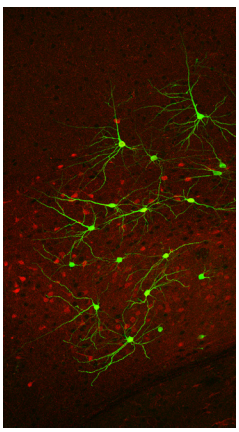

Lucifer Yellow was injected into neurons (green) in the insular cortex and the claustrum of a rat. To delineate the border, the slice was immunostained with anti-latexin antibody (red) after the dye injection. The claustrum can be identified by rich latexin-positive neuropil staining. Latexin-positive neurons are also scattered along the border regions. The dendritic morphology exhibits dramatic differences across the border.
Watakabe A, Ohsawa S, Ichinohe N, Rockland KS and Yamamori T (2014) Characterization of claustral neurons by comparative gene expression profiling and dye-injection analyses. Front. Syst. Neurosci. 8:98. doi: 10.3389/fnsys.2014.00098

The claustrum is a long, band-like grey matter structure situated in the ventrolateral telencephalon of most, if not all, mammalian brains. Due to its shape and close proximity to white matter structures and insular cortex, the anatomy and behavioral relevance of the claustrum have proven difficult to study. As a result, disagreements in the literature exist over ontogeny, phylogeny, anatomical boundaries, and connectivity. Despite this, it is generally regarded that the claustrum contains excitatory projection neurons that reciprocally connect to most regions of the cerebral cortex, a feature that has fostered varying hypotheses as to its function. These hypotheses propose multisensory integration, coordination of cortical activity for the generation of conscious percepts, or saliency filtration. The articles of this e-book consider the historical and recent highlights in claustrum structure, hodology, and function and seek to provide a compelling way forward for this "hidden" nucleus.

Citation: Deutch, A. Y., Mathur, B. N., eds. (2015). The Claustrum: Charting a Way Forward for the Brain's Most Mysterious Nucleus. Lausanne: Frontiers Media. doi: 10.3389/978-2-88919-542-8

Table of Contents

frontiers in Systems Neuroscience

EDITORIAL
published: 15 July 2015
doi: 10.3389/fnsys.2015.00103

Editorial: The Claustrum: charting a way forward for the brain's most mysterious nucleus

Ariel Y. Deutch[1]* *and Brian N. Mathur*[2]

[1] Departments of Psychiatry and Pharmacology, Vanderbilt University Medical Center, Nashville, TN, USA, [2] Department of Pharmacology, University of Maryland School of Medicine, Baltimore, MD, USA

Keywords: insula, insular cortex, prefrontal cortex, cingulate cortex, attention, conciousness, comparative anatomy, connectivity

There are many reasons why investigators decide to expend their energy on studying a particular nucleus in the brain. Sometimes the choice of structures has little to do with new insights that may be gleaned but is more attributable to the tractability of the site to experimental manipulation. However, some sites remain relatively obscure because their structure almost seems designed to impede research. The claustrum belongs to the latter group. Entombed between tightly constricting white matter bundles, the claustrum both escaped and resisted significant attention for much of the twentieth century. However, over the past decade there has been a resurgence in interest in the claustrum. This renewed attention is in large part attributable to a paper by Crick and Koch (2005), which advanced the hypothesis that the claustrum plays a central role in binding and consciousness. Seductively written, and with Crick and Koch's imprimatur, a flurry of studies ensued. While it appeared that this opened the door to experimental studies of claustral function, over the past decade it has become apparent that the door is merely ajar.

This collection of papers is an attempt to bring together many of the key recent findings on the claustrum. Perusing the volume quickly reveals that there is a striking emphasis on the anatomy of the claustrum, with most contributions emphasizing comparative anatomy of the claustrum, localization of different types of chemically-coded neurons within the claustrum, and new details on the morphology of claustral neurons. This selective attention to the anatomy of the claustrum has led some wags to comment that the anatomy of the claustrum should by now have been defined. However, striking differences in claustral organization and the anatomy of the region surrounding the claustrum across various species led to confusion regarding the boundaries of the claustrum. This resulted in some definitions being overly inclusive, adding to the claustrum several cortical regions that are now considered to be distinct. Other definitions were too restrictive and did not account for the ontogeny of the claustrum. This situation led Crick and Koch (2005) to decry the lack of objective criteria for the definition of the claustrum. The past decade has mainly been spent trying to respond to their plea.

This collection of papers appears to have arrived at a consensus regarding the definition of the claustrum, as seen from the vantage point of anatomical studies. Although there remain some small bones of contention, these are relatively minor and will no doubt soon be resolved. In light of the evolutionary expansion of the claustrum to its (discontinuous) presence in humans and other animals with large cortices, it is not surprising that about half of the manuscripts involve studies of primates (Baizer et al., 2014; Gattass et al., 2014; Hinova-Palova et al., 2014; Johnson et al., 2014; Pirone et al., 2014; Reser et al., 2014), with two papers on cetaceans (Baizer et al., 2014; Cozzi et al., 2014), and still others on rodents (Rockland, 2014; Patzke et al., 2014; Watakabe et al., 2014). There are somewhat fewer papers on the transmitters and molecules present in different populations of claustral cells (Cozzi et al., 2014; Hinova-Palova et al., 2014; Pirone et al., 2014; Rockland, 2014; Watakabe et al., 2014).

OPEN ACCESS

Edited and reviewed by:
Maria V. Sanchez-Vives, ICREA-IDIBAPS, Spain

***Correspondence:**
Ariel Y. Deutch, ariel.deutch@vanderbilt.edu

Received: *25 March 2015*
Accepted: *01 July 2015*
Published: *15 July 2015*

Citation:
Deutch AY and Mathur BN (2015) Editorial: The Claustrum: charting a way forward for the brain's most mysterious nucleus. Front. Syst. Neurosci. 9:103. doi: 10.3389/fnsys.2015.00103

Baizer and colleagues, in their paper on the structure of the claustrum in higher order species, reminds us to ask "what does structure tell us about function?," a query echoed by Mathur (2014) in his review. In addition to the aesthetic qualities of neuroanatomical preparations, neuroscience labors under the assumption that structure defines function, and that understanding morphology and hodology allows us to formulate testable hypotheses of neural function. In the current collection of papers, intended as a survey of the claustrum, only the Smith and Alloway (2014) contribution and that of Remedios et al. (2014) empirically explore the functions of the claustrum. We are obviously at a crossroads in claustral research, where our knowledge of the anatomy is sufficient to warrant testing the hypotheses of claustral function that almost every paper in this collection have advanced.

As noted earlier, the claustrum's peculiar shape has historically been a major impediment to functional studies of the claustrum. Fortunately, the advent of new methods and improvements in existing methods has made it possible to probe claustral function at the molecular, physiological, and behavioral levels. One can now study the physiology of the claustrum using optogenetic or chemogenetic approaches in slice preparations and *in vivo*, and image the activity of subpopulations of genetically defined claustral neurons using calcium imaging in awake, behaving animals. The use of laser capture microdissection and other methods such as immunopanning permits one to obtain claustral neurons without fear of contamination from adjacent structures, and analyze the proteome or transcriptome of these cells; this can even be done in claustral cells identified as projecting to specific targets. Non-invasive *in vivo* imaging methods can now be applied to both human and non-human studies: the resolution of structural imaging is now sufficient (7T) to undertake longitudinal studies of claustrum volume in health and disease, and with co-registration algorithms it may be possible to differentiate the contribution of the claustrum and insular cortex to fMRI signal changes. Finally, advances in methods for producing knockout and transgenic animals, such as that afforded by CRISPR/cas approaches, has made the rapid generation of such animals possible, opening the door to behavioral studies of claustral function.

Over the decade since the publication of Crick and Koch's cry for molecular studies of the claustrum and their hypothesis on claustral involvement in binding of percepts, a consensus regarding claustral structure has been reached. Over the next decade we look forward to a comparable blossoming of functional studies that unlock the deep secrets of the claustrum.

References

Baizer, J. S., Sherwood, C. C., Noonan, M., and Hof, P. R. (2014). Comparative organization of the claustrum: what does structure tell us about function? *Front. Syst. Neurosci.* 8:117. doi: 10.3389/fnsys.2014.00117

Crick, F. C., and Koch, C. (2005). What is the function of the claustrum? *Philos. Trans. R. Soc. Lond. B Biol. Sci.* 360, 1271–1279. doi: 10.1098/rstb.2005.1661

Cozzi, B., Roncon, G., Granato, A., Giurisato, M., Castagna, M., Peruffo, A., et al. (2014). The claustrum of the bottlenose dolphin *Tursiops truncatus* (Montagu 1821). *Front. Syst. Neurosci.* 8:42. doi: 10.3389/fnsys.2014.00042

Gattass, R., Soares, J. G., Desimone, R., and Ungerleider, L. G. (2014). Connectional subdivision of the claustrum: two visuotopic subdivisions in the macaque. *Front. Syst. Neurosci.* 8:63. doi: 10.3389/fnsys.2014.00063

Hinova-Palova, D. V., Edelstein, L., Landzhov, B., Minkov, M., Malinova, L., Hristov, S., et al. (2014). Topographical distribution and morphology of NADPH-diaphorase-stained neurons in the human claustrum. *Front. Syst. Neurosci.* 8:96. doi: 10.3389/fnsys.2014.00096

Johnson, J. I., Fenske, B. A., Jaswa, A. S., and Morris, J. A. (2014). Exploitation of puddles for breakthroughs in claustrum research. *Front. Syst. Neurosci.* 8:78. doi: 10.3389/fnsys.2014.00078

Mathur, B. N. (2014). The claustrum in review. *Front. Syst. Neurosci.* 8:48. doi: 10.3389/fnsys.2014.00048

Patzke, N., Innocenti, G. M., and Manger, P. R. (2014). The claustrum of the ferret: afferent and efferent connections to lower and higher order visual cortical areas. *Front. Syst. Neurosci.* 8:31. doi: 10.3389/fnsys.2014.00031

Pirone, A., Castagna, M., Granato, A., Peruffo, A., Quilici, F., Cavicchioli, L., et al. (2014). Expression of calcium-binding proteins and selected neuropeptides in the human, chimpanzee, and crab-eating macaque claustrum. *Front. Syst. Neurosci.* 8:99. doi: 10.3389/fnsys.2014.00099

Remedios, R., Logothetis, N. K., and Kayser, C. (2014). A role of the claustrum in auditory scene analysis by reflecting sensory change. *Front. Syst. Neurosci.* 8:44. doi: 10.3389/fnsys.2014.00044

Reser, D. H., Richardson, K. E., Montibeller, M. O., Zhao, S., Chan, J. M., Soares, J. G., et al. (2014). Claustrum projections to prefrontal cortex in the capuchin monkey (Cebus apella). *Front. Syst. Neurosci.* 8:123. doi: 10.3389/fnsys.2014.00123

Rockland, K. S. (2014). Zinc-positive and zinc-negative connections of the claustrum. *Front. Syst. Neurosci.* 8:37. doi: 10.3389/fnsys.2014.00037

Smith, J. B., and Alloway, K. D. (2014). Interhemispheric claustral circuits coordinate sensory and motor cortical areas that regulate exploratory behaviors. *Front. Syst. Neurosci.* 8:93. doi: 10.3389/fnsys.2014.00093

Watakabe, A., Ohsawa, S., Ichinohe, N., Rockland, K. S., and Yamamori, T. (2014). Characterization of claustral neurons by comparative gene expression profiling and dye-injection analyses. *Front. Syst. Neurosci.* 8:98. doi: 10.3389/fnsys.2014.00098

Conflict of Interest Statement: The authors declare that the research was conducted in the absence of any commercial or financial relationships that could be construed as a potential conflict of interest.

frontiers in
SYSTEMS NEUROSCIENCE

REVIEW ARTICLE
published: 04 April 2014
doi: 10.3389/fnsys.2014.00048

The claustrum in review

Brian N. Mathur*

Department of Pharmacology, University of Maryland School of Medicine, Baltimore, MD, USA

Edited by:
Federico Bermudez-Rattoni, Universidad Nacional Autónoma de México, Mexico

Reviewed by:
Natasha Sigala, University of Sussex, UK
Jorge A. Larriva-Sahd, Universidad Nacional Autónoma de México, Mexico

Correspondence:
Brian N. Mathur, Department of Pharmacology, University of Maryland School of Medicine, BRB 4-011, 655 W. Baltimore St., Baltimore, MD 21201, USA
e-mail: bmathur@som.umaryland.edu

The claustrum is among the most enigmatic of all prominent mammalian brain structures. Since the 19th century, a wealth of data has amassed on this forebrain nucleus. However, much of this data is disparate and contentious; conflicting views regarding the claustrum's structural definitions and possible functions abound. This review synthesizes historical and recent claustrum studies with the purpose of formulating an acceptable description of its structural properties. Integrating extant anatomical and functional literature with theorized functions of the claustrum, new visions of how this structure may be contributing to cognition and action are discussed.

Keywords: claustrum, cerebral cortex, connections, function, attention

INTRODUCTION

Despite centuries of investigation, the claustrum continues to evade complete structural and functional characterization. In their comprehensive study of comparative neuronanatomy, Ariëns Kappers et al. (1936, 1960) described the "Problem of the Claustrum", which largely centered on the debate over claustral gross and fine morphology, connectivity, and function. Though much has been learned since this time through the application of modern neuroscience techniques, several problems persist. Notably, the exact borders of the claustrum have been called into question, an issue that carries implications for connectivity and functional conclusions, including those based on functional imaging, lesioning, electrophysiological single-unit recording, and optogenetic approaches. Thus, it is essential that a cogent structural definition should be established to inform functional conclusions for the ultimate purpose of solving the "problem" of the claustrum.

Contributing to the mysterious nature of the claustrum is the varied nomenclature used since its initial description. This structure was originally named the "nucleus taeniaformis" by the French comparative anatomist Vicq d'Azyr around the turn of the 18th century, and would soon thereafter be renamed the "claustrum" by Burdach (Rae, 1954). "Claustrum" often collectively refers to both "dorsal claustrum", otherwise known as the "insular claustrum" or "field 8" (Brodmann, 1909), and a structure that is ventrally contiguous called the "ventral claustrum", otherwise known as the "endopiriform nucleus" (Loo, 1931), or "claustrum ventrale" (Druga, 1966; Druga et al., 1990, 1993). The endopiriform nucleus can further be subdivided into the dorsal endopiriform nucleus and the ventral endopiriform nucleus (Paxinos and Watson, 1997); the ventral endopiriform nucleus, which also is known as the "claustrum praefiriforme" (Brockhaus, 1940; Narkiewicz, 1964), is very poorly described. The term claustrum will be used to refer to the "dorsal claustrum" while the term endopiriform nucleus will be used to refer to the "ventral claustrum" hereafter, following current conventions.

MORPHOLOGY

MACROSCOPIC MORPHOLOGY

Structurally, the claustrum is a long, band-like gray matter structure in the ventrolateral telencephalon of all therian mammals (marsupials and placentals), and arguably in monotremes (Loo, 1931; Butler et al., 2002; Ashwell et al., 2004). Therian mammals can be divided into two groups based on claustrum morphologies: species lacking an extreme capsule of white matter (hedgehog, bat, mouse, and rat), and species possessing an extreme capsule of white matter (guinea pig, rabbit, cow, carnivores, non-human primates, and human).

Among species lacking an extreme capsule, the structural organization of the claustrum has been most heavily studied in the rat. Nonetheless, views on the structural boundaries of the claustrum in this species (and other extreme capsule-lacking species) have been historically inconsistent, in part because no claustrum-specific neuroanatomical marker had been identified. It is, therefore, not surprising that accounts of claustral borders for the rat vary between brain atlases (Swanson, 2004; Paxinos and Watson, 2007), as well as across various primary research sources (Krettek and Price, 1977; Bayer and Altman, 1991; Druga et al., 1993; Kowiański et al., 1999; McKenna and Vertes, 2004; Mathur et al., 2009). Paxinos and Watson do not cite a source for their definition, but Swanson cites Krettek and Price (1977, 1978). Krettek and Price (1977) define the claustrum as extending along the entire rostrocaudal length of the striatum, where it resides immediately adjacent to the medially-lying external capsule (EC). However, both the Paxinos and Swanson atlases, as well as primary literature sources such as McKenna and Vertes (2004),

extend the claustrum much further rostrally than the descriptions of Krettek and Price (1977) or Bayer and Altman (1991), well into the frontal pole where it lies immediately ventrolateral to the forceps minor. The reason for this rostral extension is unclear. Paxinos and Watson (2007) noted in their atlas a new, dorsally-lying component to the claustrum, which they termed the "dorsal claustrum". This area has yet to be examined.

In species possessing an extreme capsule, the structural organization of the claustrum is ostensibly easier to define; it is historically defined as the thin strip of gray matter interposed between the striatum and the insular cortex. Consistent with the definition of its name, meaning "hidden" or "enclosed space", the claustrum appears completely enveloped by the medially-lying EC and the laterally-lying extreme capsule of white matter. The arbitrary border created by this surrounding white matter and the gray matter that is enclosed within thus defines the structural boundaries of the claustrum. In humans, as an example of a species possessing an extreme capsule, the claustrum is present along the entire rostrocaudal extent of the striatum (Jennes et al., 1995). Dorsoventrally, the claustrum extends along the entire medial face of the adjacent insula. Along this dorsoventral axis, the claustrum undulates slightly, following the contours of the insula. From an oblique angle, then, the claustrum appears as a wavy sheet of gray matter (Rae, 1954).

NEW MACROSCOPIC MORPHOLOGICAL DEFINITIONS

The varying definitions of the borders of the rat claustrum arose from the absence of a claustrum-specific marker protein. In 2009, however, we found a claustral marker, G protein gamma 2 subunit (Gng2), to be enriched in the claustrum and in register with parvalbumin-immunoreactive (PV-ir) neuropil (Mathur et al., 2009). The Gng2/parvalbumin (PV)-based definition of the claustrum alters the borders proposed by rat brain atlases. Paxinos and Watson (2007), for example, show the claustrum to extend well beyond the rostral pole of the striatum, lying ventrolaterally to the forceps minor (**Figure 1A**). However, Gng2 and PV immunostaining data, AChE and cytochrome oxidase histochemistry and tract tracing data indicate that the rostral most extension of the claustrum does not actually reach beyond the rostral pole of the striatum (Mathur et al., 2009; Smith and Alloway, 2010). Moreover, co-immunostaining for PV and crystallin mu (Crym), a marker of insular layer VI (Arlotta et al., 2005), does not readily reveal the presence of the claustrum at levels rostral to the striatum (**Figure 1B**; see Mathur et al., 2009 for methods). This suggests the rat claustrum is only present at striatal levels (**Figure 1C**). The PV and Crym immunohistochemistry data also indicate that the claustrum is situated not between the EC and the insular cortex, but embedded within layer VI of insular cortex. The PV-positive cloud of neuropil that defines the claustrum lies

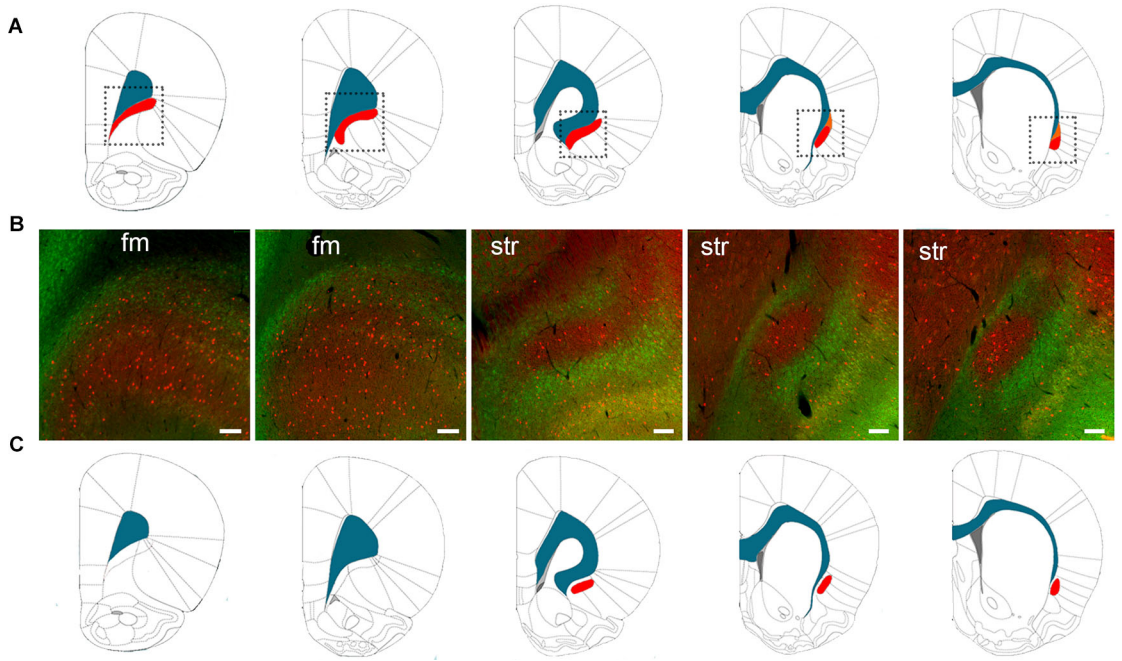

FIGURE 1 | (A) The structural boundaries of the rat claustrum (shown in red) and its proximity to the white matter (shown in blue) of the forceps minor (fm) and EC as defined by Paxinos and Watson (2007) (used with permission from Elsevier). The dotted lines in **(A)** indicate the regions depicted in **(B)**, which shows immunohistochemical staining for parvalbumin (PV) (red) and crystallin mu (Crym), a marker of insular cortex (staining originally published in Mathur et al., 2009). At levels of the striatum (str), the body of the claustrum is labeled by PV-immunoreactivity (-ir) and surrounded by Crym-ir, indicating that the claustrum is not immediately juxtaposed to the white matter. At the level of the fm, however, PV-ir and Crym-ir does not reveal structural boundaries of the claustrum as defined by Paxinos and Watson (2007). **(C)** The structural boundaries of the claustrum redrawn to depict the definition based on PV-ir and Crym-ir, as well as G protein gamma 2 subunit (Gng2)-ir (Mathur et al., 2009). Scale bars: 200 μm for fm sections; 100 μm for str sections.

lateral to the Crym-ir deep layer VI cells of the insula, and not immediately adjacent to the white matter of the EC as is depicted by Paxinos and Watson (2007), for example (**Figures 1A–C**).

For the rat claustrum then, protein expression data finally exists to define this structure: this Gng2/PV-based definition excludes the pregenual extent of the claustrum proposed by atlases, which derive their definition from Krettek and Price (1977). It should be noted that the manuscript by Krettek and Price (1977) is focused on the prefrontal cortex, only tangentially mentions the claustrum, and does not provide a rationale for the anatomical definitions of this nucleus. As such, the borders outlined in **Figure 1C** represent the first empirical anatomical definition for the claustrum.

MICROSCOPIC MORPHOLOGY

Following early investigations of the gross anatomy of the claustrum by Dejerine (1895) and others, Rae (1954) published a careful microscopic analysis in the human. Using silver impregnation studies, he found that the interface of capsular fibers and the gray matter body of the claustrum, which represents the structural boundaries of the claustrum, are not clearly demarcated; the dense collection of cell bodies and fibers in the core of the claustrum gradually change toward the border with capsular fibers. Specifically, he observed that fusiform-shaped cells, became more prevalent toward the perimeter of the claustrum. Interestingly, both Meynert (1884) and Brodmann (1909) also observed the prevalence of fusiform somata in the claustral perimeter, which they found to be enriched in the insular cortex. It has yet to be investigated whether the fusiform somata on the claustral periphery are actually insular cortex cells, as would be suggested by the finding that the claustrum is surrounded by insular cortex (Mathur et al., 2009). Besides the heterogeneous distribution of fusiform cells in the claustrum, Rae (1954) found a homogenous distribution of other cell types within the claustrum, including ovoid, triangular, and polygonal types.

The significance of these ovoid, triangular, and polygonal types remains unclear as golgi impregnation analysis of human tissue has only defined two types of neurons, type I and type II (Braak and Braak, 1982). Golgi type I neurons comprise roughly 85% of all claustral neurons and are evenly distributed throughout the body of the claustrum (Braak and Braak, 1982; Spahn and Braak, 1985; Sherk, 1986). They have spiny dendrites with axons projecting out of the claustrum, and have cell body diameters of 15–29 nm. The type I neurons represent the excitatory neurons that send projections to and receive projections from the cortex. A combined neuronal tract tracer and in situ hybridization study in rat demonstrated that the claustral projection neurons express the gene encoding the vesicular glutamate transporter (Vglut) 2 (Hur and Zaborszky, 2005). Because Vgluts (1 and 2) are considered to be unambiguous markers of cells that use glutamate as a neurotransmitter, it can reasonably be inferred that these claustral projection neurons are glutamatergic.

The less common Golgi type II neurons, comprising the remaining 15% of claustral cells, have cell body diameters of 10–15 nm, are aspiny, and have axons that do not project outside the body of the claustrum, as evidenced by human and cat studies (LeVay and Sherk, 1981; Braak and Braak, 1982). Type II neurons are therefore thought to be interneurons. This suggestion is bolstered by the fact that retrograde tract tracing studies have found that these cells do not accumulate tracer. These cells may express one of three types of calcium-binding proteins: PV, calbindin (CB), and calretinin (CR; Druga et al., 1993; Reynhout and Baizer, 1999). The rat claustrum is rich in PV-positive interneurons, but relatively poor in CB and CR-positive interneurons (Druga et al., 1993; Paxinos et al., 1999). Immunohistochemical analysis reveals a dense cloud of PV-ir neuropil with interspersed PV-ir somata in the rat claustrum, while a plexus of neuropil rich in CR-ir surrounds the claustrum in what appears as a ring around the nucleus. However, overlap exists between the PV-ir and the CR-ir plexuses.

Unlike the rat claustrum, the non-human primate claustrum has a much more homogenous distribution of interneuron populations compared to the rat, although the density between these populations varies. Reynhout and Baizer (1999) found PV-ir neurons to be large, multipolar cells with smooth dendrites in the macaque (*Macaca fascicularis*). In comparison, CR-ir cells are smaller, have elongated somata, are bipolar, and exhibit beaded dendrites. The CB-ir neurons were shown to exist in three forms: a dense population with small cell bodies and winding dendrites, a second multipolar type not unlike the PV-positive neurons, and a third bipolar type resembling the CR-positive neurons. Similar cell types have been observed in several different species, including human (Brand, 1981; LeVay and Sherk, 1981; Braak and Braak, 1982; Mamos, 1984; Mamos et al., 1986; Rahman and Baizer, 2007; Hinova-Palova et al., 2013).

Not unlike the cortex, then, the claustrum is composed of inhibitory-like interneurons and excitatory projection neurons; it is highly likely that several subclasses of both types of neurons await identification. Unlike the cortex, the claustrum does not exhibit a layered organization. Moreover, the dendrites of the type I projection neurons are not oriented in any specific direction, and these neurons express Vglut2, which is typically restricted to subcortical cells (Hur and Zaborszky, 2005). This suggests that the claustrum is a subcortical, or at least non-cortical, structure despite its physical apposition to and high connectivity with cortex, as well as its presence of inhibitory interneurons and excitatory projection neurons.

ONTOGENY

Early in the 20th century, the ontogenic and phylogenic derivations of the claustrum were intensely contested by several comparative anatomists. Investigators agreed that the claustrum is of pallial derivation. However, a dispute arose over whether the claustrum should be considered a derivative of cortex or a subcortical (albeit pallial) structure. Holl (1899) viewed the claustrum as a doubling of the insular cortex, and Smith (1910, 1917) later independently concluded that the claustrum derived from the upturned aspect of the piriform cortex. This notion of a doubling of adjacent cortex was also supported by Brodmann (1909) and others who concluded that the claustrum is cortical in origin. De Vries shared this view, but submitted that this did not necessarily mean that the claustrum was derived from cortex (Ariëns Kappers et al., 1936, 1960).

Carrying the cortical derivation hypothesis further, Sonntag and Woollard (1925) noted the resemblance of layer VI cells of the insular cortex and claustral cells in the aardvark. They concluded that the deepest layer of insular cortex is a "two-layered lamina multiformis" that is separated by the extreme capsule. Under this model, the superficial layer of this "lamina multiformis" is layer VI of insular cortex, with the deep layer being the claustrum. Similarly, Rose (1928) held that in mammals lacking an extreme capsule, the claustrum is the innermost extension of insular layer VI. In mammals possessing an extreme capsule, both Rose (1928) and Brodmann (1909) suggested that the claustrum is differentiated into an independent cortical layer, with what was termed insular layer VII representing the extreme capsule and layer VIII representing the claustrum. By this definition, the claustrum is cortical, but does not appear layered because it, itself, is a layer of insular cortex. Again, the finding that the claustrum is surrounded by insular cortex cells may have led to the close alignment of the claustrum with the insular cortex by these early researchers.

Standing in opposition to the notion that the claustrum is a cortical component, Landau (1919), and later Faul (1926), believed the claustrum to be subcortical, grouping it with striatal areas, though considering it not to be developmentally related to either striatum or cortex. Holmgren (1925) held a similar view but made the insightful assertion that the claustrum is a pallial structure not derived from cortex. He submitted that the claustrum derives from the ventricular surface, rather than as an in-folding of the overlying insular cortex, and should be grouped along with the amygdaloid complex. His perspective was largely ignored, however, as the bulk of opinions regarded the claustrum as a component part of the insular cortex (Ariëns Kappers et al., 1936, 1960).

It would take 75 years of speculation and investigation before convincing evidence was found to support Holmgren's view of claustrum ontogeny. Performing an elegant analysis of pallial and subpallial genetic markers in the developing chicken and mouse brains, Puelles et al. (2000) demonstrated the existence of four distinct pallial regions in the developing telencephalon. In addition to the medial, dorsal, and lateral pallial areas previously identified, a new "ventral pallium" was also defined. Based on these findings, Puelles et al. (2000) assigned the claustrum to the lateral pallium, along with the dorsal piriform cortex and basolateral amygdala. The new "ventral pallium" gives rise to the endopiriform nucleus, as well as other sites including the ventral piriform cortex, olfactory bulb, and lateral and intercalated nuclei of the amygdala. This view suggests that because the claustrum lacks a laminar organization and is derived from lateral pallium along with the basolateral amygdala, it should not be considered cortical.

If the claustrum is not a cortical structure, and is derived separately from the endopiriform nucleus, one might predict that the birth date of claustral neurons differs from that of cells in endopiriform nucleus and cortex. Bayer and Altman (1991) used tritiated thymidine birth-dating analysis to determine that rat claustral neurons primarily arise on embryonic day (E) 15 and 16, while endopiriform neurons are born earlier, on E14 and E15. Interestingly, cortical layer VI neurons are born at approximately E12.5, with the more superficial layers completing development by E15.5 (Valverde et al., 1989; Molyneaux et al., 2007). Despite the distinct birth-dating difference between the claustrum and the cortex, Bayer and Altman (1991) showed that claustrum neurons are derived from the cortical epithelium. This finding is consistent with the lateral pallial derivation findings of Puelles et al. (2000), and the position held by Holmgren (1925). In contrast, the endopiriform nucleus derives from the palliostriatal ventricular angle, a zone that straddles the border between the primordia of the basal ganglia and cortex (Bayer and Altman, 1991). Further distinguishing the claustrum from the endopiriform nucleus, claustral neurons migrate ventrally along the axis of the EC where they populate in a caudal to rostral fashion. Endopiriform neurons form a gradient in the orthogonal axis to that of the claustrum, with older neurons populating ventrally, and younger neurons populating dorsally (Bayer and Altman, 1991). So, despite the lack of clear boundaries between the claustrum and the endopiriform nucleus, these structures appear to be developmentally distinct.

CONNECTIVITY

In order to clearly delineate the connections of the claustrum it is imperative to analyze tract tracing data on the basis of an empirical definition of claustrum boundaries. Thus, existing connectivity data will be discussed in light of the Mathur et al. (2009) Gng2/PV-based definition (see **Figure 1C**).

CORTICAL CONNECTIONS

Through the mid-20th century, degeneration studies in rabbit, cat, and macaque (Carman et al., 1964; Narkiewicz, 1964, 1972; Druga, 1966, 1968; Kemp and Powell, 1970; Chadzypanagiotis and Narkiewicz, 1971) suggested that the claustrum is connected with all areas of cortex. A general feature that arose from these studies was that the claustrum is topographically organized, with rostral areas of cortex innervating rostral areas of the claustrum and caudal cortical sites projecting to the more caudal claustrum. Using tract tracing methods, these findings have been substantiated and extended by showing that the cortical projections to the claustrum are reciprocated (Sanides and Buchholtz, 1979; Olson and Graybiel, 1980; Edelstein and Denaro, 2004; Crick and Koch, 2005). Today it is generally accepted that the claustrum is reciprocally connected with all cortical sites (Sherk, 1986), though this position likely requires experimental confirmation. Regardless, it is clear that the claustrum is not equally connected with each cortical area (Alloway et al., 2009; Colechio and Alloway, 2009; Smith and Alloway, 2010). The claustrum appears to project primarily ipsilaterally to the cortex, while a weaker contralateral projection does exist (Norita, 1977; Olson and Graybiel, 1980; Squatrito et al., 1980; Li et al., 1986; Colechio and Alloway, 2009; Mathur et al., 2009; Smith and Alloway, 2010). The reverse appears to be true for cortico-claustral projections, with contralateral projections being denser than their ipsilateral counterparts (Alloway et al., 2009; Smith and Alloway, 2010).

Regarding layer specificity of claustral projections, LeVay (1986) and Olson and Graybiel (1980) showed using a discrete

deposit of an anterograde tracer into the claustrum of cat that the claustrum projects to all layers, with the densest innervation to layers IV and VI. Claustral axons synapse with spiny dendrites (of presumptive excitatory cells) in all layers, but in layer IV they also synapse onto aspiny dendrites (LeVay, 1986). Projections from the cortex to claustrum appear to arise predominantly from pyramidal and fusiform cells of layer VI (Olson and Graybiel, 1980; LeVay and Sherk, 1981). Approximately 3–4% of layer VI cells in the visual cortex, for example, project to the claustrum, and this population is distinct from neurons projecting to the lateral geniculate nucleus of the thalamus (Olson and Graybiel, 1980; LeVay and Sherk, 1981). Electron microscopy studies show that cortical projections form asymmetric synapses onto spiny (presumed excitatory) and aspiny (presumed inhibitory) cells of the claustrum (LeVay and Sherk, 1981).

Perhaps the most detailed demonstration of discrete claustral territories is the work done by Olson and Graybiel (1980) in the cat and later confirmed by Remedios et al. (2010) in the rhesus macaque. Olson and Graybiel (1980) used electrophysiological recordings from subregions of the cat claustrum following various sensory stimuli and found that the cortical representation for visual and tactile information within the claustrum maintained an orderly retinotopic and somatotopic organization. By injecting tracers into the claustral site from which they recorded, Olson and Graybiel (1980) found that discrete subdivisions within the claustrum receive projections from and send projections to cognate sensory cortices. In contrast to the rat claustrum, the claustrum of felines and primates, which has expanded along with the cortex, appears far more segregated in its zonal distribution.

Based on the widespread connectivity of claustrum with cortex, and the zones of cortical targeting in the claustrum, it appears that the organization of the claustrum resembles that of the thalamus (Olson and Graybiel, 1980). Are there connections within the claustrum that link these cortical recipient and projection zones together? Following the discrete injections of horseradish peroxidase into the claustrum by Olson and Graybiel (1980) and later LeVay (1986), these investigators reported no inter-zonal connections. However, Smith and Alloway (2010) were able to deposit a retrograde tracer into the rat claustrum and found extensive labeling along the rostro-caudal axis of the claustrum. Further work is needed to completely resolve this issue.

Brodmann (1909), Loo (1931), Rae (1954) and others noted similarities between the insular cortex and the claustrum. The insular cortex, like the claustrum, has widespread connections with other parts of the brain. Studies have shown that the insula projects to or receives inputs from the nucleus of the solitary tract, olfactory bulb, amygdala, hippocampus, the parvicellular part of the posteromedial ventral thalamic nucleus, as well as the entorhinal, motor, primary and secondary somatosensory, prefrontal, orbitofrontal, primary auditory, auditory association, and visual association cortices (Mufson and Mesulam, 1982; van der Kooy et al., 1984; Augustine, 1985, 1996; Nakashima et al., 2000). While the claustrum and the insular cortex share many sites in their respective connectivity profiles, there has been no indication in the literature that these profiles are identical. Based on structural, developmental, and connectivity lines of evidence, the claustrum is not part of insular cortex, despite appearing embedded within layer VI (Mathur et al., 2009).

SUBCORTICAL CONNECTIONS

In addition to the claustrum's reciprocal connections with cortex, modern tract tracing studies have suggested the presence of subcortical projections. Studies in the hedgehog, rat, cat, tree shrew, and macaque have reported claustral projections to the dorsal thalamic nuclei (LeVay and Sherk, 1981; Carey and Neal, 1986; Dinopoulos et al., 1992; Erickson et al., 2004; McKenna and Vertes, 2004; Vertes and Hoover, 2008), striatum (Arikuni and Kubota, 1985), hippocampus (Amaral and Cowan, 1980), and hypothalamus (LeVay and Sherk, 1981; Vertes, 1992; Yoshida et al., 2006). Interestingly, in many of these studies the retrogradely-labeled somata in the claustrum were to seen to form a ring-like pattern around the body of the claustrum (**Figure 2**). These findings can be interpreted as a segregation of the claustrum into a PV-ir rich "core" surrounded by a Vglut2-enriched "shell", as proposed by Real et al. (2006) in the mouse. According to this, the "shell" may be connected to

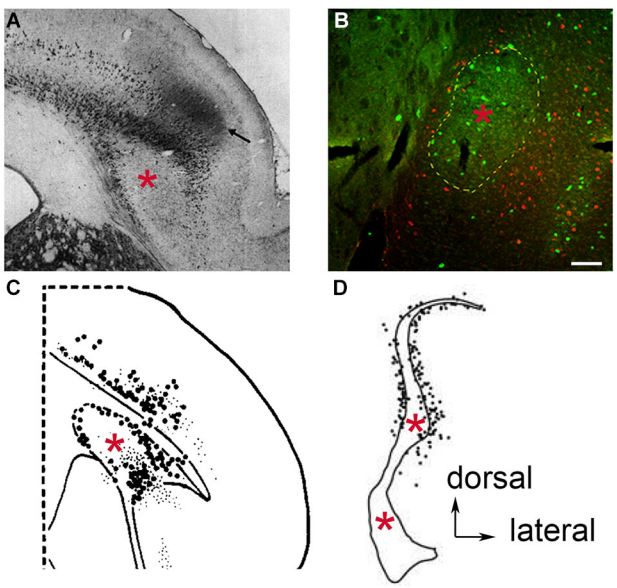

FIGURE 2 | Retrograde neuronal tract tracer labeling in the region of the claustrum following tracer deposit into the thalamic mediodorsal nucleus of various species. Examples of species lacking an extreme capsule, **(A)** the hedgehog, (used by permission from John Wiley and Sons; Dinopoulos et al., 1992), and **(B)** the rat, where PV-ir is depicted in green and retrogradely labeled cells in red (see original publication by Mathur et al., 2009). In both cases, the retrogradely labeled cells appear to reside in the insular cortex and surround the body of the claustrum (red asterisk), which in the case of the rat is defined by PV-ir. In species containing an extreme capsule, **(C)** the tree shrew (used by permission from Elsevier; Carey and Neal, 1986), and **(D)** the cynomolgus monkey (used by permission from Elsevier; Erickson et al., 2004) both exhibit a similar pattern of retrograde labeling. The rat data **(B)** suggests that the labeled cells in **(C)** and **(D)** are insular cortex cells that have been separated from the rest of the more superficial insular cortex cell layers through time by the development of the extreme capsule. Scale bar: 100 μm.

subcortical sites, while the "core" may be connected with cortex. However, if the "core" and "shell" concept of the claustrum were valid, one might expect that other lines of evidence would distinguish the "shell" from deep layers of insular cortex. However, the rat claustrum was found to be enriched in netrin G-2 protein and cholecystokinin mRNA expression in a pattern consistent with Gng2 expression (Miyashita et al., 2005; Watakabe et al., 2012), while the entire insular cortex was found to be enriched for purkinje cell protein 4 mRNA in a pattern that surrounds the body of the claustrum (Watakabe et al., 2012). Moreover, following retrograde tract tracer injection into subcortical sites, retrogradely-labeled somata surrounding the claustrum typically extend into more superficial layers of the insula as well (**Figure 2**). The pattern of purkinje cell protein 4 mRNA expression and retrograde labeling throughout the insula further supports that the claustrum is surrounded by insular cortex, rather than being arranged into "core" and "shell" subcomponents that have differential connectivity.

The redefinition of claustral structural boundaries by Gng2/PV expression not only accounts for much of the disagreement over claustrum ontogeny through history, but it also accounts for the abundance of subcortical connection findings. The Gng2/PV-based definition posits the thalamic and lateral hypothalamic connections once believed to be claustral are actually assigned to layer VI of insular cortex. Examination of existing anatomical studies reveals this distinction in several species. Injections of retrograde tracers into the dorsal thalamus of the hedgehog showed retrogradely labeled cell bodies encapsulating the apparent body of claustrum (Dinopoulos et al., 1992; **Figure 2A**). This is also apparent in rat following injection of retrograde tract tracer into the mediodorsal nucleus of the thalamus (**Figure 2B**).

Through time, as species developed an extreme capsule following the elaboration of cortex, the claustrum became enveloped by white matter. Prior to the complete encapsulation of the claustrum, this structure was partially bordered laterally by an inchoate extreme capsule in certain species. One example of this is the tree shrew. Injection of a retrograde tract tracer into the dorsal thalamus of this species results in labeled cells again completely surrounding the claustrum notably on the lateral aspect of the claustrum where the extreme capsule borders this structure (Carey and Neal, 1986; **Figure 2C**). In the macaque, in which the claustrum is completely enveloped in white matter, Erickson et al. (2004) revealed retrogradely-labeled cells surrounding the body of the claustrum again following injection of tracer into the dorsal thalamus (**Figure 2D**). It should be noted that in these tracer studies, the authors interpreted the findings as a demonstration that the claustrum connects to the dorsal thalamus. However, in light of the Gng2/PV-based definition of claustral boundaries, the retrogradely-labeled cells are likely insular layer VI neurons that populate the perimeter of the white matter-encapsulated claustrum. Interestingly, in the Erickson et al. (2004) study, a large number of retrogradely-labeled cells were observed in the dorsal extension of the macaque claustrum; Crym immunolocalization indicates that this area of the "claustrum" is actually composed of an admixture of insular layer VI and claustral cells (Mathur et al., 2009).

Evidence suggesting the claustrum *receives* subcortical projections is less controversial. Immunohistochemical studies suggest that the claustrum in rats and cats receives a diffuse serotonergic innervation, presumably from the brainstem dorsal raphe nucleus (Baizer, 2001; Rahman and Baizer, 2007). This serotonergic input was reported to be evenly distributed across the entire claustrum (Rahman and Baizer, 2007). Consistent with these findings, some evidence exists for expression of five subtypes of serotonin receptors within the claustrum, including 5-HT_{1A}, 5-HT_{1F}, 5-HT_{2A}, and 5-HT_{2C} receptors (Pompeiano et al., 1994; Wright et al., 1995; Mengod et al., 1996; Pasqualetti et al., 1999). The significance of this potential subcortical connection has yet to be experimentally elucidated.

Another subcortical structure that has been reported to project to the claustrum is the endopiriform nucleus, which lies immediately ventral to the claustrum. Lipowska et al. (2000) found that the endopiriform nucleus in the rat and rabbit projects to the perimeter of the claustrum. This connectivity pattern would again appear to be consistent with the notion of a "core" and "shell" organization of the claustrum. Thus, the "shell" of the claustrum projects to endopiriform nucleus. Alternatively, and in accordance with the Gng2/PV-based definition of the claustrum, these projections to the endopiriform nucleus arise instead from the insular cortex. It should be noted that discrete tracer injections into the endopiriform nucleus are extremely difficult to achieve. Because the endopiriform nucleus borders white matter, claustrum, and insula, endopiriform connectivity data based on tract tracing carries a note of caution.

FUNCTION

The final, and most puzzling, "problem" of the claustrum lies in its function. Relative to other prominent telencephalic structures such as the cortex, striatum, and thalamus, knowledge of claustral function is sorely lacking. Despite waves of interest in the claustrum over the last century, only a few nuggets of functional information and some controversial hypotheses on its functional attributes exist. Why has the function of the claustrum proven to be so hard to unlock? The shape of the claustrum has made complete and discrete claustrum lesions impossible to achieve using conventional chemical or mechanical means. Clinical pathological correlation studies have yielded extraordinary information about the function of many brain sites, but no convincing selective claustral lesions have been reported in humans following cerebral hemorrhage or ischemia. Without the ability to generate reproducible, discrete lesions of the claustrum in animals, the functional roles of this nucleus remain a mystery.

MULTISENSORY INTEGRATION

Based on its bidirectional cortical connectivity, the claustrum has been proposed to function as a multisensory integrator; serving to bind information from disparate sensory cortices. Supporting this notion, Segundo and Machne (1956) and later Spector et al. (1974) found electrophysiological evidence for sensory convergence in the claustrum. Both groups recorded from claustral neurons in awake and anesthetized cats that were exposed to sensory stimuli of different modalities. They

showed that 75% claustral cells responded to more than one sensory modality (Spector et al., 1974). The polymodal neurons responded to as few as two modalities, and to as many as six (touches, flashes, clicks, smells, vagal, and tooth pulp stimulation). The most common convergences observed were somato-olfactory, somato-visceral, and somato-nocioceptive (Segundo and Machne, 1956). Polymodal cells were distributed throughout the claustrum (Spector et al., 1974), and these cells displayed unique firing patterns for each type of modality-specific stimulus (Segundo and Machne, 1956). Given that the claustrum may be surrounded/intermingled with insular cortical cells (Mathur et al., 2009), these previous studies are called into question.

Two different theories for multisensory integration have been proposed. The first theory states that multisensory integration occurs in polymodal sites that only process specific sensory combinations; these types of cells have been reported in a variety of areas including arcuate sulcus, superior temporal sulcus, inferior and posterior parietal lobules, the amygdaloid complex, hippocampus, and the superior colliculus (Thompson and Shaw, 1965; Ettlinger and Wilson, 1990). Because the claustrum appears to have multisensory-responsive cells, the claustrum may serve to bind some types of sensory modalities. The second theory, proposed by Ettlinger and Wilson (1990), states that no one structure in brain executes the processes required for cross-modal performance. Instead, only a subcortical relay nucleus is required through which different sensory cortices can access each other in order to associate modalities. This subcortical relay nucleus was proposed to be the claustrum. In this way, the claustrum theoretically synchronizes cortical areas to accomplish the feat of crossing modalities. Ettlinger and Wilson (1990) did not state, however, how this may be accomplished or where the binding of multimodal information would occur.

In vivo functional imaging studies exploring multisensory integration largely support the second theory, which places the claustrum as the necessary subcortical relay nucleus. This support is due to a growing body of evidence showing activation of the claustrum/insula region in cross-modal matching tasks (Hörster et al., 1989; Lewis et al., 2000; Olson et al., 2002; Naghavi et al., 2007; Kavounoudias et al., 2008). A possible representative finding comes from Hadjikhani and Roland (1998) positron emission tomography (PET) study that involved a task that had subjects attempting to identify objects in their hand (to which they were blind) to a matching object in their visual field (but out of reach) that was amongst a series of similar, but non-identically-shaped objects. They found that the insula-claustrum region, with a center of gravity situated closer to the claustrum, was the only area constantly activated in these tasks. A caveat with this study is that the claustrum and insula are impossible to distinguish with the imaging resolution provided by PET. Other studies using functional magnetic resonance imaging (fMRI) have gone on to show that a combination of the appropriate sensory cortices and the claustrum were activated during similar matching paradigms (Olson et al., 2002; Naghavi et al., 2007; Kavounoudias et al., 2008). Thus, a relay function for the claustrum enjoys support.

Arguing against multisensory integration is recent work by Remedios et al. (2010) who improved targeting of the claustrum using magnetic resonance to guide the placement of the recording electrode in awake monkeys. They found that claustral neurons are relatively quiescent and, supporting the earlier work by Olson and Graybiel (1980), that the claustrum is subdivided into discrete sensory zones. That is, the visual zone of the claustrum preferentially and transiently responds to suddenly presented visual cues, while the auditory subdivision of the claustrum does the same for auditory cues (Remedios et al., 2010). Polymodal responses were rarely observed.

The imaging studies that do support a role for the claustrum in multisensory integration do not address the question of where polymodal information is being bound exactly, and again suffer from the inability to discriminate between claustral vs. insular activation. Moreover, it is quite possible that, given the negative multisensory findings by Remedios et al. (2010) that claustral activation under multisensory tasks may be an effect of activity pooling, wherein the BOLD activity threshold for the claustrum is achieved only when multiple, discrete sensory zones of the claustrum are simultaneously activated.

CRICK AND KOCH'S HYPOTHESIS

Crick and Koch (2005) hypothesized that the claustrum is where sensory information is bound, functioning as a generator of the unified perception of a multitude of sensory stimuli in one's environment (conscious percepts). That is, putting individual stimuli together, one is able to recognize an object as a whole rather than experiencing each stimulus as a separate sensory entity. Crick and Koch argued that since almost all theories attempting to explain the neural correlate of such an experience (consciousness) require a "need to rapidly integrate and bind information in neurons that are situated across distinct cortical and thalamic regions" (see also Bachmann, 2000; Llinas, 2001), that the claustrum may be perfectly suited to subserve such a function due to its unique feature of reciprocal connectivity with the cortex, its central positioning in brain, and its connections with the thalamus (which are now called into question, see Mathur et al., 2009). Crick and Koch (2005) went on to propose that the binding of multisensory information in the claustrum underlies the unification of sensory experiences. This hypothesis has received further theoretical support from Smythies et al. (2012), who propose that the claustrum functions as a detector, modulator, and integrator of synchronous oscillations for the purpose of subserving cognitive processes such as consciousness.

Though the claustrum does appear to have many of the attributes required of a sensory binding site, some problems exist with this concept. First, a well-recognized physiological trait of claustral cells consistently found across functional studies is their quiescent nature (Segundo and Machne, 1956; Spector et al., 1974). The spontaneous firing rate is quite low, usually only becoming activated following the presentation of a sudden sensory stimulus in awake monkeys (Remedios et al., 2010). If the claustrum is binding sensory stimuli for the purpose of generating conscious percepts, one would predict that the claustrum would display near constant activation during awake, behaving conditions. Secondly, the Crick and Koch model places the high computational load requirement of binding in a structure that is not layered, or at least not organized (by sensory subdivisions) in

such a way that would suggest processing power as we currently know it.

FROM STRUCTURE TO FUNCTION?

The Gng2/PV-based anatomical definition of the claustrum indicates this structure may be largely restricted to (reciprocal) connections with cortical sites, and does not project subcortically to structures including the lateral hypothalamus and mediodorsal thalamic nucleus (Mathur et al., 2009). Given the normally quiescent nature of claustral cells that respond transiently to suddenly presented stimuli then (Remedios et al., 2010), the claustrum could serve as a saliency filter for cortico-cortico communication. Given that the claustrum preferentially projects to the ipsilateral anterior cingulate cortex (Smith and Alloway, 2010), an area known to be involved in error detection and attentional processing (Muir et al., 1996; Botvinick, 2007; Carter and van Veen, 2007; Johnston et al., 2007), the claustrum may be acting as a component part of a sensorimotor/sensory association cortex-to-claustrum-to-cingulate pathway for encoding the salience of incoming stimuli. This would allow only the most salient signals to propagate through the claustrum to the cingulate cortex. It is also possible that a cingulate cortex-to-claustrum-to-sensorimotor cortex/association cortex circuit may be recruited for allocation of attentional load to the necessary cortical sites demanded of a particularly salient stimulus. These hypotheses could possibly be tested using optogenetic activation/inactivation of cingulate fibers projecting to the claustrum during a modified 5-choice reaction test in rodents. This is the standard assay for assessing attentional ability in rodents. It involves presenting a brief light stimulus in one of five possible holes arrayed in a horizontal arc in front of the animal. Once the cue is presented, the animal must successfully nose-poke the hole where the light flashed and a food reward is delivered. The task basically tests the ability to sustain attention to a number of locations over a series of trials (Robbins, 2002).

The saliency detection concept fits with existing structural and functional data and presents testable predictions. The first prediction is that the claustrum is most intimately connected to higher order association cortices, rather than primary sensory cortices. If the claustrum is indeed involved in attention, then attentional resources should be allocated to cortices encoding for complex representations (faces) rather than those encoding the component parts of objects (lines). This could easily be tested using a series of traditional anterograde and retrograde neuronal tract tracer injections into the necessary cortical sites. The second prediction would be that the claustrum would be expected to be recruited during tasks requiring attentional shifting or the early phase of attentional focusing. Based on connectivity studies over several decades, including recent work in rats showing that claustro-cortical connections are significantly stronger ipsilaterally and cortico-claustral projections display the opposite configuration (Alloway et al., 2009; Colechio and Alloway, 2009; Mathur et al., 2009; Smith and Alloway, 2010), one could then hypothesize that claustral activation may be commonly observed to be unilateral, unless the salient stimulus was presented bilaterally. This could possibly be tested using functional imaging in humans (given sufficient resolution of the claustrum) or *in vivo* electrophysiology in non-human primate subjects presented with unilateral vs. bilateral stimuli during attentional tasks.

For an incoming, salient sensory stimulus encoded by sensorimotor or association cortices, once a certain threshold of salience is achieved, the contralateral claustrum would be activated (**Figure 3**). Claustral activation would signal to ipsilateral cingulate cortex. Through the claustrum, then, the cingulate cortex enjoys an online saliency map of the cortical mantle. Cingulate processing may then result in contralateral activation of claustrum that would, in turn, result in claustral activation of the original sensorimotor or association cortical site for the allocation of attentional demand to the perceived salient stimulus (**Figure 3**). The zonal organization of cortical representation in the claustrum again becomes necessary in this context. Using this organization, the cingulate cortex channels signals through the appropriate claustrum sensory subdivision to prime the cognate

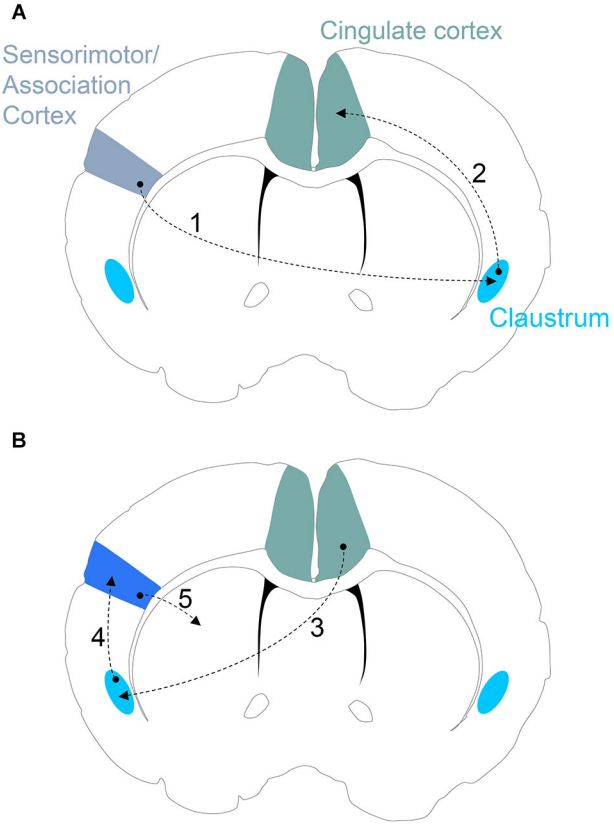

FIGURE 3 | (A) Proposed claustrum circuitry involved in stimulus encoding. Neural activity encoding a novel/salient sensory stimulus in sensorimotor and/or association cortices activates the corresponding subdivision of the contralateral claustrum (*Step 1*). If the sensory stimulus is salient enough to pass the claustral filter, the ipsilateral cingulate cortex receives and processes the incoming claustral signal (*Step 2*). **(B)** Proposed circuitry involved in an action response to a salient stimulus. The cingulate cortex signals to the appropriate subdivision of the contralateral claustrum (*Step 3*) that, in turn, provides attentional allocation to the original sensorimotor/association cortex encoding the salient stimulus (*Step 4*). The activated sensorimotor/association cortex finally signals to the striatal complex for selection of an appropriate action (*Step 5*).

sensorimotor/association cortical site. If the claustrum was not arranged into discrete zones, and these sensory subdivisions were intermixed, it would seem likely that the categorical allocation of attention to distinct sensory cortices would be blurred.

If the claustrum is functioning as a component part of a distributed network for attentional allocation, a role for this circuit in instigating cortico-basal ganglia circuitry for action selection can be envisioned. In response to a salient stimulus, claustral activation of a sensorimotor/association cortex may prime subsets of corticostriatal circuits for initiation/selection of a particular action (or inaction) through enhanced synaptic drive or synchrony at select corticostriatal synapses. It is also plausible that claustral priming of a select corticostriatal circuit may enhance learning of a motor sequence or skill response to a salient stimulus. As novel stimuli are often perceived as salient, the claustrum may also be involved in attentional allocation to cortical sites signaling to the striatal complex during the learning of novel actions. These predictions could be tested using optogenetic manipulation of claustral afferents to cortical sites projecting to the striatum, such as motor cortex, during acquisition of a skill.

CONCLUSIONS

The expression of Gng2 and PV immunoreactivity offers an empirical definition of claustral boundaries and describes the relationship of the claustrum to contiguous structures. In doing so, the Gng2/PV-based definition challenges the currently held view of claustral connectivity. That is, the claustrum appears to connect (reciprocally) to cortex, and not to project to other prominent subcortical sites (lateral hypothalamus and mediodorsal nucleus of the thalamus) as once thought (Mathur et al., 2009). However, afferent connections from subcortical sites such as the dorsal raphe nucleus remain a possibility.

It is clear that a consensus on the structural boundaries of the claustrum is required. Such a consensus would result in agreement on the claustrum's connectivity profile and, in turn, shed light on the possible functional attributes of this nucleus. Towards this end, it is imperative that mouse lines expressing green fluorescent protein or Cre recombinase under control of a claustral-specific gene (e.g., Gng2) promoter are generated to allow for the next generation of cell type classification, functional characterization and microcircuit mapping of the claustrum. Such tools would allow for *in vivo* control of claustral activation with light, ultimately providing a long-sought and elegant means of testing existing and future functional hypotheses of the "problem" that is the claustrum.

ACKNOWLEDGMENTS

I would like to thank Dr. Ariel Y. Deutch for helpful comments. This work was supported by the NIAAA K22 Career Development Award.

REFERENCES

Alloway, K. D., Smith, J. B., Beauchemin, K. J., and Olson, M. L. (2009). Bilateral projections from rat MI whisker cortex to the neostriatum, thalamus and claustrum: forebrain circuits for modulating whisking behavior. *J. Comp. Neurol.* 515, 548–564. doi: 10.1002/cne.22073

Amaral, D. G., and Cowan, W. M. (1980). Subcortical afferents to the hippocampal formation in the monkey. *J. Comp. Neurol.* 189, 573–591. doi: 10.1002/cne.901890402

Ariëns Kappers, C. U., Huber, G. C., and Crosby, E. C. (1936, 1960). *The Comparative Anatomy of the Nervous System of Vertebrates, Including Man*. New York: Hafner Publishing Company.

Arikuni, T., and Kubota, K. (1985). Claustral and amygdaloid afferents to the head of the caudate nucleus in macaque monkeys. *Neurosci. Res.* 2, 239–254. doi: 10.1016/0168-0102(85)90003-3

Arlotta, P., Molyneaux, B. J., Chen, J., Inoue, J., Kominami, R., and Macklis, J. D. (2005). Neuronal subtype-specific genes that control corticospinal motor neuron development in vivo. *Neuron* 45, 207–221. doi: 10.1016/j.neuron.2004.12.036

Ashwell, K. W., Hardman, C., and Paxinos, G. (2004). The claustrum is not missing from all monotreme brains. *Brain Behav. Evol.* 64, 223–241. doi: 10.1159/000080243

Augustine, J. R. (1985). The insular lobe in primates including humans. *Neurol. Res.* 7, 2–10.

Augustine, J. R. (1996). Circuitry and functional aspects of the insular lobe in primates including humans. *Brain Res. Brain Res. Rev.* 22, 229–244. doi: 10.1016/s0165-0173(96)00011-2

Bachmann, T. (2000). *Microgenetic Approach to the Conscious Mind.* Amsterdam: Johns Benjamins.

Baizer, J. S. (2001). Serotonergic innervation of the primate claustrum. *Brain Res. Bull.* 55, 431–434. doi: 10.1016/s0361-9230(01)00535-4

Bayer, S. A., and Altman, J. (1991). Development of the endopiriform nucleus and the claustrum in the rat brain. *Neuroscience* 45, 391–412. doi: 10.1016/0306-4522(91)90236-H

Botvinick, M. M. (2007). Conflict monitoring and decision making: reconciling two perspectives on anterior cingulate function. *Cogn. Affect. Behav. Neurosci.* 7, 356–366. doi: 10.3758/cabn.7.4.356

Braak, H., and Braak, E. (1982). Neuronal types in the claustrum of man. *Anat. Embryol. (Berl)* 163, 447–460. doi: 10.1007/bf00305558

Brand, S. (1981). A serial section Golgi analysis of the primate claustrum. *Anat. Embryol. (Berl)* 162, 475–488. doi: 10.1007/bf00301872

Brockhaus, H. (1940). Die cyto- and myeloarchitectonik des cortex claustralis and des claustrum biem menschen. *J. Psychol. Neurol.* 49, 249–349.

Brodmann, K. (1909). *Vergleichende Lokalisationslehre der Grosshirnrinde in Ihren Prinzipien Dargestellt Auf Grund des Zellenbaues.* Leipzig: J. A. Barth.

Butler, A. B., Molnár, Z., and Manger, P. R. (2002). Apparent absence of claustrum in monotremes: implications for forebrain evolution in amniotes. *Brain Behav. Evol.* 60, 230–240. doi: 10.1159/000066698

Carey, R. G., and Neal, T. L. (1986). Reciprocal connections between the claustrum and visual thalamus in the tree shrew (Tupaia glis). *Brain Res.* 386, 155–168. doi: 10.1016/0006-8993(86)90152-6

Carman, J. B., Cowan, W. M., and Powell, T. P. (1964). The cortical projection upon the claustrum. *J. Neurol. Neurosurg. Psychiatry* 27, 46–51. doi: 10.1136/jnnp.27.1.46

Carter, C. S., and van Veen, V. (2007). Anterior cingulate cortex and conflict detection: an update of theory and data. *Cogn. Affect. Behav. Neurosci.* 7, 367–379. doi: 10.3758/cabn.7.4.367

Chadzypanagiotis, D., and Narkiewicz, O. (1971). Connections of the visual cortex with the claustrum. *Acta Neurobiol. Exp. (Wars)* 31, 291–311.

Colechio, E. M., and Alloway, K. D. (2009). Differential topography of the bilateral cortical projections to the whisker and forepaw regions in rat motor cortex. *Brain Struct. Funct.* 213, 423–439. doi: 10.1007/s00429-009-0215-7

Crick, F. C., and Koch, C. (2005). What is the function of the claustrum? *Philos. Trans. R. Soc. Lond. B Biol. Sci.* 360, 1271–1279. doi: 10.1098/rstb.2005.1661

Dejerine, J. (1895). *Anatomie des Centres Nerveux*. Vols. I and II, Paris: Rueff.

Dinopoulos, A., Papadopoulos, G. C., Michaloudi, H., Parnavelas, J. G., Uylings, H. B., and Karamanlidis, A. N. (1992). Claustrum in the hedgehog (Erinaceus europaeus) brain: cytoarchitecture and connections with cortical and subcortical structures. *J. Comp. Neurol.* 316, 187–205. doi: 10.1002/cne.903160205

Druga, R. (1966). Cortico-claustral connections. I. Fronto-claustral connections. *Folia Morphol. (Praha)* 14, 391–399.

Druga, R. (1968). Cortico-claustral connections. II. Connections from the parietal, temporal and occipital cortex to the claustrum. *Folia Morphol. (Prague)* 16, 142–149.

Druga, R., Chen, S., and Bentivoglio, M. (1993). Parvalbumin and calbindin in the rat claustrum: an immunocytochemical study combined with retrograde tracing frontoparietal cortex. *J. Chem. Neuroanat.* 6, 399–406. doi: 10.1016/0891-0618(93)90014-U

Druga, R., Rokyta, R., and Benes, V. Jr. (1990). Claustro-neocortical projections in the rhesus monkey (projections to area 6). *J. Hirnforsch.* 31, 487–494.

Edelstein, L. R., and Denaro, F. J. (2004). The claustrum: a historical review of its anatomy, physiology, cytochemistry and functional significance. *Cell. Mol. Biol. (Noisy-le-grand)* 50, 675–702.

Erickson, S. L., Melchitzky, D. S., and Lewis, D. A. (2004). Subcortical afferents to the lateral mediodorsal thalamus in cynomolgus monkeys. *Neuroscience* 129, 675–690. doi: 10.1016/j.neuroscience.2004.08.016

Ettlinger, G., and Wilson, W. A. (1990). Cross-modal performance: behavioral processes, phylogenetic considerations and neural mechanisms. *Behav. Brain Res.* 40, 169–192. doi: 10.1016/0166-4328(90)90075-P

Faul, J. (1926). The comparative ontogenetic development of the corpus striatum in reptiles. *Proc. Sect. Sci.* 29, 150–162.

Hadjikhani, N., and Roland, P. E. (1998). Cross-modal transfer of information between the tactile and the visual representations in the human brain: a positron emission tomographic study. *J. Neurosci.* 18, 1072–1084. doi: 10.1016/s1053-8119(96)80365-X

Hinova-Palova, D. V., Edelstein, L., Landzhov, B. V., Braak, E., Malinova, L. G., Minkov, M., et al. (2013). Parvalbumin-immunoreactive neurons in the human claustrum. *Brain Struct. Funct.* doi: 10.1007/s00429-013-0603-x. [Epub ahead of print].

Holl, M. (1899). Ueber die insel des carnivorenhirns. *Arch. f. Anat. und Physiol.*

Holmgren, N. (1925). Points of view concerning forebrain morphology in higher vertebrates. *Acta Zool.* 6, 413–459. doi: 10.1111/j.1463-6395.1925.tb00271.x

Hörster, W., Rivers, A., Schuster, B., Ettlinger, G., Skreczek, W., and Hesse, W. (1989). The neural structures involved in cross-modal recognition and tactile discrimination performance: an investigation using 2-DG. *Behav. Brain Res.* 33, 209–227. doi: 10.1016/s0166-4328(89)80052-x

Hur, E. E., and Zaborszky, L. (2005). Vglut2 afferents to the medial prefrontal and primary somatosensory cortices: a combined retrograde tracing in situ hybridization study. *J. Comp. Neurol.* 483, 351–373. doi: 10.1002/cne.20444

Jennes, L., Traurig, H. H., and Conn, P. M. (1995). *Atlas of the Human Brain.* Philadelphia: Lippincott Williams and Wilkins.

Johnston, K., Levin, H. M., Koval, M. J., and Everling, S. (2007). Top-down control-signal dynamics in anterior cingulate and prefrontal cortex neurons following task switching. *Neuron* 53, 453–462. doi: 10.1016/j.neuron.2006.12.023

Kavounoudias, A., Roll, J. P., Anton, J. L., Nazarian, B., Roth, M., and Roll, R. (2008). Proprio-tactile integration for kinesthetic perception: an fMRI study. *Neuropsychologia* 46, 567–575. doi: 10.1016/j.neuropsychologia.2007.10.002

Kemp, J. M., and Powell, T. P. (1970). The cortico-striate projection in the monkey. *Brain* 93, 525–546. doi: 10.1093/brain/93.3.525

Kowiański, P., Dziewiatkowski, J., Kowianski, J., and Morys, J. (1999). Comparative anatomy of the claustrum in selected species: a morphometric analysis. *Brain Behav. Evol.* 53, 44–54. doi: 10.1159/000006581

Krettek, J. E., and Price, J. L. (1977). The cortical projections of the mediodorsal nucleus and adjacent thalamic nuclei in the rat. *J. Comp. Neurol.* 171, 157–191. doi: 10.1002/cne.901710204

Krettek, J. E., and Price, J. L. (1978). A description of the amygdaloid complex in the rat and cat with observations on intra-amygdaloid axonal connections. *J. Comp. Neurol.* 178, 255–280. doi: 10.1002/cne.901780205

Landau, E. (1919). The comparative anatomy of the nucleus amygdalae, the claustrum and the insular cortex. *J. Anat.* 53, 351–360.

LeVay, S. (1986). Synaptic organization of claustral and geniculate afferents to the visual cortex of the cat. *J. Neurosci.* 6, 3564–3575.

Lewis, J. W., Beauchamp, M. S., and DeYoe, E. A. (2000). A comparison of visual and auditory motion processing in human cerebral cortex. *Cereb. Cortex* 10, 873–888. doi: 10.1093/cercor/10.9.873

LeVay, S., and Sherk, H. (1981). The visual claustrum of the cat. I. Structure and connections. *J. Neurosci.* 9, 956–980.

Li, Z. K., Takada, M., and Hattori, T. (1986). Topographic organization and collateralization of claustrocortical projections in the rat. *Brain Res. Bull.* 17, 529–532. doi: 10.1016/0361-9230(86)90220-0

Lipowska, M., Kowianski, P., Majak, K., Jagalska-Majewska, H., and Morys, J. (2000). The connections of the endopiriform nucleus with the insular claustrum in the rat and rabbit. *Folia Morphol. (Warsz)* 59, 77–83.

Llinas, R. R. (2001). *I of the Vortex: From Neurons to Self.* Cambridge, MA: MIT Press.

Loo, Y. T. (1931). The forebrain of the opossum, Didelphis virginiana. *J. Comp. Neurol.* 52, 1–148. doi: 10.1002/cne.900520102

Mamos, L. (1984). Morphology of claustral neurons in the rat. *Folia Morphol. (Warsz)* 43, 73–78.

Mamos, L., Narkiewicz, O., and Morys, J. (1986). Neurons of the claustrum in the cat; a Golgi study. *Acta Neurobiol. Exp. (Wars)* 46, 171–178. doi: 10.1007/bf00239531

Mathur, B. N., Caprioli, R. M., and Deutch, A. Y. (2009). Proteomic analysis illuminates a novel structural definition of the claustrum and insula. *Cereb. Cortex* 19, 2372–2379. doi: 10.1093/cercor/bhn253

McKenna, J. T., and Vertes, R. P. (2004). Afferent projections to nucleus reuniens of the thalamus. *J. Comp. Neurol.* 480, 115–142. doi: 10.1002/cne.20342

Mengod, G., Vilaró, M. T., Raurich, A., López-Giménez, J. F., Cortés, R., and Palacios, J. M. (1996). 5-HT receptors in mammalian brain: receptor autoradiography and in situ hybridization studies of new ligands and newly identified receptors. *Histochem. J.* 28, 747–758. doi: 10.1007/bf02272148

Meynert, T. (1884). *Psychiatrie. Klinik der Erkrankungen des Vorderhirns.* Wien: W. Braumüller.

Miyashita, T., Nishimura-Akiyoshi, S., Itohara, S., and Rockland, K. S. (2005). Strong expression of NETRIN-G2 in the monkey claustrum. *Neuroscience* 136, 487–496. doi: 10.1016/j.neuroscience.2005.08.025

Molyneaux, B. J., Arlotta, P., Menezes, J. R., and Macklis, J. D. (2007). Neuronal subtype specification in the cerebral cortex. *Nat. Rev. Neurosci.* 6, 427–437. doi: 10.1038/nrn2151

Mufson, E. J., and Mesulam, M. M. (1982). Insula of the old world monkey. II: afferent cortical input and comments on the claustrum. *J. Comp. Neurol.* 212, 23–37. doi: 10.1002/cne.902120103

Muir, J. L., Everitt, B. J., and Robbins, T. W. (1996). The cerebral cortex of the rat and visual attentional function: dissociable effects of mediofrontal, cingulate, anterior dorsolateral and parietal cortex lesions on a five-choice serial reaction time task. *Cereb. Cortex* 6, 470–481. doi: 10.1093/cercor/6.3.470

Naghavi, H. R., Eriksson, J., Larsson, A., and Nyberg, L. (2007). The claustrum/insula region integrates conceptually related sounds and pictures. *Neurosci. Lett.* 422, 77–80. doi: 10.1016/j.neulet.2007.06.009

Nakashima, M., Uemura, M., Yasui, K., Ozaki, H. S., Tabata, S., and Taen, A. (2000). An anterograde and retrograde tract-tracing study on the projections from the thalamic gustatory area in the rat: distribution of neurons projecting to the insular cortex and amygdaloid complex. *Neurosci. Res.* 36, 297–309. doi: 10.1016/s0168-0102(99)00129-7

Narkiewicz, O. (1964). Degenerations in the claustrum after regional neocortical ablations in the cat. *J. Comp. Neurol.* 123, 335–356. doi: 10.1002/cne.901230304

Narkiewicz, O. (1972). Frontoclaustral interrelations in cats and dogs. *Acta Neurobiol. Exp. (Wars)* 32, 141–150.

Norita, M. (1977). Demonstration of bilateral claustro-cortical connections in the cat with the method of retrograde axonal transport of horseradish peroxidase. *Arch. Histol. Jpn.* 40, 1–10. doi: 10.1679/aohc1950.40.1

Olson, I. R., Gatenby, J. C., and Gore, J. C. (2002). A comparison of bound and unbound audio-visual information processing in the human cerebral cortex. *Brain Res. Cogn. Brain Res.* 14, 129–138. doi: 10.1016/s0926-6410(02)00067-8

Olson, C. R., and Graybiel, A. M. (1980). Sensory maps in the claustrum of the cat. *Nature* 288, 479–481. doi: 10.1038/288479a0

Pasqualetti, M., Ori, M., Castagna, M., Marazziti, D., Cassano, G. B., and Nardi, I. (1999). Distribution and cellular localization of the serotonin type 2C receptor messenger RNA in human brain. *Neuroscience* 92, 601–611. doi: 10.1016/s0306-4522(99)00011-1

Paxinos, G., Kus, L., Ashwell, K. W. S., and Watson, C. R. R. (1999). *Chemoarchitectonic Atlas of the Rat Forebrain.* San Diego: Academic Press.

Paxinos, G., and Watson, C. (1997). *The Rat Brain in Stereotaxic Coordinates.* 3rd Edn. San Diego: Academic Press.

Paxinos, G., and Watson, C. (2007). *The Rat Brain in Stereotaxic Coordinates.* 6th Edn. London, Amsterdam: Elsevier, Academic Press.

Pompeiano, M., Palacios, J. M., and Mengod, G. (1994). Distribution of the serotonin 5-HT2 receptor family mRNAs: comparison between 5-HT2A and 5-HT2C receptors. *Brain Res. Mol. Brain Res.* 23, 163–178. doi: 10.1016/0169-328x(94)90223-2

Puelles, L., Kuwana, E., Puelles, E., Bulfone, A., Shimamura, K., Keleher, J., et al. (2000). Pallial and subpallial derivatives in the embryonic chick and

mouse telencephalon, traced by the expression of the genes Dlx-2, Emx-1, Nkx-2.1, Pax-6 and Tbr-1. *J. Comp. Neurol.* 424, 409–438. doi: 10.1002/1096-9861(20000828)424:3<409::aid-cne3>3.0.co;2-7

Rae, A. S. (1954). The form and structure of the human claustrum. *J. Comp. Neurol.* 100, 15–39. doi: 10.1002/cne.901000103

Rahman, F. E., and Baizer, J. S. (2007). Neurochemically defined cell types in the claustrum of the cat. *Brain Res.* 1159, 94–111. doi: 10.1016/j.brainres.2007.05.011

Real, M. A., Dávila, J. C., and Guirado, S. (2006). Immunohistochemical localization of the vesicular glutamate transporter VGLUT2 in the developing and adult mouse claustrum. *J. Chem. Neuroanat.* 31, 169–177. doi: 10.1016/j.jchemneu.2005.12.002

Remedios, R., Logothetis, N. K., and Kayser, C. (2010). Unimodal responses prevail within the multisensory claustrum. *J. Neurosci.* 30, 12902–12907. doi: 10.1523/JNEUROSCI.2937-10.2010

Reynhout, K., and Baizer, J. S. (1999). Immunoreactivity for calcium-binding proteins in the claustrum of the monkey. *Anat. Embryol. (Berl)* 199, 75–83. doi: 10.1007/s004290050211

Robbins, T. W. (2002). The 5-choice serial reaction time task: behavioural pharmacology and functional neurochemistry. *Psychopharmacology (Berl)* 163, 362–380. doi: 10.1007/s00213-002-1154-7

Rose, M. (1928). Die inselrinde des menschen und der tiere. *J. Psychol. Neurol.* 37, 467–624.

Sanides, D., and Buchholtz, C. S. (1979). Identification of the projection from the visual cortex to the claustrum by anterograde axonal transport in the cat. *Exp. Brain Res.* 34, 197–200. doi: 10.1007/bf00238353

Segundo, J. P., and Machne, X. (1956). Unitary responses to afferent volleys in lenticular nucleus and claustrum. *J. Neurophysiol.* 19, 325–339.

Sherk, H. (1986). "The claustrum and the cerebral cortex," in *Cerebral Cortex*, eds E. G. Jones and A. Peters (Vol. 5), (New York: Plenum Press), 467–499.

Smith, G. E. (1910). *On Some Problems Relating to the Evolution of Brain*. Lancet: Arris and Gale Lectures.

Smith, G. E. (1917). "The central nervous system," in *Cunningham's Text-book of Anatomy*, ed A. Robinson (New York: W. Wood).

Smith, J. B., and Alloway, K. D. (2010). Functional specificity of claustrum connections in the rat: interhemispheric communication between specific parts of motor cortex. *J. Neurosci.* 30, 16832–16844. doi: 10.1523/JNEUROSCI.4438-10.2010

Smythies, J., Edelstein, L., and Ramachandran, V. (2012). Hypotheses relating to the function of the claustrum. *Front. Integr. Neurosci.* 6:53. doi: 10.3389/fnint.2012.00053

Sonntag, C. F., and Woollard, H. H. (1925). A monograph of Orycteropus afer. II. Nervous system, sense organs and hairs. *Proc. Zool. Soc. London* 95, 1185–1235. doi: 10.1111/j.1469-7998.1925.tb07118.x

Spahn, B., and Braak, H. (1985). Percentage of projection neurons and various types of interneurons in the human claustrum. *Acta Anat. (Basel)* 122, 245–248. doi: 10.1159/000146023

Spector, I., Hassmannova, J., and Albe-Fessard, D. (1974). Sensory properties of single neurons of cat's claustrum. *Brain Res.* 66, 39–65. doi: 10.1016/0006-8993(74)90077-8

Squatrito, S., Battaglini, P. P., Galletti, C., and Riva Sanseverino, E. (1980). Projections from the visual cortex to the contralateral claustrum of the cat revealed by an anterograde axonal transport method. *Neurosci. Lett.* 19, 271–275. doi: 10.1016/0304-3940(80)90272-4

Swanson, L. (2004). *Brain Maps: Structure of the Rat Brain.* 3rd Edn. San Diego: Elsevier, Academic Press.

Thompson, R. F., and Shaw, J. A. (1965). Behavioral correlates of evoked activity recorded from association areas of the cerebral cortex. *J. Comp. Physiol. Psychol.* 60, 329–339. doi: 10.1037/h0022556

Valverde, F., Facal-Valverde, M. V., Santacana, M., and Heredia, M. (1989). Development and differentiation of early generated cells of sublayer VIb in the somatosensory cortex of the rat: a correlated Golgi and autoradiographic study. *J. Comp. Neurol.* 290, 118–140. doi: 10.1002/cne.902900108

van der Kooy, D., Koda, L. Y., McGinty, J. F., Gerfen, C. R., and Bloom, F. E. (1984). The organization of projections from the cortex, amygdala and hypothalamus to the nucleus of the solitary tract in rat. *J. Comp. Neurol.* 224, 1–24. doi: 10.1016/0006-8993(78)91125-3

Vertes, R. P. (1992). PHA-L analysis of projections from the supramammillary nucleus in the rat. *J. Comp. Neurol.* 326, 595–622. doi: 10.1002/cne.903260408

Vertes, R. P., and Hoover, W. B. (2008). Projections of the paraventricular and paratenial nuclei of the dorsal midline thalamus in the rat. *J. Comp. Neurol.* 508, 212–237. doi: 10.1002/cne.21679

Watakabe, A., Hirokawa, J., Ichinohe, N., Ohsawa, S., Kaneko, T., Rockland, K. S., et al. (2012). Area-specific substratification of deep layer neurons in the rat cortex. *J. Comp. Neurol.* 520, 3553–3573. doi: 10.1002/cne.23220

Wright, D. E., Seroogy, K. B., Lundgren, K. H., Davis, B. M., and Jennes, L. (1995). Comparative localization of serotonin1A, 1C and 2 receptor subtype mRNAs in rat brain. *J. Comp. Neurol.* 351, 357–73. doi: 10.1002/cne.903510304

Yoshida, K., McCormack, S., España, R. A., Crocker, A., and Scammell, T. E. (2006). Afferents to the orexin neurons of the rat brain. *J. Comp. Neurol.* 494, 845–861. doi: 10.1002/cne.20859

Conflict of Interest Statement: The author declares that the research was conducted in the absence of any commercial or financial relationships that could be construed as a potential conflict of interest.

Received: 06 February 2014; accepted: 17 March 2014; published online: 04 April 2014.
Citation: Mathur BN (2014) The claustrum in review. Front. Syst. Neurosci. ***8****:48. doi: 10.3389/fnsys.2014.00048*
This article was submitted to the journal Frontiers in Systems Neuroscience.

frontiers in
SYSTEMS NEUROSCIENCE

OPINION ARTICLE
published: 18 March 2014
doi: 10.3389/fnsys.2014.00037

Zinc-positive and zinc-negative connections of the claustrum

Kathleen S. Rockland [1,2]*

[1] *Department of Anatomy and Neurobiology, Boston University School Medicine, Boston, MA, USA*
[2] *Cold Spring Harbor Laboratory, Cold Spring Harbor, NY, USA*
**Correspondence: krock@bu.edu*

Edited by:
Brian N. Mathur, University of Maryland School of Medicine, USA

Reviewed by:
Richard H. Dyck, University of Calgary, Canada

Keywords: amygdala, epilepsy, feedback, layer 1, reuniens

Three features often mentioned as characteristic of the claustrum are its widespread connections with cortical areas, the reciprocity of these connections in general, and the origin of cortico-claustral connections from a distinctive subtype of layer 6 pyramidal cells (Sherk, 1986; Katz, 1987; Tanne-Gariepy et al., 2002; Crick and Koch, 2005; Smythies et al., 2012). Another feature, often overlooked, is that a proportion of claustral-cortical neurons use synaptic zinc and that zinc+ terminations are moderately dense in the claustrum. This article will summarize data about zinc and the claustrum and present the case that cortico-claustral neurons might also be zinc-positive (Zn+). I conclude with comments on the likely implications for claustral identity and function.

ZINC-CONTAINING NEURONS

There are several excellent reviews on the importance of synaptic zinc in the central nervous system (Frederickson et al., 2000, 2005; Nakashima and Dyck, 2009; Sensi et al., 2009). In brief, Zn+ neurons are predominantly in the cerebral cortex and amygdala. Zn+ neurons (i.e., those in which zinc is highly concentrated in the synaptic vesicles) are a subset of glutamatergic neurons, exclusive of corticothalamic. The projections between thalamus and cortex are zinc-negative (Zn−). Zinc is considered an activity- and calcium-dependent neuromodulator of excitation and as being important in synaptic plasticity. It interacts with a wide range of zinc-sensitive postsynaptic membrane targets (see Table 1 in Frederickson et al., 2005 and Figure 2 in Sensi et al., 2009). In general, Zn+ neurons have been preferentially associated with limbic projections; and the hippocampal mossy fibers are well-known to have a high concentration of synaptic zinc.

The brainwide distribution of Zn+ neurons is demonstrated by intraperitoneal injection of sodium selenite, which produces a zinc–selenium precipitate that is retrogradely transported from axon terminals to cell bodies of origin (e.g., Brown and Dyck, 2004). Focal intra-cerebral injections of sodium selenite are used to retrogradely label target-specific projection neurons. Terminations are visualized by modifications of the classic Timm stain.

CLAUSTRAL-CORTICAL PROJECTIONS

Zinc–selenium histochemistry reveals a subset of Zn+ neurons in the mouse claustrum (Brown and Dyck, 2004); and focal injections of sodium selenite in different cortical areas in rodent directly demonstrate a subset of Zn+ cortically projecting neurons in the claustrum. These are reported as sparse or moderate for projections, respectively, to visual and barrel cortex, but more abundant for those to frontal and orbital cortical areas (Garrett et al., 1992; Casanovas-Aquilar et al., 1998; Brown and Dyck, 2005). Experiments using standard retrograde tracers report a small proportion of double labeled neurons projecting to two different cortical areas (in rat: Li et al., 1986; in cat: Clasca et al., 1992). Whether these are Zn+ or not is unknown.

The claustrum also sends projections to the amygdala (for monkey: Stefannacci and Amaral, 2000), to parts of the subicular complex (Witter et al., 1988; Zhang et al., 2013), and to nucleus reuniens (for rat: McKenna and Vertes, 2004). There are no data as to the proportion of claustral-amygdala or claustral-hippocampal neurons that might be Zn+; and claustral-thalamic projections can be assumed as Zn−.

Claustral-cortical projections labeled with standard anterograde tracers terminate in layers 1–4 and 6 (Clasca et al., 1992; da Costa et al., 2010). This partially coincides with the pattern of Zn+ terminations, which are elevated in layers 1b, 2, 3, and 5/6, depending on the cortical area. As layer 4 is relatively Zn−, claustral-cortical terminations in this layer can be inferred to originate from a separate subset of Zn− neurons in the claustrum. The proportion of Zn+ terminations may be taken to vary depending on the species and projection system. For claustral-cortical projections, an initial guess might be 25–50% as being Zn+, largely based on the density of Zn+ neurons retrogradely labeled in the claustrum following focal injections of sodium selenite in cortical areas in rodents.

By comparison, cortical feedback projections from monkey temporal cortex have been shown to consist of a mix of Zn+ and Zn− components by cortical injections of sodium selenite. In confirmation, injections of the anterograde tracer BDA in area TE were coupled with a terminal intravenous injection of sodium sulfide to precipitate Zn+ terminations. Subsequent ultrastructural inspection of BDA-labeled terminations in areas targeted by TE neurons (V1, V4, TEO, and the depth of the superior temporal sulcus) revealed about one-third of the synapses as Zn+, except for a higher proportion in V1 (four of five identified synapses;

Ichinohe et al., 2010). As a second comparison, projections from the basolateral amygdala to medial prefrontal cortex were all found to be Zn+ in the monkey (Miyashita et al., 2007), although only 35% of the amygdalo-cortical terminations were Zn+ in rats (Cunningham et al., 2007).

CORTICO-CLAUSTRAL NEURONS

Layer 6 contains a mixed population of pyramidal neurons, of which the four major groups are intrinsically projecting, and extrinsically projecting to the thalamus, to other cortical areas, and to the claustrum (Briggs, 2010; Thomson, 2010). Corticothalamic neurons are Zn−; and feedback cortically projecting neurons in layer 6 are intermixed Zn+ and Zn− (for monkey: Ichinohe et al., 2010). There have been no appropriate injections in the claustrum to determine directly whether any cortico-claustral projecting neurons are Zn+, but this possibility is supported by indirect evidence, as discussed next.

First, as noted above, Zn+ terminations are moderately dense in the claustrum (rat: Perez-Clausell, 1996; Valente et al., 2002; monkey: Figure 1 in Ichinohe and Rockland, 2005a; Figure 10 in Miyashita et al., 2007). Zn+ cortico-claustral neurons are one of three possible sources of the Zn+ terminations in the claustrum. Another is the claustrum itself, since it has both Zn+ neurons (Brown and Dyck, 2004) and widespread intrinsic connections (Smith and Alloway, 2010). The amygdala is a third possible source. Several claustral projecting subnuclei in the amygdala contain Zn+ neurons, demonstrated by intraperitoneal (Brown and Dyck, 2004) or focal injections of sodium selenite in cortical areas (for the rat: Majak et al., 2002; for monkey: Ichinohe and Rockland, 2005b). There are projections from midline thalamus to the claustrum (Vertes et al., 2006), but like almost all thalamic projections (except those from anterior dorsal thalamus to the subiculum), these can be considered as zinc-negative.

A second, indirect line of evidence is the dendritic morphology of pyramidal neurons in layer 6 (Katz, 1987; Ojima et al., 1992; Olsen et al., 2012; and reviewed in Briggs, 2010; Thomson, 2010). Corticothalamic neurons have short, thin apical dendrites typically not extending much above layer 4. At least a subset of cortical feedback projecting neurons also have short, non-tufted apical dendrites (for monkey: Lund et al., 1981; Figure 9 in Rockland, 1994; Berezovskii et al., 2012). Cortico-claustral neurons have nontufted apical dendrites ascending to layer 1 (Katz, 1987). Of these three groups, corticothalamic neurons can be assumed to be Zn−. Cortico-cortical neurons, in monkey, are a mix of Zn+ and Zn−, as noted above. An interesting possibility is that some cortico-claustral neurons, which have a nontufted apical dendrite (even though this appears to ascend more superficially than cortical neurons), are Zn+. The proportion of layer 6 neurons with long apical dendrites (i.e., putative cortico-claustral) is likely to be area and species specific. From intracellular fills, these are reported as unusually abundant—almost 40% of the filled neurons—in layer 6 of rat medial prefrontal cortex, although the projectional identity is unknown (Van Aerde and Feldmeyer, 2013).

If cortico-claustral neurons, or a subset of these, are Zn+, we can further speculate whether individual neurons might send collaterals to cortical areas and the claustrum. There are so far no relevant data for cortico-claustal neurons, either from double retrograde tracers or intercellular labeling; and this possibility waits for future investigations.

What can we conclude about the claustrum as part of a Zn+ associational system? One clear point is that claustral-cortical neurons are a mixed population, of Zn+ and Zn− neurons, and are presumably functionally mixed as well. Less clear is the specific role or roles of zinc in the claustrum. In general, synaptic Zn is associated with activity-dependent plasticity (reviewed in Frederickson et al., 2005; Nakashima and Dyck, 2009). Consistent with plasticity effects, a sizeable proportion of claustral-cortical synapses are perforated (∼33% in cat visual cortex; da Costa et al., 2010). By comparison, 27% of amygdalo-cortical terminations (putatively Zn+ but neurochemically uncharacterized) were identified as perforated in temporal cortex, 39% in visual cortex (for monkey: Freese and Amaral, 2006), and ∼25% of those in orbitofrontal (identified as Zn+ for monkey: Miyashita et al., 2007). Perforated synapses are specifically implicated in memory-related plasticity (Calverley and Jones, 1990; Hara et al., 2012).

Alterations in the regulation of zinc release, either as protective or harmful, have been associated with epilepsy, among other neuropathological disorders (reviewed in Paoletti et al., 2009). The well-established susceptibility of the claustrum to kindling and its implication with generalized seizures may thus be related to the presence of zinc in intrinsic claustro-claustral connections and/or in the connections between the claustrum and amygdala or the claustrum and cortex. A recent study, concerned with the role of zinc homeostasis in epileptogenicity, found that epilepsy-resistant rat strains had significantly lower levels of synaptic zinc as compared to epilepsy-prone strains (Flynn et al., 2007).

CLAUSTRUM AS CORTICAL?

The identification of the claustrum, as cortical or striatal, has generated considerable discussion. On developmental grounds, the claustrum has been considered (1) as a derivative of the insula, with a pallial origin; (2) as derived from the ganglionic eminence along with the basal ganglia; or (3) as having both a pallial and subpallial derivation (reviewed in Inda et al., 2009; Pirone et al., 2012). Gene expression studies show the claustrum as having pallial markers, like the amygdala but unlike striatal structures (Miyashita et al., 2005; Pirone et al., 2012); and the claustrum is consistently reported as expressing genes in common with cortical areas (Miyashita et al., 2005; Mathur et al., 2009; Watakabe et al., under review). From a somewhat different perspective, chandelier cells, a specific type of cortical interneuron, are found in both the claustrum and amygdala, but not striatum (Inda et al., 2009). From the perspective of zinc, both the claustrum and basal ganglia have moderate levels of Zn+ terminations, at least in part of a cortical origin; but Zn+ neurons do not occur in the striatum (Frederickson et al., 2000). The existence of Zn+ neurons in the claustrum is consistent with a cortical association, but is a feature shared as well with the amygdala.

CLAUSTRAL FUNCTION?

One of the ideas consistently put forth for claustral function is that it is concerned with multisensory integration (Sherk, 1986; Edelstein and Denaro, 2004; Crick and Koch, 2005). This is consistent with its pattern of widespread connectivity, although physiological recording in alert monkeys have identified distinct claustral zones comprised of unimodal, not multimodal, neurons associated with the auditory and visual modalities (Remedios et al., 2010).

Reciprocal and widespread connectivity architecture, often seen as indicating an integrative role (Tanne-Gariepy et al., 2002; Crick and Koch, 2005), is not anatomically unique to the claustrum, but applies to other structures as well; for example, the amygdala and midline thalamus. Thus, it is not yet clear that this connectivity architecture in itself is strong support for a distinctively integrative role. Continuing work in rat, in fact, has concluded that while the efferent connectivity of the claustrum might well subserve interhemispheric coordination of motor and somatosensory whisker representations, its role as an integrator of somesthetic and motor information is less likely, since there are no projections from the somatosensory whisker representation to the claustrum (Smith et al., 2012).

Worth noting is that claustral-cortical projections terminate in both layers 1 and 4, presumably from separate subpopulations, given that Zn+ terminations are dense in layer 1 and very sparse in layer 4. Layer 1 and layer 4 terminations are also spatially dissociable to some extent in that those in layer 1 are typically widely divergent, in contrast with the more topographically organized termination systems in layer 4. Amygdalo-cortical projections to layer 1 are widely divergent (Freese and Amaral, 2006), as are thalamo-cortical (Rubio-Garrido et al., 2009), and cortical feedback (Rockland, 1994). Widespread terminations in layer 1 might contribute to the generation of synchronized oscillations, another role associated with the claustrum (Smythies et al., 2012), although more data are needed specifically concerning neurons postsynaptic to claustral inputs. In particular, is there a neuron-to-neuron reciprocity with claustral projections targeting cortico-claustral neurons?

The architecture that emerges is not so much structure-to-structure reciprocity, as a wider constellation of closely interconnected networks; namely, claustral-cortex-amygdala (Zn+ or mixed), claustral-hippocampus-amygdala (Zn+ or mixed), claustral-reuniens-cortex (Zn−), possibly hippocampus-reuniens-claustrum (Zn−), among others.

SUMMARY

The importance of synaptic zinc for claustral connections has been largely overlooked, despite abundant evidence of Zn+ inputs and outputs. Synaptic zinc has been associated with activity-driven plasticity; and one might propose that the functional role of zinc for the claustrum is "similar" to that of zinc as used by the basolateral amygdala and feedback cortical connections from layer 6. More immediately, a practical consequence is that the wide range of manipulations targeting Zn+ terminations and Zn+ neurons (reviewed in Nakashima and Dyck, 2009) offer new tools to probe claustral organization and function. Potential approaches might include comparisons across species and mouse lines, across developmental stages, or in different environmental or pathological conditions.

REFERENCES

Berezovskii, V., Born, R. T., and Nassi, J. J. (2012). Detailed morphology of feedforward and feedback neurons in area V2 of primate visual cortex studied with genetically modified rabies virus. *Soc. Neurosci Abstr.* 464.13.

Briggs, F. (2010). Organizing principles of cortical layer 6. *Front. Neural Circuits* 4:3. doi: 10.3389/neuro.04.003.2010

Brown, C. E., and Dyck, R. H. (2004). Distribution of zincergic neurons in the mouse forebrain. *J. Comp. Neurol.* 479, 156–167. doi: 10.1002/cne.20308

Brown, C. E., and Dyck, R. H. (2005). Retrograde tracing of the subset of afferent connections in mouse barrel cortex provided by zincergic neurons. *J. Comp. Neurol.* 486, 48–60. doi: 10.1002/cne.20522

Calverley, R. K., and Jones, D. G. (1990). Contributions of dendritic spines and perforated synapses to synaptic plasticity. *Brain Res. Brain Res. Rev.* 15, 215–249. doi: 10.1016/0165-0173(90)90002-6

Casanovas-Aquilar, C., Reblet, C., Perez-Clausell, J., and Bueno-Lopez, J. L. (1998). Zinc-rich afferents to the rat neocortex: projections to the visual cortex traced with intracerebral selenite injections. *J. Chem. Neuroanat.* 15, 97–109. doi: 10.1016/S0891-0618(98)00035-0

Clasca, F., Avendano, C., Roman-Guindo, A., Llamas, A., and Reinoso-Suarez, F. (1992). Innervation from the claustrum of the frontal association and motor areas: axonal transport studies in the cat. *J. Comp. Neurol.* 326, 402–422. doi: 10.1002/cne.903260307

Crick, F., and Koch, C. (2005). What is the function of the claustrum? *Philos. Trans. R. Soc. Lond. B Biol. Sci.* 360, 1271–1279. doi: 10.1098/rstb.2005.1661

Cunningham, M. G., Ames, H. M., Christensen, M. K., and Sorensen, J. C. (2007). Zincergic innervation of medial prefrontal cortex by basolateral projection neurons. *Neuroreport* 18, 531–535. doi: 10.1097/WNR.0b013e328091c212

da Costa, N. M., Fursinger, D., and Martin, K. A. C. (2010). The synaptic organization of the claustral projection to the cat's visual cortex. *J. Neurosci.* 30, 13166–13170. doi: 10.1523/JNEUROSCI.3122-10.2010

Edelstein, L. R., and Denaro, F. J. (2004). The claustrum: a historical review of its anatomy, physiology, cytochemistry and functional significance. *Cell. Mol. Biol. (Noisy-le-grand)* 50, 675–702.

Flynn, C., Brown, C. E., Calasso, S. L., McIntyre, D. C., Campbell Teskey, G., and Dyck, R. H. (2007). Zinergic innervation of the forebrain distinguishes epilepsy-prone from epilepsy-resistant rat strains. *Neuroscience* 144, 1409–1414. doi: 10.1016/j.neuroscience.2006.11.005

Frederickson, C. J., Koh, J.-Y., and Bush, A. I. (2005). The neurobiology of zinc in health and disease. *Nat. Rev. Neurosci.* 6, 449–462. doi: 10.1038/nrn1671

Frederickson, C. J., Suh, S. W., Silva, D., Frederickson, C. J., and Thompson, R. B. (2000). Importance of zinc in the central nervous system: the zinc-containing neuron. *J. Nutr.* 130, 1471S–1483S.

Freese, J. I., and Amaral, D. G. (2006). Synaptic organization of projections from the amygdala to visual cortex areas TE and V1 in the macaque monkey. *J. Comp. Neurol.* 496, 655–667. doi: 10.1002/cne.20945

Garrett, B., Sorensen, J. C., and Slomianka, L. (1992). Fluoro-gold tracing of zinc-containing afferent connections in the mouse visual cortices. *Anat. Embryol.* 156, 451–459.

Hara, Y., Rapp, P. R., and Morrison, J. H. (2012). Neuronal and morphological bases of cognitive decline in aged rhesus monkeys. *Age* 34, 1051–1073. doi: 10.1007/s11357-011-9278-5

Ichinohe, N., Matsushita, A., Ohta, K., and Rockland, K. S. (2010). Pathway-specific utilization of synaptic zinc in the macaque ventral visual cortical areas. *Cereb. Cortex* 20, 2818–2831. doi: 10.1093/cercor/bhq028

Ichinohe, N., and Rockland, K. S. (2005a). Distribution of synaptic zinc in the macaque amygdala. *J. Comp. Neurol.* 489, 135–147. doi: 10.1002/cne.20632

Ichinohe, N., and Rockland, K. S. (2005b). Zinc-enriched amygdalo- and hippocampo-cortical connections to the inferotemporal cortices in macaque monkey. *Neurosci. Res.* 53, 57–68. doi: 10.1016/j.neures.2005.06.002

Inda, M. C., DeFelipe, J., and Munoz, A. (2009). Morphology and distribution of chandelier cell axon terminals in the mouse cerebral cortex and claustroamydaloid complex. *Cereb. Cortex* 19, 1941–1954. doi: 10.1093/cercor/bhn057

Katz, L. C. (1987). Local circuitry of identified projection neurons in cat visual cortex brain slices. *J. Neurosci.* 7, 1233–1249.

Li, Z. K., Takada, M., and Hattori, T. (1986). Topographic organization and collateralization of claustrocortical projections in the rat. *Brain Res. Bull.* 17, 529–532. doi: 10.1016/0361-9230(86)90220-0

Lund, J. S., Hendrickson, A. E., Ogren, M. P., and Tobin, E. A. (1981). Anatomical organization of primate cortex area VII. *J. Comp. Neurol.* 202, 19–45. doi: 10.1002/cne.902020104

Majak, K., Pikkarainen, M., Kemppainen, S., Jolkkonen, E., and Pitkanen, A. (2002). Projections from the amydaloid complex to the claustrum and the endopiriform nucleus: a *Phaseolus vulgaris* leucoagglutinin study in the rat. *J. Comp. Neurol.* 451, 236–246. doi: 10.1002/cne.10346

Mathur, B. N., Caprioli, R. M., and Deutsch, A. Y. (2009). Proteomic analysis illuminates a novel structural definition of the claustrum and insula. *Cereb. Cortex* 19, 2372–2379. doi: 10.1093/cercor/bhn253

McKenna, J. T., and Vertes, R. P. (2004). Afferent projections to nucleus reuniens of the thalamus. *J. Comp. Neurol.* 480, 115–142. doi: 10.1002/cne.20342

Miyashita, T., Ichinohe, N., and Rockland, K. S. (2007). Differential modes of termination of amygdalothalamic and amygdalocortical projections in the monkey. *J. Comp. Neurol.* 502, 309–324. doi: 10.1002/cne.21304

Miyashita, T., Nishimura-Akiyoshi, S., Itohara, S., and Rockland, K. S. (2005). Strong expression of *NETRIN-G2* in the monkey claustrum. *Neuroscience* 136, 487–496. doi: 10.1016/j.neuroscience.2005.08.025

Nakashima, A. S., and Dyck, R. H. (2009). Zinc and cortical plasticity. *Brain Res. Rev.* 59, 347–373. doi: 10.1016/j.brainresrev.2008.10.003

Ojima, H., Honda, C. N., and Jones, E. G. (1992). Characteristics of intracellularly injected infragranular pyramidal neurons in cat primary auditory cortex. *Cereb. Cortex* 2, 197–216. doi: 10.1093/cercor/2.3.197

Olsen, S. R., Bortone, D. S., Adesnik, H., and Scanziani, M. (2012). Gain control by layer six in cortical circuits of vision. *Nature* 483, 47–52. doi: 10.1038/nature10835

Paoletti, P., Vergnano, A. M., Barbour, B., and Casado, M. (2009). Zinc at glutamatergic synapses. *Neuroscience* 158, 126–136. doi: 10.1016/j.neuroscience.2008.01.061

Perez-Clausell, J. (1996). Distribution of terminal fields stained for zinc in the neocortex of the rat. *J. Chem. Neuroanat.* 11, 99–111. doi: 10.1016/0891-0618(96)00131-7

Pirone, A., Cozzi, B., Edelstein, L., Peruffo, A., Lenzi, C., Quilici, F., et al. (2012). Topography of Gng2- and Netrin G2-expression suggests an insular origin of the human claustrum. *PLoS ONE* 7:e44745. doi: 10.1371/journal.pone.0044745

Remedios, R., Logothetis, N. K., and Kayser, C. (2010). Unimodal responses prevail within the multisensory claustrum. *J. Neurosci.* 30, 12902–12907. doi: 10.1523/JNEUROSCI.2937-10.2010

Rockland, K. S. (1994). "The organization of feedback connections from area V2 (18) to V1 (17)," in *Cerebral Cortex*,Vol. 10, eds A. Peters and K. Rockland (New York, NY: Plenum Press), 261–299.

Rubio-Garrido, P., Perez-de-Manzo, F., Porrero, C., Galazo, M. J., and Clasca, F. (2009). Thalamic input to distal apical dendrites in neocortical layer 1 is massive and highly convergent. *Cereb. Cortex* 19, 2380–2395. doi: 10.1093/cercor/bhn259

Sensi, S. L., Paoletti, P., Bush, A. I., and Sekler, I. (2009). Zinc in the physiology and pathology of the CNS. *Nat. Rev. Neurosci.* 10, 780–791. doi: 10.1038/nrn2734

Sherk, H. (1986). "The claustrum and the cerebral cortex," in *Cerebral Cortex*, Vol. 5, eds E. G. Jones and A. Peters (New York, NY: Plenum Press), 467–499.

Smith, J. B., and Alloway, K. D. (2010). Functional specificity of claustrum connections in the rat: interhemispheric communication between specific parts of motor cortex. *J. Neurosci.* 30, 16832–16844. doi: 10.1523/JNEUROSCI.4438-10.2010

Smith, J. B., Radhakrishnan, H., and Alloway, K. D. (2012). Rat claustrum coordinates but does not integrate somatosensory and motor cortical information. *J. Neurosci.* 32, 8583–8588. doi: 10.1523/JNEUROSCI.1524-12.2012

Smythies, J., Edelstein, L., and Ramachandran, V. (2012). Hypotheses relating to the function of the claustrum. *Front. Integr. Neurosci.* 6:53. doi: 10.3389/fnint.2012.00053

Stefannacci, L., and Amaral, D. G. (2000). Topographic organization of cortical inputs to the lateral nucleus of the macaque monkey amygdala: a retrograde tracer study. *J. Comp. Neurol.* 421, 52–79. doi: 10.1002/(SICI)1096-9861(20000522)421:1<52::AID-CNE4>3.0.CO;2-O

Tanne-Gariepy, J., Boussaoud, D., and Rouiller, E. M. (2002). Projections of the claustrum to the primary motor, premotor, and prefrontal cortices in the macaque monkey. *J. Comp. Neurol.* 454, 140–157. doi: 10.1002/cne.10425

Thomson, A. M. (2010). Neocortical layer 6, a review. *Front. Neuroanat.* 4:13. doi: 10.3389/fnana.2010.00013

Valente, T., Auladell, C., and Perez-Clausell, J. (2002). Postnatal development of zinc-rich terminal fields in the brain of the rat. *Exp. Neurol.* 174, 215–229. doi: 10.1006/exnr.2002.7876

Van Aerde, K. I., and Feldmeyer, D. (2013). Morphological and physiological characterization of pyramidal neuron subtypes in rat medial prefrontal cortex. *Cereb. Cortex.* doi: 10.1093/cercor/bht278. [Epub ahead of print].

Vertes, R. P., Hoover, W. B., Do Valle, A. C., Sherman, A., and Rodriguez, J. J. (2006). Efferent projections of reuniens and rhomdoid nuclei of the thalamus in the rat. *J. Comp. Neurol.* 499, 768–796. doi: 10.1002/cne.21135

Witter, M. P., Room, P., Groenewegen, H. J., and Lohman, A. H. (1988). Reciprocal connections of the insular and piriform claustrum with limbic cortex: an anatomical study in the cat. *Neuroscience* 24, 519–539. doi: 10.1016/0306-4522(88)90347-8

Zhang, S.-J., Ye, J., Miao, C., Tsao, A., Cerniauskas, I., Ledergerber, D., et al. (2013). Optogenetic dissection of entorhinal-hippocampal functional connectivity. *Science* 340, 44–58. doi: 10.1126/science.1232627

Received: 29 January 2014; accepted: 28 February 2014; published online: 18 March 2014.

Citation: Rockland KS (2014) Zinc-positive and zinc-negative connections of the claustrum. Front. Syst. Neurosci. ***8****:37. doi: 10.3389/fnsys.2014.00037*

This article was submitted to the journal Frontiers in Systems Neuroscience.

frontiers in
SYSTEMS NEUROSCIENCE

ORIGINAL RESEARCH ARTICLE
published: 23 May 2014
doi: 10.3389/fnsys.2014.00098

Characterization of claustral neurons by comparative gene expression profiling and dye-injection analyses

Akiya Watakabe[1,2]*, Sonoko Ohsawa[1], Noritaka Ichinohe[3], Kathleen S. Rockland[4] and Tetsuo Yamamori[1,2]

[1] *Division of Brain Biology, National Institute for Basic Biology, Okazaki, Japan*
[2] *Department of Basic Biology, The Graduate University for Advanced Studies (Sokendai), Hayama, Japan*
[3] *Department of Ultrastructural Research, National Center of Neurology and Psychiatry, National Institute of Neuroscience, Kodaira, Japan*
[4] *Department of Anatomy and Neurobiology, Boston University School of Medicine, Boston, MA, USA*

Edited by:
Brian N. Mathur, University of Maryland School of Medicine, USA

Reviewed by:
Robert N. S. Sachdev, Yale University, USA
Charles R. Watson, Curtin University, Australia; Prince of Wales Medical Research Institute, Australia

****Correspondence:***
Akiya Watakabe, Division of Brain Biology, National Institute for Basic Biology, Nishigonaka 38, Myodaiji, Okazaki, 444-8585 Aichi, Japan
e-mail: watakabe@nibb.ac.jp

The identity of the claustrum as a part of cerebral cortex, and in particular of the adjacent insular cortex, has been investigated by connectivity features and patterns of gene expression. In the present paper, we mapped the cortical and claustral expression of several cortical genes in rodent and macaque monkey brains (*nurr1, latexin, cux2*, and *netrinG2*) to further assess shared features between cortex and claustrum. In mice, these genes were densely expressed in the claustrum, but very sparsely in the cortex and not present in the striatum. To test whether the cortical vs. claustral cell types can be distinguished by co-expression of these genes, we performed a panel of double ISH in mouse and macaque brain. *NetrinG2* and *nurr1* genes were co-expressed across entire cortex and claustrum, but *cux2* and *nurr1* were co-expressed only in the insular cortex and claustrum. *Latexin* was expressed, in the macaque, only in the claustrum. The *nurr1*$^+$ claustral neurons expressed *VGluT1*, a marker for cortical glutamatergic cells and send cortical projections. Taken together, our data suggest a partial commonality between claustral neurons and a subtype of cortical neurons in the monkey brain. Moreover, in the embryonic (E110) macaque brain, many *nurr1*$^+$ neurons were scattered in the white matter between the claustrum and the insular cortex, possibly representing their migratory history. In a second set of experiments, we injected Lucifer Yellow intracellularly in mouse and rat slices to investigate whether dendrites of insular and claustral neurons can cross the border of the two brain regions. Dendrites of claustral neurons did not invade the overlying insular territory. In summary, gene expression profile of the claustrum is similar to that of the neocortex, in both rodent and macaque brains, but with modifications in density of expression and cellular co-localization of specific genes.

Keywords: non-human-primate, layer 6, neocortex, migration, ctgf, Gng2, Nr4a2

INTRODUCTION

Historically, there have been long debates about the identity of the claustrum as belonging with cortex or basal ganglia (see Edelstein and Denaro, 2004; Miyashita et al., 2005; Pirone et al., 2012). Classic morphological studies, for example, have shown that the most common cell type in the claustrum is a type I cell with spiny dendrites and with axon projecting at a distance, as well as with local collaterals (summarized in Crick and Koch, 2005). Owing to rapid advances in molecular data, we now have several molecular markers that can help to clarify the developmental and evolutionary identity of the main claustral neuron subtypes. For example, Mathur and coworkers searched for claustral molecular markers by proteomic approach (Mathur et al., 2009). Of particular note, in this paper, are two genes, latexin, a carboxypeptidase inhibitor (Arimatsu et al., 1992), and nurr1, a nuclear receptor subtype of transcription factor. Both these genes exhibit a strikingly similar expression pattern in the rodent brain; namely, continuous with dense expression in the claustrum and endopiriform nucleus, they are expressed in layer 6 of lateral neocortex (e.g., S2). Despite sparse expression in the neocortex, these two genes are co-expressed in the same cells (nurr 1 has additional expression in layer 6b), and these cells are associated with cortical projections (Arimatsu et al., 2003; Bai et al., 2004; Watakabe et al., 2007). Given the shared features of gene expression and extrinsic connectivity, the possibility arises that Latexin$^+$/nurr1$^+$ neurons in the cortical deep layers and the claustrum may be categorized as the same subclass of neurons.

To examine the evolutionarily conserved expression of these genes, we previously performed ISH analyses in the macaque brain (Watakabe et al., 2007; Watakabe, 2009). By this search, we found that nurr1$^+$ neurons are present in both the claustrum and cortex in the macaque brain, like in the rodent. However, as opposed to lateral-restricted expression in the rodent brain, nurr1 mRNA was expressed in layer 6 across the entire neocortex in macaques, even while latexin mRNA was not detected in the neocortical regions in this species. The differential gene expression in rodent and macaque led us to further

investigations to clarify the evolutionary fingerprint of the claustral neurons.

In this paper, we addressed the question of whether the claustrum is more appropriately viewed as cortical or basal ganglial by two approaches. First, we selected additional molecular markers that are enriched in the claustrum in either rodents or macaques with the intention of extending the comparison of cortical and claustral gene expression phenotypes in these two species: Cux2 is a transcription factor that specifies upper layer neuron fate (Nieto et al., 2004; Cubelos et al., 2010; Franco et al., 2012). It is, however, also expressed in the deep layers of the lateral cortex of rodents, where it exhibits a "latexin-like" expression pattern. NetrinG2 is an axon guidance molecule implicated in synapse specification (Nishimura-Akiyoshi et al., 2007). Netrin G2 mRNA in monkeys is expressed in layer 6 of the insular cortex and claustrum (Miyashita et al., 2005).

We aimed to clarify by double ISH whether these genes exhibit similar distribution patterns as that of nurr1 in the two species. Whether they are co-expressed outside claustrum would be a good measure to understand the significance of their expression in both cortex and claustrum. In addition, we reexamined the latexin mRNA expression in the insular/claustral regions of the macaque brain. We also examined the expression of the nurr1 gene in the embryonic monkey and postnatal mouse cortex to see if we could differentiate cortical and claustral neurons in the earlier developmental time point.

As a second approach, we examined the morphology of claustral neurons to ascertain whether their dendrites extend beyond the insular/claustral border in rodents. If the claustral neurons exhibit long dendrites that cross into insular cortex, this could be taken as strong support for a cortical identity.

MATERIALS AND METHODS

Tracer injection into the adult macaque monkey was performed in RIKEN Institute in accordance with the protocol approved by the Experimental Animal Committee of the RIKEN Institute, which was also concordant with the National Institutes of Health Guide for the Care and Use of Laboratory Animals (NIH Publications No. 80-23), revised 1996. Adult macaque monkey brain sections for ISH were obtained from the samples that were used in a previous study (Watakabe et al., 2007). Embryonic macaque monkey brain was obtained from Tsukuba Primate Research Center, National Institute of Infectious Diseases. Tracer injection into rat brain and perfusion of mice and rats for ISH and Lucifer Yellow injection followed the animal care guidelines of the National Institute for Basic Biology and National Institute for Physiological Sciences, Japan, and the National Institutes of Health, USA.

IN SITU HYBRIDIZATION (ISH)

Coronal sections were cut at 40 μm thickness for single-color ISH, 15–20 μm for double ISH, and 15–20 μm for tracer-ISH using a freezing microtome. The detailed description of ISH method can be found in a previous paper (Watakabe et al., 2010) or on the web (http://www.nibb.ac.jp/brish/). The FastBlue injection and the subsequent ISH were performed as previously (Watakabe et al., 2007). The FluoroGold injection and the following ISH was performed as previously (Watakabe et al., 2012).

The ISH probes for the mouse and monkey nurr1 and VGluT1 gene have been described previously (Watakabe et al., 2007). To clone cDNA fragments of the cux2, netrinG2, and latexin genes, PCR was performed on the mouse and monkey cDNAs using the following primer sets. For the cux2 gene, 5′-TGGAGTGGGA GTTCTGAAAG-3′ and 5′-GGAAACTTCCTGGGTTGTGC-3′; for the netrinG2 gene, 5′-ATGCCGAAGGCCTCCATGCA-3′, and 5′-CTGTCACAATTTGAGAGTCTGC-3′. For the latexin gene, 5′-TTGGTGGCACAGAACTACATCA-3′ and 5′-GTGACA CTTTGGGATTATTTGG-3′.

LUCIFER YELLOW INJECTION

To investigate dendritic morphology, Lucifer Yellow injection was performed essentially as described previously (Oga et al., 2013). Briefly, 11-week old male BL6 mice (∼30 g) or 7-week old male Wistar rats (∼150 g) were perfused with 30 and 150 ml of 4% paraformaldehyde/0.1 M phosphate buffer, at the rate of 1 or 10 ml/min for mice and rats, respectively. The fixed brain was excised and sliced at 200 μm, in the coronal plane, using a vibratome. After counterstaining with 1 μg/ml DAPI, Lucifer Yellow was injected into individual cells under the visual guidance of ultraviolet illumination. In the low-power view of the dark field image, the insular/claustral regions appeared as a dark column next to the rhinal fissure, which itself was sandwiched between the brighter neocortex and piriform cortices. The injections were targeted from the posterior side of the slices.

To identify the precise border between the claustrum and the insular cortex, and to enhance the fluorescent signals of the Lucifer Yellow, the injected slices were processed for immunostaining using the biotinylated rabbit antibody to Lucifer Yellow (Invitrogen, A5751) and the mouse monoclonal antibody to latexin (Arimatsu et al., 1992, 1:500) or parvalbumin (Swant235; 1:1000) in 2% bovine serum albumin, 1% Triton X-100, 0.1% sodium azide, and 5% sucrose in 0.1 M phosphate buffer for 5–7 days at room temperature, followed by detection with streptavidin-Alexa488 and Cy3-conjugated anti-mouse antibody.

DATA ACQUISITION AND PROCESSING

The fluorescent images were captured by an Olympus DP71 digital camera attached to a BX51 microscope (Olympus). The confocal images were taken by a Nikon confocal laser microscope system A1. Maximum intensity projection images for the confocal data were created by NIS-Elements imaging software (Nikon). All the images were processed by Adobe photoshop for proper contrast for presentation. The dendritic morphologies of the Lucifer Yellow injected cells were traced using Imaris FilamentTracer (Bitplain AG, Zurich, Switzerland). To examine the polarity of dendrite extensions, the horizontal and vertical axes were determined, using the low-power image (10×), with the external capsule horizontal below the claustrum and the insula above the claustrum. The tips of the dendrites and the cell body of the targeted cells were marked and their X–Y positions within the image were measured using ImageJ (http://imagej.nih.gov/ij/). The distance between the "Top," "Bottom," "Right," and "Left"

borders and the center of the cell body was calculated based on these values.

RESULTS

cux2 AND netrinG2 mRNAs ARE EXPRESSED IN THE nurr1$^+$ NEURONS IN THE MOUSE CORTEX AND CLAUSTRUM

To clarify whether the cux2 and netrin G2 genes are expressed in the same cell populations that express latexin and nurr1, we first performed double ISH using these gene markers in the mouse cortex and later in the macaque brain.

Figure 1A shows the typical upper layer (layers 2–4) expression of cux2 mRNA, together with latexin-like expression in the lateral cortex of mice. By double ISH, we found that the cux2 and nurr1 genes are densely expressed in the claustrum and co-expressed, as expected from such high density of expression (**Figure 1B**). In the adjacent insular cortex, they exhibited scattered pattern, but still mostly co-expressed in layers 5–6 (**Figures 1C–E**). The high coincidence of expression even in such a scattered pattern strongly suggests that the two genes are expressed in a cell-type specific fashion. The co-expression was not observed in layer 6b, where we observed nurr1 mRNA-single positive cells. This subpopulation is considered to correspond to the latexin$^-$/CTGF$^+$ subpopulation of nurr1$^+$ cells (Arimatsu et al., 2003; Watakabe et al., 2007). More posteriorly, both cux2 and nurr1 mRNA expression were observed in layer 6 of S2 (**Figures 1F–H**) and this was precisely co-localized (**Figures 1I–O**).

We next examined the expression pattern of the netrinG2 gene in the mouse brain. As **Figure 2A** shows, the netrinG2 gene exhibited a latexin-like pattern in the adult mouse cortex. Importantly, double ISH demonstrated that netrinG2 and nurr1 mRNAs are exactly co-localized in the claustrum and in the deep layer neurons in the adjacent cortical areas (**Figures 2A–H**). Like latexin, the netrinG2 gene was not expressed in layer 6b. Other than that, we observed few neurons that expressed netrinG2 mRNA but not nurr1 mRNA (**Figures 2F–H**, arrows). We conclude that latexin, nurr1, cux2, and netrinG2 gene are all expressed in the same neuronal population that is enriched both in the claustrum and in layer 6 and some in layer 5 of the mouse lateral cortical areas.

EXPRESSION PROFILING OF MONKEY CLAUSTRUM AND INSULAR CORTEX FOR THE cux2, netrinG2, latexin, nurr1, AND VGluT1 GENES

If the cell-type specific expressions of latexin, nurr1, cux2, and netrinG2 genes have functional importance, we might expect their expression patterns to be conserved across species. To test this, we examined the expression of these genes in the monkey claustrum and the adjacent insular cortex. We first examined whether cux2 and nurr1 mRNAs are co-expressed in the monkey cortex. **Figure 3** shows double ISH of cux2 and nurr1 mRNAs in the monkey insular cortex and the claustrum. The double ISH demonstrated that cux2 mRNA is co-expressed with nurr1 mRNA in exactly the same cells, both in layer 6 and claustrum (**Figures 3A–I**); but we observed some nurr1$^+$ neurons in the lower half of layer 6 that do not co-express cux2 mRNA (compare **Figures 3B,E,H**). This cux2$^-$/nurr1$^+$ subpopulation is considered to correspond to the CTGF$^+$/nurr1$^+$ population that we previously described in monkeys (Watakabe et al., 2007). In addition, cux2 mRNA was also expressed in the upper layers, which is consistent with the mouse and human data (Nieto et al., 2004; Arion et al., 2007). Intriguingly, unlike nurr1 mRNA, cux2 mRNA was not expressed in layer 6 neurons of all areas. In area TE, for example, cux2 mRNA expression was restricted to the upper layers (**Figures 3J,K**), suggesting further differentiation of nurr1-mRNA expressing cortical neurons.

In a previous study, the netrinG2 gene was reported to be expressed in the claustrum and layer 6 neurons of the insular cortex (Miyashita et al., 2005). As shown in **Figures 4A–H**, we found by double ISH that the netrinG2 gene is co-expressed with the nurr1 gene in layer 6 of the insular cortex as well as in the claustrum. Like cux2 gene, we observed nurr1mRNA-positive cells in layer 6b that do not express netrinG2 mRNA. The expression of netrinG2 and nurr1 mRNAs in the insular cortex, however, generally coincided in limited subpopulation. The coexpression of netrinG2 and nurr1 genes were observed in all the areas we examined including, frontal, motor, somatosensory, temporal, and visual areas (data not shown).

We have examined the latexin mRNA expression in the monkey cortex. As shown in **Figures 4J–L**, latexin mRNA was not expressed in the insular cortex. However, we found it to be expressed in the claustrum where it co-localized with nurr1 mRNA. The expression of latexin mRNA was somewhat heterogeneous and some claustral nurr1 mRNA-positieve cells expressed only low levels of latexin mRNA (see the magnified images indicated by the arrows in **Figures 4J–L**).

In the adult rodent brain, claustral neurons are reported to express vesicle glutamate transporter 2 (VGluT2) mRNA (Fremeau et al., 2001; Hur and Zaborszky, 2005). However, we detected only low level of VGluT2 mRNA in the monkey claustrum in comparison to that in the thalamus (data not shown). So, we tested the expression of VGluT1 mRNA, which has been used as a marker for excitatory glutamatergic neurons of the cerebral cortex (Komatsu et al., 2005). As shown in **Figures 4M–P**, VGluT1 mRNA was expressed in the insular cortex and claustrum of the monkey brain. In the claustrum, most but not all of the VGluT1mRNA-positive neurons co-expressed nurr1 mRNA. VGluT1 mRNA-positive/nurr1 mRNA-negative cells were present in the white matter that surround the claustrum (**Figure 4M**). We conclude that claustral expression of latexin, nurr1, cux2, and netrinG2 genes is conserved across mice and monkeys, whereas cortical expression patterns are modified in monkeys.

CLAUSTRAL nurr1 mRNA-POSITIVE NEURONS HAVE CORTICAL PROJECTIONS

It is well established that claustral cells have widespread cortical projections (LeVay and Sherk, 1981; Carey and Neal, 1985; Tanne-Gariepy et al., 2002). To directly test whether such projections originate from the nurr1$^+$ populations, we carried out tracer-ISH experiments. FastBlue was injected into areas V4 and 7a of a monkey to produce retrogradely labeled neurons. As shown in **Figures 5B–D**, all the FastBlue-positive cells expressed nurr1 mRNA in the claustrum. We injected FluoroGold into V1 in a rat and found retrograde labeling in the claustrum (**Figure 5E**). The FluoroGold-positive cells in the claustrum expressed nurr1 mRNA (**Figures 5E–H**).

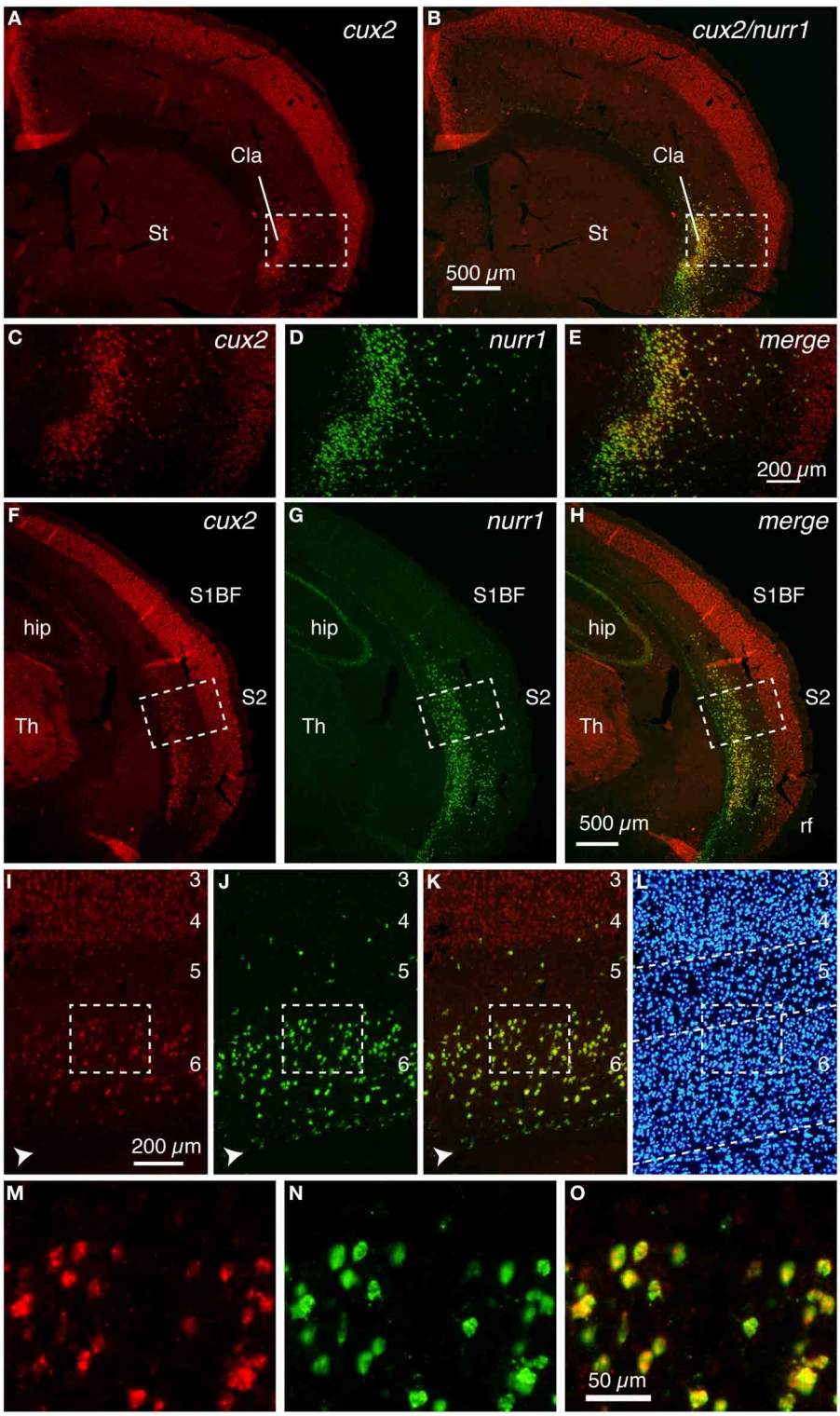

FIGURE 1 | Colocalization of cux2 and nurr1 mRNAs in the claustrum and cortical deep layer of the mouse brain. DIG-labeled cux2 antisense probe (detected in red) and FITC-labeled nurr1 antisense probe (detected in green) were hybridized to the coronal sections of the mouse brain. **(A,B)** Double ISH of cux2 (red) and nurr1 (green) mRNAs in the frontal section. **(A)** shows only the red channel (cux2 signal), while **(B)** shows the merged view for red and green channels of the same section. **(C–E)** The dashed rectangles in **(A,B)** were magnified and shown for different channels. **(C,D)** show the signals for cux2 and nurr1 mRNAs and **(E)** shows the merged image of **(C,D)**. **(F–H)** Double ISH of cux2 and nurr1 in the more posterior section. **(F,G)** show red (cux2 signal) and green (nurr1) channels, while **(H)** shows the merged

(Continued)

FIGURE 1 | Continued
view for red and green channels. **(I–K)** Dashed rectangles in **(F–K)** were magnified. The arrowheads in panels **(I–K)** indicate the nurr1^{+}/cux2^{-} cells in layer 6b. **(L)** Hoechst nuclear staining to confirm lamina boundaries in **(I–K)**. The dashed lines indicate the lamina borders determined by the density of nuclear staining. **(M–O)** Dashed rectangles in **(I–K)** were magnified. Note exact colocalization of the two mRNAs in **(O)**. Cla, claustrum; hip, hippocampus; rf, rhinal fissure; S1BF, somatosensory barrel field; S2, secondary somatosensory area; St, striatum; Th, thalamus.

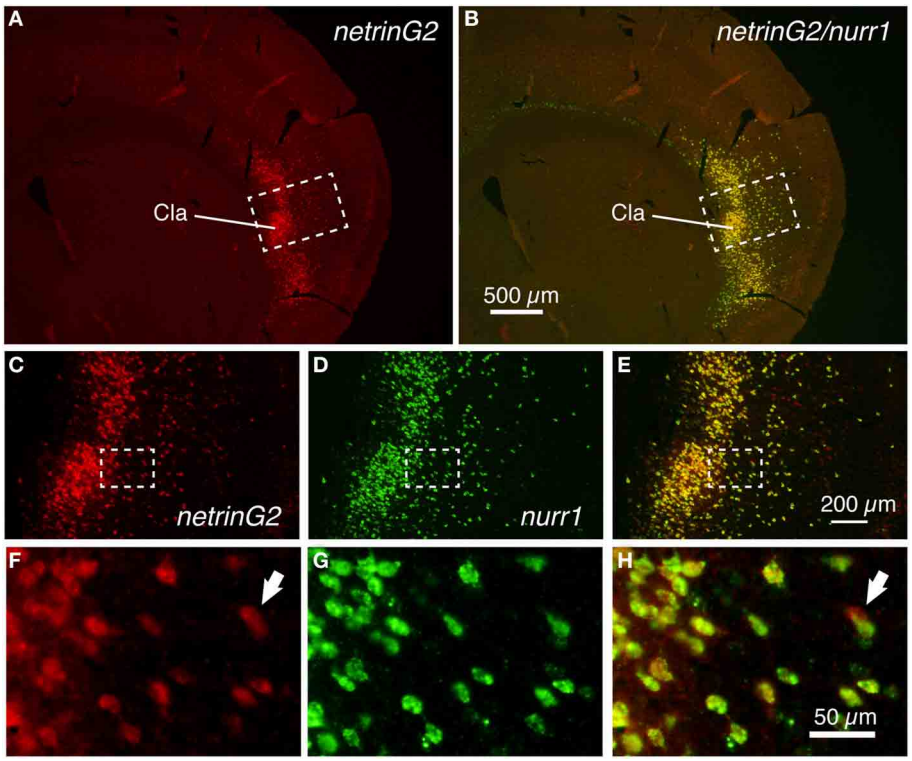

FIGURE 2 | Colocalization of netrinG2 and nurr1 mRNAs in the mouse brain. (A,B) Double ISH of netrinG2 (red) and nurr1 (green) mRNAs in the mouse frontal section. **(A)** shows only the red channel (netrinG2), while **(B)** shows the merged view for red and green channels of the same section. **(C–E)** Dashed rectangles in **(A,B)** were magnified and shown for netrinG2 **(C)**, nurr1 **(D)**, and merged **(E)** signals. **(F–H)** Dashed rectangles in **(C–E)** were magnified. The arrows in **(F,H)** indicate a netrinG2-single positive cell.

ISH OF nurr1 GENE IN THE EMBRYONIC MONKEY AND POSTNATAL MOUSE

To categorize cell types in the adult brain, it is informative to investigate the ontogenic origin. Toward this goal, we investigated the expression of nurr1 gene in the embryonic monkey brain. In **Figures 6E–H**, we illustrate the nurr1 mRNA distribution in the embryonic E110 monkey. We found that the adult pattern of nurr1 mRNA distribution (**Figures 6A–D**) is already established at this stage. One difference was the abundance of nurr1 mRNA-positive cells in the white matter that separates the insular cortex and the claustrum, as if these were persistent residuals of the migratory cells (**Figure 6F**). Such a white matter population was also present in the adult monkey brain, although fewer than that in the E110 brain (**Figure 6B**). The mRNA distribution in the proximal dendrites was well visualized in the embryonic tissue (**Figures 6G,H**) to show morphology of the cell body. Inverted pyramids (**Figure 6H**) or multipolar cells (**Figure 6G**) were easily observed in the claustrum and the white matter, but "standard" pyramidal neurons (i.e., with a discernible apical dendrites oriented toward the pia), only rarely.

For comparison, we investigated the distribution of nurr1 mRNA in P0 and P8 mice (**Figures 6I–K**). The distribution of nurr1 mRNA was almost identical to that in the adult brain at this stage. As in the embryonic monkey, the proximal dendrites were more evident in the postnatal mice (**Figures 6I–K**).

MORPHOLOGICAL ANALYSES OF CLAUSTRAL NEURONS IN RODENTS BY LUCIFER YELLOW INJECTION

The claustrum is separated from the insular cortex by white matter in monkeys, but in the rodent brain, the two structures appear continuous. We wondered whether the neurons in the insular cortex and claustrum of rodents have segregated or intermingled dendrites. To test this, we injected Lucifer Yellow randomly within the mouse insular/claustral regions. As shown in **Figures 7A–D**, the random injection resulted in a meshwork of dendrites that appeared to cover both insular cortex and claustrum. On closer examination, however, dendrites appeared to be differentiable between claustrum and insular cortex. While the upper layer neurons in the insular cortex exhibited typical pyramidal shape with conspicuous, vertically oriented apical dendrites, the lower part of

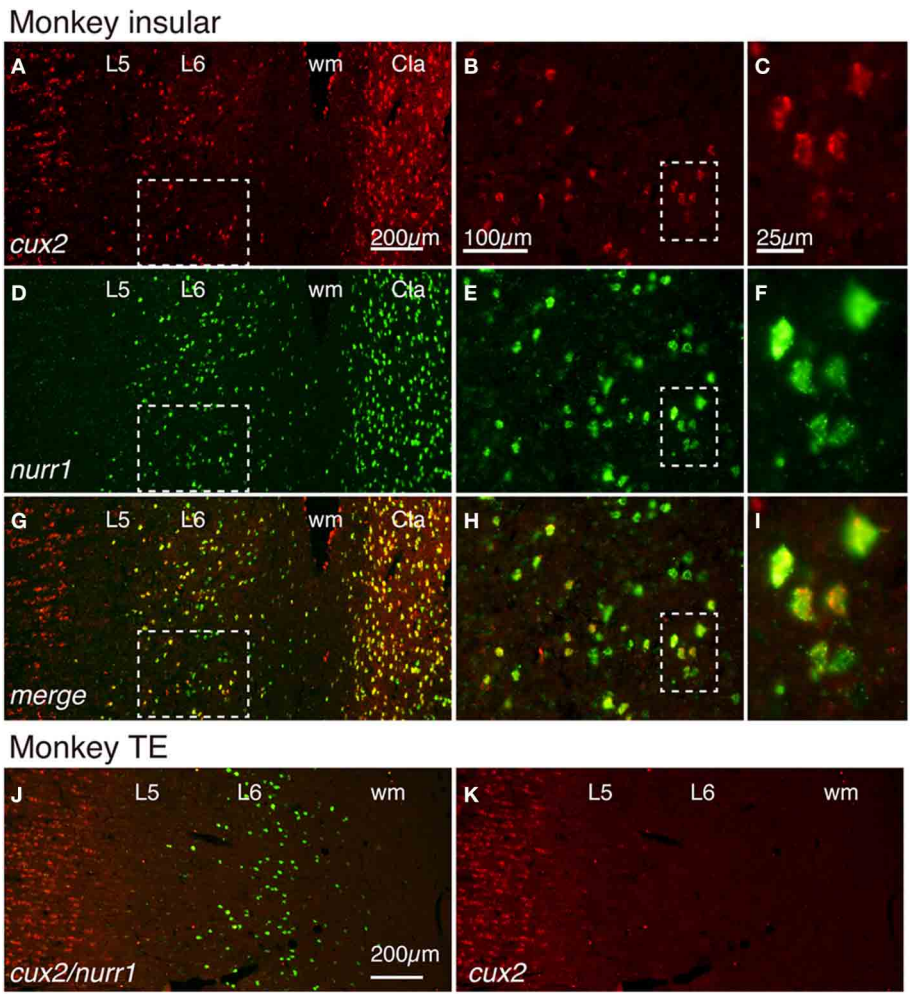

FIGURE 3 | Colocalization of cux2 and nurr1 mRNAs in the claustrum and insular cortex of the monkey brain. (A,D,G) Double ISH of cux2 (red) and nurr1 (green) mRNAs in the monkey brain section that spans the deep layers 5 (L5) and 6 (L6) of the insular cortex and the claustrum. Left side is to the pia matter. Red **(A)**, green **(D)**, and merged **(G)** channels were shown for the same section to demonstrate the colocalization of cux2 and nurr1 mRNA signals. **(B,E,H)** Dashed rectangles in **(A,D,G)** were magnified. **(C,F,I)** Dashed rectangles in **(B,E,H)** were magnified. **(J,K)** Double ISH of cux2 and nurr1 mRNAs in monkey TE. In **(J)**, both cux2 (red) and nurr1 (green) mRNA signals are shown as merged, while in **(K)**, only the cux2 mRNA signals are shown. Note the absence of cux2 mRNA signals in the deep layers in this area. Cla, claustrum; wm, white matter.

this region that should correspond to the claustrum had neurons without such dendrites. The dye-injected neurons were mostly spiny, although we encountered some smooth neurons as well. In this mouse experiment, we were not sure of the precise border between the insular cortex and the claustrum. With the rat preparations, we were able to stain the slice with monoclonal latexin antibody (Arimatsu et al., 1992) after the Lucifer Yellow injection, which enabled us to determine the precise border between insular cortex and the claustrum.

As shown in **Figures 7E,F**, **8A**, the heavy fiber staining of the latexin antibody clearly delimited the border between the insular cortex and the claustrum for the slices used for intracellular Lucifer Yellow injections. Morphologically, the claustral and insular cells were similar to those in the mouse cortex in that the claustral cells lacked apical dendrites and tended to extend dendrites within the claustrum (**Figure 7G**). To quantify this feature, we measured the extent of dendritic elongation in the coronal plane in maximum intensity projection images as detailed in the methods section. **Figure 8B** shows the radar charts for 28 claustral cells (e.g., C-13, C-14) and 29 cells outside the claustrum (outer cells; e.g., O-19). Only the spiny neurons were chosen for this analysis. The difference of dendritic elaboration was clearly visible in this panel and the average values were statistically significant (**Figure 8C**). **Figure 8D** show five representative tracings for claustral and outer cell dendrites. As these images show, the cell bodies of the outer cells were generally "pyramidal" and had one apical dendrite elongated toward the pial surface (red arrowhead). On the other hand, the claustral cells generally did not have typical apical dendrites that elongate toward the pial surface. In the 3D image, some claustral cells appeared to have "apical" dendrites oriented vertically to the slice surface. Cell C-15, for example, had a thick dendrite with secondary branches that

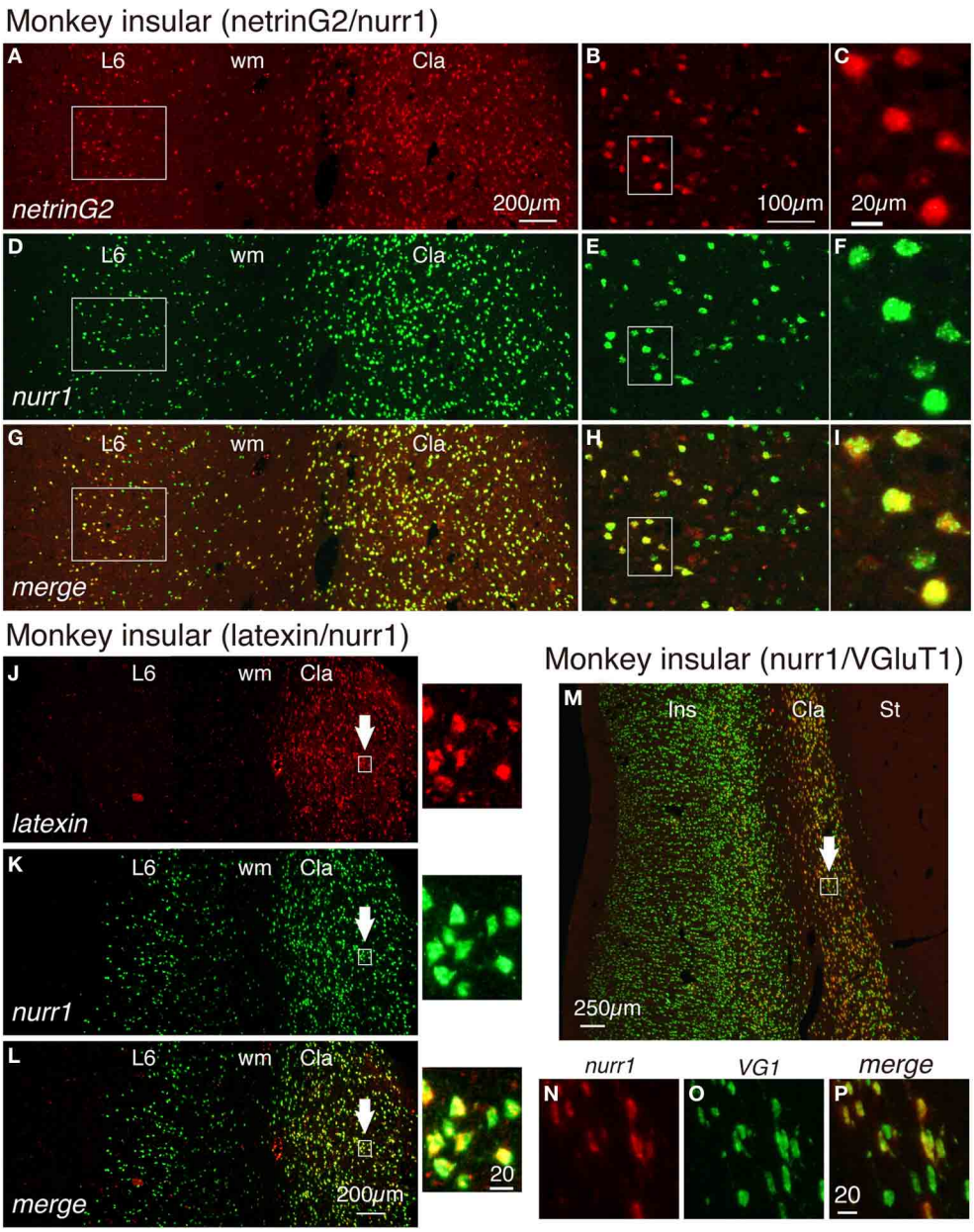

FIGURE 4 | Gene expression profiling for insular and claustral neurons by netrin G2, nurr1, latexin, and VGluT1 genes. (A,D,G) Double ISH of netrinG2 (red) and nurr1 (green) mRNAs in the monkey brain section that spans layer 6 (L6) of the insular cortex and the claustrum (Cla). Left side is to the pia matter. Red **(A)**, green **(D)**, and merged **(G)** channels were shown for the same section to demonstrate the colocalization of netrinG2 and nurr1 mRNA signals. **(B,E,H)** Rectangles in **(A,D,G)** were magnified. **(C,F,I)** Rectangles in **(B,E,H)** were magnified. **(J–L)** Double ISH of latexin (red) and nurr1 (green) mRNAs in the monkey brain section that spans layer 6 (L6) of the insular cortex and the claustrum (Cla). Left side is to the pia matter. The rectangles in the claustrum indicated by the arrows were magnified on the right side of each panel. **(M)** A merged view for double ISH of nurr1 (red) and VGluT1 (green) mRNAs in the monkey brain section that spans the entire layers of the insular cortex (Ins), the claustrum (Cla) and the striatum (St) is shown. Left side is to the pia matter. Red **(N)**, green **(O)**, and merged **(P)** channels were shown for the rectangle in the claustrum indicated by the white arrow. All the nurr1$^+$ neurons were VGluT1$^+$ glutamatergic in this analysis, while some VGluT1$^+$ cells in the claustrum exhibited only low level expression of nurr1 mRNA (compare **N–P**). Cla, claustrum; Ins, insular cortex; St, striatum; wm, white matter.

orient toward the bottom of the slices (C-15: **Figures 9A–C**). Since we always injected from the posterior side of the coronal slice, this means that C-15 may have a dendrite oriented toward the anterior side. Conversely, cell C-13 had a protrusion that looks like a severed dendrite (**Figures 9C,D**). C-13 may have a dendrite toward the posterior side. These examples suggest that lack of vertically orienting apical dendrites for at least some claustral cells may be because they are oriented along the longitudinal axis. We conclude that while there does not appear to exist clear-cut border of dendritic fields for claustral and insular

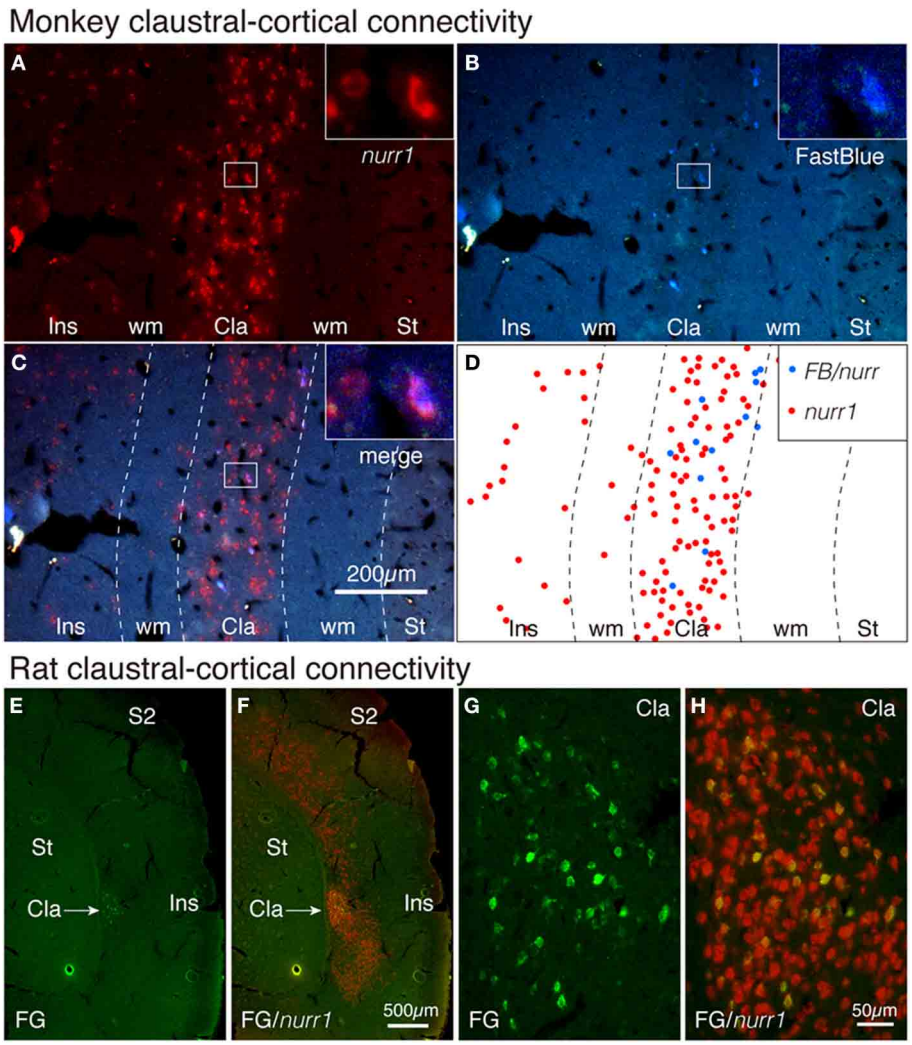

FIGURE 5 | Tracer-ISH of monkey and rat claustrum. (A–D) FastBlue was injected into areas V4 and 7a and several claustral cells were retrogradely labeled **(B,D)**. The same section processed for nurr1 ISH **(A,C)** exhibited nurr1 expression in all the FastBlue-labeled cells (see the insets). The rectangles within the claustrum are shown magnified in the insets for each panel. **(D)** indicate the schematic plot for **(C)**; the nurr1 single-positive cells were plotted in red, and the nurr1/FastBlue double positive cells were plotted in blue. **(E,F)** FluoroGold was injected into V1 and the claustral cells were retrogradely labeled. The same section was processed for nurr1 ISH. **(G,H)** The claustral regions of **(A,B)** were magnified. Cla, claustrum; Ins, insular cortex; S2, secondary somatosensory area; ST, striatum; wm, white matter.

cells, the dendrites of these cells are mostly contained within each territory.

DISCUSSION

In this paper, we set out to ask whether the claustral neurons are best considered as belonging to the cortex or the basal ganglia, in part using gene expression as a criterion. As we have demonstrated, nurr1, cux2, and netrinG2 genes are all expressed in both claustrum and cortical layer 6 in rodents and monkeys (summarized in **Table 1**). This observation supports previous proposals based on molecular marker expression that would favor a cortical phenotype of claustral neurons (Miyashita et al., 2005; Pirone et al., 2012). On the other hand, (1) latexin mRNA was expressed only in the claustrum in macaques and (2) cux2 mRNA was expressed only in the insular cortex and the claustrum (in contrast with the widespread cortical expression of nurr1 and netrinG2 mRNAs). Considering their sparse distribution, these genes would not be co-expressed simply by coincidence in the cortex. Despite obvious species difference, the exact matching of distribution outside claustrum demonstrates the significant similarity of the claustral cells and a subtype of cortical deep layer neuron.

The previous literature has identified several candidates for claustral-specific genes; so far these seem to have cortical expression as well. For example, a proteomic analysis has identified G-protein gamma2 (Gng2) subunit as claustral-specific (Mathur et al., 2009). However, Pirone et al., detected Gng2 immunoreactivity in the insular cortex of human brain (Pirone et al., 2012); and Allen brain atlas data (http://mouse.brain-map.org/) show that Gng2 gene is expressed in both the mouse cortex

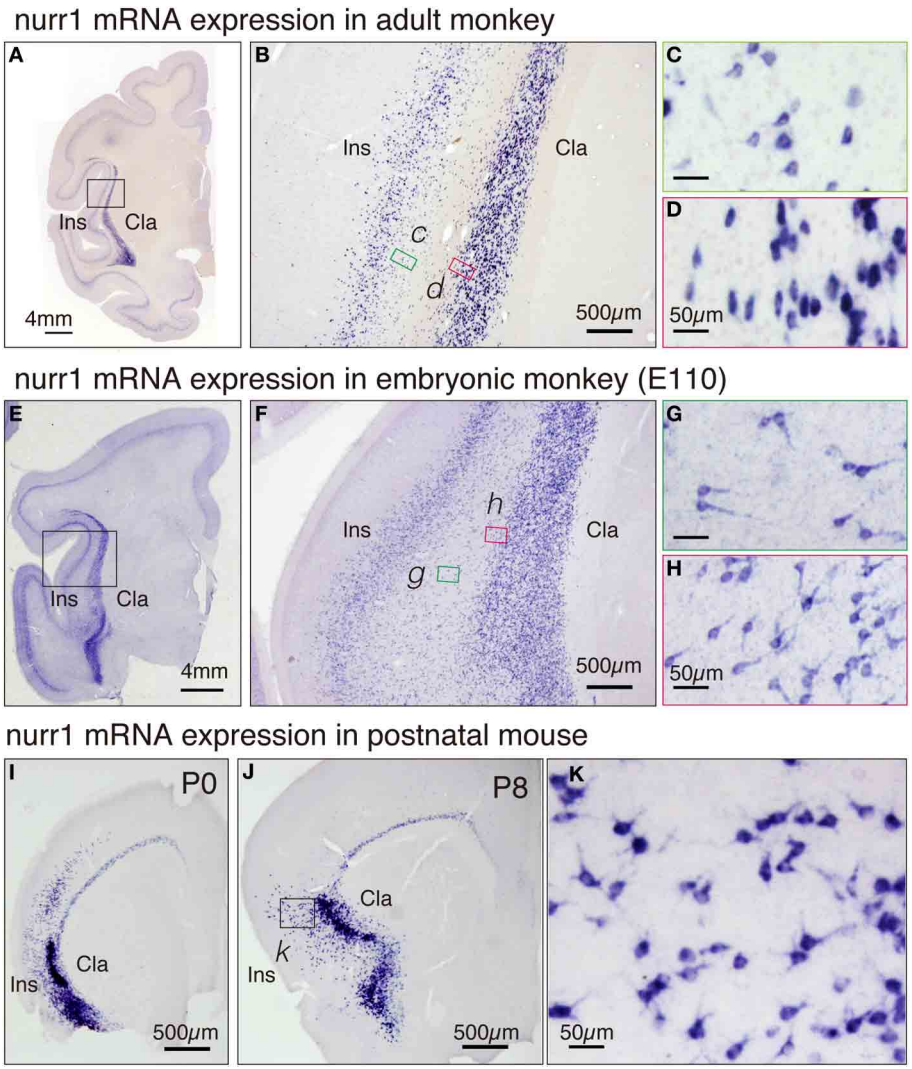

FIGURE 6 | Expression of nurr1 mRNA in the embryonic monkey and postnatal mice. (A) Single ISH of nurr1 mRNA in the coronal section of the adult monkey brain hemisphere. Note a dense expression of nurr1 mRNA in the claustrum and layer 6 of the insular cortex. **(B)** The rectangle in **(A)** was magnified. Note the scattered cell population in the white matter between the insular cortex and the claustrum. **(C,D)** The rectangles in **(B)** were magnified. **(C)** shows the shapes of the cell bodies at the bottom of the insular cortex, most of which were typical pyramidal except those at the very bottom (right side of the panel). **(D)** shows the shapes of the cell bodies at the top of the claustrum, which are elongated in horizontal direction. **(E)** ISH of nurr1 mRNA in the coronal section of the embryonic E110 monkey brain hemisphere. **(F)** The rectangle in **(E)** was magnified. Note the abundant scattered cell population in the white matter between the insular cortex and the claustrum. **(G,H)** The rectangles in **(F)** were magnified. **(G)** shows the shapes of the cell bodies in the white matter, many of which appear like inverted pyramidal cells. **(H)** shows the cell bodies at the top of the claustram, which are irregularly shaped. **(I,J)** ISH of nurr1 mRNA in the coronal section of the postnatal P0 and P8 mouse brain hemisphere. **(K)** The rectangle in **(J)** was magnified. Note similarity of the shapes of the cells to those in the monkey claustrum **(G)**.

and claustrum in a latexin-like pattern. mRNA for another gene, LGR7, is reported also to exhibit a latexin-like pattern of expression (Piccenna et al., 2005), and we found by double ISH that LGR7 mRNA colocalizes with nurr1 mRNA in the mouse brain (data not shown).

Other more general markers support a cortical, as opposed to striatal signature for claustral neurons. (1) VGluT1 and VGluT2 genes are glutamatergic marker genes, neither of which is expressed in the striatum, where GABAergic cells are the principal cell type. By double ISH, we found that the nurr1$^+$ neurons in both mouse and macaque claustrum co-express VGluT1 mRNA (**Figure 4** and data not shown). (2) In our previous study, moreover, we reported that excitatory neurons in layer 6 of rats can be classified as either pcp4$^+$ or cck$^+$ cells, and that nurr1$^+$ cells express cck mRNA (Watakabe et al., 2012). In both rodents and monkeys, cck mRNA was expressed in the claustrum but not in the striatum (data not shown). These data are consistent with our tracer-ISH data showing that nurr1$^+$ neurons project to the cortex (**Figure 5**).

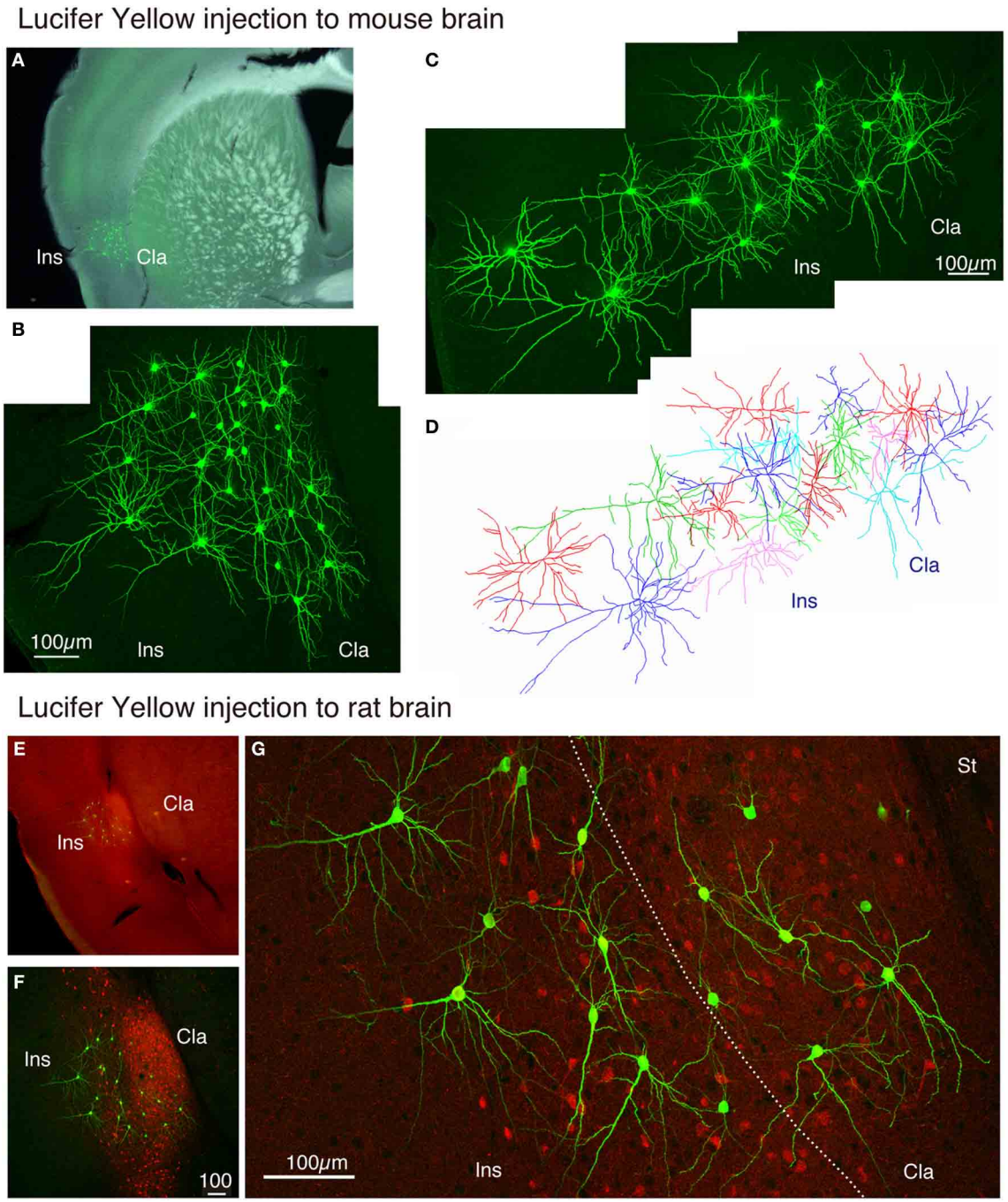

FIGURE 7 | Lucifer Yellow injection to the mouse and rat claustral neurons. (A) Dark field image of the mouse slice that received Lucifer Yellow injection to the insular/claustral region. The fluorescent image of the antibody-enhanced Lucifer Yellow-filled neurons is superimposed to indicate the location of clustered injection. **(B)** Maximal projection stacks of confocal sections for magnified view of the insular/claustral region of **(A)**. Note the meshwork of dendrites that cover the insular cortex and the claustrum. **(C)** Another injection into the mouse slice. The pia is to the left. **(D)** Reconstruction of the Lucifer Yellow injected neurons shown in **(C)**. Different cells are shown by different colors for better representation of each cell. **(E)** Merged view for latexin (red) and Lucifer Yellow (green)-stained slice of the rat brain. The densely stained oval at the bottom of the insular cortex is considered as the claustrum. **(F)** Maximal projection stacks of confocal sections for magnified view of the insular/claustral region of **(E)**. Note that the insular/clautral border can be delineated by the dense fiber staining of latexin within the claustrum. Latexin^{+} neurons were observed in a scattered manner outside the claustrum as well. **(G)** Magnified view of the insular/claustral border of **(F)**. Note the differential dendritic arborization of the claustral and insular cells. The dotted line indicates the insular/claustral border identified on the basis of latexin fiber staining. Cla, claustrum; Ins, insular cortex; St, striatum.

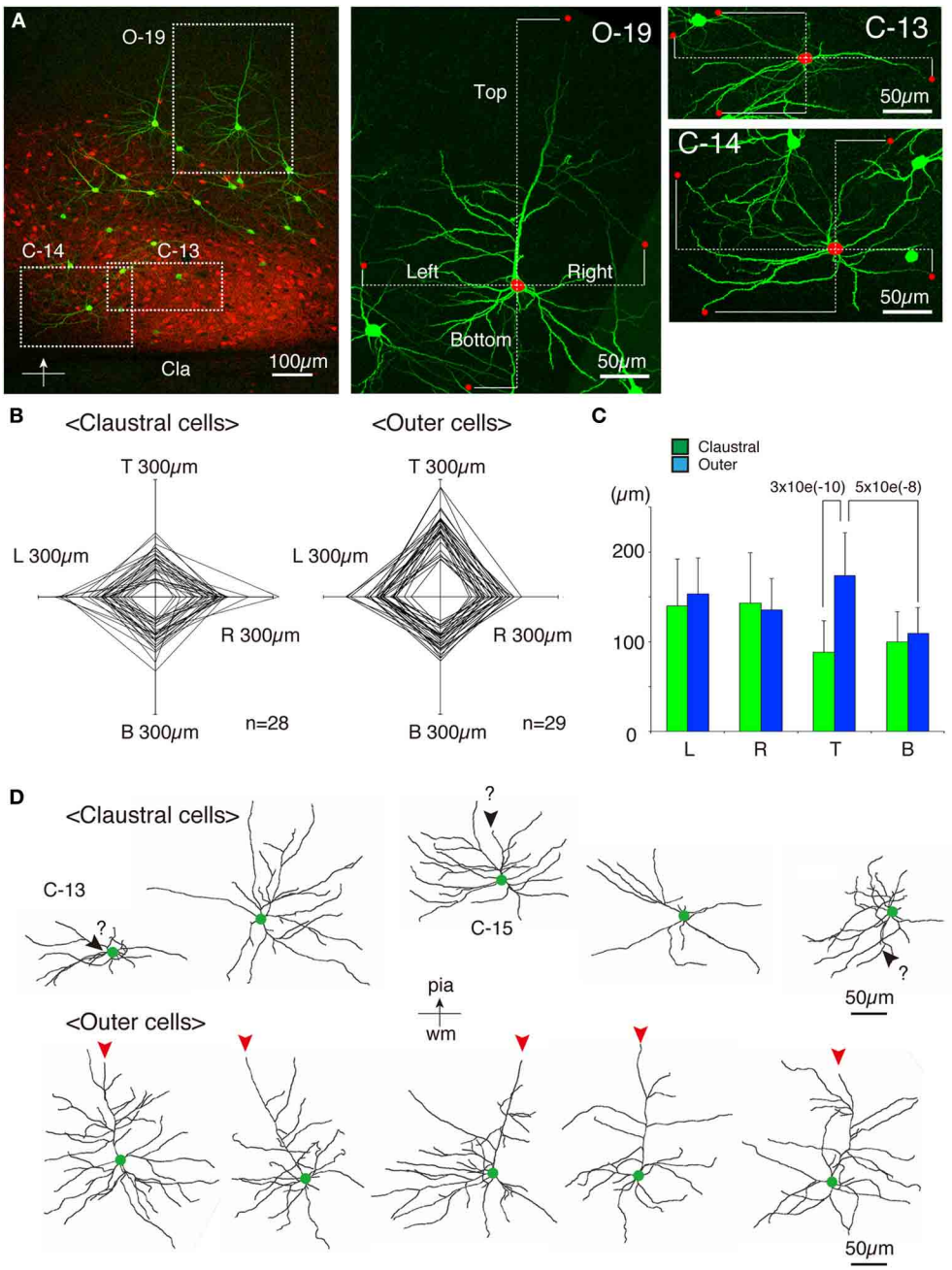

FIGURE 8 | Quantitative analysis of dendritic field extension for Lucifer-Yellow injected cells. (A) A typical example of the fluorescent image of the analyzed insular/claustral region. The axis of analysis (shown by the bar and the arrow at the bottom) was determined so that the pia is to the "Top." This panel was taken from the same section shown in **Figures 7E–G**. Three analyzed cells, C-13, C-14, and O-19, were magnified on the right. The red dots on each cell indicate the tips of the dendrites that determined the "Top," "Bottom," "Right," and "Left" borders of the dendritic field of the cell of interest. The distance from the center of the cell body to these borders were measured (dotted lines) to examine the polarity of dendritic extensions. Because we wanted to measure the overlaps between the insular and claustral territory, we measured the distance in these max projection images, and not the 3D distance from the tips to the cell body. **(B)** Rader plots for 28 claustral and 29 outer cells chosen from eight slices of two rats were superimposed. The ends of each axis correspond to 300 μm from the center. The "claustral" cells were determined based on the counterstaining by latexin or parvalubumin. The "outer" cells were those that were located outside the dense latexin-positive regions but within the regions containing scattered latexin$^+$ cells. **(C)** The averages and standard deviations for Left (L), Right (R), Top (T), and Bottom (B) values for claustral and outer cells are shown. The difference of the "Top" values between the claustral and outer cells or the difference of the "Top" and "Bottom" values for the outer cells were statistically significant with the indicated *p*-value. **(D)** Five representative examples each of the dendritic reconstruction for the claustral and outer cells by Imaris FilamentTracer. All these neurons are oriented so that the top is to the pia. Green dots indicate the position of the cell bodies. The red arrowheads of the outer cells indicate the apical dendrites that were clearly different from other basal dendrites by morphology. Most of the claustral cells lacked such apical dendrites. However, candidates for apical dendrites which may be oriented toward the anterior or posterior directions (orthogonal to the slice plane) were present in some cells, which were shown by black arrowheads with question marks.

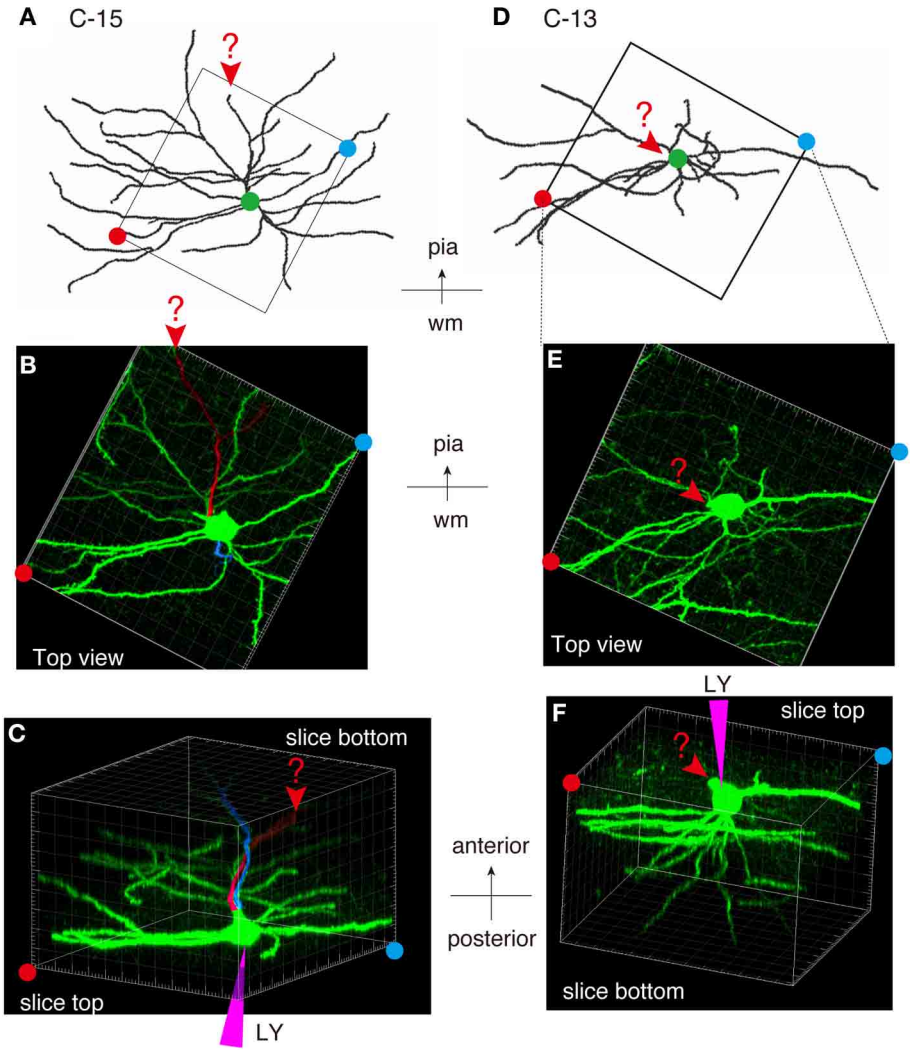

FIGURE 9 | Examples of atypically oriented pyramidal cells in the claustrum. (A) Dendritic reconstruction of a claustral cell (C-15) shown in **Figure 8D**. The region indicated by the square was cut off for 3D reconstruction of the confocal stack images in **(B,C)**. Note the orientation of the neuron: the top is to the pia matter of the insular cortex. **(B)** A maximal projection stack of confocal images of the region shown by a rectangle in **(A)** was viewed from the top surface of the slice. In this view, there does not appear to exist apical dendrites. **(C)** The 3D reconstruction of the confocal images for C-15 was rotated so that the slice is viewed obliquely from the bottom side. Note the positions of the red and blue circles, which indicated the slice tops. The purple triangle represents the pipette position for Lucifer Yellow (LY) injection. The candidate primary and secondary apical dendrites that are oriented toward the bottom of the slice were colored in red and blue, respectively. The arrowheads and the question mark indicates the potential apical dendrites that may be severed. Since we injected from the posterior side of the coronal slice, this means that the candidate apical dendrites are oriented toward the anterior side of the mouse brain. **(D–F)** Dendritic reconstruction of a claustral cell (C-13). The same as for C-15. The rotation of the 3D-reconstruction revealed an appendage that appears like an apical dendrite severed at the slice top surface.

In addition, ontogenic data are suggestive of a cortical origin of the claustrum, as has been discussed in previous studies (Miyashita et al., 2005; Pirone et al., 2012). In the embryonic brain, the claustrum expresses TBr1 but not Dlx1, markers; these are associated with pallial (cortical) and striatal structures, respectively (Puelles et al., 2000). Furthermore, autoradiographic birthdating, followed by developmental tracing of the labeled cortical neurons, suggests that claustral neurons are produced in the neocortical neuroepithelium and migrate ventrolaterally to reach their final destination (Bayer and Altman, 1991). Relevant to this point, our ISH data for nurr1 mRNA expression in the embryonic E110 monkey brain revealed many positive cells located within the white matter that separates the insular cortex and the claustrum (**Figure 6**). The cell body morphology of these neurons is consistent with the migratory pathway proposed by Bayer and Altman (1991) rather than with the typical radial migration for pyramidal cells.

At present, we cannot conclude whether this migratory neuron population is the same subtype as that scattered in layer 6 of the insular and other cortical areas. It is likely that the claustral neurons migrate from distant pallial primordium to the proximity of insular cortex. Note that the

Table 1 | Summary of expression patterns for claustral enriched genes.

	Gene	latexin	nurr1	cux2	netrinG2	cux2$^+$/nurr1$^+$	netrinG2$^+$/nurr1$^+$
Rodent	Cortex (upper)	No	No	Yes	No	No	No
	Cortex (deep)	Yes*1	Yes*1	Yes*1	Yes*1	Yes*1	Yes*1
	Cortex (layer 6b)	No	Yes	No	No	No	No
	Claustrum	Yes	Yes	Yes	Yes	Yes	Yes
Monkey	Cortex (upper)	No	No	Yes	No	No	No
	Cortex (deep)	No	Yes*2	Yes*3	Yes*4	Only upper layer 6	Only upper layer 6
	Claustrum	Yes	Yes	Yes	Yes	Yes	Yes

**1, Only in the lateral cortical areas including the insular cortex, S2, and others; *2, Both upper and lower part of layer 6 across areas; *3, Only in the insular cortex, not inV1, S1, M1, TE, or frontal areas; *4, Only in the upper part of layer 6 but across areas including V1, S1, M1, TE, or frontal areas.*

radial glia for the insular cortex are reported as anchored at the pial surface and the neuroepithelium of lateral and ventral pallial portions, bypassing the claustrum (Reblet et al., 2002). Further, Mathur and co-workers found that Crym, a marker for cortical deep layer neurons, is expressed in the cells that surround the claustrum (Mathur et al., 2009). Consistent with this finding, we observed VGluT1 mRNA-positive cells in the white matter that surrounds the monkey claustrum.

CLAUSTRAL DENDRITES DO NOT EXTEND INTO OVERLYING INSULAR CORTEX

Since Brodmann, there has been discussion that the claustrum may be an additional layer of the insular cortex (reviewed in Swanson and Petrovich, 1998; Swanson, 2000; Edelstein and Denaro, 2004). From this perspective, and given that the claustrum directly abuts the insular cortex in rodents, one might expect some degree of dendritic incursion, at least at the border. Previous Golgi studies (Brand, 1981; LeVay and Sherk, 1981; Braak and Braak, 1982; Mamos, 1984; Mamos et al., 1986; Dinopoulos et al., 1992; Rowniak et al., 1994; Wasilewska and Najdzion, 2001), however, have provided no evidence of dendritic incursion; and, in fact, our Lucifer Yellow filled neurons had dendrites that were clearly skewed, avoiding the overlying insular territory. By simultaneous visualization of the claustral/insular border by latexin immunotaining, we consolidated the past morphological studies. We also performed side-by-side comparison of the insular and claustral cells within the same experimental condition, which clearly showed the different morphological features of these neurons. Our intracellular fills did show some orientation preference of apparently multipolar cells, but the dendritic elongation was along the longitudinal axis (**Figure 9**). This confirms *in vivo*-labeling and 3D reconstruction demonstrating the existence of a neuron with rostrally-extending apical dendrite in the rostral part of the rat claustrum (Shibuya and Yamamoto, 1998), suggestive of extensive intra-claustral connectivity. Unfortunately, we could not succeed in filling claustral axons in the postmortem slice preparation; but extensive intra-claustral axonal arborization can be inferred from the presence of "hundreds of retrogradely labeled neurons" after localized injections of retrograde tracer in the rat claustrum (Smith and Alloway, 2010).

THE nurr1$^+$ SUBCLASS OF CORTICAL LAYER 6 NEURONS

The expression analyses performed in this study strongly suggest the existence of a distinct cortical cell type defined by expression of latexin, nurr1, cux2, and netrinG2 genes in the rodent brain. The expression of these genes in both mouse and monkey claustrum implies similar properties of the claustral and cortical neurons. This could be based in connectivity from the deep cortical layers to claustrum. In our previous study, we proposed that nurr1$^+$/CTGF$^-$ cells in layer 6 of monkey cortex that cover the entire neocortex may be equivalent to the lateral-restricted nurr1$^+$/CTGF-cells in the rodent cortex (Watakabe et al., 2007). Consistent with this idea, we found that netrinG2 mRNA is expressed in the upper subpopulation of nurr1-mRNA positive cells in all the areas examined including motor, somatosensory, TE, frontal and visual cortices (data not shown). Nevertheless, we found that cux2 mRNA is not expressed in the deep layers outside the insular cortex in the macaque cortex. In addition, latexin mRNA was not expressed even in the insular cortex, where cux2 mRNA is co-expressed with nurr1 mRNA. One possible interpretation would be that latexin and cux2 mRNA expression is downregulated as a result of cortical differentiation. Alternatively, the nurr1$^+$ neurons in the monkey brain may be ontogenetically independent from those of rodent cortex. Further study is needed to clarify this point and to understand the functional significance of species difference observed here.

ACKNOWLEDGMENTS

We thank Dr. Tetsuya Sasaki in National Institute of Neuroscience for helping us with the Lucifer Yellow injection. We thank Drs Yumiko Hatanaka and Yasuyoshi Arimatsu for providing latexin antibody. We thank Dr. Sachi Okabayashi of the Corporation for Production and Research of Laboratory Primates; Dr. Yasuhiro Yasutomi of the Tsukuba Primate Research Center, National Institute of Infectious Diseases for providing the embryonic monkey tissue. Confocal images were acquired at Spectrography and Bioimaging Facility, NIBB Core Research Facilities. Supported by the grant from the JSPS to Akiya Watakabe (KAKENHI19500304 and 22500300) and Scientific Research on Innovative Areas (Neocortical Organization) (22123009 to Tetsuo Yamamori).

REFERENCES

Arimatsu, Y., Ishida, M., Kaneko, T., Ichinose, S., and Omori, A. (2003). Organization and development of corticocortical associative neurons expressing

the orphan nuclear receptor Nurr1. *J. Comp. Neurol.* 466, 180–196. doi: 10.1002/cne.10875

Arimatsu, Y., Miyamoto, M., Nihonmatsu, I., Hirata, K., Uratani, Y., Hatanaka, Y., et al. (1992). Early regional specification for a molecular neuronal phenotype in the rat neocortex. *Proc. Natl. Acad. Sci. U.S.A.* 89, 8879–8883. doi: 10.1073/pnas.89.19.8879

Arion, D., Unger, T., Lewis, D. A., and Mirnics, K. (2007). Molecular markers distinguishing supragranular and infragranular layers in the human prefrontal cortex. *Eur. J. Neurosci.* 25, 1843–1854. doi: 10.1111/j.1460-9568.2007.05396.x

Bai, W. Z., Ishida, M., and Arimatsu, Y. (2004). Chemically defined feedback connections from infragranular layers of sensory association cortices in the rat. *Neuroscience* 123, 257–267. doi: 10.1016/j.neuroscience.2003.08.056

Bayer, S. A., and Altman, J. (1991). Development of the endopiriform nucleus and the claustrum in the rat brain. *Neuroscience* 45, 391–412. doi: 10.1016/0306-4522(91)90236-H

Braak, H., and Braak, E. (1982). Neuronal types in the claustrum of man. *Anat. Embryol. (Berl).* 163, 447–460. doi: 10.1007/BF00305558

Brand, S. (1981). A serial section golgi analysis of the primate claustrum. *Anat. Embryol. (Berl).* 162, 475–488. doi: 10.1007/BF00301872

Carey, R. G., and Neal, T. L. (1985). The rat claustrum: afferent and efferent connections with visual cortex. *Brain Res.* 329, 185–193. doi: 10.1016/0006-8993(85)90524-4

Crick, F. C., and Koch, C. (2005). What is the function of the claustrum? *Philos. Trans. R. Soc. Lond. B Biol. Sci.* 360, 1271–1279. doi: 10.1098/rstb.2005.1661

Cubelos, B., Sebastian-Serrano, A., Beccari, L., Calcagnotto, M. E., Cisneros, E., Kim, S., et al. (2010). Cux1 and Cux2 regulate dendritic branching, spine morphology, and synapses of the upper layer neurons of the cortex. *Neuron* 66, 523–535. doi: 10.1016/j.neuron.2010.04.038

Dinopoulos, A., Papadopoulos, G. C., Michaloudi, H., Parnavelas, J. G., Uylings, H. B., and Karamanlidis, A. N. (1992). Claustrum in the hedgehog (*Erinaceus europaeus*) brain: cytoarchitecture and connections with cortical and subcortical structures. *J. Comp. Neurol.* 316, 187–205. doi: 10.1002/cne.903160205

Edelstein, L. R., and Denaro, F. J. (2004). The claustrum: a historical review of its anatomy, physiology, cytochemistry and functional significance. *Cell. Mol. Biol. (Noisy-le-grand).* 50, 675–702. doi: 10.1170/T558

Franco, S. J., Gil-Sanz, C., Martinez-Garay, I., Espinosa, A., Harkins-Perry, S. R., Ramos, C., et al. (2012). Fate-restricted neural progenitors in the mammalian cerebral cortex. *Science* 337, 746–749. doi: 10.1126/science.1223616

Fremeau, R. T. J., Troyer, M. D., Pahner, I., Nygaard, G. O., Tran, C. H., Reimer, R. J., et al. (2001). The expression of vesicular glutamate transporters defines two classes of excitatory synapse. *Neuron* 31, 247–260. doi: 10.1016/S0896-6273(01)00344-0

Hur, E. E., and Zaborszky, L. (2005). Vglut2 afferents to the medial prefrontal and primary somatosensory cortices: a combined retrograde tracing in situ hybridization study [corrected]. *J. Comp. Neurol.* 483, 351–373. doi: 10.1002/cne.20444

Komatsu, Y., Watakabe, A., Hashikawa, T., Tochitani, S., and Yamamori, T. (2005). Retinol-binding protein gene is highly expressed in higher-order association areas of the primate neocortex. *Cereb. Cortex* 15, 96–108. doi: 10.1093/cercor/bhh112

LeVay, S., and Sherk, H. (1981). The visual claustrum of the cat. I. Structure and connections. *J. Neurosci.* 1, 956–980.

Mamos, L. (1984). Morphology of claustral neurons in the rat. *Folia Morphol. (Warsz).* 43, 73–78.

Mamos, L., Narkiewicz, O., and Morys, J. (1986). Neurons of the claustrum in the cat; a Golgi study. *Acta Neurobiol. Exp. (Wars).* 46, 171–178.

Mathur, B. N., Caprioli, R. M., and Deutch, A. Y. (2009). Proteomic analysis illuminates a novel structural definition of the claustrum and insula. *Cereb. Cortex* 19, 2372–2379. doi: 10.1093/cercor/bhn253

Miyashita, T., Nishimura-Akiyoshi, S., Itohara, S., and Rockland, K. S. (2005). Strong expression of NETRIN-G2 in the monkey claustrum. *Neuroscience* 136, 487–496. doi: 10.1016/j.neuroscience.2005.08.025

Nieto, M., Monuki, E. S., Tang, H., Imitola, J., Haubst, N., Khoury, S. J., et al. (2004). Expression of Cux-1 and Cux-2 in the subventricular zone and upper layers II-IV of the cerebral cortex. *J. Comp. Neurol.* 479, 168–180. doi: 10.1002/cne.20322

Nishimura-Akiyoshi, S., Niimi, K., Nakashiba, T., and Itohara, S. (2007). Axonal netrin-Gs transneuronally determine lamina-specific subdendritic segments. *Proc. Natl. Acad. Sci. U.S.A.* 104, 14801–14806. doi: 10.1073/pnas.0706919104

Oga, T., Aoi, H., Sasaki, T., Fujita, I., and Ichinohe, N. (2013). Postnatal development of layer III pyramidal cells in the primary visual, inferior temporal, and prefrontal cortices of the marmoset. *Front. Neural Circuits* 7:31. doi: 10.3389/fncir.2013.00031

Piccenna, L., Shen, P. J., Ma, S., Burazin, T. C., Gossen, J. A., Mosselman, S., et al. (2005). Localization of LGR7 gene expression in adult mouse brain using LGR7 knock-out/LacZ knock-in mice: correlation with LGR7 mRNA distribution. *Ann. N.Y. Acad. Sci.* 1041, 197–204. doi: 10.1196/annals.1282.030

Pirone, A., Cozzi, B., Edelstein, L., Peruffo, A., Lenzi, C., Quilici, F., et al. (2012). Topography of Gng2- and NetrinG2-expression suggests an insular origin of the human claustrum. *PLoS ONE* 7:e44745. doi: 10.1371/journal.pone.0044745

Puelles, L., Kuwana, E., Puelles, E., Bulfone, A., Shimamura, K., Keleher, J., et al. (2000). Pallial and subpallial derivatives in the embryonic chick and mouse telencephalon, traced by the expression of the genes Dlx-2, Emx-1, Nkx-2.1, Pax-6, and Tbr-1. *J. Comp. Neurol.* 424, 409–438. doi: 10.1002/1096-9861(20000828)424:3<409::AID-CNE3>3.0.CO;2-7

Reblet, C., Alejo, A., Blanco-Santiago, R. I., Mendizabal-Zubiaga, J., Fuentes, M., and Bueno-Lopez, J. L. (2002). Neuroepithelial origin of the insular and endopiriform parts of the claustrum. *Brain Res. Bull.* 57, 495–497. doi: 10.1016/S0361-9230(01)00719-5

Rowniak, M., Szteyn, S., Robak, A., and Klawon, M. (1994). The types of neurons in the claustrum of bison bonasus: nissl and golgi study. *Folia Morphol. (Warsz).* 53, 231–237.

Shibuya, H., and Yamamoto, T. (1998). Electrophysiological and morphological features of rat claustral neurons: an intracellular staining study. *Neuroscience* 85, 1037–1049. doi: 10.1016/S0306-4522(97)00609-X

Smith, J. B., and Alloway, K. D. (2010). Functional specificity of claustrum connections in the rat: interhemispheric communication between specific parts of motor cortex. *J. Neurosci.* 30, 16832–16844. doi: 10.1523/JNEUROSCI.4438-10.2010

Swanson, L. W. (2000). Cerebral hemisphere regulation of motivated behavior. *Brain Res.* 886, 113–164. doi: 10.1016/S0006-8993(00)02905-X

Swanson, L. W., and Petrovich, G. D. (1998). What is the amygdala? *Trends Neurosci.* 21, 323–331. doi: 10.1016/S0166-2236(98)01265-X

Tanne-Gariepy, J., Boussaoud, D., and Rouiller, E. M. (2002). Projections of the claustrum to the primary motor, premotor, and prefrontal cortices in the macaque monkey. *J. Comp. Neurol.* 454, 140–157. doi: 10.1002/cne.10425

Wasilewska, B., and Najdzion, J. (2001). Types of neurons of the claustrum in the rabbit–Nissl, Kluver-Barrera and Golgi studies. *Folia Morphol. (Warsz).* 60, 41–45.

Watakabe, A. (2009). Comparative molecular neuroanatomy of mammalian neocortex: what can gene expression tell us about areas and layers? *Dev. Growth Differ.* 51, 343–354. doi: 10.1111/j.1440-169X.2008.01085.x

Watakabe, A., Hirokawa, J., Ichinohe, N., Ohsawa, S., Kaneko, T., Rockland, K. S., et al. (2012). Area-specific substratification of deep layer neurons in the rat cortex. *J. Comp. Neurol.* 520, 3553–3573. doi: 10.1002/cne.23160

Watakabe, A., Ichinohe, N., Ohsawa, S., Hashikawa, T., Komatsu, Y., Rockland, K. S., et al. (2007). Comparative analysis of layer-specific genes in Mammalian neocortex. *Cereb. Cortex* 17, 1918–1933. doi: 10.1093/cercor/bhl102

Watakabe, A., Komatsu, Y., Ohsawa, S., and Yamamori, T. (2010). Fluorescent *in situ* hybridization technique for cell type identification and characterization in the central nervous system. *Methods* 52, 367–374. doi: 10.1016/j.ymeth.2010.07.003

Conflict of Interest Statement: The authors declare that the research was conducted in the absence of any commercial or financial relationships that could be construed as a potential conflict of interest.

Received: 31 January 2014; accepted: 07 May 2014; published online: 23 May 2014.
Citation: Watakabe A, Ohsawa S, Ichinohe N, Rockland KS and Yamamori T (2014) Characterization of claustral neurons by comparative gene expression profiling and dye-injection analyses. Front. Syst. Neurosci. ***8****:98. doi: 10.3389/fnsys.2014.00098*
This article was submitted to the journal Frontiers in Systems Neuroscience.

frontiers in
SYSTEMS NEUROSCIENCE

ORIGINAL RESEARCH ARTICLE
published: 28 February 2014
doi: 10.3389/fnsys.2014.00031

The claustrum of the ferret: afferent and efferent connections to lower and higher order visual cortical areas

Nina Patzke[1], Giorgio M. Innocenti[2,3] and Paul R. Manger[1]*

[1] School of Anatomical Sciences, Faculty of Health Sciences, University of the Witwatersrand, Johannesburg, South Africa
[2] Department of Neuroscience, Karolinska Institutet, Stockholm, Sweden
[3] Brain and Mind Institute, École Polytechnique Fédérale de Lausanne, Lausanne, Switzerland

Edited by:
Brian Neil Mathur, University of Maryland School of Medicine, USA

Reviewed by:
Jon H. Kaas, Vanderbilt University, USA
David Reser, Monash University, Australia

Correspondence:
Paul R. Manger, School of Anatomical Sciences, Faculty of Health Sciences, University of the Witwatersrand, 7 York Road, Parktown, 2193 Johannesburg, South Africa
e-mail: paul.manger@wits.ac.za

The claustrum, a subcortical telencephalic structure, is known to be reciprocally interconnected to almost all cortical regions; however, a systematic analysis of claustrocortical connectivity with physiologically identified lower and higher order visual cortical areas has not been undertaken. In the current study we used biotinylated dextran amine to trace the connections of the ferret claustrum with lower (occipital areas 17, 18, 19 and 21) and higher (parietal and temporal areas posterior parietal caudal visual area (PPc), posterior parietal rostral visual area (PPr), 20a, 20b, anterior ectosylvian visual area (AEV)) order visual cortical areas. No connections between the claustrum and area 17 were observed. Occipital visual areas 18, 19 and 21 revealed a reciprocal connectivity mainly to the caudal part of the claustrum. After injection into parietal areas PPc and PPr labeled neurons and terminals were found throughout almost the entire rostrocaudal extent of the dorsal claustrum. Area 20b revealed reciprocal connections mainly to the caudal-ventral claustrum, although some labeled neurons and terminals were observed in the dorso-central claustrum. No projection from the claustrum to areas AEV and 20a could be observed, though projections from AEV and 20a to the claustrum were found. Only injections placed in areas PPr and AEV resulted in anterogradely labeled terminals in the contralateral claustrum. Our results suggest that lower order visual areas have clearly defined connectivity zones located in the caudal claustrum, whereas higher order visual areas, even if not sending and/or receiving projections from the entire claustrum, show a more widespread connectivity.

Keywords: cerebral cortex, claustrum, connections, ferret, visual cortex

INTRODUCTION

The claustrum is a thin subcortical unlaminated telencephalic structure located between the dorsal striatopallidal complex, specifically the putamen, and the insular cortex, or claustrocortex in mammals that lack the insular formation and a sylvian fissure. A precise definition of the anatomical location of the claustrum within the mammalian brain has been recently advanced based on proteomic studies, and indicates that the claustrum is surrounded by layer VI neurons and is connected to the cerebral cortex, but it does not connect to sub-cortical structures (Mathur et al., 2009). The claustrum appears to be present in all mammals (Jakubowska-Sadowska et al., 1998; Kowianski et al., 1999), but evidence for its existence in all monotremes is equivocal (Butler et al., 2002; Ashwell et al., 2004). Various anatomical tract-tracing experiments, mostly in cats and monkeys, but also in other species, have demonstrated that the claustrum is reciprocally interconnected to almost all cortical regions. Those cortical regions for which claustrocortical connectivity has been observed include: visual cortex, parieto-occipital and posterior parietal cortex, temporal and temporopolar cortex, motor and premotor cortex, prefrontal cortex, cingulate cortex, the frontoparietal operculum, somatosensory cortex, prepiriform olfactory cortex and the entorhinal cortex (for details see Tanné-Gariépy et al., 2002; Edelstein and Denaro, 2004; Crick and Koch, 2005). Tractographic anatomical studies in humans have demonstrated claustral projections to the superior frontal, precentral, postcentral, posterior parietal, orbitofrontal, prefrontal, temporal and occipital cortical regions (Fernández-Miranda et al., 2008).

The claustrocortical connections are topographically organized, forming cortical projection zones within the claustrum; however, these projection zones are not strictly separated from each other and appear to overlap. The degree of overlap, the extent and the location of the projection zones within the claustrum are species-specific (Jakubowska-Sadowska et al., 1998). Examples for such a species-specific variation are the claustral visual projection zones. For example, the claustral projections zones to areas 17 and 18 show a full overlap in rat and rabbit, but are completely separate in the cat (Jakubowska-Sadowska et al., 1998). Moreover the visual projection zones in the claustrum of rat, rabbit and primates are located in the caudoventral claustrum, whereas in the cat and guinea pig they occupy the caudodorsal claustrum

(LeVay and Sherk, 1981; Jakubowska-Sadowska et al., 1998). The claustrum is mainly reciprocally connected to the ipsilateral cortex, but inconsistent data concerning the presence of a weaker contralateral projection has been reported for different species (e.g., Jakubowska-Sadowska et al., 1998).

Contrasting with the topographically organized functional/connectional subdivisions of the claustrum, immunohistochemical and Golgi studies have revealed a homogeneous architecture without any parcellation (Sherk, 1986; Reynhout and Baizer, 1999). Due to this uniform organization, it has been suggested that neuronal information processing within the claustrum may entail specialized mechanisms that allow information to travel widely within its rostral-caudal and dorsal-ventral extent (Crick and Koch, 2005). In light of the extensive connectivity of the claustrum to virtually all cortical areas, and its intra-claustral organization, Crick and Koch (2005) postulated that the claustrum may synchronize information both within and across sensory, motor and cognitive modalities, thus enabling a conscious perception of environmental stimuli.

Although many studies of claustrocortical connectivity have been conducted, there is a lot of inconsistency in the reports. Importantly, a systematic analysis of claustrocortical connectivity with established and physiologically identifiable lower and higher order visual cortical areas is missing from the literature—i.e., are systematic differences in the extent, location and connectivity type evident as one proceeds from lower order to higher order areas? In the current study we used biotinylated dextran amine (BDA) tracing to examine the connectivity of the ferret claustrum with physiologically identified lower (occipital areas 17, 18, 19 and 21; Innocenti et al., 2002; Manger et al., 2002a) and higher (parietal and temporal posterior parietal caudal visual area (PPc), posterior parietal rostral visual area (PPr), 20a, 20b, anterior ectosylvian visual area (AEV; Manger et al., 2002b, 2004, 2005)) order visual cortical areas to specifically answer the question.

MATERIALS AND METHODS

Nine adult female ferrets (*Mustela putorius*) weighing between 600 and 1000 g were used in the current study. All experiments were performed according to Swedish and European Community guidelines for the care and use of animals in scientific experiments. The animals were initially anesthetized with i.m. doses of ketamine hydrochloride (Ketalar, 10 mg/kg) and medetomidin hydrochloride (Domitor, 0.08 mg/kg), supplemented with atropine sulfate (0.15 mg/kg) and placed in a stereotaxic frame. A mixture of 1% isoflurane in a 1:1 nitrous oxide and oxygen mixture was delivered through a mask while the animal maintained its own respiration. Anesthetic level was monitored using the eye blink and withdrawal reflexes, in combination with measurement of the heart rate. The visual cortex was exposed under aseptic conditions and in each animal a number (less than 20) of electrophysiological recordings were taken to ensure placement of the tracer within a specific cortical area near the representation of the horizontal meridian (Manger et al., 2002a,b, 2004, 2005). Approximately 500 nl of tracer (biotinylated dextran amine, BDA 10 k, 5% in 0.1 M phosphate buffer; Molecular Probes) was delivered at each injection site (one site per animal) through a Hamilton microsyringe (**Figure 1**).

After completion of the injection, a soft contact lens was cut to fit over the exposed cortex, the retracted dura mater pulled over the contact lens, and the excised portion of bone repositioned and held in place with dental acrylic. The temporal muscle was

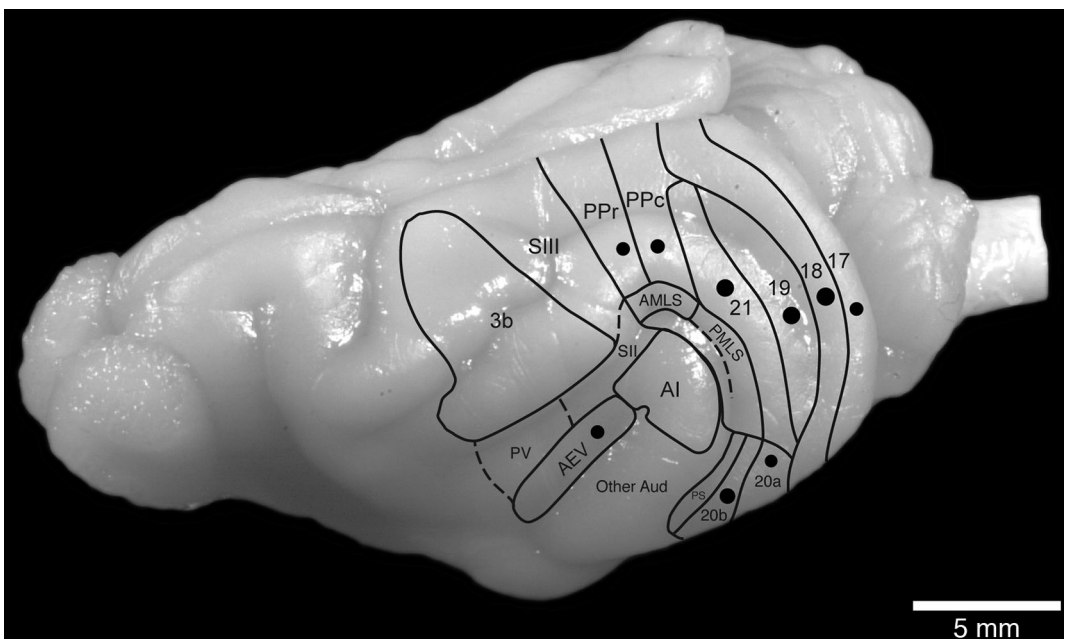

FIGURE 1 | Location and approximate size of the injection sites analyzed in the current study in relation to the known boundaries of visual cortical areas in the ferret brain.

reattached using surgical glue and the midline incision of the skin sutured. Antibiotics were administered in all cases (Terramycin, 40 mg/kg, each day for 5 days). These animals were given a 2-week recovery period to allow for tracer transport. At the end of this period, the animals were given a lethal dose of sodium pentobarbital (80 mg/kg, i.p.) and perfused intracardially, initially with a rinse of 0.9% saline (4°C, 500 ml/kg), followed by fixation with 4% paraformaldehyde in 0.1 M phosphate buffer (4°C, 1000 ml/kg). The brain was removed from the skull and post-fixed overnight in the same solution, then transferred to a 30% sucrose solution in 0.1 M phosphate buffer (at 4°C) and allowed to equilibrate. The brains were then frozen in dry ice and sectioned on a freezing microtome in a coronal plane and a one in four series of stains made for Nissl substance (with cresyl violet), myelin (Gallyas, 1979), cytochrome oxidase (Carroll and Wong-Riley, 1984) and BDA. For visualization of BDA, the sections were incubated in 0.5% bovine serum albumin in 0.05 M Tris buffer for 1 h. This was followed by incubation in an avidin-HRP solution for 3 h. A 10 min pre-incubation in 0.2% $NiNH_4SO_4$ preceded the addition of H_2O_2 (200 μl/l) to this solution, at which time the sections were monitored visually for the reaction product. The reaction was stopped by placing the sections in 0.05 M Tris buffer. All sections were mounted on 0.5% gelatine coated slides, dehydrated in graded series of alcohols, cleared in xylene and coverslipped with Depex mounting medium.

The stained sections were examined at both low and high power with light microscopes to determine in which sections through the claustrum labeled cell bodies and terminals were present. Under low power stereomicroscopy, the architectonic outlines of the claustrum and adjacent regions were drawn using the Nissl, myelin and cytochrome oxidase sections with the aid of a camera lucida. The sections reacted for the anatomical tract tracer were then matched to these drawing and the locations of individual retrogradely labeled cells plotted and regions of anterogradely labeled axonal terminal demarcated. The drawings were scanned and redrawn using the Canvas 8 drawing program. Digital photomicrographs were captured using a Zeiss Axioskop and the Axiovision software. No pixilation adjustments, or manipulation of the captured images were undertaken, except for the adjustment of contrast, brightness, and levels using Adobe Photoshop 7.

RESULTS

The position of the claustrum and its extent was identified using Nissl, myelin and cytochrome oxidase stained sections that were made adjacent to the sections on which the BDA labeling was revealed and analyzed. The claustrum of the ferret shows the typical mammalian shape of a thin, curved, irregular sheet of gray matter, located between the putamen and the claustrocortex (**Figure 2**). In the rostrocaudal axis, the claustrum was found to extend from the most rostral part of globus pallidus to the rostral border of the habenular complex (**Figure 2**).

CLAUSTRAL CONNECTIONS WITH THE LOWER ORDER/OCCIPITAL VISUAL AREAS 17, 18, 19 AND 21

No BDA positive neurons or terminals were observed in the claustrum after injection of the tracer into area 17. As a control we examined the potential connections with the dorsal lateral geniculate nucleus (dLGN) and observed labeled cells (**Figure 3A**). This connectivity with the dLGN in the ferret following area 17 injections indicates that the lack of labeled cells in the claustrum is not a result of methodological issues. Additional examples of dorsal thalamic connectivity following injections into the different visual areas indicates that in all cases the injections were correctly placed in the cerebral cortex (**Figure 3**).

Injections into visual areas 18, 19 and 21 revealed similar projection zones in the claustrum (**Figures 4**, **5**). Retrogradely labeled neurons were exclusively found in the caudal third of the ipsilateral claustrum. In the caudal half of the projection zone labeled neurons were located throughout the whole cross section of the claustrum, with the highest cell density in the middle portion of the cross section. Injections into areas 18 and 19 revealed a few labeled neurons in a more rostral location occupying the ventral portion of the cross section. Injections into area 21 revealed the smallest projection zone in the claustrum and at the most rostral location where labeled cell were present, they were observed in the dorsal portion of the cross section. For all three visual areas the presence of anterogradely labeled axonal terminals was concurrent with the territories where retrogradely BDA labeled neurons were observed. No BDA positive cells or terminals were observed in the contralateral claustrum following injection into these cortical areas.

CLAUSTRAL CONNECTIONS WITH THE POSTERIOR PARIETAL VISUAL AREAS PPc AND PPr

Following injection into area PPc, BDA positive neurons were found throughout the majority of the rostrocaudal extent of the ipsilateral claustrum, and were seen to occupy the dorsal half of the cross section (**Figure 6**). The number of labeled cells exhibited a greater density towards the caudal pole of the claustrum; however, at the most rostral and caudal poles of the claustrum no labeled neurons were observed. Anterogradely labeled axonal terminals were coincident with the regions where retrogradely BDA labeled neurons were observed.

Injections of anatomical tract tracer into area PPr resulted in a labeling of neurons mostly in the caudal half of the ipsilateral claustrum. BDA positive neurons were observed to occupy the dorsal portion of the cross section, with the highest density of labeled cells observed in the caudal part of the claustrum; however, as with the PPc injections no labeled neurons were observed at the most caudal pole of the claustrum. The region of the claustrum in which retrogradely labeled neurons were observed also contained anterograde labeling, but this extended over greater rostrocaudal extent of the claustrum. Interestingly, anterogradely labeled terminals were observed in the dorsal caudal aspect of the contralateral claustrum following injection of BDA into area PPr (**Figure 6**).

INJECTION INTO THE TEMPORAL VISUAL AREAS 20a, 20b AND AEV

Although areas 20a and 20b are small adjacent visual areas in the temporal lobe (Manger et al., 2004), the labeling in the claustrum following cortical injection showed quite distinct and differing patterns for each area (**Figure 5**). The injections into 20b resulted in the labeling of cell and axonal terminals in the caudal third of

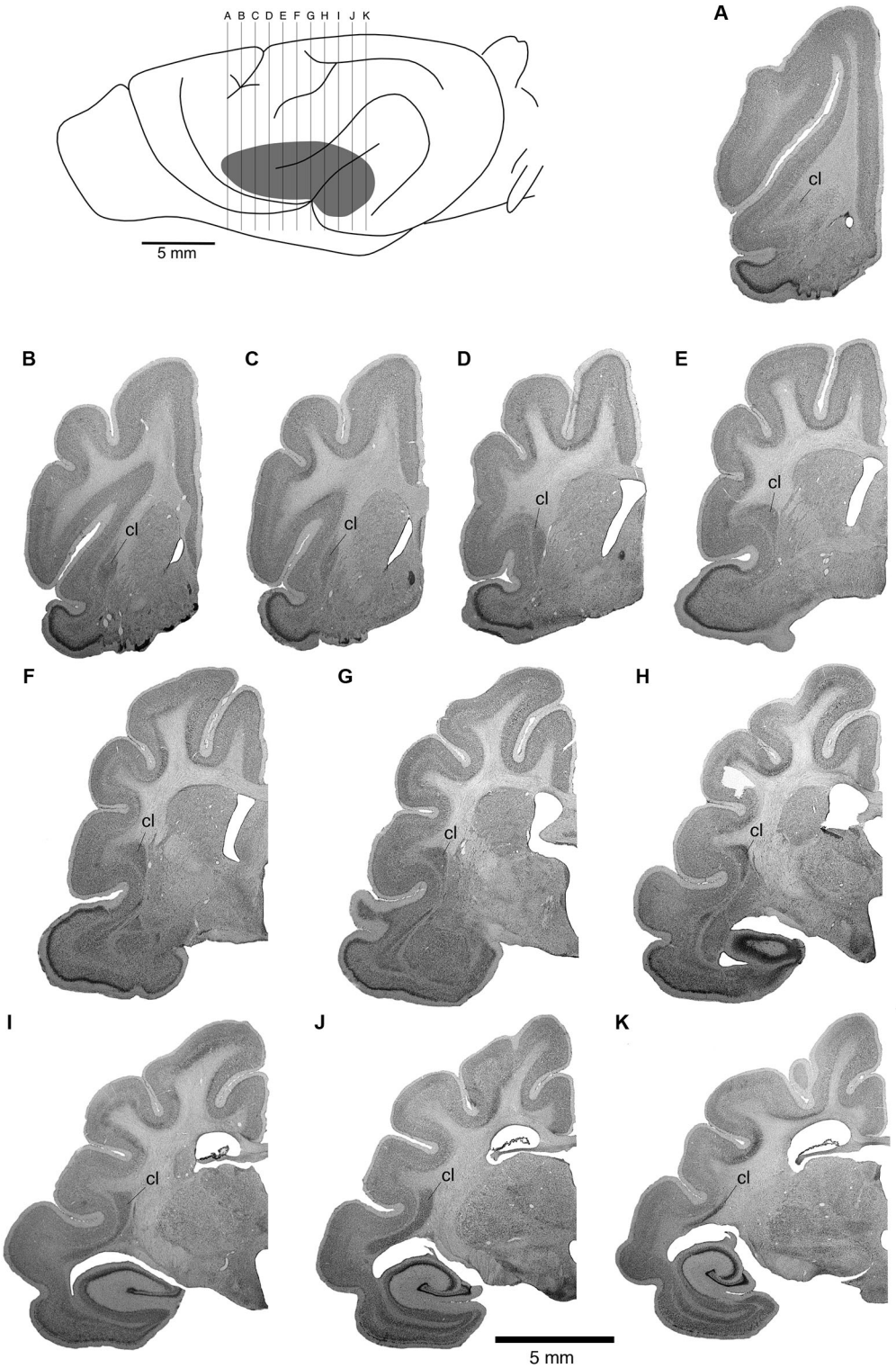

FIGURE 2 | Location of the ferret claustrum (cl). The drawing of the lateral view of the ferret brain demarcates the location of the claustrum below the cerebral cortex, as well as the level of section corresponding to each of the images of the rostral to caudal Nissl stained sections **A** through **K** which are approximately 1 mm apart.

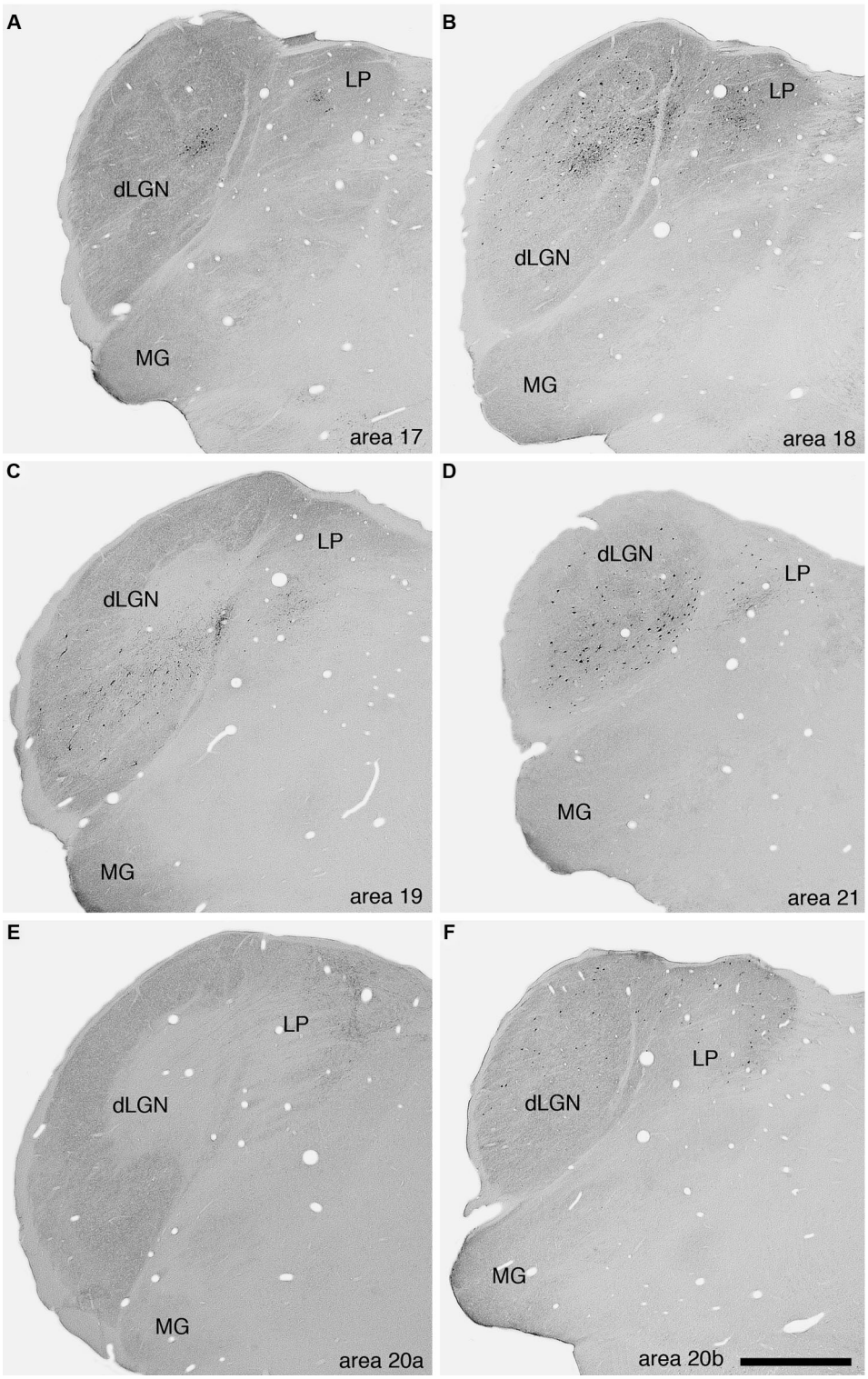

FIGURE 3 | Photomicrographs of labeled cells and axon terminals in the visual regions of the dorsal thalamus of the ferret following injection of BDA into various visual cortical areas. A—area 17, **B**—area 18, **C**—area 19, **D**—area 21, **E**—area 20a, **F**—area 20b. Note the presence of labeled cells or axon terminals in the **dLGN** or the lateral posterior nucleus (**LP**) following the injections into the different cortical areas. Scale bar in **F** = 1 mm and applies to all. Dorsal to the top and medial to the right in all images. **MG**—medial geniculate body.

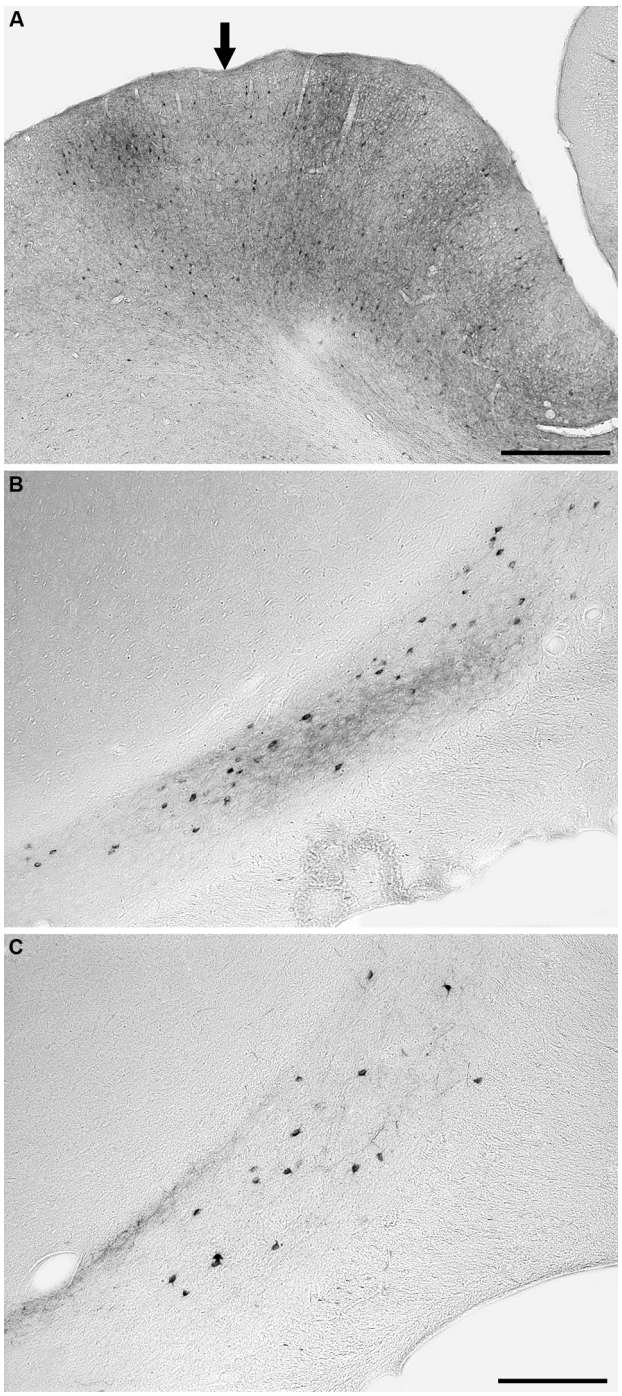

FIGURE 4 | Photomicrographs of an example injection site in area 21 (A) and labeled cells and terminals in the claustrum following injections into area 18 (B) and area 21 (C). Note that the injected tracer has been mostly taken up from the injection site (entry of microsyringe into cortex marked with an **arrow**) and that the injection sites did not encompass any of the underlying white matter. Following injections in both areas 18 and 21, retrogradely labeled neurons and anterogradely labeled terminals were observed, but in the depicted cases the anterograde labeling was far stronger after injection into area 18. In all images medial is to the right and dorsal to the top. The scale bar in **A** = 500 μm, the scale bar in **C** = 250 μm and applies to **B** and **C**.

the ipsilateral claustrum, mostly located in the ventral half of the claustrum; however, in the most rostral part of the projection zone labeled cells were observed in the dorsal half of the claustrum.

In contrast, no labeled cells were observed in the claustrum after injection into area 20a (**Figure 5**); however, anterogradely labeled axonal terminals were scattered through the entire ipsilateral claustrum. Similar to the claustral projection observed with area 20a, no labeled neurons were observed in the claustrum following injection into area AEV (**Figure 6**). Here again anterogradely labeled axonal terminals were observed throughout the entire ipsilateral claustrum; however, no labeling was found at the most rostral and caudal poles of the claustrum. As with area PPr, a few randomly scattered labeled axonal terminals were observed in the caudal half of the contralateral claustrum following injection into area AEV (**Figure 6**).

DISCUSSION

Claustrocortical connectivity has been the subject of several studies on different animals (see below); however, a systematic analysis of the connectivity with established and physiologically identified visual cortical areas has not been undertaken. In the current study, the interconnections of several physiologically identified lower and higher order visual areas with the claustrum was systematically examined in the ferret.

CLAUSTROCORTICAL CONNECTIVITY WITH THE LOWER ORDER VISUAL AREA 17

No connectivity between the claustrum and area 17 was observed in the present study; however, BDA positive neurons were found in the lateral geniculate nucleus—the principal thalamic input neurons to area 17—indicating that the injection site was correctly placed. Previous studies describing claustrocortical connectivity with area 17 present inconsistent results. While some studies show no connectivity of the claustrum with area 17 in rat (Hadley and Trachtenberg, 1978; Carey and Neal, 1985), hamster (Lent, 1982) and owl monkey (Graham et al., 1979), other tracing studies show contrary results. For example, a comparative tracing study by Jakubowska-Sadowska et al. (1998) demonstrated claustrocortical connectivity with area 17 in rat, rabbit, guinea pig and cat. Other studies on rats (Shameem et al., 1984; Sloniewski et al., 1986), cats (Jayaraman and Updyke, 1979; Olson and Graybiel, 1980; LeVay and Sherk, 1981; LeVay, 1986), tree shrews (Carey et al., 1979, 1980), baboons (Riche and Lanoir, 1978) and macaques (Mizuno et al., 1981; Doty, 1983; Kennedy and Bullier, 1985; Perkel et al., 1986) also revealed connections of the claustrum with area 17. Nevertheless, in some studies it is not clear if the projection from the claustrum to area 17 is a result of the injection or through tracer spread to adjacent cortical areas or the underlying white matter (Riche and Lanoir, 1978; Sloniewski et al., 1986). In addition, an interesting observation was made by Carey et al. (1979) in the tree shrew, where they observed that after injection into area 17, retrogradely labeled cells were not seen in the claustrum in every case, but all cases showed labeled cells in the lateral geniculate nucleus. Rather, they observed that retrogradely cells were only found in the claustrum in cases with large injection sites. It seems that the claustrocortical projection to area 17 is quite weak and large injections sites are required in order to visualize

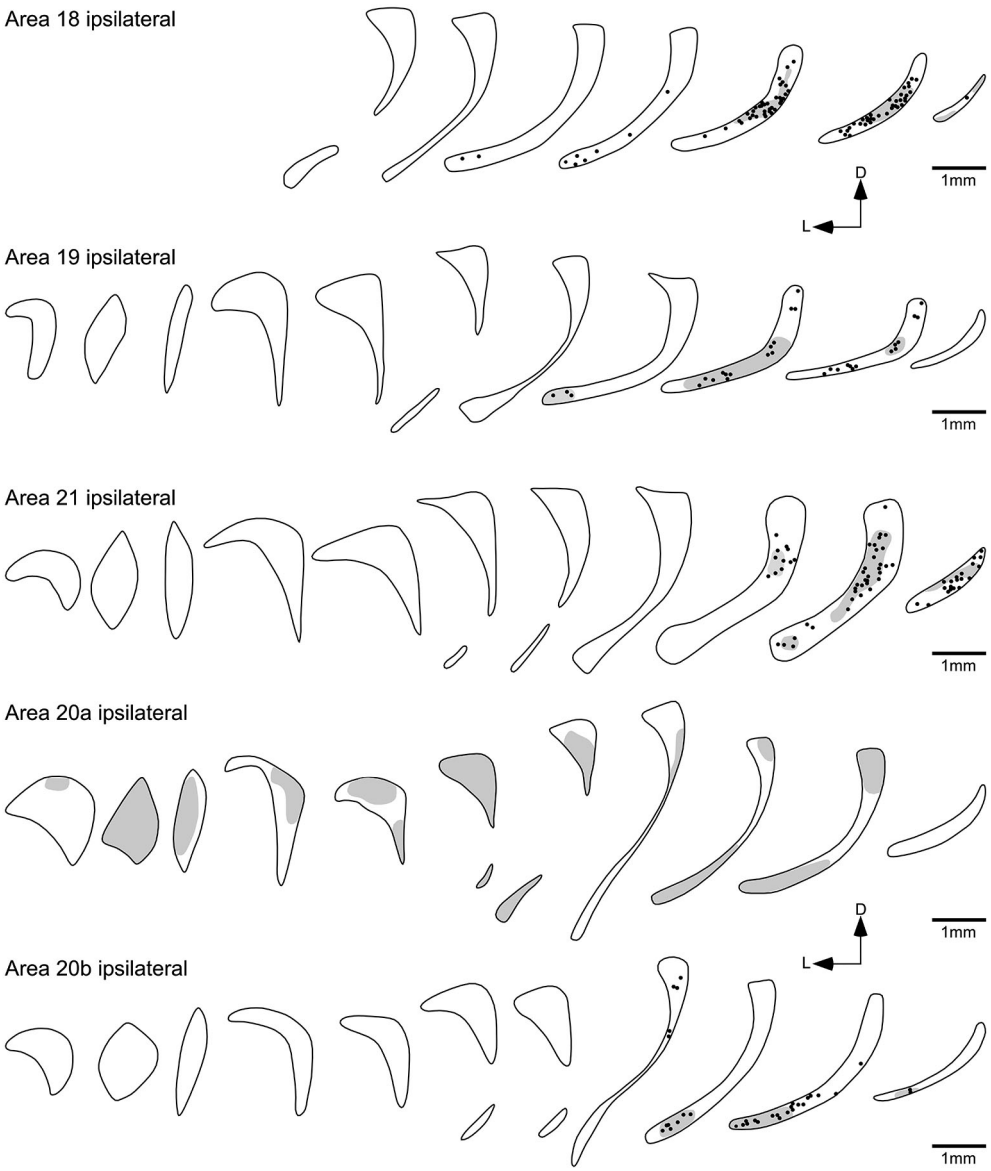

FIGURE 5 | Diagrammatic reconstructions of the ipsilateral claustral connectivity following injections of biotinylated dextran amine into cortical visual areas 18, 19, 21, 20a and 20b. Each figurine, which are spaced approximately 1 mm apart in the rostrocaudal plane, represents a coronal section through the claustrum (see **Figure 2**) with the rostral sections to the left and caudal sections to the right and for each figurine medial is to the right and dorsal to the top. In each figurine, the dots represent retrogradely labeled neurons, while the shading represents regions of labeled anterograde axonal terminals. Note the caudally located reciprocal connectivity of the occipital (18, 19, 21) visual areas and also the temporal visual area 20b, while temporal visual area 20a shows a widespread anterograde connectivity to the claustrum.

this projection. In our study, the injection site was relatively small in order to avoid tracer spread to adjacent areas and the underlying white matter, and this likely resulted in our inability to detect this potential connection. Taken together, the evidence indicates that the claustrum may be connected with area 17; however, this connection is presumably fairly weak and requires large application sites in order to be visualized. It is also possible, given the topographic discontinuities in the representation of the visual field in area 17 of the ferret (Innocenti et al., 2002; Manger et al., 2002a), that our small injections were restricted to a portion of the visual field, for example the peripheral visual field, which does not connect with the claustrum.

CLAUSTROCORTICAL CONNECTIVITY TO THE LOWER ORDER OCCIPITAL VISUAL AREAS 18, 19 AND 21

Injection into the visual areas 18, 19 and 21 resulted in a similar overlapping pattern of connectivity, where labeled neurons axon terminals were exclusively found in the caudal third of

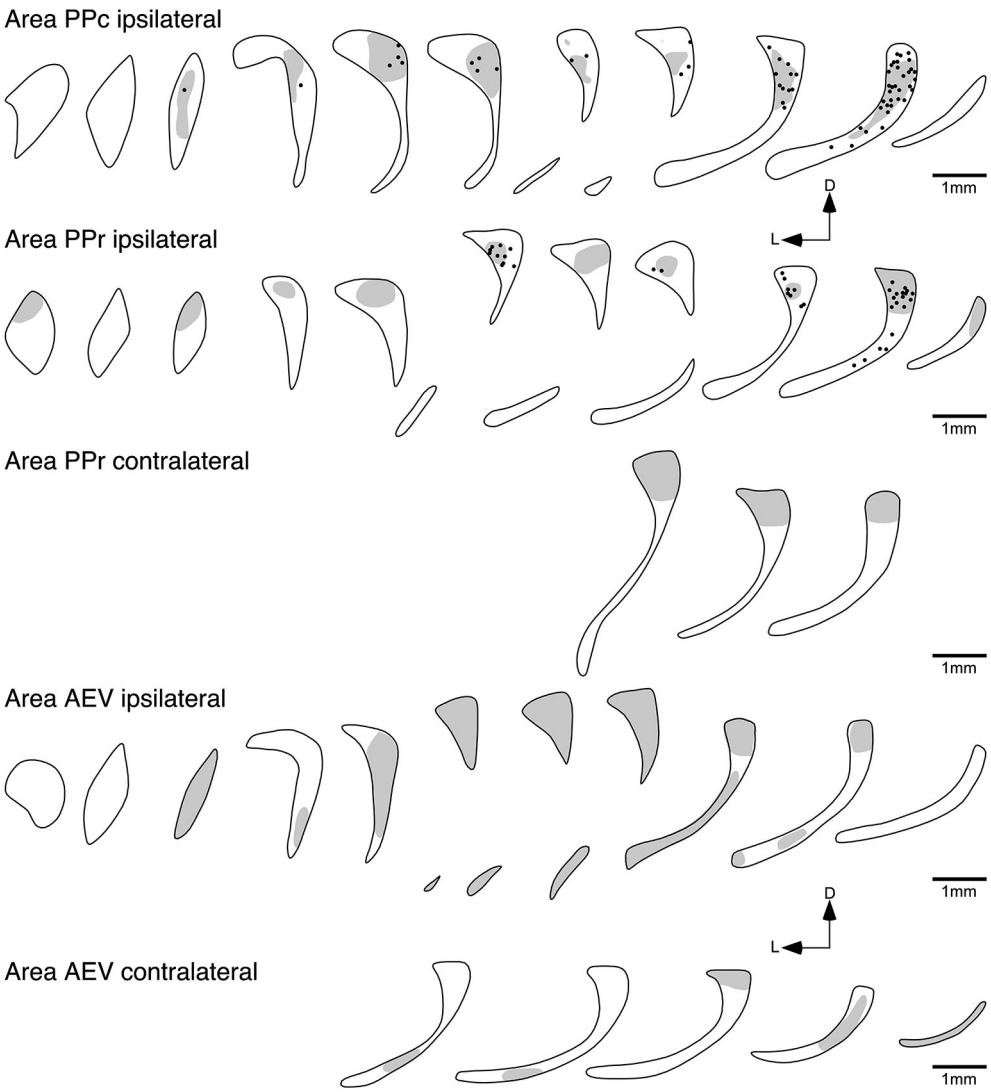

FIGURE 6 | Diagrammatic reconstructions of the ipsilateral and contralateral claustral connectivity following injections of biotinylated dextran amine into cortical visual areas PPc, PPr and AEV. Each figurine, which are spaced approximately 1 mm apart in the rostrocaudal plane, represents a coronal section through the claustrum (see **Figure 1**), with the rostral sections to the left and caudal sections to the right and for each figurine medial is to the right and dorsal to the top. In each figurine, the dots represent retrogradely labeled neurons, while the shading represents regions of labeled anterograde axonal terminals. Note the widespread ipsilateral reciprocal connectivity of areas PPc and PPr, the widespread ipsilateral anterograde connectivity of area AEV, with a small amount of contralateral anterograde connectivity following injections in areas PPr and AEV.

the ipsilateral claustrum. The rostral extent of the claustral projection zone was highest after injection into area 18, slightly smaller after injection into area 19, and occupied the caudoventral claustrum. The smallest projection zone was observed after injection into area 21, which was limited to the caudal part of the claustrum.

Several studies in the cat (Narkiewicz, 1964; Jayaraman and Updyke, 1979; LeVay and Sherk, 1981; Updyke, 1993; Jakubowska-Sadowska et al., 1998) indicate that the occipital visual areas projection zones in the claustrum are located in the dorsocaudal portion of the claustrum. This is more or less concurrent with the area 21 projection zone in the ferret, where at the most rostral region of connectivity labeled cell were found in the dorsal half of the claustrum. In contrast, visual projection zones of area 18 and 19 were located in the ventral portion of the ferret claustrum, and hence showed an inversion in comparison to the cat. In addition to the claustral connectivity inversion between the cat and the ferret, an inverted retinotopic organization of area 20a, 20b (Manger et al., 2004) and anteromedial lateral suprasylvian visual area (AMLS; Manger et al., 2008) has been observed in the ferret when compared to the cat. Moreover, the ferret retinotopic map within the lateral geniculate nucleus of the

thalamus seems to be rotated by approximately 90° in comparison to the cat (Bishop et al., 1968; Zahs and Stryker, 1985), while other visual areas including areas 17, 18, 19, posteromedial lateral suprasylvian visual area (PMLS) and AEV (Manger et al., 2002a, 2005; Cantone et al., 2006) show a similar retinotopy to the cat. Why the retinotopic organization of some of the visual cortical areas and claustral connectivity of ferret differs to those in cat and others not remains uncertain. A possible explanation was provided by Manger et al., 2008, postulating that depending on the developmental time point and maturation of the visual dorsal thalamus and the different cortical areas the retinotopic maps of certain cortical areas are inverted or not (for a detail explanation see Manger et al., 2008). How far this time-dependent developmental concept can be applied to the inverted occipital visual projection zones in the claustrum of ferret is not certain at the moment and requires further investigation.

CLAUSTROCORTICAL CONNECTIVITY TO THE TEMPORAL VISUAL AREAS 20a, 20b AND AEV

Areas 20a and 20b are functionally related and adjacent visual areas in the ferret temporal lobe. Nevertheless their claustral labeling showed very different patterns. Injection into area 20b resulted in the labeling of cell and axonal terminals in the caudal third of the ipsilateral claustrum, mostly located in the ventral half. In contrast no projection from the claustrum to area 20a was observed, but area 20a shows an extensive and widespread projection to the claustrum. Anterograde tracing studies with ^{3}H-proline in cats demonstrated terminal labeling in the dorsal portion of the claustrum after injection into areas 20a and 20b (LeVay and Sherk, 1981; Updyke, 1993), which agrees with our results after injection in to area 20b in the ferret; however, the terminal field in the claustrum after injection into area 20a in the ferret is more extensive than that seen in the cat. The absence of a claustral projection to area 20a appeared unusual, but this projection has not been analyzed in other animal and thus we cannot exclude that this projection in general exists, it may just be something specific to the ferret. Nevertheless the extensive presence of axon terminals and well-labeled cells following injections into nearby cortical areas makes it very unlikely that the absence of this claustro-area 20a was the result of a methodical problem. Similar to area 20a, AEV seems to project extensively to the entire extent of the contralateral claustrum in the ferret, and it similarly does not receive input from the claustrum. The unidirectional connectivity of areas 20a and AEV, clearly higher order visual areas forming part of the ventral processing stream, is in contrast to the occipital visual areas. It would then appear that these higher order visual areas influence claustral processing, while the claustrum does not directly influence their functionality. What affect this differential connectivity may have on neural processing in these visual areas and the claustrum is presently unknown.

CLAUSTROCORTICAL CONNECTIVITY TO THE PARIETAL VISUAL AREAS PPc AND PPr

PPc and PPr are functionally related visual areas located in the caudal parietal lobe. After injection into areas PPc and PPr labeled cells were found in the dorsal portion of the claustrum. To date a similar connectivity has been demonstrated for the owl monkey (Graham et al., 1979) but not in other species. Area PPc of the ferret seems to have a much broader claustral projection zone than area PPr, which only occupied the caudal third. Nevertheless the projection zone of axonal terminals was more expansive after injection into area PPr than area PPc.

CONNECTIVITY WITH THE CONTRALATERAL CLAUSTRUM

No visual cortical area studied herein was observed to receive projections from the contralateral claustrum. Interestingly, only areas PPr and AEV, arguably areas at the terminus of the dorsal and ventral cortical visual processing streams, revealed anterograde projections to the contralateral claustrum. Tracing studies in cats demonstrated that the contralateral claustrum is reciprocally connected to all visual areas studied to date, although these contralateral projections were reported to be far weaker than the ipsilateral ones (Norita, 1977; Squatrito et al., 1980; LeVay and Sherk, 1981; Macchi et al., 1981). It is not clear why in our study we only could visualize the projections from PPr and AEV to the contralateral claustrum; however, since our injection areas were relatively small, in order to avoid tracer spread to adjacent areas, it is possible that given the small amount of tracer it was not sufficient to visualize these rather weak projections. Jakubowska-Sadowska et al. (1998) also failed to visualize the bilateral projection of the claustrum, but they also argue that it is possibly related to small injection sites. Thus, the contralateral corticoclaustral connectivity might be very weak and require large amounts of tracer to be revealed. This indicates that the physiological effect of this connection on neural processing is likely not to be very significant.

SUMMARY

With the exceptions of areas AEV and 20a, all visual areas that we analyzed appear to be reciprocally connected with the ipsilateral claustrum and the highest density of retrogradely labeled cells were found in the caudal third of the claustrum. Previous studies on different animals (rat, cat, guinea pig, rabbit, Jakubowska-Sadowska et al., 1998; monkey, Graham et al., 1979; cat and baboon, Riche and Lanoir, 1978; cat, LeVay and Sherk, 1981) demonstrated cells projecting to lower order visual cortical areas in the caudal claustrum. Our data reveals that even if the higher order temporal and parietal visual areas have broader projection zones in the claustrum, the ferret caudal claustrum is particularly involved in visual information processing. This finding provides further evidence that the distribution of claustral projection zones along the rostrocaudal axis is phylogenetically stable (Mincinacchi et al., 1985; Jakubowska-Sadowska et al., 1998).

Previous studies have also demonstrated that cortico-claustral connectivity is reciprocal. This was the case for areas 18, 19, 21, PPc and 20b in the ferret, but areas PPr and AEV appear to be an exception to this general pattern of connectivity. Claustral projection neurons to area PPc were found in the caudal half of the claustrum, whereas area PPr seems to project to the entire claustrum. Moreover all higher order visual areas (PPr, PPc, 20a, AEV) studied herein, with the exception of 20b, appear to project, more or less, to the entire claustrum. This broad connectivity with the claustrum may be reflective of the complex types of neuronal information processed in higher order areas. Taken together our results suggest that lower order visual areas reveal more or less

clearly defined projection zones located in the caudal claustrum. In comparison to that higher order visual areas, even if not sending and/or receiving projection from the entire claustrum, show a more widespread claustral connectivity rather than a strictly defined projection zone. It would be of interest to compare or combine the results of the connectional studies provided herein with a proteomic redefinition of the claustrum in the ferret as previously done for the rat and monkey (Mathur et al., 2009).

REFERENCES

Ashwell, K. W., Hardman, C., and Paxinos, G. (2004). The claustrum is not missing from all monotreme brains. *Brain Behav. Evol.* 64, 223–241. doi: 10.1159/000080243

Bishop, P. O., Burke, W., and Davis, R. (1968). The identification of single units in central visual pathways. *J. Physiol.* 162, 409–431.

Butler, A. B., Molnár, Z., and Manger, P. R. (2002). Apparent absence of claustrum in monotremes: implications for forebrain evolution in amniotes. *Brain Behav. Evol.* 60, 230–240. doi: 10.1159/000066698

Cantone, G., Xiao, L., and Levitt, J. B. (2006). Retinotopic organization of ferret suprasylvian cortex. *Vis. Neurosci.* 23, 61–77. doi: 10.1017/s0952523806231067

Carey, R. G., and Neal, T. L. (1985). The rat claustrum: afferent and efferent connections with visual cortex. *Brain Res.* 329, 185–193. doi: 10.1016/0006-8993(85)90524-4

Carey, R. G., Bear, M. F., and Diamond, I. T. (1980). The laminar organization of the reciprocal projections between the claustrum and striate cortex in the tree shrew, *Tupaia glia*. *Brain Res.* 184, 193–198. doi: 10.1016/0006-8993(80)90597-1

Carey, R. G., Fitzpatrick, D., and Diamond, I. T. (1979). Layer I of striate cortex of *Tupaia glis* and *Galago senegalensis*: projections from thalamus and claustrum revealed by retrograde transport of horseradish peroxidase. *J. Comp. Neurol.* 186, 393–437. doi: 10.1002/cne.901860306

Carroll, E. W., and Wong-Riley, M. T. (1984). Quantitative light and electron microscopic analysis of cytochrome oxidase-rich zones in the striate cortex of the squirrel monkey. *J. Comp. Neurol.* 222, 1–17. doi: 10.1002/cne.902220102

Crick, F. C., and Koch, C. (2005). What is the function of the claustrum? *Philos. Trans. R. Soc. Lond. B Biol. Sci.* 360, 1271–1279. doi: 10.1098/rstb.2005.1661

Doty, R. W. (1983). Nongeniculate afferents to striate cortex in macaques. *J. Comp. Neurol.* 218, 159–173. doi: 10.1002/cne.902180204

Edelstein, L. R., and Denaro, F. J. (2004). The claustrum: a historical review of its anatomy, physiology, cytochemistry and functional significance. *Cell. Mol. Biol. (Noisy-le-grand)* 50, 675–702.

Fernández-Miranda, J. C., Rhoton, A. L., Kakizawa, Y., Choi, C., and Alvarez-Linera, J. (2008). The claustrum and its projection system in the human brain: a microsurgical and tractographic anatomical study. *J. Neurosurg.* 108, 764–774. doi: 10.3171/jns/2008/108/4/0764

Gallyas, F. (1979). Silver staining of myelin by means of physical development. *Neurol. Res.* 1, 203–209.

Graham, J., Lin, C. S., and Kaas, J. H. (1979). Subcortical projections of six visual cortical areas in the owl monkey, *Aotus trivirgatus*. *J. Comp. Neurol.* 187, 557–580. doi: 10.1002/cne.901870307

Hadley, R. T., and Trachtenberg, M. C. (1978). Poly-L-ornithine enhances the uptake of horseradish peroxidase. *Brain Res.* 158, 1–14. doi: 10.1016/0006-8993(78)90002-1

Innocenti, G. M., Manger, P. R., Masiello, I., Colin, I., and Tettoni, L. (2002). Architecture and callosal connections of visual areas 17, 18, 19 and 21 in the ferret (*Mustela putorius*). *Cereb. Cortex* 12, 411–422. doi: 10.1093/cercor/12.4.411

Jakubowska-Sadowska, K., Morys, J., Sadowski, M., Kowianski, P., Karwacki, Z., and Narkiewicz, O. (1998). Visual zone of the claustrum shows localizational and organizational differences among rat, guinea pig, rabbit and cat. *Anat. Embryol. (Berl)* 198, 63–72. doi: 10.1007/s004290050165

Jayaraman, A., and Updyke, B. V. (1979). Organization of visual cortical projections to the claustrum in the cat. *Brain Res.* 178, 107–115. doi: 10.1016/0006-8993(79)90091-x

Kennedy, H., and Bullier, J. (1985). A double-labeling investigation of the afferent connectivity to cortical areas V1 and V2 of the macaque monkey. *J. Neurosci.* 5, 2815–2830.

Kowianski, P., Dziewiatkowski, J., Kowianska, J., and Morys, J. (1999). Comparative anatomy of the claustrum in selected species: a morphometric analysis. *Brain Behav. Evol.* 53, 44–54. doi: 10.1159/000006581

Lent, R. (1982). The organization of subcortical projections of the hamster's visual cortex. *J. Comp. Neurol.* 206, 227–242. doi: 10.1002/cne.902060303

LeVay, S. (1986). Synaptic organization of claustral and geniculate afferents to the visual cortex of the cat. *J. Neurosci.* 6, 3564–3575.

LeVay, S., and Sherk, H. (1981). The visual claustrum of the cat. I. Structure and connections. *J. Neurosci.* 1, 956–980.

Macchi, G., Bentivoglio, M., Minciacchi, D., and Molinari, M. (1981). The organization of the claustroneocortical projections in the cat studied by means of the HRP retrograde axonal transport. *J. Comp. Neurol.* 195, 681–695. doi: 10.1002/cne.901950411

Manger, P. R., Engler, G., Moll, C. K., and Engel, A. K. (2005). The anterior ectosylvian visual area of the ferret: a homologue for an enigmatic visual cortical area of the cat? *Eur. J. Neurosci.* 22, 706–714. doi: 10.1111/j.1460-9568.2005.04246.x

Manger, P. R., Engler, G., Moll, C. K., and Engel, A. K. (2008). Location, architecture, and retinotopy of the anteromedial lateral suprasylvian visual area (AMLS) of the ferret (*Mustela putorius*). *Vis. Neurosci.* 25, 27–37. doi: 10.1017/s0952523808080036

Manger, P. R., Kiper, D., Masiello, I., Murillo, L., Tettoni, L., Hunyadi, Z., et al. (2002a). The representation of the visual field in three extrastriate areas of the ferret (*Mustela putorius*) and the relationship of retinotopy and field boundaries to callosal connectivity. *Cereb. Cortex* 12, 423–437. doi: 10.1093/cercor/12.4.423

Manger, P. R., Masiello, I., and Innocenti, G. M. (2002b). Areal organization of the posterior parietal cortex of the ferret (*Mustela putorius*). *Cereb. Cortex* 12, 1280–1297. doi: 10.1093/cercor/12.12.1280

Manger, P. R., Nakamura, H., Valentiniene, S., and Innocenti, G. M. (2004). Visual areas in the lateral temporal cortex of the ferret (*Mustela putorius*). *Cereb. Cortex* 14, 676–689. doi: 10.1093/cercor/bhh028

Mathur, B. N., Caprioli, R. M., and Deutch, A. Y. (2009). Proteomic analysis illuminates a novel structural definition of the claustrum and insula. *Cereb. Cortex* 19, 2372–2379. doi: 10.1093/cercor/bhn253

Mincinacchi, D., Molinari, M., Bentivoglio, M., and Macchi, G. (1985). The organization of the ipsi- and contralateral claustrocortical system in rat with notes on the bilateral claustrocortical projections in cat. *Neuroscience* 16, 557–576. doi: 10.1016/0306-4522(85)90192-7

Mizuno, N., Uchida, K., Nomura, S., Nakamura, Y., Sugimoto, T., and Uemura-Sumi, M. (1981). Extrageniculate projections to the visual cortex in the macaque monkey: an HRP study. *Brain Res.* 212, 454–459. doi: 10.1016/0006-8993(81)90477-7

Narkiewicz, O. (1964). Degenerations in the claustrum after regional neocortical ablations in the cat. *J. Comp. Neurol.* 123, 335–355. doi: 10.1002/cne.901230304

Norita, M. (1977). Demonstration of bilateral claustro-cortical connections in the cat with the method of retrograde axonal transport of horseradish peroxidase. *Arch. Histol. Jpn.* 40, 1–10. doi: 10.1679/aohc1950.40.1

Olson, C. R., and Graybiel, A. M. (1980). Sensory maps in the claustrum of the cat. *Nature* 288, 479–481. doi: 10.1038/288479a0

Perkel, D. J., Bullier, J., and Kennedy, H. (1986). Topography of the afferent connectivity of area 17 in the monkey: a double-labelling study. *J. Comp. Neurol.* 253, 374–402. doi: 10.1002/cne.902530307

Reynhout, K., and Baizer, J. S. (1999). Immunoreactivity for calcium-binding proteins in the claustrum of the monkey. *Anat. Embryol. (Berl)* 199, 75–83. doi: 10.1007/s004290050211

Riche, D., and Lanoir, J. (1978). Some claustro-cortical connections in the cat and baboon as studied by retrograde horseradish peroxidase transport. *J. Comp. Neurol.* 177, 435–444. doi: 10.1002/cne.901770306

Shameem, N., Sanderson, K., and Dreher, B. (1984). Claustral afferents to the rat's visual cortex. *Neurosci. Lett.* 49, 247–252. doi: 10.1016/0304-3940(84)90297-0

Sherk, H. (1986). Location and connections of visual cortical areas in the cat's suprasylvian sulcus. *J. Comp. Neurol.* 247, 1–31. doi: 10.1002/cne.902470102

Sloniewski, P., Usunoff, K. G., and Pilgrim, C. (1986). Retrograde transport of fluorescent tracers reveals extensive ipsi- and contralateral claustrocortical connections in the rat. *J. Comp. Neurol.* 246, 467–477. doi: 10.1002/cne.902460405

Squatrito, S., Battaglini, P. P., Galleti, C., and Riva Sansaverini, E. (1980). Autoradiographic evidence for projections from cortical visual areas 17, 18, 19 and the Clare-Bishop area to the ipsilateral claustrum in the cat. *Neurosci. Lett.* 19, 265–269. doi: 10.1016/0304-3940(80)90271-2

Tanné-Gariépy, J., Boussaoud, D., and Rouiller, E. M. (2002). Projections of the claustrum to the primary motor, premotor, and prefrontal cortices in the macaque monkey. *J. Comp. Neurol.* 454, 140–157. doi: 10.1002/cne.10425

Updyke, B. V. (1993). Organization of visual corticostriatal projections in the cat, with observations on visual projections to claustrum and amygdala. *J. Comp. Neurol.* 327, 159–193. doi: 10.1002/cne.903270202

Zahs, K. R., and Stryker, M. P. (1985). The projection of the visual field onto the lateral geniculate nucleus of the ferret. *J. Comp. Neurol.* 241, 210–224. doi: 10.1002/cne.902410208

Conflict of Interest Statement: The authors declare that the research was conducted in the absence of any commercial or financial relationships that could be construed as a potential conflict of interest.

Received: 16 January 2014; accepted: 11 February 2014; published online: 28 February 2014.

Citation: Patzke N, Innocenti GM and Manger PR (2014) The claustrum of the ferret: afferent and efferent connections to lower and higher order visual cortical areas. Front. Syst. Neurosci. ***8****:31. doi: 10.3389/fnsys.2014.00031*

This article was submitted to the journal Frontiers in Systems Neuroscience.

frontiers in
SYSTEMS NEUROSCIENCE

ORIGINAL RESEARCH ARTICLE
published: 28 March 2014
doi: 10.3389/fnsys.2014.00042

The claustrum of the bottlenose dolphin *Tursiops truncatus* (Montagu 1821)

Bruno Cozzi[1]*, Giulia Roncon[1], Alberto Granato[2], Maristella Giurisato[1], Maura Castagna[3], Antonella Peruffo[1], Mattia Panin[1], Cristina Ballarin[1], Stefano Montelli[1] and Andrea Pirone[4]

[1] Department of Comparative Biomedicine and Food Science, University of Padova, Legnaro, Italy
[2] Department of Psychology, Catholic University, Milan, Italy
[3] Department of Translational Research on New Technologies in Medicine and Surgery, University of Pisa, Pisa, Italy
[4] Department of Veterinary Sciences, University of Pisa, Pisa, Italy

Edited by:
Brian N. Mathur, University of Maryland School of Medicine, USA

Reviewed by:
Preston E. Garraghty, Indiana University, USA
Stefan Huggenberger, University of Cologne, Germany

***Correspondence:**
Bruno Cozzi, Department of Comparative Biomedicine and Food Science, University of Padova, Viale dell'Università 16, 35020 Legnaro, Italy
e-mail: bruno.cozzi@unipd.it

The mammalian claustrum is involved in processing sensory information from the environment. The claustrum is reciprocally connected to the visual cortex and these projections, at least in carnivores, display a clear retinotopic distribution. The visual cortex of dolphins occupies a position strikingly different from that of land mammals. Whether the reshaping of the functional areas of the cortex of cetaceans involves also modifications of the claustral projections remains hitherto unanswered. The present topographic and immunohistochemical study is based on the brains of eight bottlenose dolphins and a wide array of antisera against: calcium-binding proteins (CBPs) parvalbumin (PV), calretinin (CR), and calbindin (CB); somatostatin (SOM); neuropeptide Y (NPY); and the potential claustral marker Gng2. Our observations confirmed the general topography of the mammalian claustrum also in the bottlenose dolphin, although (a) the reduction of the piriform lobe modifies the ventral relationships of the claustrum with the cortex, and (b) the rotation of the telencephalon along the transverse axis, accompanied by the reduction of the antero-posterior length of the brain, apparently moves the claustrum more rostrally. We observed a strong presence of CR-immunoreactive (-ir) neurons and fibers, a diffuse but weak expression of CB-ir elements and virtually no PV immunostaining. This latter finding agrees with studies that report that PV-ir elements are rare in the visual cortex of the same species. NPY- and somatostatin-containing neurons were evident, while the potential claustral markers Gng2 was not identified in the sections, but no explanation for its absence is currently available. Although no data are available on the projections to and from the claustrum in cetaceans, our results suggest that its neurochemical organization is compatible with the presence of noteworthy cortical inputs and outputs and a persistent role in the general processing of the relative information.

Keywords: claustrum, bottlenose dolphin, calcium binding proteins, NPY, somatostatin, insular cortex

INTRODUCTION

Dolphins (Delphinidae) are carnivore marine mammals belonging to the Infraorder Odontoceti (toothed whales). Together with the Infraorder Mysticeti (baleen whales) toothed whales belong to the taxon Cetacea which is today grouped together with Artiodactyla (even-toed hooved mammals) into the single order Cetartiodactyla (Geisler and Uhen, 2005; Thewissen et al., 2007). This relationship may explain some of their anatomical conformities and common evolutionary adaptations with domestic animals like the cow and the pig (for general reference see Slijper, 1979). However the brain of dolphins possesses some strikingly unique features, including compression of the longitudinal axis and expansion of the temporal width, pronounced rotation along the transverse (inter-insular) axis, essential absence of the olfactory lobe and nerves, intense folding of the cerebral cortex accompanied by reduced thickness, and general uniformity of columnar organization in the different topographical areas. On the other hand, the virtual absence of a typical layer IV in cetaceans (for a comprehensive review see Manger, 2006) is common also to other Cetartiodactyla and Ungulates in general (Hof et al., 1999, 2000). Physiological studies on brain functions and internal connections are obviously restricted by ethical reasons and by the consequent limited number of published studies. However, a review of the available information suggests that functional localizations differ from terrestrial mammals (Oelschläger and Oelschläger, 2009). The visual cortex is not located in the occipital pole, but shifted dorsally and placed longitudinally, separated from the inter-hemispheric scissure by the peculiar paralimbic lobe, and accompanied laterally by the elongated acoustic cortex (Lende and Akdikmen, 1968; Kesarev and Malofeeva, 1969; for review see Morgane et al., 1986). Motor and somatosensory cortices are pushed rostrally almost entirely on the frontal aspect of the

brain, in relation also to the particularly advanced position of the cruciate sulcus (Lende and Akdikmen, 1968; Kesarev and Malofeeva, 1969).

The claustrum is considered to be reciprocally connected to several cortical areas, and to possess direct involvement in the processing of sensorimotor information (Crick and Koch, 2005), with a special relationship to the visual cortex in the cat (Olson and Graybiel, 1980; Minciacchi et al., 1995) and monkey (Remedios et al., 2010). The topographic shift of the dolphin visual cortex to a location parallel to the inter-hemispheric cleft, and the profound modifications of several modalities of somatosensory inputs (i.e., related to the virtual absence of taste buds in the tongue, reduction of the hand, and disappearance of the hind limb) suggest possible functional adaptative modifications of the claustrum. The claustrum of dolphins (and cetaceans in general) has never been specifically described, although references to its position and relationship with the complex insular cortex and pocket (Jacobs et al., 1984) indicate a predominance of the infrainsular part, corresponding to the central core of the insular cortex in parasagittal section. In fact the same authors report that in the posterior and dorsal insular regions of the bottlenose dolphin (*Tursiops truncatus*), the claustrum is "either absent or present as a discontinuous cell band beneath the insular cortex", and in their study the diagrams show a close proximity, if not contiguity, of the ventral claustrum with the sylvian cleft in the more caudal extension (Jacobs et al., 1984). The contiguity of the cetacean claustrum with the cerebral cortex was noted by other authors in the harbor porpoise (Jelgersma, 1934) and reported in a comprehensive review (Jansen and Jansen, 1969).

In the present study we intend to investigate the topography and selected neurochemical characteristics of the claustrum in the bottlenose dolphin, the most widely studied member of the Family Delphinidae. The neurochemical organization of the claustrum, as defined by the expression of calcium-binding proteins (CBPs), selected modulators (neuropeptide Y, NPY; somatostatin, SOM), and the recognized claustral marker Gng2 (Mathur et al., 2009) may help understand whether this structure maintains in dolphins the organization now considered typical of terrestrial mammals, and whether its neurochemical characteristics are similar to those of other mammalian models.

MATERIALS AND METHODS

TISSUE SAMPLES

In this study we used samples of the claustrum obtained from the brains of eight bottlenose dolphins (see **Table 1**) stored in the *Mediterranean marine mammal tissue bank* (MMMTB) of the University of Padova at Legnaro, Italy. The MMMTB is a CITES recognized (IT020) research center and tissue bank (Ballarin et al., 2005), sponsored by the Italian Ministry of the Environment and the University of Padova, with the aim of harvesting tissues from wild and captive cetaceans and distributing them to qualified research centers worldwide.

Tissue samples consisted of blocks approximately 1 cm thick, including the claustrum, surrounded by portions of the adjoining structures (extreme and external capsules, insular cortex, putamen), carefully dissected (**Figure 1**) during post-mortem procedures performed in the necropsy room of the Department of Comparative Biomedicine and Food Science of the University of Padova at Legnaro. Post-mortem delay before actual sampling varied between 18 and 40 h. The samples were fixed by immersion in 4% buffered formalin, washed in phosphate saline buffer (PBS) 0.1 M, pH 7.4 and subsequently either processed for paraffin embedding or frozen by immersion in liquid nitrogen-chilled isopentane at −30°C. Sections were cut either with a microtome (6 μm) or a cryostat (20 μm) and subsequently processed for immunohistochemistry (see below). For each tissue block, one section out of ten was treated for Nissl stain for general outline, reference and topography.

Table 1 | Details of the sampled bottlenose dolphins.

Specimen	Sex	Origin	Age (years)/length/weight	Formalin	Frozen
ID # 95	F	wild	11 (pregnant adult)/285 cm		x
ID # 107	M	captive	9 /250 cm	x	x
ID # 110	M	wild	>2/190 cm /74 kg		x
ID # 114	M	captive	newborn/115 cm	x	
ID # 133	F	captive	adult (age uncertain) /248 cm	x	
ID # 139	M	captive	12 /268 cm/198 kg	x	x
ID # 146	M	captive	3.5/226 cm	x	
ID # 159	M	captive	>40 /328 cm	x	

IMMUNOHISTOCHEMISTRY

A rabbit polyclonal anti-calretinin (CR) antibody (sc-50453; Santa Cruz Biotech., Inc., Santa Cruz, CA; dilution 1:200), a mouse monoclonal anti-parvalbumin (PV) antibody (Clone PA-235, Cat. # P-3171; Sigma-Aldrich, St. Louis, MO, USA; dilution

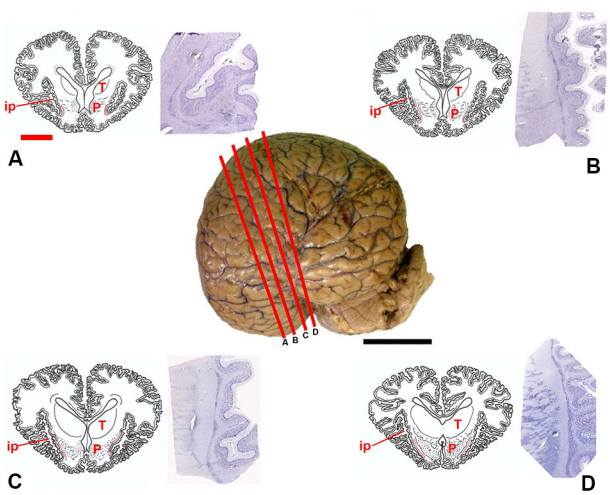

FIGURE 1 | Position of the claustrum in *Tursiops truncatus*. Center, lateral photograph of the adult brain; the orange bars **(A–D)** approximate the levels of subsequent sections. The drawings **(A–D)** are based on composite renderings of coronal sections of the dolphin brain, sided by Nissl preparations obtained approximately at the corresponding levels. In the drawings the claustrum is represented by a thin red line. Note the reduction of the endopiriform cortex ventral to the basal ganglia; P, putamen; T, thalamus; ip, insular pocket. Black scale bar (lateral photograph of the dolphin brain) = 5 cm; orange scale bar (drawings) = 2 cm.

1:3000), a mouse monoclonal anti-calbindin-D-28K (CB) antibody (Clone CB-955, Cat. # C9848, Sigma-Aldrich, St. Louis, MO, USA; dilution 1:3000), a rabbit polyclonal anti-CB-D-28K antibody (Cat. # CB38A, Swant, Bellinzona, Switzerland; diluition 1:10000), a rabbit polyclonal anti-NPY antibody (ab30914; abcam; dilution 1:3000), a rabbit polyclonal anti-Gng2 antibody (HPA003534; Sigma-Aldrich, dilution 1:100), and a rabbit polyclonal anti-SOM antibody (ab103790; abcam; dilution 1:700) were used in this study. Epitope retrieval was carried out at 120°C in a pressure cooker for 5 min using a Tris/EDTA buffer pH 9.0. Sections were rinsed in PBS and incubated in 1% H_2O_2-PBS for 10 min, then pre-incubated in PBS with 0.3% Triton X-100 (TX) (Sigma-Aldrich, St. Louis, MO, USA) and 5% normal goat serum (Vector Labs, Burlingame, CA) to reduce non-specific staining. Sections were subsequently incubated overnight in a humid chamber at 4°C with the primary antibody diluted in PBS with 0.3% TX and 1% normal goat serum. After several washings in PBS, sections were incubated for 1 h at room temperature with biotinylated goat anti-rabbit (for CR, NPY and SOM) or biotinylated goat anti-mouse secondary antibodies (for PV and CB) (Vector Labs, Burlingame, CA), diluted 1:300 in PBS. Sections were then washed for 3 × 10 min in PBS, and incubated for 1 h at room temperature in avidinbiotin-horseradish peroxidase complex (PK-6100; Vector Labs, Burlingame, CA). After washing for 3 × 10 min in Tris/HCl (pH 7.6), peroxidase activity was detected by incubation in a solution of 0.125 mg/ml diaminobenzidine (Sigma-Aldrich, St. Louis, MO, USA) and 0.1% H_2O_2 in the same buffer for 10 min or by a VIP substrate Kit for peroxidase (Cat. # SK-4600, Vector Labs, Burlingame, CA).

The amino acid sequence of the proteins investigated in this article in the claustrum of *Tursiops truncatus* were compared with those of other mammals (and especially the rat). For this aim we used the Ensembl genomic database.[1] The sequence of NPY, SOM, CB and CR is shared for over 93%, whereas correspondence for Gng2 and PV is over 70%. The specificity of the immunohistochemical staining was tested in repeated trials as follows: substitution of either the primary antibody, the anti-rabbit or anti-mouse IgG, or the ABC complex by PBS or non-immune serum. Under these conditions the staining was abolished.

RESULTS

GENERAL TOPOGRAPHY AND SHAPE

Based on the examinations of macroscopic slices of the brain, followed by analysis of Nissl-stained sections, the claustrum was detected in all the examined specimens, including newborns. The topography of the claustrum observed in our experimental series reflects the general orientation of the dolphin brain, in which the lateral (temporal) lobes grow considerably, and the lower (partially olfactory) divisions of the telencephalon are reduced. The position of the claustrum was clearly identified lateral to the conspicuous putamen and medial to the insular formation and relative insular pocket (**Figure 1**).

In Nissl-stained sections the claustrum appeared thin (not thicker than 1–2 mm) and dorso-ventrally elongated (up to 3.5 cm), without an evident endopiriform root as commonly found in terrestrial mammals. The ventralmost limits of the claustrum apparently touch the insular cortex with virtual disappearance of the *capsula extrema*.

IMMUNOHISTOCHEMICAL DATA

Calretinin

In our experimental series, we observed a strong presence of CR-immunoreactive (-ir) neurons and fibers, both in paraffin-embedded (**Figures 2A–E**) and frozen sections (**Figures 2F, G**). Positive cells appeared as mono- and bi-polar small (approx. 10 μm) neurons, with a round or fusiform soma. The morphology of CR-ir neurons in the claustrum was very different from that of the typical CR-ir neurons in the cortical columns of the adjacent insula (**Figure 2E**).

The distribution of CR-ir elements (**Figures 2H–J**) did not show any specific segregation and the neurons were diffuse in all the parts of the claustrum, although immunostained cells were scarcer at its dorsal and ventral extremities.

Calbindin

The examined sections showed a diffuse but weak expression of CB-ir elements (**Figures 3A–C**). The few positive elements displayed a small (approx. 10 μm) mono- or bipolar soma. Positive fibers were evident throughout the claustrum.

Parvalbumin

The immunostaining for PV revealed no positive cell or fiber in the claustrum of all the animals examined.

Neuropeptide Y

The whole length of the claustrum is crossed by a mesh of NPY-ir beaded nerve fibers (**Figures 4A, B**), with some unipolar, pseudo-unipolar, and multipolar small-medium (15–20 μm) neurons (**Figures 4C, D**). In cryostat cut sections some of these neurons displayed a well-ramified dendrite arborization (**Figures 4E, F**). Also the distribution of NPY-ir elements (**Figures 4G–I**) did not show any specific segregation, although immunostained cells were scarcer at the dorsal and ventral extremities of the claustrum.

Somatostatin

In our experimental series, we identified a few SOM-ir neurons in the claustrum (**Figure 5**). Immunostained elements appeared either as slender bipolar neurons or spherical, with medium dimensions (approx. 20–25 μm). Fibers were rare.

Gng2

In our experimental series the claustral marker Gng2 was not identified in any cell or fiber of the claustrum or adjacent brains structures.

DISCUSSION

The position and relationships of the claustrum in the bottlenose dolphin described here is based on the analysis of macroscopic brain slices and Nissl stained sections. The location of the claustrum (**Figure 6**) reflects the changes in the general outline of the

[1] www.ensembl.org

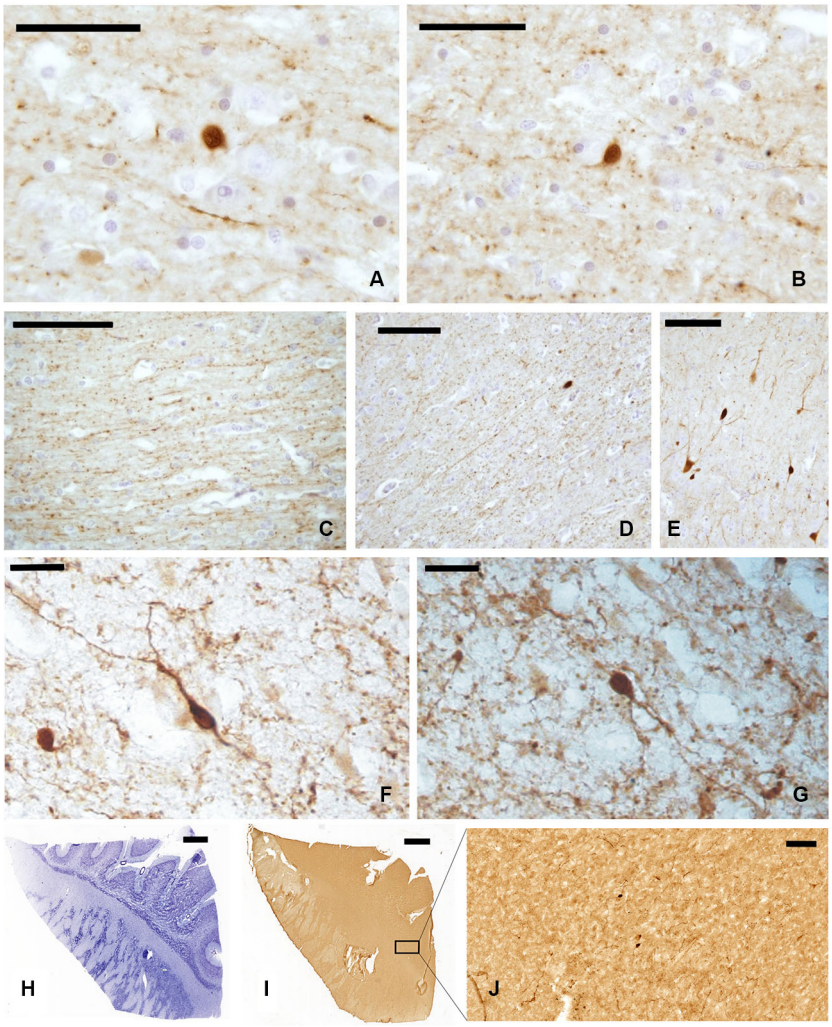

FIGURE 2 | CR-ir neurons and fibers in the claustrum. **(A–D)** Images derive from paraffin-embedded sections. **(A, B)** Small unipolar neurons surrounded by beaded fibers; **(C, D)** several CR-ir beaded fibers cross the whole length of the claustrum. **(E)** CR-ir neurons in the insular cortex. **(F, G)** Immunostained neurons in frozen sections; **(H–J)** localization of CR-ir neurons in whole sections (**(H)** Nissl stain, **(I–J)** immunocytochemistry); **J** represent an enlargement of the black rectangle in **I** Scale bars: **A, B** = 50 μm; **C, D, E, J** = 100 μm; **F, G** = 20 μm; **H, I** = 2 mm.

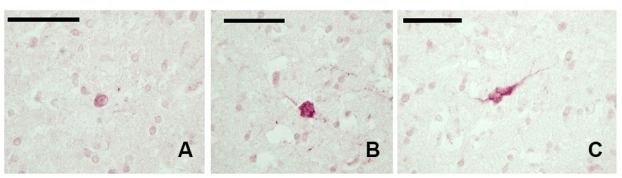

FIGURE 3 | CB-ir neurons in the claustrum. (A–C) Immunoreactive neurons in paraffin-embedded sections. Scale bars etc.

brain and consequently the modifications of its internal organization and topography. The absence of a complete endopiriform cortex as such (due to the lack of olfactory bulbs and related structures) limits the development of the so-called "endopiriform" part of the claustrum, and modifies its ventral outline. The rostro-ventral part of the dolphin claustrum surrounds the ventral borders of the insular pocket, but shows no medial projections towards the midsagittal plane as in terrestrial mammals including man. The extreme reduction of the Ammon's horn and the hippocampal formation in general (Morgane et al., 1982), sensibly changes the disposition of ventro-lateral structures in the temporal lobe, and their reciprocal relationships. In man and other primates the caudalmost part of the claustrum terminates dorsal to the tail of the caudate nucleus and the hippocampus. This latter disposition is absent in the dolphin, in which the pronounced rotation of cerebral components along the transverse (inter-insular) axis (**Figure 1**; for detailed description and an interpretation see Morgane et al., 1980), and the reduction of olfaction-related limbic structures places the caudal extremity of the claustrum more anteriorly (see **Figure 6**). In a dated but well known review on the cetacean nervous system (Jansen and Jansen,

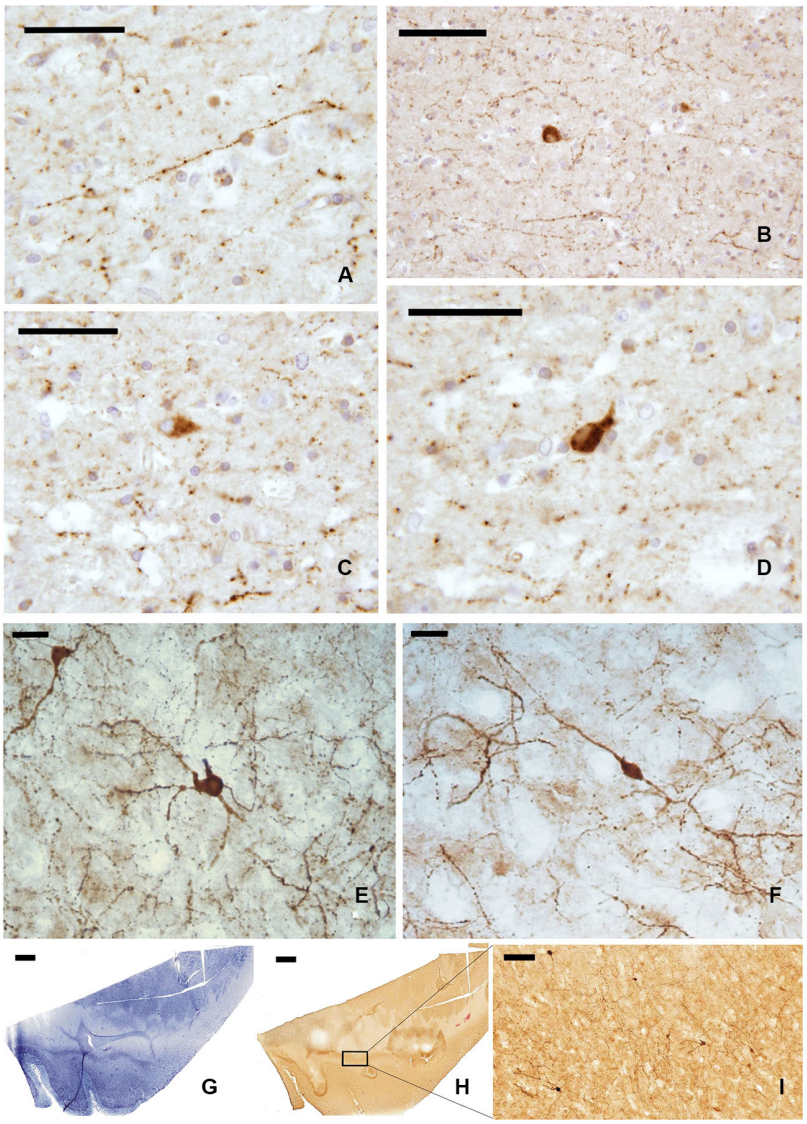

FIGURE 4 | NPY-ir fibers (A, B) and neurons (C, D) in paraffin-embedded sections of the claustrum; (E, F) NPY positive neurons in frozen sections; (G–I) localization of NPY-ir neurons in whole sections ((G) Nissl stain, (H–I) immunocytochemistry); I represent an enlargement of the black rectangle in H. Scale bars = **A, C, D** = 50 μm; **B, I** = 100 μm; **E, F** = 20 μm;. **G, H** = 2 mm.

1969), it was noted that "the claustrum extends rostrolaterally beyond the limits of the putamen", with reference to the harbor porpoise (Jelgersma, 1934). The disposition of the claustrum that we describe here in *Tursiops truncatus* overlaps what reported for the common dolphin *Delphinus delphis*, at least based on a series of transverse sections of the brain (Pilleri et al., 1980).

Our data confirm what was reported in the drawings of the seminal paper on the bottlenose dolphin insula by Jacobs et al. (1984), in which the ventral extremity of the claustrum is attached to the insular cortex and the opercular gyri at the level of the insular pocket. We also noted contiguity between the insular cortex and the ventral extremity of the claustrum. We emphasize this topographical relationship in view of its ontogenetic significance for the origin of the claustrum. As well known, the claustrum may derive from (a) the putamen and basal ganglia; (b) the insular cortex; or possibly (c) a combination of both (Edelstein and Denaro, 2004). A recent study (Pirone et al., 2012), performed on post-mortem human brains, identified the presence of a potential claustral marker, the protein Gng2, formerly developed in rodents (Mathur et al., 2009), in the insular cortex and claustrum, but not in the putamen, thus suggesting a possible common origin of the former two structures. There is presently no information on how much the structure of Gng2 is conservative among mammals, and the eventual presence of different isoforms of this protein in cetaceans may explain the lack of immunoreactivity in our experimental series. However, contiguity between cortex and claustrum, as we observed in the bottlenose dolphin, may reinforce the insular hypothesis.

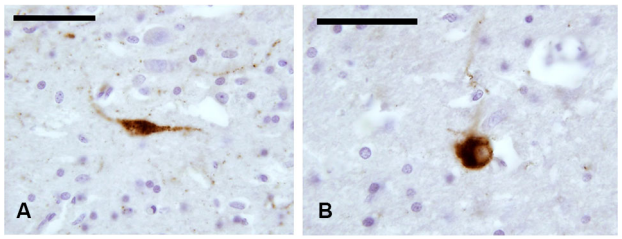

FIGURE 5 | SOM-ir fibers and neurons in the claustrum. (A–B) Images from paraffin-embedded sections. Scale bars etc.

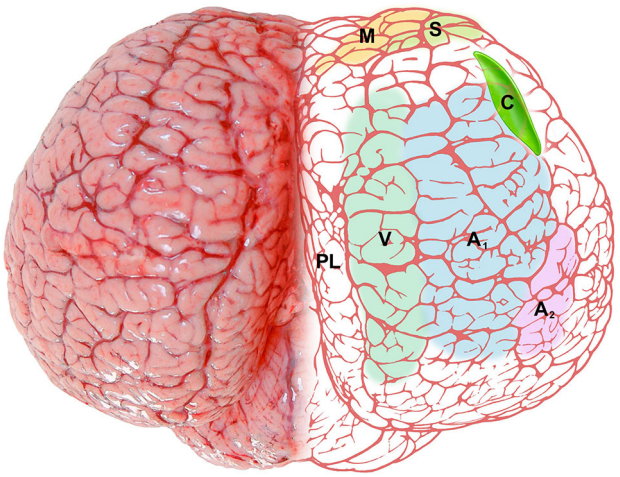

FIGURE 6 | Schematic representation of the claustrum (C, bright green) of the bottlenose dolphin shown through the dorsal aspect of the brain. The pale colors on the right side represent functional areas of the cortex: M (yellow), motor cortex; S (green), somatosensory cortex; V (gray-green), visual cortex; A_1 (pale blue), primary auditory cortex; A_2 (pale pink), secondary auditory cortex; PL (no color), paralimbic lobe.

The presence of CBPs in the claustrum has been described in several mammalian species (Reynhout and Baizer, 1999; Ángeles Real et al., 2003; Wojcik et al., 2004; Rahman and Baizer, 2007), and a recent detailed study reports the distribution of PV in the human claustrum (Hinova-Palova et al., 2013). Former studies on the distribution of CBPs in the auditory and visual cortex of the bottlenose dolphin (Glezer et al., 1995, 1998) identified only very few PV-ir neurons, contrarily to what observed in the macaque *Macaca fascicularis*, in which PV was present or even prevalent in both systems. Furthermore, PV-ir neurons in the visual cortex of selected cetacean species were scarce except in layers IIIc/V and VI (Glezer et al., 1993). On the other hand, the GABA component seems not different between cetaceans and terrestrial mammals (Garey et al., 1989). Our data indicate that PV is not expressed in the claustrum of the bottlenose dolphin, a fact that may be related to the paucity of PV-ir neurons in the visual cortex of the same species described in the reports cited above. Considering that the PV amino acid sequence in dolphins shows a 70% identity with the corresponding protein of terrestrial mammals, additional studies are required to further clarify this issue and its important implications in terms of claustro-visual projections. However we'd like to emphasize that our experimental procedures were performed under the same conditions applied in our laboratory to the primate claustrum in which a clear, well evident presence of a network of PV-containing elements was observed (data not shown), even when the brains suffered a post-mortem interval prior to sampling possibly longer than that of the bottlenose dolphins described here.

CR-ir neurons were described in the visual cortex of *Tursiops truncatus* (Glezer et al., 1992) and CR- and CB-ir neurons were identified especially in the auditory system of the same species (Reynhout and Baizer, 1999). In our series mono- or bi-polar neurons CR-ir were easily identified in the claustrum, and a few CB-ir neurons were also evident. The dorsal claustrum receives important visual projections from the occipital cortex in the cat (LeVay and Sherk, 1981), while the visual claustrum is instead ventral in primates (Remedios et al., 2010). The apparent reduction of the ventral part of the claustrum that takes place in the bottlenose does not imply curtailed visual projections, but may simply reflect a different topography of visual inputs/outputs as reported in other species. We emphasize here that the dolphin visual cortex shifts dorsally (see **Figure 6**), and a re-shaping of the internal organization of the claustrum may be plausible, with the visual domains potentially moving dorsally within the nucleus. The visual cortex of the dolphins shows a specific organization, containing both a heterolaminar part/component, with an incipient layer IV, and a homolaminar one, where layer IV is absent, as elsewhere in the cortex (Morgane et al., 1988), a feature typical of Cetartiodactyla (Hof et al., 1999, 2000). The mostly agranular visual cortex of the bottlenose dolphin has been discussed in details (Garey et al., 1985; Morgane et al., 1990), but its projections remain undetected. In a retrograde tracer study performed on *Phocoena phocoena* (Revishchin and Garey, 1990), the visual cortex was found to project to the lateral geniculate nucleus and inferior pulvinar, but no connection was precisely identified outside the thalamus. We note here that PV-ir elements are particularly abundant in layer IV of the somatosensory and auditory cortices of several mammalian orders (Sherwood et al., 2009), but CR and CB are the predominant CBPs in the Cetartiodactyla cortex (Hof et al., 1999, 2000), lacking layer IV. Our data indicate that in the bottlenose dolphin CR is the prevalent CBP in the claustrum, thus suggesting its potential role for reciprocal claustro-cortical connections.

The cellular types that we illustrate here correspond to those described in other species (for review see Edelstein and Denaro, 2004). NPY and SOM are expressed in neurons of the primate (Smith et al., 1985) and rodent claustrum (Kowiański et al., 2008). Due to the plausible common origin of claustrum and insular cortex (Pirone et al., 2012), we can only speculate that claustral and cortical interneurons may play similar functional roles. In the neocortex, Martinotti cells, which target the apical tuft of pyramidal dendrites, express SOM (Markram et al., 2004). Similarly, NPY expressing neurons are able to modulate Ca^{2+}-dependent currents in the distal dendrites in pyramidal neurons (Hamilton et al., 2013). On the contrary, PV interneurons mainly

target the soma and proximal dendrites of principal neurons (Markram et al., 2004). Therefore, given the presence of NPY and SOM interneurons in the dolphin claustrum, along with the absence of PV, it is possible that the cetacean claustrum might display a prevalence of interneurons with putative synapses onto distal dendrites of projecting neurons. The functional significance of this peculiar feature would deserve further examination.

Our observations confirmed the general outline of the mammalian claustrum also in the bottlenose dolphin, even if the reduction of the piriform lobe modifies the ventral relationships with the cortex.

Although no data are available on the projections to and from the claustrum in cetaceans, our results provide evidence that its neurochemical organization is compatible with the presence of cortical inputs and outputs and a persistent role in the general processing of the relative information. PV-containing interneurons, absent in the claustrum of the bottlenose dolphin, are important fast-spiking elements in the cortex (Moore et al., 2010) and neostriatum (Tepper et al., 2004). Whether the particular display of CBPs in the dolphin claustrum may be functionally related to the structural organization of the cortex (Morgane and Jacobs, 1972; Kern et al., 2011); to the shift in the functional areas (Oelschläger and Oelschläger, 2009); to the virtual absence of binocular vision and the fact that the retina projects almost exclusively to the contralateral hemisphere (Ridgway, 1990; Tarpley et al., 1994); or to the peculiar mono-hemispheric sleep pattern (Mukhametov et al., 1977; see Lyamin et al., 2008 for a recent review), awaits further verification.

ACKNOWLEDGMENTS

The Authors willingly acknowledge the precious contribution of Massimo Demma who drew the three-dimensional image of the dolphin brain represented in **Figure 6**.

REFERENCES

Ángeles Real, M., Dávila, J. C., and Guirado, S. (2003). Expression of calcium-binding proteins in the mouse claustrum. *J. Chem. Neuroanat.* 25, 151–160. doi: 10.1016/s0891-0618(02)00104-7

Ballarin, C., Papini, L., Bortolotto, A., Butti, C., Peruffo, A., Sassu, R., et al. (2005). An on-line bank for marine mammals of the Mediterranean Sea and adjacent waters. *Hystrix It. J. Mamm.* 16, 127–133. doi: 10.4404/hystrix-16.2-4350

Crick, F. C., and Koch, C. (2005). What is the function of the claustrum? *Philos. Trans. R. Soc. Lond. B Biol. Sci.* 360, 1271–1279. doi: 10.1098/rstb.2005.1661

Edelstein, L. R., and Denaro, F. J. (2004). The claustrum: a historical review of its anatomy, physiology, cytochemistry and functional significance. *Cell. Mol. Biol. (Noisy-le-grand)* 50, 675–702. doi: 10.1170/T558

Garey, L. J., Takás, J., Revishchin, A. V., and Hámori, J. (1989). Quantitative distribution of GABA-immunoreactive neurons in cetacean visual cortex is similar to that in land mammals. *Brain Res.* 485, 278–284. doi: 10.1016/0006-8993(89)90571-4

Garey, L. J., Winkelmann, E., and Brauer, K. (1985). Golgi and Nissl studies of the visual cortex of the bottlenose dolphin. *J. Comp. Neurol.* 240, 305–321. doi: 10.1002/cne.902400307

Geisler, J. H., and Uhen, M. D. (2005). Phylogenitic relationships of extinct cetartiodactyls: results of simultaneous analyses of molecular, morphological, and stratigraphic data. *J. Mammal. Evol.* 12, 145–160. doi: 10.1007/s10914-005-4963-8

Glezer, I. I., Hof, P. R., Istomin, V. V., and Morgane, P. J. (1995). "Comparative immunocytochemistry of calcium-binding protein-positive neurons in visual and auditory systems of cetacean and primate brains," in *Sensory Systems of Aquatic Mammals*, eds R. A. Kastelein, J. A. Thomas and P. E. Nachtigall (The Netherlands: De Spil Publishers, Woerden), 477–513.

Glezer, I. I., Hof, P. R., Leranth, C., and Morgane, P. J. (1993). Calcium-binding protein-containing neuronal populations in mammalian visual cortex: a comparative study in whales, insectivores, bats, rodents and primates. *Cereb. Cortex* 3, 249–272. doi: 10.1093/cercor/3.3.249

Glezer, I. I., Hof, P. R., and Morgane, P. J. (1992). Calretinin-immunoreactive neurons in the primary visual cortex of dolphin and human brains. *Brain Res.* 595, 181–188. doi: 10.1016/0006-8993(92)91047-i

Glezer, I. I., Hof, P. R., and Morgane, P. J. (1998). Comparative analysis of calcium-binding protein-immunoreactive neuronal populations in the auditory and visual systems of the bottlenose dolphin (*Tursiops truncatus*) and the macaque monkey (*Macaca fascicularis*). *J. Chem. Neuroanat.* 15, 203–237. doi: 10.1016/s0891-0618(98)00022-2

Hamilton, T. J., Xapelli, S., Michaelson, S. D., Larkum, M. E., and Colmers, W. F. (2013). Modulation of distal calcium electrogenesis by neuropeptide Y receptors inhibits neocortical long-term depression. *J. Neurosci.* 33, 11184–11193. doi: 10.1523/jneurosci.5595-12.2013

Hinova-Palova, D. V., Edelstein, L., Landzhov, B. V., Braak, E., Malinova, L. G., Minkov, M., et al. (2013). Parvalbumin-immunoreactive neurons in the human claustrum. *Brain Struct. Funct.* doi: 10.1007/s00429-013-0603-x. [Epub ahead of print].

Hof, P. R., Glezer, I. I., Condé, F., Flagg, R. A., Rubin, M. B., Nimchinsky, E. A., et al. (1999). Cellular distribution of the calcium-binding proteins parvalbumin, calbindin, and calretinin in the neocortex of mammals: phylogenetic and developmental patterns. *J. Chem. Neuroanat.* 16, 77–116. doi: 10.1016/s0891-0618(98)00065-9

Hof, P. R., Glezer, I. I., Nimchinsky, E. A., and Erwin, J. M. (2000). Neurochemical and cellular specializations in the mammalian neocortex reflect phylogenetic relationships: evidence from primates, cetaceans, and artiodactyls. *Brain Behav. Evol.* 55, 300–310. doi: 10.1159/000006665

Jacobs, M. S., Galaburda, A. M., McFarland, W. L., and Morgane, P. J. (1984). The insular formations of the dolphin brain: quantitative cytoarchitectonic studies of the insular component of the limbic lobe. *J. Comp. Neurol.* 225, 396–432. doi: 10.1002/cne.902250307

Jansen, J., and Jansen, J. K. S. (1969). "The nervous system of cetacean," in *The Biology of Marine Mammals*, ed H. T. Andersen (New York, USA: Academic Press), 175–252.

Jelgersma, G. (1934). *Das Gehirn der Wassersäugetiere. Eine Anatomische Untersuchung*. Leipzig: Von Johann Ambrosium Bart Verlag, 82–91.

Kern, A., Siebert, U., Cozzi, B., Hof, P. R., and Oelschläger, H. H. (2011). Stereology of the neocortex in Odontocetes: qualitative, quantitative and functional implications. *Brain Behav. Evol.* 77, 79–90. doi: 10.1159/000323674

Kesarev, V. S., and Malofeeva, L. I. (1969). Structural organization of the motor zone of the cerebral cortex in dolphins. *Arkh. Anat. Gistol. Embriol.* 56, 48–55.

Kowiański, P., Moryś, J. M., Dziewiatkowski, J., Wójcik, S., Sidor-Kaczmarek, J., and Moryś, J. (2008). NPY-, SOM- and VIP-containing interneurons in postnatal development of the rat claustrum. *Brain Res. Bull.* 76, 565–571. doi: 10.1016/j.brainresbull.2008.04.004

Lende, R. A., and Akdikmen, S. (1968). Motor field in cerebral cortex of the bottlenose dolphin. *J. Neurosurg.* 29, 495–499. doi: 10.3171/jns.1968.29.5.0495

LeVay, S., and Sherk, H. (1981). The visual claustrum of the cat. I. Structure and connections. *J. Neurosci.* 1, 956–980.

Lyamin, O. I., Manger, P. R., Ridgway, S. H., Mukhametov, L. M., and Siegel, J. M. (2008). Cetacean sleep: an unusual form of mammalian sleep. *Neurosci. Biobehav. Rev.* 32, 1451–1484. doi: 10.1016/j.neubiorev.2008.05.023

Manger, P. R. (2006). An examination of cetacean brain structure with a novel hypothesis correlating thermogenesis to the evolution of a big brain. *Biol. Rev. Camb. Philos. Soc.* 81, 293–338. doi: 10.1017/s1464793106007019

Markram, H., Toledo-Rodriguez, M., Wang, Y., Gupta, A., Silberberg, G., and Wu, C. (2004). Interneurons of the neocortical inhibitory system. *Nat. Rev. Neurosci.* 5, 793–807. doi: 10.1038/nrn1519

Mathur, B. N., Caprioli, R. M., and Deutch, A. Y. (2009). Proteomic analysis illuminates a novel structural definition of the claustrum and insula. *Cereb. Cortex* 19, 2372–2379. doi: 10.1093/cercor/bhn253

Minciacchi, D., Granato, A., Antonini, A., Tassinari, G., Santarelli, M., Zanolli, L., et al. (1995). Mapping subcortical extrarelay afferents onto primary somatosensory and visual areas in cats. *J. Comp. Neurol.* 362, 46–70. doi: 10.1002/cne.903620104

Moore, C. I., Carlen, M., Knoblich, U., and Cardin, J. A. (2010). Neocortical interneurons: from diversity, strength. *Cell* 142, 189–193. doi: 10.1016/j.cell.2010.07.005

Morgane, P. J., Glezer, I. I., and Jacobs, M. S. (1988). Visual cortex of the dolphin: an image analysis study. *J. Comp. Neurol.* 273, 3–25. doi: 10.1002/cne.902730103

Morgane, P. J., Glezer, I. I., and Jacobs, M. S. (1990). "Comparative anatomy of the visual cortex of the dolphin," in *Cerebral Cortex* (Vol. 8B), eds E. G. Jones and A. Peters (New York, USA: Plenum Publishing Co.), 215–262.

Morgane, P. J., and Jacobs, M. S. (1972). "Comparative anatomy of the cetacean nervous system," in *Functional Anatomy of Marine Mammals* (Vol. 1), ed R. J. Harrison (London, UK: Academic Press), 117–244.

Morgane, P. J., Jacobs, M. S., and Galaburda, A. (1986). "Evolutionary morphology of the dolphin brain," in *Dolphin Cognition and Behavior. A Comparative Approach*, eds R. Schusterman, J. Thomas and F. Wood (Hillsdale, New Jersey: Lawrence Erlbaum Associates), 5–28.

Morgane, P. J., Jacobs, M. S., and McFarland, W. L. (1980). The anatomy of the brain of the bottlenose dolphin (*Tursiops truncatus*). Surface configuration of the telencephalon of the bottlenose dolphin with comparative anatomical observations in four other cetacean species. *Brain Res. Bull.* 5(Suppl. 3), 1–107. doi: 10.1016/0361-9230(80)90272-5

Morgane, P. J., McFarland, W. L., and Jacobs, M. S. (1982). The limbic lobe of the dolphin brain: a quantitative cytoarchitectonic study. *J. Hirnforsch.* 23, 465–552.

Mukhametov, L. M., Supin, A. Y., and Polyakova, I. G. (1977). Interhemispheric asymmetry of the electroencephalographic sleep pattern in dolphins. *Brain Res.* 134, 581–584. doi: 10.1016/0006-8993(77)90835-6

Oelschläger, H. H. A., and Oelschläger, J. S. (2009). "Brain," in *Encyclopedia of Marine Mamamals* (2nd Edn.), eds W. F. Perrin, B. Würsing and J. G. M. Thewissen (Amsterdam: Academic Press), 134–149.

Olson, C. R., and Graybiel, A. M. (1980). Sensory maps in the claustrum of the cat. *Nature* 288, 479–481. doi: 10.1038/288479a0

Pilleri, G., Peixun, C., and Zuohua, S. (1980). *Concise Macroscopical Atlas of the Brain of the Common Dolphin (Delphinus delphis Linnaeus, 1758)*. Waldau-Berne Switzerland: Brain Anatomy Institute, University of Berne.

Pirone, A., Cozzi, B., Edelstein, L., Peruffo, A., Lenzi, C., Quilici, F., et al. (2012). Topography of Gng2- and NetrinG2-expression suggests an insular origin of the human claustrum. *PLoS One* 7:e44745. doi: 10.1371/journal.pone.0044745

Rahman, F. E., and Baizer, J. S. (2007). Neurochemically defined cell types in the claustrum of the cat. *Brain Res.* 1159, 94–111. doi: 10.1016/j.brainres.2007.05.011

Remedios, R., Logothetis, N. K., and Kayser, C. (2010). Unimodal responses prevail within the multisensory claustrum. *J. Neurosci.* 30, 12902–12907. doi: 10.1523/JNEUROSCI.2937-10.2010

Revishchin, A. V., and Garey, L. J. (1990). The thalamic projection to the sensory neocortex of the porpoise, *Phocoena phocoena*. *J. Anat.* 169, 85–102.

Reynhout, K., and Baizer, J. S. (1999). Immunoreactivity for calcium-binding proteins in the claustrum of the monkey. *Anat. Embryol. (Berl)* 199, 75–83. doi: 10.1007/s004290050211

Ridgway, S. H. (1990). "The central nervous system of the bottlenose dolphin," in *The Bottlenose Dolphin*, eds S. Leatherwood and R. R. Reeves (San Diego, USA: Academic Press), 69–97.

Sherwood, C. C., Stimpson, C. D., Butti, C., Bonar, C. J., Newton, A. L., Allman, J. M., et al. (2009). Neocortical neuron types in Xenarthra and Afrotheria: implications for brain evolution in mammals. *Brain Struct. Funct.* 213, 301–328. doi: 10.1007/s00429-008-0198-9

Slijper, E. J. (1979). *Whales* 2nd Edn. London: Hutchinson. 511pp.

Smith, Y., Parent, A., Kerkérian, L., and Pelletier, G. (1985). Distribution of neuropeptide Y immunoreactivity in the basal forebrain and upper brainstem of the squirrel monkey (*Saimiri sciureus*). *J. Comp. Neurol.* 236, 71–89. doi: 10.1002/cne.902360107

Tarpley, R. Y., Gelderd, J. B., Bauserman, S., and Ridgway, S. H. (1994). Dolphin peripheral visual pathway in chronic unilateral ocular atrophy: complete decussation apparent. *J. Morphol.* 222, 91–102. doi: 10.1002/jmor.1052220109

Tepper, J. M., Koós, T., and Wilson, C. J. (2004). GABAergic microcircuits in the neostriatum. *Trends Neurosci.* 27, 662–669. doi: 10.1016/j.tins.2004.08.007

Thewissen, J. G. M., Cooper, L. N., Clementz, M. T., Bajpai, S., and Tiwari, B. N. (2007). Whales originated from aquatic artiodactyls in the Eocene epoch of India. *Nature* 450, 1190–1194. doi: 10.1038/nature06343

Wojcik, S., Dziewiatkowski, J., Spodnik, E., Ludkiewicz, B., Domaradzka-Pytel, B., Kowianski, P., et al. (2004). Analysis of calcium binding protein immunoreactivity in the claustrum and the endopiriform nucleus of the rabbit. *Acta Neurobiol. Exp. (Wars)* 64, 449–460.

Conflict of Interest Statement: The authors declare that the research was conducted in the absence of any commercial or financial relationships that could be construed as a potential conflict of interest.

*Received: 25 January 2014; accepted: 10 March 2014; published online: 28 March 2014. Citation: Cozzi B, Roncon G, Granato A, Giurisato M, Castagna M, Peruffo A, Panin M, Ballarin C, Montelli S and Pirone A (2014) The claustrum of the bottlenose dolphin Tursiops truncatus (Montagu 1821). Front. Syst. Neurosci. **8**:42. doi: 10.3389/fnsys.2014.00042*

This article was submitted to the journal Frontiers in Systems Neuroscience.

frontiers in
SYSTEMS NEUROSCIENCE

ORIGINAL RESEARCH ARTICLE
published: 07 May 2014
doi: 10.3389/fnsys.2014.00063

Connectional subdivision of the claustrum: two visuotopic subdivisions in the macaque

Ricardo Gattass[1]*, Juliana G. M. Soares[1], Robert Desimone[2,3] and Leslie G. Ungerleider[4]

[1] *Program of Neurobiology, Institute of Biophysics Carlos Chagas Filho, Universidade Federal do Rio de Janeiro, Rio de Janeiro, Brazil*
[2] *Laboratory of Neuropsychology, National Institute of Mental Health, National Institutes of Health, Bethesda, MD, USA*
[3] *McGovern Institute for Brain Research at MIT, Cambridge, MA, USA*
[4] *Laboratory of Brain and Cognition, National Institute of Mental Health, National Institutes of Health, Bethesda, MD, USA*

Edited by:
Ariel Y. Deutch, Vanderbilt University Medical Center, USA

Reviewed by:
Alexander Maier, Vanderbilt University, USA
David A. Leopold, National Institutes of Health, USA
Daniel Jay Felleman, University of Texas Medical School-Houston, USA

****Correspondence:***
Ricardo Gattass, Institute of Biophysics, Federal University of Rio de Janeiro, Av. Carlos Chagas 373, CCS Bl. G, Rio de Janeiro, 21941-902, Brazil
e-mail: rgattass@gmail.com

The claustrum is a surprisingly large, sheet-like neuronal structure hidden beneath the inner surface of the neocortex. We found that the portions of the claustrum connected with V4 appear to overlap considerably with those portions connected with other cortical visual areas, including V1, V2, MT, MST and FST, TEO and TE. We found extensive reciprocal connections between V4 and the ventral portion of the claustrum (vCl), which extended through at least half of the rostrocaudal extent of the structure. Additionally, in approximately 75% of the cases, we found reciprocal connections between V4 and a more restricted region located farther dorsal, near the middle of the structure (mCl). Both vCl and mCl appear to have at least a crude topographic organization. Based on the projection of these claustrum subdivisions to the amygdala, we propose that vCl and mCl are gateways for the transmission of visual information to the memory system. In addition to these crude visuotopically organized regions, there are other parts of the claustrum that obey the topographical proximity principle, with considerable overlap of their connections. There is only an overall segregation of claustrum regions reciprocally connected to the occipital, parietal, temporal and frontal lobes. The portion of the claustrum connected to the visual cortex is located ventral and posterior; the one connected to the auditory cortex is located dorsal and posterior; the one connected to the somatosensory cortex is located dorsal and medial; the one connected to the frontal premotor and motor cortices is located dorsal and anterior; while the one connected to the temporal cortex is located ventral and anterior. The extensive reciprocal connections of the claustrum with almost the entire neocortex and its projections to the hippocampus, amygdala and basal ganglia prompt us to propose its role as a gateway for perceptual information to the memory system.

Keywords: V4, visual topography, cortical connections, integration of visual maps, cross-modal association

INTRODUCTION

The claustrum is a thin, irregular, sheet-like neuronal structure hidden beneath the inner surface of the neocortex. It is a very narrow nucleus (1–6 mm), except for its ventral portion (3–16 mm). Laterally, it wraps around the basal nuclei, mainly putamen (and a very small portion of the anterior thalamus). It resembles a leaf with two segments, one extending anteriorly into the frontal lobe and the other extending anteriorly into the temporal lobe. A lateral reconstruction of the claustrum reveals that this nucleus is surprisingly large in its anterior-to-posterior extent (30 × 20 mm). There was a debate concerning the ontogenetic origin of the claustrum, with three different opinions being argued: that the structure is derived from the adjacent insular cortex (Meynert, 1868), that it is part of the basal ganglia (Edelstein and Denaro, 2004), and that the claustrum does not have cortical or subcortical origins (Filimonoff, 1966). A more recent proteomics study of the rat claustrum agreed with this third view. The authors found that the claustrum is an intermediate structure between the striatum and the cortex, although having an affinity with layer VI of the insular cortex (Mathur et al., 2009). We favor its pallidal origin based on the mapping of transcription factors and data from its early morphogenesis (Edelstein and Denaro, 2004).

Crick and Koch (2005) summarized what was known about the claustrum, and speculated on its possible relationship with the processes that give rise to integrated conscious percepts. The portions of the claustrum connected with V4 appear to overlap considerably with portions that are connected to other visual cortical areas, including V1 (Mizuno et al., 1981; Doty, 1983), V2 (Pearson et al., 1982), MT (Maunsell and van Essen, 1983; Ungerleider et al., 1984), MST and FST (Boussaoud et al., 1992), TEO (Webster et al., 1993), and TE (Nauta and Whitlock, 1956; Kemp and Powell, 1970; Turner et al., 1980; Baizer et al., 1993; Webster et al., 1993). Evidence in other species suggests that the claustrum may be specialized for visuomotor tasks due to its connections with the different visual and motor subdivisions of the cortex (Olson and Graybiel, 1980). Based mainly on findings from a study using 2-Deoxy-d-glucose (2-DG), Ettlinger and Wilson (1990) speculated that the claustrum is involved in cross-modal associations. We found extensive reciprocal connections between

V4 and vCl that extended through at least half of the rostrocaudal extent of the structure (Gattass et al., 2014). Additionally, in approximately 75% of the cases, we found reciprocal connections between V4 and a more restricted region in the claustrum located farther dorsal, near the middle of the structure (mCl). Both vCl and mCl appear to have a crude topographic organization, based on the visuotopic location of the V4 injection sites. Based on the projection of these portions of the claustrum to the amygdala (Turner et al., 1980), we propose that vCl and mCl are gateways for the transmission of visual information to the memory system.

In this study, we review the total extent of the connections of V4 with the claustrum, as well as their topographic organization in the context of the connections of the claustrum with other cortical areas. We describe the overall extent of the claustrum in one macaque and its connections in nine macaque monkeys with combined tritiated amino acid (^{3}H), wheat germ agglutinin conjugated to horseradish peroxidase (HRP) and retrograde fluorescent tracer injections, placed under physiological control, into 19 different retinotopic locations of V4. We compare the organization of these visual regions of the claustrum with other portions of the claustrum connected with other sensory, motor, and association cortices.

MATERIALS AND METHODS

The shape and location of the claustrum in the macaque was determined in a series of Nissl-stained coronal sections from an adult *Macaca mulatta*. ^{3}H, HRP, and the fluorescent tracers fast blue (FB), diamidino yellow (DY), and bisbenzimide (Bis) were injected in 10 hemispheres of 9 adult *Macaca mulatta*, weighing between 3.2 and 4.4 kg. In all animals, the injections of the tracers were placed into retinotopically specified sites ($n = 21$) in V4, which were determined by electrophysiological recordings. The injection sites, two or more in each animal, spanned eccentricities from central to peripheral vision (**Figure 1**) in both the upper ($n = 3$) and lower ($n = 18$) visual fields (Gattass et al., 1988).

RECEPTIVE FIELD RECORDING

All experimental procedures were approved by the NIMH Animal Care and Use Committee and described in detail previously (Gattass et al., 2014). The procedures for multi-unit recordings and cortical injections have been reported in detail elsewhere (Gattass and Gross, 1981). Briefly, prior to the first recording session, under ketamine and sodium pentobarbital anesthesia, the animal was implanted with a bolt that was used to hold its head in the stereotaxic apparatus and the stainless steel recording chamber. During each recording session, the animal was anesthetized with 2% halothane, followed by a mixture containing 70% N_2O and 30% O_2. Muscular paralysis was induced by pancuronium bromide, and a respiratory pump connected to an endotracheal tube maintained artificial ventilation. The level of CO_2, heart rate, and rectal temperature were continuously monitored and kept within the normal physiological range. The right eye was protected by a contact lens that focused the eye on the surface of a 57-cm radius translucent hemisphere placed in front of the animal. The locations of the fovea and the center of the optic disc were projected onto the hemisphere using the target of an ophthalmoscope reflected by a corner cube prism (Edmund Scientifics, Barrington, New Jersey). The horizontal meridian was considered a line through both these points, and the vertical meridian was an orthogonal line that passes through the fovea.

Prior to the injections, we mapped the pertinent portion of V4 with the aid of varnish-coated tungsten microelectrodes. The electrodes were assembled in a micromanipulator that could be used to record from small clusters of neurons or could hold a pre-aligned micro syringe to deliver the anatomical tracer. Visual receptive fields were plotted by moving manually white or colored 2D-bars onto the surface of the translucent hemisphere, under light-adapted conditions. Recordings continued until the desired visual field representation within V4 was located.

INJECTIONS OF V4

We injected anterograde and retrograde tracers into 21 sites in 9 macaques under electrophysiological guidance. Pressure injections into the cortex were done using a 1-μl Hamilton syringe with a beveled 27-gauge needle that was guided into the appropriate site with the aid of an operating microscope. Sulcal and gyral landmarks were used to identify the location of area V4 (Zeki, 1978; Gattass et al., 1988). In six animals, injections were placed at physiologically determined sites on the prelunate gyrus under direct visualization of the cortex. In the remaining three animals, after the desired injection site was located electrophysiologically, a guide tube was inserted through the dura and placed approximately 300 μm above the intended injection site. The microelectrode was then advanced through the guide tube and the visuotopic location of the injection site was confirmed. The electrode was then withdrawn from the guide tube and replaced with a 1-μl Hamilton syringe. For the remainder of the paper, we refer to each injection site as a case.

In 9 cases, we injected 0.15–0.3 μl of a 1:1 mixture of tritiated proline (New England Nuclear L-[2,3,4,5-3H], specific activity 100–140 Ci/mmol), and tritiated leucine (New England Nuclear L-[3,4,5-3H(N)], specific activity 100–140 Ci/mmol). The labeled amino acids, which had been evaporated and then reconstituted in 0.9% saline to give a final concentration of 50 μCi/μl, were injected at the rate of 0.02 μl/2 min. To minimize leakage of the tracer up the electrode track, the syringe was left in place for 30 min after the injection and then withdrawn into the guide tube, which was then removed from the brain. In 7 cases, one to three injections (0.15–0.3 μl each at each site) of aqueous solutions of 2% FB, 4% DY, or 10% Bis were placed in V4. In 5 cases, two to four injections (0.2 μl each) of 5% of HRP were placed in V4. In the animals with injections involving both HRP and other tracers, the other tracer(s) were injected into the designated V4 sites during one procedure; then, 4–6 days later, HRP was injected into another V4 site.

The amount, concentration, and liquid vehicle of the tracer injections as well as the survival times were selected to produce anterograde and retrograde labeling of equivalent size. However, the nature of the tracers caused small differences in sensitivity. Among the tracers used, HRP was the most effective as both an anterograde and a retrograde tracer. Among the fluorescent dyes, the most effective retrograde tracer was FB, which was closely followed by DY.

Inj Site	Case	Tracer	Ecc	Claustrum			
				Ventral		Mid	
1	1c&p	^{3}H	-2 to-16		t		-
4	8c	^{3}H	-8		t		t
7	3c	^{3}H	-3		t		t
8	9c	^{3}H	-8		-		-
11	2p	^{3}H	-16		t		-
12	4p	^{3}H	-18		t		t
13	1p	^{3}H	-22		t		-
17	7p	^{3}H	-25		t		t
20	5p	^{3}H	10		t		-
3	2c	HRP	-2	c	t	c	t
9	3p	HRP	-14	c	t	c	t
18	8p	HRP	-30	c	t	c	-
19	5c	HRP	4	c	t	c	t
21	6p	HRP	20	c	t	c	t
2	8c	FB	-1	c		c	
5	4c	FB	-2	c		c	
6	5c	FB	-2	c		c	
10	3p	Bis	-10	c		c	
14	7p	Bis	-25	c		c	
15	4p	D Y	-18	c		c	
16	1p	Bis	-20	x		x	

c = cells
t = terminals

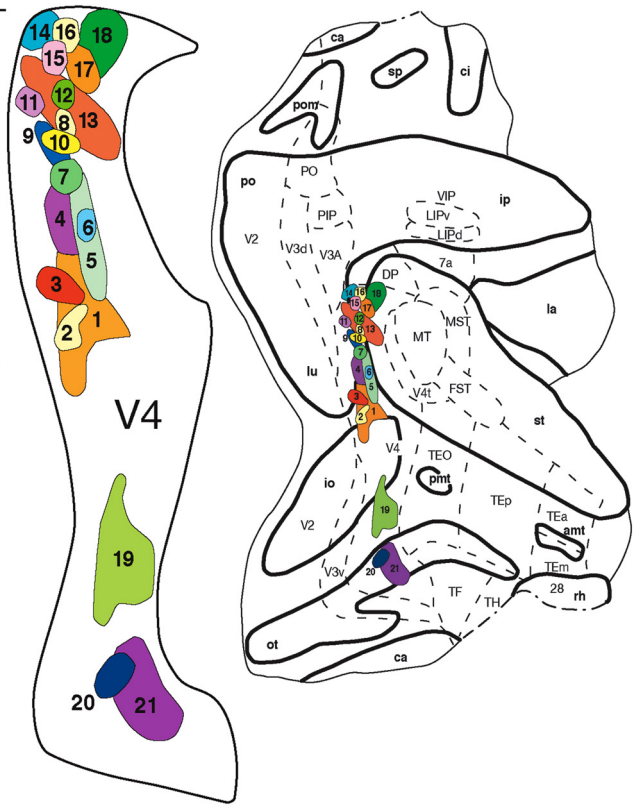

FIGURE 1 | ***Left:*** Table with the summary of the projections from and to V4. c, cells; t, terminals; gray areas, not applicable for the tracer; –, relevant sections with no label; x, relevant sections not analyzed; ECC, eccentricity of the injection. ***Right:*** Injection sites in V4 shown in a flattened map of extra-striate cortex. Tracers were placed in 21 injections sites at central and peripheral locations in V4, in 9 animals (cases) in 10 hemispheres. Each injection site is numbered and colored to match data from other figures. Myeloarchitectonic borders of visual areas are indicated with dashed lines. The injections from the individual cases were plotted on this map to best retain their locations relative to myeloarchitectonic borders and sulci. Abbreviations: *Cortical visual areas:* FST, visual area FST; LIPd, dorsal portion of lateral intraparietal area; LIPv, ventral portion of lateral intraparietal area; MIP, medial intraparietal area; MST, medial superior temporal area; MT, visual area MT; MTp, peripheral portion of MT; PIP, posterior intraparietal area; PO, parieto-occipital area; TEm, medial portion of area TE; TEO, posterior inferior temporal cortex; TEp, posterior portion of area TE; TH, cytoarchitectonic area TH; V1, primary visual cortex; V2, second visual area; V3A, visual complex V3, part A; V3d, dorsal portion of visual area 3; V3v, ventral portion of visual area 3; V4, visual area 4; V4t, V4 transition zone; VIP, ventral intraparietal area; VTF, visual portion of parahippocampal TF; *Claustrum:* fCl, frontal subdivision of the claustrum; tCl, temporal subdivision of the claustrum; pCl, parietal subdivision of the claustrum; mCl, mid claustrum; vCl, ventral claustrum; *Cortical sulci:* amt, anterior middle temporal sulcus; ar, arcuate sulcus; ca, calcarine fissure; ce, central sulcus; ec, external calcarine sulcus; io, inferior occipital sulcus; ip, intraparietal sulcus; la, lateral sulcus; lu, lunate sulcus; ot, occipitotemporal sulcus; p, principal sulcus; po, parietal occipital cleft; pmt, posterior middle temporal sulcus; rh, rhinal sulcus; sp, subparietal sulcus; st, superior temporal sulcus.

HISTOLOGICAL PROCESSING

After survival times of 2 days for HRP and 6–8 days for the other tracers, the animals received a lethal dose of sodium pentobarbital and were then transcardially perfused with 0.9% saline followed by 10% formaldehyde-saline. The brains were blocked with the aid of a stereotaxic apparatus, removed from the skull, photographed, and stored in 30% sucrose in 10% formaldehyde-saline until they sank. Frozen sections, 33 μm in thickness, were cut in the frontal plane. One case (Case 6) was cut in the parasagittal plane. Every fifth section was mounted onto gelatinized slides, dehydrated, defatted and processed for autoradiography according to the procedures of Cowan et al. (1972). These sections were dipped in Kodak NTB2 emulsion and exposed at 4°C for at least 12 weeks. Subsequently, the autoradiographs were developed in Kodak D19, fixed, and counterstained with thionin. Another series of sections, which were 250 μm apart, was processed for HRP histochemistry according to a modified tetramethylbenzidine protocol (Gibson et al., 1984). Of these sections, one in four (i.e., 1 section for each mm) was counterstained with thionin, whereas the remaining sections were left unstained and were coverslipped. Anterograde and retrograde labeling was plotted on enlarged photographs (10×) of the myelin-stained and/or thionin-stained sections for subsequent analysis. The boundaries of the various thalamic nuclei were determined from the thionin-stained sections. The Atlas of Olszewski (1952) was used as a reference for nomenclature and for delineating the thalamic boundaries. The locations of concentrations of silver grains, HRP-labeled cells and terminals and fluorescent-labeled cells were assigned to specific subcortical structures in each animal and then combined to evaluate the topographical organization of the connections. Alternate sections were stained for myelin according to the Gallyas' (1979) method.

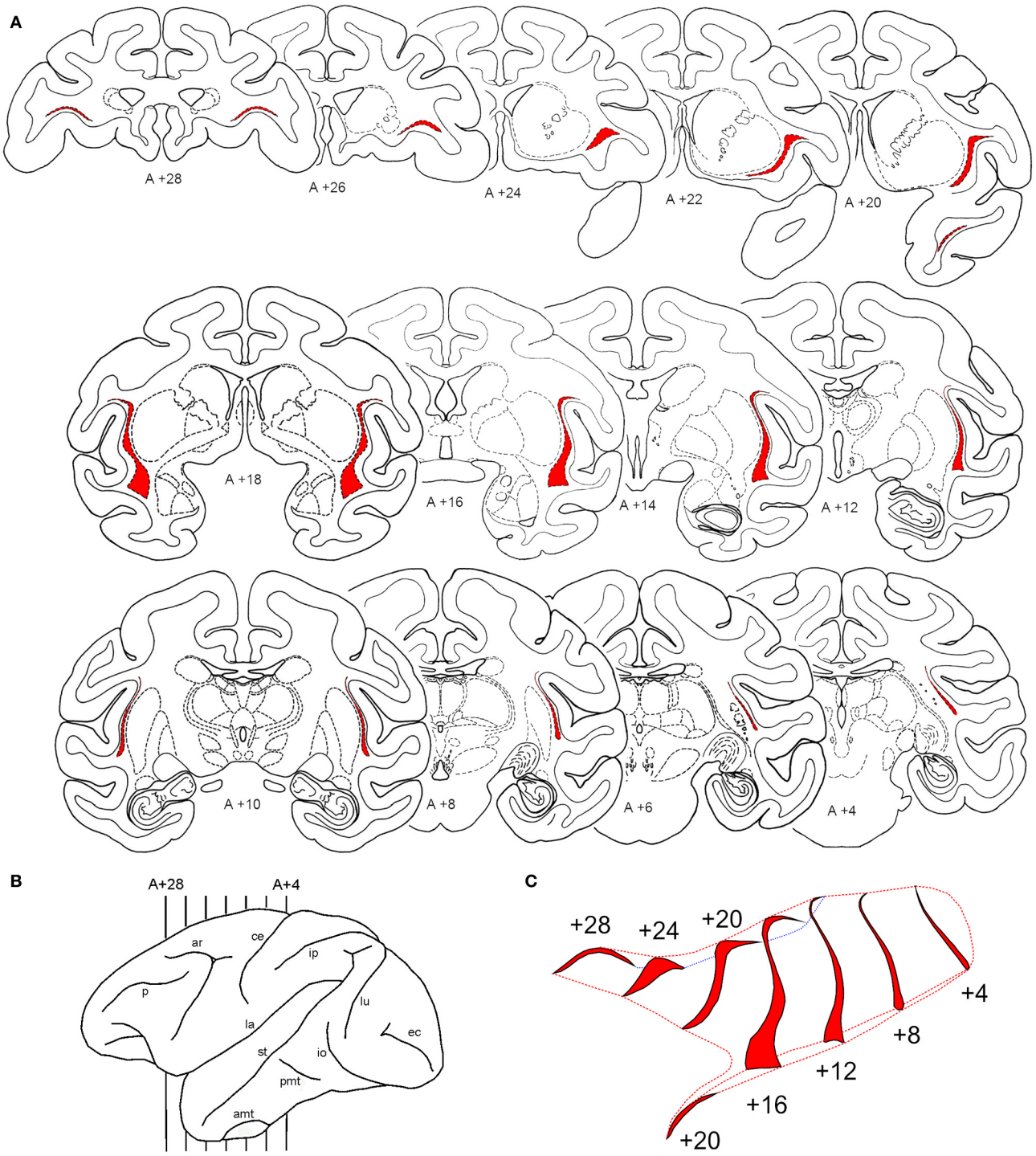

FIGURE 2 | Shape and location of the claustrum. Cororonal sections stained for Nissl through the rostral-to-caudal (top-to-bottom) extent of the claustrum. Series of coronal sections, 2 mm apart, with the claustrum shown in red **(A)** from the levels A +28 to A +4 shown in the lateral reconstruction of the left hemisphere **(B)**. An elongated 3D representation in the anterior-to-posterior dimension of the claustrum surface is shown in **(C)**. For abbreviations see legend for **Figure 1**.

RESULTS

In this section, we show the size, shape and location of the claustrum in the macaque and we revisit the data on the connections of the claustrum with V4 to reveal the location and organization of two visuotopic organized regions in the claustrum that are connected to virtually all visual areas of the occipital, temporal, and parietal lobes.

SHAPE AND LOCATION OF THE CLAUSTRUM IN CORONAL SECTIONS

The claustrum is a narrow nucleus (1–6 mm in most of its extent, and 3–16 mm in its ventral portion) that laterally wraps around the basal nuclei, mainly putamen and a very small portion of the anterior thalamus (see **Figure 2**). For most of its extent the claustrum is lateral to the putamen and medial to the insular cortex. It resembles a leaf with two segments, one extending anteriorly, into the frontal lobe and the other extending anteriorly into the temporal lobe. A lateral reconstruction of the claustrum reveals that this nucleus is surprisingly large in its anterior-to-posterior extent and typically extends over 30 mm. **Figure 2** shows the shape and location of the claustrum in coronal sections extending from A + 28 to A + 4 mm in one animal. To better visualize this narrow nucleus, we show the regions containing densely packed cells in red in sections spaced 2 mm apart (**Figure 2A**). The lateral view of the hemisphere (**Figure 2B**) shows its anterior-to-posterior extent from the level anterior to the arcuate sulcus to the posterior portion of the central sulcus. To illustrate its complex convoluted surface, we reconstructed the claustrum every 4 mm with additional spaces in the rostrocaudal dimension (**Figure 2C**). Using an elongated view in this dimension, one can see the convexity of the claustrum and its lateral fold that wraps around the insular cortex (lateral sulcus). Ventrally, the claustrum presents a broader base that extends into the temporal pole (**Figure 2**, A +20).

The shape and location of the claustrum is also shown in a photomontage of parasagittal sections of Case 6p (**Figure 3**). Four parasagittal sections were cut, aligned and stacked to reconstruct most of the claustrum. The more medial section (#50) shows the extent of the claustrum into the frontal pole. The next section (#46) shows the cells of the claustrum bridging from the frontal to the temporal pole. More lateral sections (#42 and #38) show more central portions of the nuclei. This parasagittal photomontage shows a sparser group of cells in the tail of the caudate, underneath the lateral sulcus. Overall, the anterior-to-posterior extent of the nucleus in this animal is larger than the one illustrated in **Figure 2**.

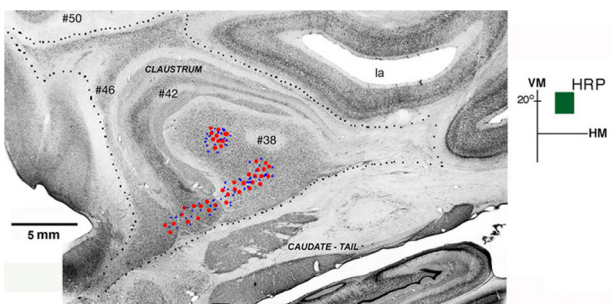

FIGURE 3 | Connections of V4 with the claustrum in a photomontage of parasagittal sections of Case 6p. Retrogradely labeled cells (*red circles*) and/or anterogradely labed terminals (*blue dots*) were found in two areas of the claustrum after injection of HRP in the upper field representation of V4 (*dark green square, in insert*). Four parasagittal sections were cut, aligned and stacked to reconstruct most of the extent of the nucleus showing two patches of labeled cells in ventral (*vCl*) and mid (*mCl*) claustrum. Black dots mark the external boundary of the claustrum. VM, vertical meridian; HM, horizontal meridian; la, lateral sulcus. Scale bar: 5 mm.

The lateral reconstruction of Case 6p and the lateral projection of the claustrum in this animal are shown in **Figure 4**. The size and location of this nucleus reveals that the surface of the claustrum is approximately 30 × 20 mm. This figure also shows the location of the two visuotopically organized regions of the claustrum, named vCl (shown in red) and mCl (shown in blue).

EVIDENCE FOR TWO COARSE VISUAL TOPOGRAPHICAL AREAS

From the 21 sites injected in V4, two sites (one in Case 1, site 8 and another in Case 9, site 16) did not reveal projections to the claustrum (see **Figure 1**). Thus, 19 injections in V4 revealed two areas with crude visual topography one located in ventral portion of the claustrum (vCl) and the other in mid (mCl) claustrum. The data are compatible with a crude and variable topography from animal to animal, but overall there are definite indications of topography, especially in more anterior portions of the claustrum. The visual topography of these areas is best seem in sections viewed in the coronal plane, inasmuch as they overlap in the

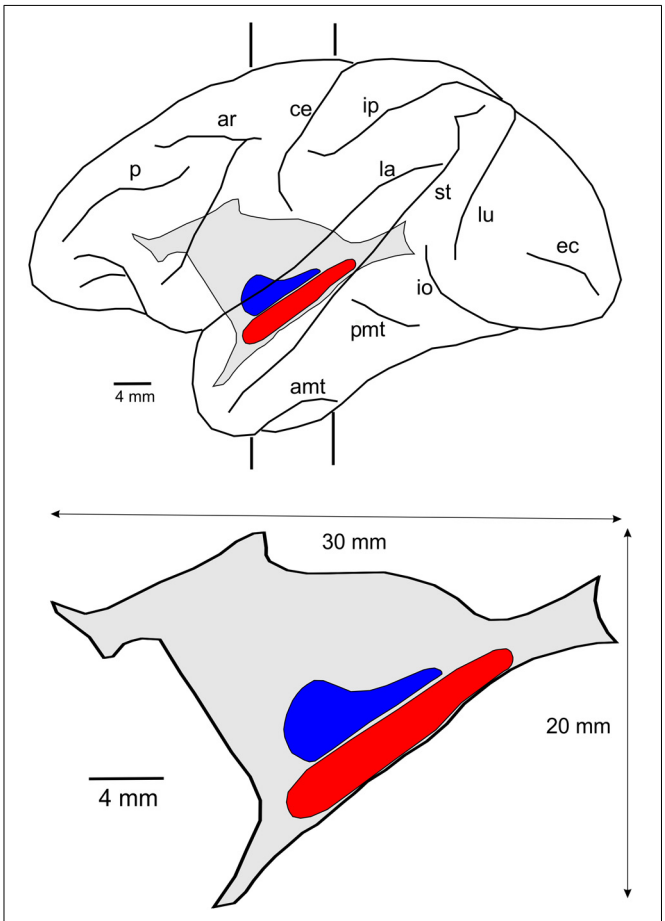

FIGURE 4 | Location and size of the claustrum. Lateral reconstruction of the left hemisphere (upper) containing the reconstruction of the claustrum with the two regions connected with V4 and other extrastriate visual areas. The contour of the lateral projection of the claustrum is shown below with an indication of its approximate dimension and the location of the two visuotopically organized regions, vCl (red) and mCl (blue). For abbreviations see legend for **Figure 1**.

lateral reconstruction. We choose to show the visual topography by showing cases with 2–3 injections at different eccentricities in V4 (**Figures 5**, **6**). First we show a case with a single upper field injection (**Figure 3**).

Figure 3 shows the result of an injection of HRP in the upper field representation (+20°) of V4 in Case 6p. Two patches of labeled cells and terminals were observed, one in ventral (vCl) and the other in mid (mCl) claustrum, showing that the upper field representation of V4 is reciprocally connected with these two regions. Retrograde labeled cells (red circles) and anterogradely labeled terminals (blue dots) were found in two segregated clusters after an injection of HRP into V4. The ventral region (vCl) had cells and terminals that appeared in three parasagittal sections (#38, #42, and #46) stacked to reconstruct most of the extent of the nucleus. Cells and terminals in the mid-region (mCl) only appeared in section #38.

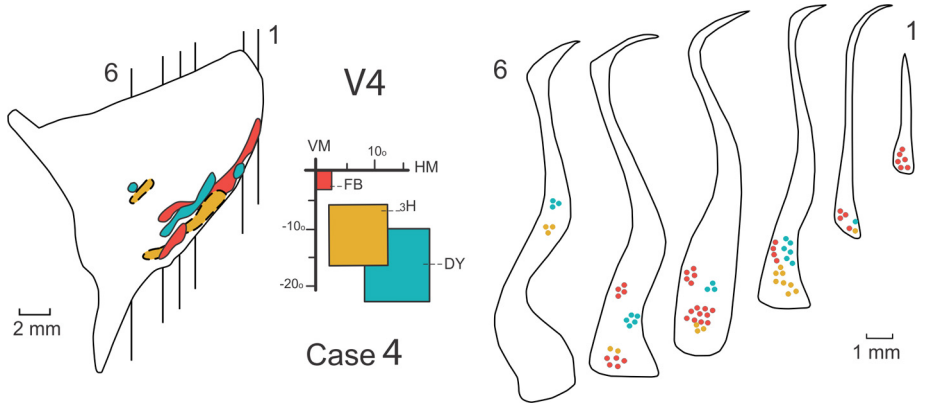

FIGURE 5 | Connections of the claustrum with area V4. Afferent and efferent connections of V4 to the claustrum are shown in 6 coronal sections at the levels indicated in the lateral reconstruction of the claustrum in Case 4. The projections from central (red), intermediate (yellow), and peripheral (blue) lower field representations of V4 are segregated into two areas of the claustrum, a medial anterior one and a ventral one. For details see text.

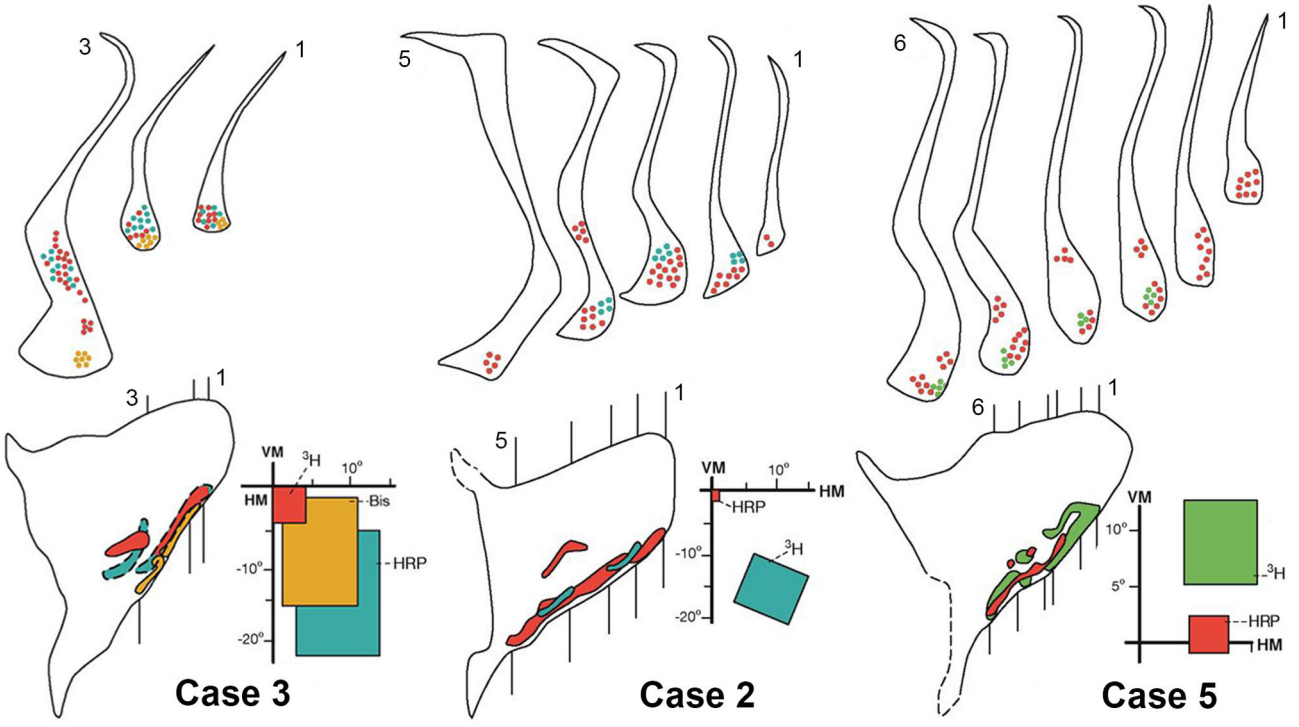

FIGURE 6 | Connections of the claustrum with area V4. Afferent and efferent connections of V4 with the claustrum are shown in coronal sections at the levels indicated in the lateral reconstruction of the claustrum in three representative cases: 2, 3, and 5. The projections from central (red), intermediate (yellow), and peripheral lower (blue) or upper (green) field representations of V4 are segregated into two areas of the claustrum, vCl and mCl. For details see text.

Figure 5 shows the result of injections of three different tracers: FB, ^{3}H, and DY in the central, intermediate and peripheral representations of the lower visual field in V4 in Case 4. Central (red) and peripheral (blue) injections reveal feedback projections from the claustrum to V4, while the intermediate injection (yellow) reveals feedforward projections to the claustrum. Six representative coronal sections show the feedback and feedforward projections in the claustrum. The lateral reconstruction of the claustrum shows that these projections are contiguous in the ventral portion of the nucleus. The projections are spatially segregated and occupy both the ventral claustrum (vCl) and the mid-claustrum (mCl). An expansion of the central field representation was observed in vCl.

Figure 6 shows the results of the central, intermediate and peripheral injections of the different tracers in the lower field representation of V4 in Cases 2 and 3 and in the upper field representation in Case 5. Injections of ^{3}H, Bis, and HRP in central (red), intermediate (yellow) and peripheral (blue) representations of the lower field of V4 in Case 3 revealed feedback and feedforward projections into two regions of the claustrum in three representative coronal sections. The receptive fields corresponding to the injections significantly overlap and the projections are poorly segregated (**Figure 6** left). Injections of HRP and ^{3}H in central (red) and peripheral (blue) representations of the lower field in V4 revealed segregated patches in the ventral portion of the claustrum and a central patch in the mid-claustrum. These bidirectional connections are shown in 5 representative coronal sections and illustrated on the lateral reconstruction of the claustrum in Case 2 (**Figure 6**, middle). The injections of HRP and ^{3}H in the central and peripheral upper field of V4 in Case 5 are shown in **Figure 6** (right). The resulting projections are shown in 6 representative coronal sections, illustrating a clear segregation in the ventral portion of the claustrum. The lateral reconstruction of the claustrum revealed that the upper field in mid-claustrum is represented ventrally, closer to the upper field representation of vCl.

COARSE VISUAL TOPOGRAPHY OF BIDIRECTIONAL CONNECTIONS

The visual topography of the reciprocal connections of V4 with vCl and mCl in 19 cases is explained in **Figure 7** and summarized in **Figure 8**. The connections found in these two regions of the claustrum were consistently observed in all animals studied, and both subdivisions appeared to have at least a coarse visuotopic organization in each area.

Figure 7 shows an intermediate level of summary data presentation between the 19 individual cases and the schematic topography shown in the next figure (**Figure 8**). This figure is built on the connections of V4 in 12 out of 19 injections in three sections at different levels of the claustrum. At the more anterior level, where the connections are more segregated and it is easier to observe a crude visuotopic organization with the upper field represented laterally in vCl and ventrally in mCl (**Figure 7**, section 1). At this level, the upper field injections corresponding to Cases 5 and 6, (**Figures 6C**, **3**) show labeling in the lower portion of mCl and in the lateral portion of vCl (dark green, Case 6) and in the ventral lateral portion of vCl (light green, Case 5). Case 6 labels

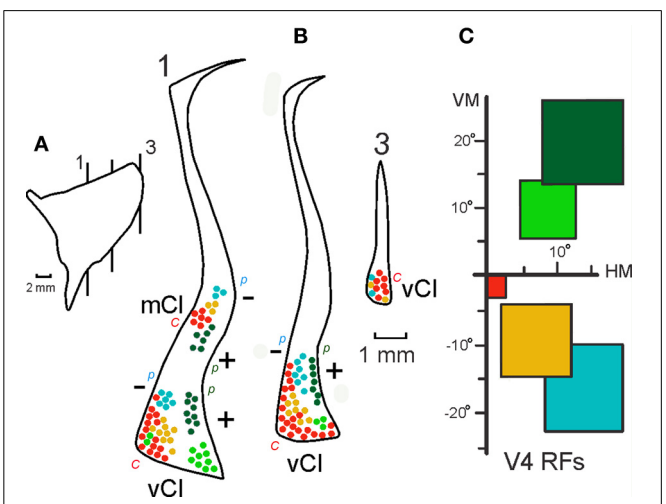

FIGURE 7 | Intermediate summary data showing the combined projections of 12 injections in V4 onto three representative sections at different levels of the claustrum. Three sections **(B)** at the level indicated in the lateral reconstruction of the claustrum **(A)** show the projections of injections at central, intermediate and peripheral upper and lower field representations in V4 **(C)**. The first section shows portions of mCl and vCl and details of the visual topography depicted in the next figure. *Labels:* c, central field representation; p, peripheral field representation; +, upper visual field; −, lower visual field representation. For details see text.

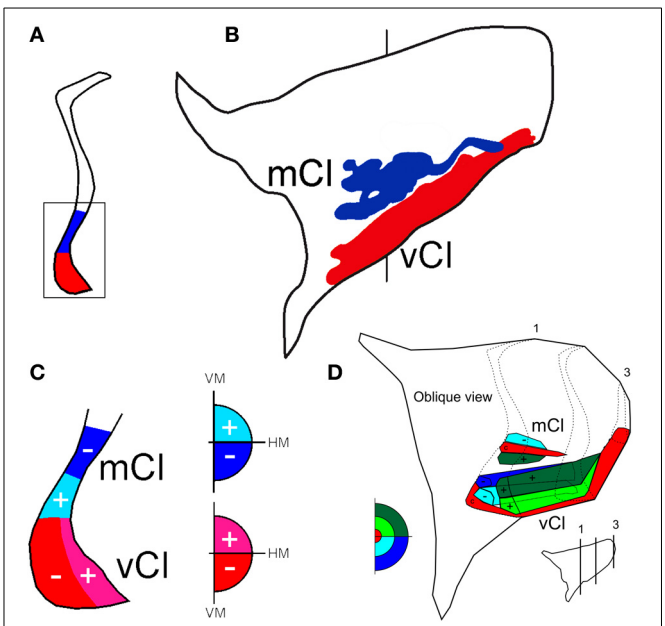

FIGURE 8 | Two topographically organized regions in the claustrum shown in a coronal section (A) at the level indicated in the lateral projection of the claustrum (B). The projections from the 19 injections in V4 were superimposed and are shown in the lateral reconstruction: mCl (blue) and vCl (red). The visual topography of these regions is shown in a representative coronal section in **(C)** and in an oblique reconstruction in **(D)**. c, indicates central field representation, (+) indicates the representation of the upper visual field, and (−) indicates the representation of the lower visual field in the claustrum.

both areas (see **Figure 3**), but Case 5 only labels vCl (**Figure 6C**). Injections in central, intermediate and peripheral lower visual field representations in V4 label sequentially portions of vCl and mCl at this level. At a more posterior section (**Figure 7B**, section 2), projections are restricted to vCl and are more superimposed. Nonetheless, it is always possible to see a central to peripheral trend as well as a segregation of lower and upper field representations. As before, the upper field is represented laterally while the lower field is represented more medially. There is a larger emphasis of the central field representation that predominates in the posterior portion of vCl. Connections at more posterior levels are more superimposed and intermingled suggesting that the topography is more complex at that level.

After 19 injections in V4, both of these regions showed labeled cells and terminals that occupied the ventral and mid-portions of the nucleus (**Figure 8A**). The lateral reconstruction of the nucleus shows two regions that are elongated in the anterior-to-posterior dimension (**Figure 8B**). In the more dorsal labeled mCl, the connections with V4's lower visual field were found dorsal to the connections with V4's upper visual field (**Figures 8C,D**). In the ventral labeled vCl, the visuotopic organization was less clear but there was a tendency for the connections with V4's upper visual field to be located laterally to the connections with V4's lower visual field (**Figures 8C,D**).

DISCUSSION

Extrastriate area V4 plays a key role in relaying information from V2 to higher-order areas in the inferior temporal cortex (areas TEO and TE) that are critical for object recognition (Ungerleider et al., 2008). In the present study, we examined the relationship between V4 and the claustrum, and compared these projections with those from other neocortical areas.

The claustrum is a thin, irregular, sheet-like neuronal structure hidden beneath the inner surface of the neocortex. We found extensive reciprocal connections between V4 and the ventral portion of the claustrum (termed vCl) that extended through at least half of the rostrocaudal extent of the structure (Gattass et al., 2014). Additionally, in approximately 75% of the cases, we found reciprocal connections between V4 and a more restricted region in the claustrum, which was located farther dorsal, near the

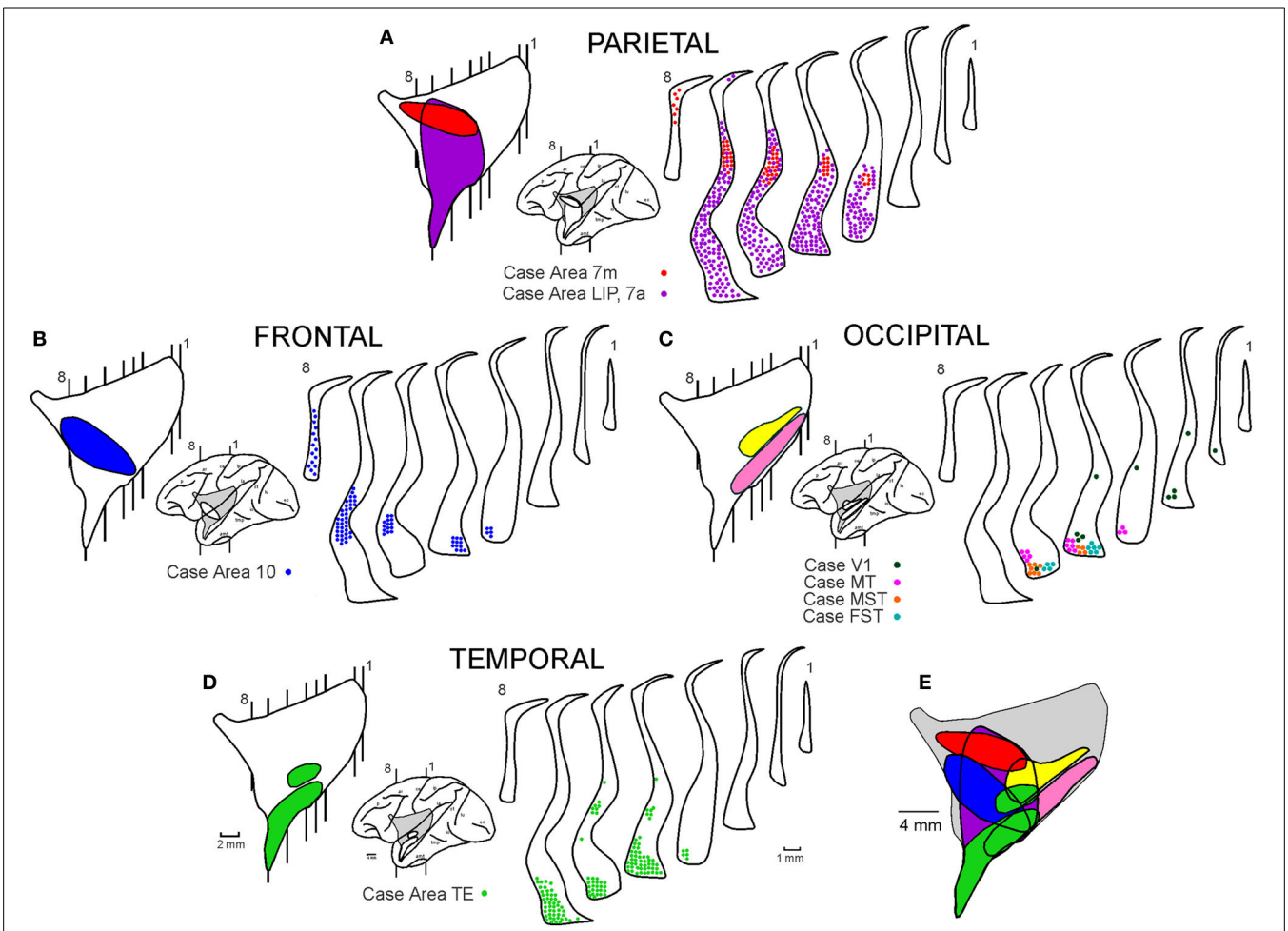

FIGURE 9 | Reciprocal connections of the claustrum with parietal (A), frontal (B), occipital (C), and temporal (D) areas. All connections were superimposed in the lateral reconstruction of the claustrum **(E)**. Data were compiled from previous publications (Ungerleider et al., 1984; Boussaoud et al., 1992; Baizer et al., 1993; Webster et al., 1993) or presentations (Ribeiro Gomes et al., 2013). For details, see text.

middle of the structure (termed mCl). Both vCl and mCl appear to have a crude topographic organization, based on the visuotopic location of our injection sites.

Figure 9 shows existing data on the connections of the claustrum, which we summarize from previous publications (Ungerleider et al., 1984; Boussaoud et al., 1992; Baizer et al., 1993; Webster et al., 1993) or presentations (Ribeiro Gomes et al., 2013). The portions of the claustrum connected with V4 appear to overlap considerably with the portions connected with other visual cortical areas, including V1 (Mizuno et al., 1981; Doty, 1983), V2 (Pearson et al., 1982), MT (Maunsell and van Essen, 1983; Ungerleider et al., 1984), MST and FST (Boussaoud et al., 1992), TEO (Webster et al., 1993), and TE (Nauta and Whitlock, 1956; Kemp and Powell, 1970; Turner et al., 1980; Baizer et al., 1993; Webster et al., 1993). The regions of the claustrum connected with V4 and with occipital areas are illustrated in pink and yellow in the lateral reconstruction of the nucleus (**Figure 9C**). The connections with V1 (Ribeiro Gomes et al., 2013), MT (Ungerleider et al., 1984), MST, and FST (Boussaoud et al., 1992) are illustrated in the coronal sections of the claustrum in **Figure 9C**. Injections in TEO (Webster et al., 1993) and TE (Baizer et al., 1993; Webster et al., 1993) revealed connections with the anterior portion of mCl and VCl, which extends into the temporal branch of the claustrum (**Figure 9D**). Injections in the frontal pole of cortex (Brodmann area 10, Ribeiro Gomes et al., 2013) revealed connections with the anterior portion of vCl which extends to the frontal branch of the claustrum (**Figure 9B**). Injections in the parietal lobe (Baizer et al., 1993; Ribeiro Gomes et al., 2013) revealed extensive connections with the anterior and ventral portions of the claustrum (**Figure 9A**). The injection of Ribeiro Gomes et al. (2013) was placed on the medial surface in area 7 m and revealed a smaller connection than that of Baizer et al. (1993) who removed the medial bank of the intraparietal sulcus and placed injections into the lateral bank of the intraparietal sulcus that included LIPv and LIPd, extending into VIP and area 7a. These lateral intraparietal sulcus injections revealed extensive connections with the anterior and ventral portions of the claustrum. **Figure 9E** shows the plot of the connections revealing a crude topographic segregation, with a considerable amount of overlap, roughly obeying the "proximity" principle, whereby a given cortical region projects to the portion of the structure that is physically closest to it (Kemp and Powell, 1970).

The scheme proposed in **Figure 9E** is compatible with the data presented in this research topic by Reser et al. (2014) for the connections of the frontal pole with the claustrum in *Cebus apella*. The connections of areas 9, 10, and 12 of the frontal lobe are clustered in areas vCl and mCl, in addition to an area located dorsally and anteriorly that they termed fCl (Figure 6B of Reser et al., 2014). This area (fCl) is comparable to the frontal subdivision shown in **Figure 9B** (Ribeiro Gomes et al., 2013).

Evidence in other species suggests that the claustrum may be specialized for visuomotor function due to of its connections with different visual and motor subdivisions of cortex (Olson and Graybiel, 1980). Based primarily on findings from a study using 2-DG, Ettlinger and Wilson (1990) speculated that the claustrum is involved in cross-modal associations.

The present results are consistent with a mixed organizational scheme, namely, a ventral visuotopic projection system combined with a dorso-ventral and anterior-posterior connectional system segregated with some degree of topographical proximity. Thus, in addition to the visuotopic subdivisions we describe here, the anatomical connections of the claustrum resemble those of the caudate nucleus, which obeys the "proximity" principle (Kemp and Powell, 1970). According to this principle, the frontal cortex would project to the head of the caudate, the parietal cortex to the body, the occipital cortex to the genu, and the temporal cortex to the tail. This organizational scheme differs somewhat from that proposed by Saint-Cyr et al. (1990) for the caudate, who found that the projection strips arising from cortical visual areas are limited in length, and thus show some degree of topographic proximity.

Based on our data and other connectional studies of the claustrum (Ungerleider et al., 1984; Boussaoud et al., 1992; Baizer et al., 1993; Webster et al., 1993; Ribeiro Gomes et al., 2013), we propose three hypotheses for the connectional organization of this nucleus. **Figure 10** is a pictorial representation of these three hypotheses. The first hypothesis addresses the two visuotopically organized areas reciprocally connected with visual cortical areas and projecting to the amygdala. This hypothesis is based on the connectional data of V4 and other visual areas. We termed this hypothesis "route to amygdala," which potentially carries information about objects in visual space (**Figure 10A**). The second hypothetical scheme is topographical, whereby reciprocal connections of the different neocortical lobules are topographically segregated in the claustrum (**Figure 10B**). In spite of the large degree of overlap, double-labeled cells projecting to the temporal

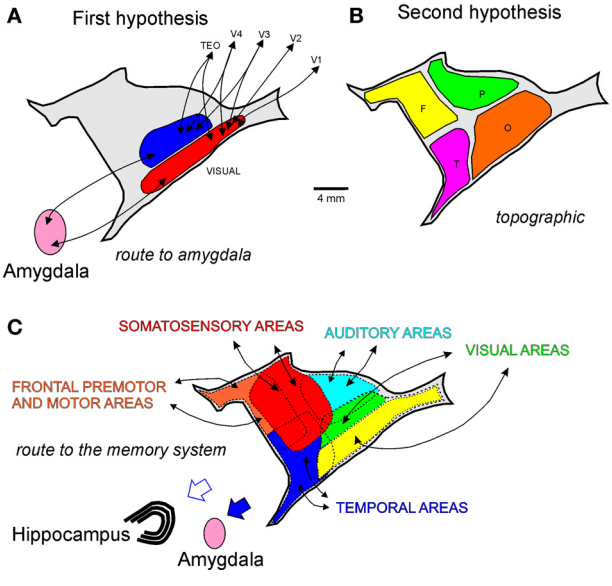

FIGURE 10 | Hypothetized anatomical organization of the claustrum. Lateral reconstructions of the claustrum with pictorial representations of three connectional hypotheses: **(A)** *route to the amygdala*; **(B)** *topographic* (O, occipital; P, parietal; T, temporal; and F, frontal connections); and **(C)** *route to the memory system.*

and parietal cortices from the claustrum are virtually nonexistent (Baizer et al., 1993). The third hypothetical scheme (**Figure 10C**) incorporates the findings of Milardi et al. (2013) described in the next paragraph. It is clear that the first and the third hypothetical scheme are compatible and that they coexist in the claustrum. The work of Reser et al. (2014) for the connections of the frontal pole with the claustrum in *Cebus apella* in this *research topic* shows that injections in visual-related areas of the frontal cortex label the fCl region (*by topographical proximity*) but also label the visual related areas vCl and mCl (*as a route to the amygdala*). It is worth noticing that neurophysiological recording in the claustrum revealed mostly unisensory responses (Remedios et al., 2010), a finding consistent with the absence of double labeling found in the claustrum (Baizer et al., 1993). The homogeneous cell type of the claustrum may convey unisensory information, but the interaction between neighboring cells may be important for multimodal integration in this structure.

Using constrained spherical deconvolution tractography, Milardi et al. (2013) described four groups of white matter fibers that connect the claustrum to the cortex. The anterior and posterior cortico-claustral tracts connect the claustrum to the prefrontal cortex and visual areas. The superior tract link the claustrum to the sensory-motor areas, while the lateral pathway connects the claustrum to the auditory cortex. Additionally, this study demonstrated a claustrum-medial pathway that connects the claustrum to the basal ganglia, specifically the caudate nucleus, putamen, and globus pallidus. Together, the first and the third hypothetical schemes best represent our current understanding of claustral connectivity. We also consider the crude visual topography of mCl and vCl useful in organizing the visual connections of several visual cortical areas to the claustrum.

ACKNOWLEDGMENTS

We wish to dedicate this work to Thelma W. Galkin, and we thank her for her help, inspiration and skillful technical assistance at every stage of this work. Thelma reconstructed the lateral view of the claustrum and prompted us to search for its connections and function. This work is a tribute to this nice, serious, lovely, and outgoing person who inspired us to look for the thin, unknown, hidden claustrum. The research reported here was supported by the NIMH Intramural Research Program and by NEI (NIH) grant RO1EY017292 (to Robert Desimone).

REFERENCES

Baizer, J. S., Desimone, R., and Ungerleider, L. G. (1993). Comparison of subcortical connections of inferior temporal and posterior cortex in monkeys. *Vis. Neurosci.* 10, 59–72. doi: 10.1017/S0952523800003229

Boussaoud, D., Desimone, R., and Ungerleider, L. G. (1992). Subcortical connections of MST and FST in the macaque. *Vis. Neurosci.* 9, 291–302. doi: 10.1017/S0952523800010701

Cowan, W. M., Gottleib, D. I., Hendrickson, A. E., Price, J. L., and Woolsey, T. A. (1972). The autoradiographic demonstration of axonal connections in the central nervous system. *Brain Res.* 37, 21–51. doi: 10.1016/0006-8993(72)90344-7

Crick, F. C., and Koch, C. (2005). What is the function of the claustrum? *Philos. Trans. R. Soc. Lond. B Biol. Sci.* 360, 1271–1279. doi: 10.1098/rstb.2005.1661

Doty, R. W. (1983). Nongeniculate afferents to striate cortex in macaques. *J. Comp. Neurol.* 218, 159–173. doi: 10.1002/cne.902180204

Edelstein, L. R., and Denaro, F. J. (2004). The claustrum: a historical review of its anatomy, physiology, cytochemistry and functional significance. *Cell. Mol. Biol.* 50, 675–702.

Ettlinger, G., and Wilson, W. A. (1990). Cross-modal performance: behavioural processes, phylogenetic considerations and neural mechanisms. *Behav. Brain Res.* 40, 169–192. doi: 10.1016/0166-4328(90)90075-P

Filimonoff, I. N. (1966). The claustrum, its origin and development. *J. Hirnforsch.* 8, 503–528.

Gallyas, F. (1979). Silver staining of myelin by means of physical development. *Neurol. Res.* 1, 203–209.

Gattass, R., Galkin, T. W., Desimone, R., and Ungerleider, L. G. (2014). Subcortical connections of V4 in the macaque. *J. Comp. Neurol.* 522, 01–25. doi: 10.1002/cne.23513

Gattass, R., and Gross, C. G. (1981). Visual topography of the striate projection zone in the posterior temporal sulcus (MT) of the macaque. *J. Neurophysiol.* 46, 621–638.

Gattass, R., Sousa, A. P. B., and Gross C. G. (1988). Visuotopic organization and extent of V3 and V4 of the macaque. *J. Neurosci.* 8, 1831–1845.

Gibson, A. R., Hansma, D. I., Houk, J. C., and Robinson, F. R. (1984). A sensitive low artifact TMB procedure for the demonstration of WGA-HRP in CNS. *Brain Res.* 298, 235–241. doi: 10.1016/0006-8993(84)91423-9

Kemp, J. M., and Powell, T. P. S. (1970). The cortico-striate projection in the monkey. *Brain* 93, 525–546. doi: 10.1093/brain/93.3.525

Mathur, B. N., Caprioli, R. M., and Deutch, A. Y. (2009). Proteomic analysis illuminates a novel structural definition of the claustrum and insula. *Cereb. Cortex* 19, 2372–2379. doi: 10.1093/cercor/bhn253

Maunsell, J. H., and van Essen, D. C. (1983). The connections of the middle temporal visual area (MT) and their relationship to a cortical hierarchy in the macaque monkey. *J. Neurosci.* 3, 2563–2586.

Meynert, T. (1868). Neue untersuchungen über den bau der grosshirnrinde und ihre örtliche verschiedenheiten. *Alleg. Wien. Medizin. Ztg.* 13, 419–428.

Milardi, D., Bramanti, P., Milazzo, C., Finocchio, G., Arrigo, A., Santoro, G., et al. (2013). Cortical and subcortical connections of the human claustrum revealed *in vivo* by constrained spherical deconvolution tractography. *Cereb. Cortex.* doi: 10.1093/cercor/bht231. [Epub ahead of print].

Mizuno, N., Uchida, K., Nomura, S., Nakamura, Y., Sugimoto, T., and Uemura-Sumi, M. (1981). Extrageniculate projections to the visual cortex in the macaque monkey: an HRP study. *Brain Res.* 212, 454–459. doi: 10.1016/0006-8993(81)90477-7

Nauta, W. J., and Whitlock, D. G. (1956). Subcortical projections from the temporal neocortex in *Macaca mulatta*. *J. Comp. Neurol.* 106, 183–212. doi: 10.1002/cne.901060107

Olson, C. R., and Graybiel, A. M. (1980). Sensory maps in the claustrum of the cat. *Nature* 288, 479–481. doi: 10.1038/288479a0

Olszewski, J. (1952). *The Thalamus of the Macaca mulatta (An Atlas for Use with the Stereotaxic Instrument)*. Basel: S. Karger.

Pearson, R. C., Brodal, P., Gatter, K. C., and Powell, T. P. (1982). The organization of the connections between the cortex and the claustrum in the monkey. *Brain Res.* 234, 435–441. doi: 10.1016/0006-8993(82)90883-6

Remedios, R., Logothetis, N. K., and Kayser, C. (2010). Unimodal responses prevail within the multisensory claustrum. *J. Neurosci.* 30, 12902–12907. doi: 10.1523/JNEUROSCI.2937-10.2010

Reser, D., Richardson, K., Montibeller, M. O., Zhao, S., Chan, J., Soares, J. G. M., et al. (2014). "Topography of claustrum projections to prefrontal cortex in *Cebus apella*," in *Frontiers in Systems Neuroscience, Research Topic: The Claustrum: Charting a Way Forward for the Brain's Most Mysterious Nucleus*, Vol. 8, eds A. Y. Deutch and B. N. Mathur.

Ribeiro Gomes, A. R., Lamy, C., Misery, C., Knoblauch, K., and Kennedy, H. (2013). *A Quantitative Analysis of the Topology of Subcortical Projections to the Macaque Cortex*. Program No. 551.10. 2013 Neuroscience Meeting Planner. San Diego, CA: Society for Neuroscience.

Saint-Cyr, J. A., Ungerleider, L. G., and Desimone, R. (1990). Organization of visual cortical inputs to the striatum and subsequent outputs to the pallido-nigral complex in the monkey. *J. Comp. Neurol.* 298, 129–156. doi: 10.1002/cne.902980202

Turner, B. H., Mishkin, M., and Knapp, M. (1980). Organization of the amygdalopetal projections from modality-specific cortical association areas in the monkey. *J. Comp. Neurol.* 191, 515–543. doi: 10.1002/cne.901910402

Ungerleider, L. G., Desimone, R., Galkin, T. W., and Mishkin, M. (1984). Subcortical projections of area MT in macaque. *J. Comp. Neurol.* 223, 368–386. doi: 10.1002/cne.902230304

Ungerleider, L. G., Galkin, T. W., Desimone, R., and Gattass, R. (2008). Cortical connections of area V4 in the macaque. *Cereb. Cortex* 18, 477–499. doi: 10.1093/cercor/bhm061

Webster, M. J., Bachevalier, J., and Ungerleider, L. G. (1993). Subcortical connections of inferior temporal areas TE and TEO in macaque monkeys. *J. Comp. Neurol.* 335, 73–91. doi: 10.1002/cne.903350106

Zeki, S. M. (1978). Uniformity and diversity of structure and function in rhesus monkey prestriate cortex. *J. Physiol. (Lond)*. 277, 273–290.

Conflict of Interest Statement: The Review Editor David A. Leopold declares that, despite being affiliated to the same institution as authors Robert Desimone and Leslie G. Ungerleider, the review process was handled objectively and no conflict of interest exists.

Received: 30 January 2014; accepted: 04 April 2014; published online: 07 May 2014.
Citation: Gattass R, Soares JGM, Desimone R and Ungerleider LG (2014) Connectional subdivision of the claustrum: two visuotopic subdivisions in the macaque. Front. Syst. Neurosci. ***8****:63. doi: 10.3389/fnsys.2014.00063*
This article was submitted to the journal Frontiers in Systems Neuroscience.

frontiers in
SYSTEMS NEUROSCIENCE

ORIGINAL RESEARCH ARTICLE
published: 03 July 2014
doi: 10.3389/fnsys.2014.00123

Claustrum projections to prefrontal cortex in the capuchin monkey (*Cebus apella*)

David H. Reser[1]*, Karyn E. Richardson[1,2], Marina O. Montibeller[1], Sherry Zhao[1], Jonathan M. H. Chan[1], Juliana G. M. Soares[3], Tristan A. Chaplin[1], Ricardo Gattass[3] and Marcello G. P. Rosa[1,4]

[1] Department of Physiology, Monash University, Clayton, VIC, Australia
[2] Department of Psychology and Psychiatric Medicine, Monash University, Clayton, VIC, Australia
[3] Programa de Neurobiologia, Instituto de Biofísica Carlos Chagas Filho, Universidade Federal do Rio de Janeiro, Rio de Janeiro, Brazil
[4] Australian Research Council Centre of Excellence for Integrative Brain Function, Clayton, VIC, Australia

Edited by:
Brian N. Mathur, University of Maryland School of Medicine, USA

Reviewed by:
Brian N. Mathur, University of Maryland School of Medicine, USA
Peter M. Kaskan, National Institutes of Mental Health, USA

***Correspondence:**
David H. Reser, Department of Physiology, Monash University Clayton, Bldg. 13F, Clayton, VIC 3800, Australia
e-mail: david.reser@monash.edu

We examined the pattern of retrograde tracer distribution in the claustrum following intracortical injections into the frontal pole (area 10), and in dorsal (area 9), and ventral lateral (area 12) regions of the rostral prefrontal cortex in the tufted capuchin monkey (*Cebus apella*). The resulting pattern of labeled cells was assessed in relation to the three-dimensional geometry of the claustrum, as well as recent reports of claustrum-prefrontal connections in other primates. Claustrum-prefrontal projections were extensive, and largely concentrated in the ventral half of the claustrum, especially in the rostral 2/3 of the nucleus. Our data are consistent with a topographic arrangement of claustrum-cortical connections in which prefrontal and association cortices receive connections largely from the rostral and medial claustrum. Comparative aspects of claustrum-prefrontal topography across primate species and the implications of claustrum connectivity for understanding of cortical functional networks are explored, and we hypothesize that the claustrum may play a role in controlling or switching between resting state and task-associated cortical networks.

Keywords: claustrum, primate, cortical networks, neuroanatomy, prefrontal

INTRODUCTION

Although it was first described over 200 years ago, the claustrum remains an enigma in modern neuroscience (Crick and Koch, 2005; Smythies et al., 2014). The convoluted geometry and difficult surgical approach to the claustrum, combined with its close proximity to the insula and putamen, have contributed to the uncertainty regarding claustrum function, as has the poor understanding of its cytoarchitectonic and chemoarchitectonic organization. The dearth of information regarding the claustrum is particularly acute among primate species. Although it has been shown that the claustrum has widespread reciprocal connectivity with the cerebral cortex, there is growing evidence for species differences in morphology, neurochemistry, and connectivity (reviewed in Baizer, 2014).

Claustrum connections to prefrontal areas have been examined in rodents (Vertes, 2004; Hoover and Vertes, 2007) and primates (Pearson et al., 1982; Tanne-Gariepy et al., 2002), as well as humans (Fernandez-Miranda et al., 2008; Milardi et al., 2013). In the rat, projections to the prelimbic area arise from the dorsal or insular portion of the claustrum, while projections to the infralimbic cortex are concentrated in the ventral (endopiriform) portion of the claustrum (Vertes, 2004). Hoover and Vertes (2007) expanded the range of observed rat prefrontal areas to include the anterior cingulate and frontal agranular areas, but reported a similar distribution of afferent projections to the earlier study, along with dense projections from the dorsal claustrum to anterior cingulate and frontal agranular areas.

In macaques, Pearson et al. (1982) and Tanne-Gariepy et al. (2002) examined claustrum afferents to lateral prefrontal areas, including areas 8, 9, 12, and 46, and to motor and premotor areas of frontal cortex. These studies showed that projections to area 46 were widespread, and extended along the majority of the rostral-caudal axis of the claustrum (this includes the injections of area 9 in Pearson et al., 1982). Projections to area 12 overlapped the distribution of area 9 connections, but extended more ventrally, especially in the more caudal portion of the claustrum. Afferent input from the claustrum to supplementary and premotor areas in both studies were segregated from prefrontal inputs along the dorsal-ventral axis of the claustrum, with less prominent separation of labeled cells along the rostral-caudal axis.

In humans, Fernandez-Miranda et al. (2008) described segregation of the claustro-cortical white matter tracts using a combination of cadaver dissection and diffusion tensor imaging, with clear separation of frontal and prefrontally projecting axons from those projecting to other cortical areas, e.g., temporal and parietal cortex. Despite advances in tractographic imaging methods (e.g., Milardi et al., 2013), non-human primates remain the best experimental model for detailed studies of connectivity of larger networks of cortical areas. It is therefore essential to understand the homology between identified cortical areas across species, in

order to make accurate comparisons. To date, there have been few studies of claustro-cortical connections in New World monkey species.

The present study describes the claustral projections to the prefrontal cortex of the *Cebus* (capuchin) monkey, a species of New World monkey. The anatomy of *Cebus* monkey prefrontal cortex has recently been described in detail by Cruz-Rizzolo et al. (2011), including identification of cytoarchitectonic and myeloarchitectonic boundaries of cortical areas corresponding to those identified in macaques (Petrides and Pandya, 1999, 2002; Chaplin et al., 2013) and marmosets (another species of New World monkey; Burman et al., 2006; Burman and Rosa, 2009; Paxinos et al., 2012). We have previously reported that the dorsal and lateral portions of the frontal pole (area 10) of the marmoset receives a rich claustrum projection (Burman et al., 2011a,b).

MATERIALS AND METHODS

Three adult *Cebus apella* monkeys were injected with fluorescent tracers, including fluororuby (FR, 10% in dH_20), fluoroemerald (FE, 10% in dH_20), diamidino yellow (DY, 2% in dH_20), and fast blue (FB, 2% in dH_20), at multiple locations in prefrontal and orbitofrontal cortex. Case details for each animal are summarized in **Table 1**. All surgical and experimental procedures were approved in advance by the Animal Ethics Committee of the Centro de Ciências da Saúde of the Universidade Federal do Rio de Janeiro (CEUA IBCCF189-06/16), and conformed to the guidelines of the Brazilian Federal Arouca law governing laboratory animal use and care, as well as the Australian Code of Practice for Care and Use of Animals for Scientific Purposes. Tracer injections and histological processing were conducted at the Instituto de Biofísica Carlos Chagas Filho, Rio de Janeiro, Brazil. Microscopic examination and data analysis were performed in the Department of Physiology of Monash University. Throughout this report, the numerical designations used for the various prefrontal areas conform to those of Cruz-Rizzolo et al. (2011). Stereotaxic location estimates are based on the Eidelberg and Saldias atlas (1960).

Table 1 | Case information and tracer injection locations.

Animal ID	Body weight (kg)	Sex	Hemisphere	Tracer	Amount (uL)	Location
FR01	3.3	M	R	FB	0.4	Area 10
				DY	0.4	Area 10
				FE	1.0	Area 10
				FR	1.0	Area 10
FR02	3.0	M	R	FB	0.5	Area 10
				FE	1.0	Area 10
				DY	0.5	Area 12
FR04	3.0	M	R	FB	0.5	Area 9
				DY	0.5	Area 12o

Summary of individual case data and injection targets. Recovery time for all animals was 2 weeks post-injection.

TRACER INJECTIONS

All tracers were injected using a 1 μL Hamilton syringe. The animals were pre-medicated with atropine (0.15 mg/kg IM) and diazepam (0.5 mg/kg IM) and anesthetized with ketamine (30 mg/kg IM) and maintained using intramuscular ketamine and xylazine (1:5). All animals received peri-operative antibiotics (penicillin G, 300,000 IU, IM) and dexamethasone (0.3 mg/kg, IM).

A craniotomy was performed over the target regions of cortex, and the tracer was deposited in 50–100 nL increments over approximately 15 min. The micropipette tip was left in place for an additional 5–10 min following the last deposit, in order to minimize leakage of tracer into non-target areas. The injection into area 12o was accessed from the dorsal surface of the frontal cortex and intervening white matter. Tracer leakage along the needle track was minimized by slow withdrawal; however, it is possible that some contamination of the adjacent white matter occurred. After the final injection, the tip was withdrawn, and the bone flap excised during the craniotomy was replaced and cemented into place. The overlying tissue was sutured and the animal was allowed to recover until it could make spontaneous and coordinated movements, after which it was returned to the home cage. Each animal was carefully monitored during the 14 day post-injection survival period, during which analgesics and antibiotics were provided as required. At the end of the survival period, each animal was humanely euthanized with an overdose of sodium pentobarbital (40 mg/kg) and transcardially perfused with saline followed by 4% paraformaldehyde in phosphate buffered saline. The brain was extracted and further post-fixed for 24 h in 4% paraformaldehyde.

HISTOLOGICAL PROCESSING

Perfused brains were cryoprotected in increasing concentrations of glycerol (5–15% in 4% PFA), then sectioned on a cryostat at 50 μm thickness. Every tenth section was mounted unstained for fluorescence microscopy. These sections were dried and coverslipped with di-n-butyl phthalate xylene (DPX) following quick dehydration (2 × 100% ethanol) and immersion in xylene. Adjacent series of sections were stained for Nissl, myelin (Gallyas, 1979), and cytochrome oxidase (Wong-Riley, 1979).

MICROSCOPY AND PHOTOGRAPHY

Fluorescence labeled sections were examined unstained using a Zeiss Axioplan fluorescence microscope, and labeled cell bodies were plotted with an X-Y stage digitizer (MD-3, Accustage) and associated software (MD-Plot, v. 5.3). Photographs of selected tissue sections and injection sites were obtained using a Zeiss ICC5 camera. The resulting images were cropped, adjusted for level, brightness, and contrast, and re-sized using Adobe Photoshop.

DATA ANALYSIS

Digital files containing cell count and position information were processed in Adobe Illustrator CS6, which was used to extract and align the claustrum outlines and surgical schematics. A three-dimensional model of the claustrum from case FR01 was created using manually aligned Nissl-stained sections with mid-thickness drawings, resulting in a series of contours that were

then reconstructed into a 3D triangular mesh (**Figure 1B**), using the program CARET (Van Essen et al., 2001). The lateral view of this 3-dimensional model was then traced and smoothed in Illustrator, and overlaid with a 200 × 200 μm square grid, which was used as a template for plotting cells from each case, in order to facilitate comparison across injections. Each case was normalized to the maximum dorsal-ventral distance of the claustrum sections, and the grid was subsequently applied across all sections (24–26 sections per case). Cells within each grid square were counted and translated to a "heat map." Color scales were derived by setting the low value to 20% of the respective color on the CMYK color scale, with the 100% value as the maximum (e.g., 20–100% yellow for the minimum-maximum range) for labeled cell density within each grid square. In practice, the cell density across all cases ranged from 1 cell to approximately 25 cells/grid, with the vast majority of grid squares containing fewer than 5 cells. Although this method yields a valuable display for comparison across injections and cases, it necessarily introduces some distortions, especially at the extreme dorsal and ventral portions of the map, where the *Cebus* claustrum varies the most in its medial-lateral extent. Moreover, the relative medial and lateral positions of labeled cells are lost in this flattened display. The distortion was considered acceptable in this study, as there were no cells in the dorsal-most or dorso-lateral portions of the insular claustrum in any of the cases studied. Spatial separation of cells in the ventral regions of the insular claustrum was observed, but this information is not captured in the flattened 2-D map format.

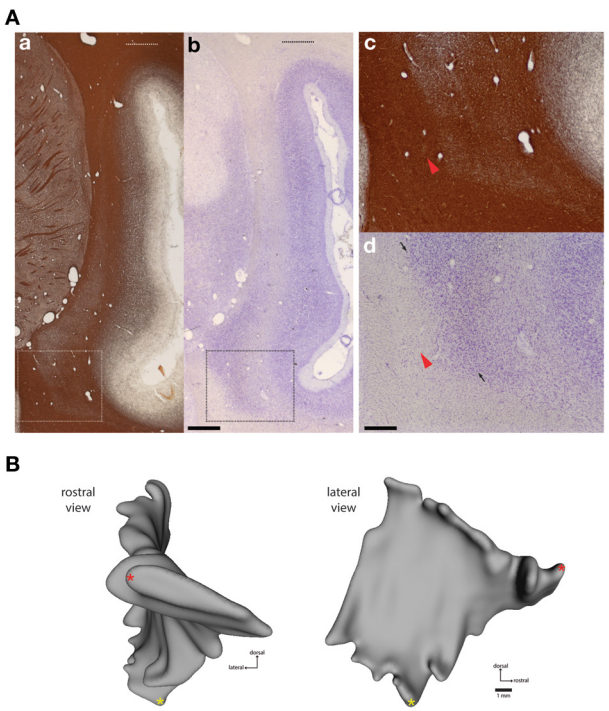

FIGURE 1 | Histological boundaries of *Cebus* claustrum. (A) Myelin **(a,c)** and nissl **(b,d)** stained frontal sections showing the dorsal and ventral extent of the claustrum at approximately A-P +13.0 in the atlas of Eidelberg and Saldias (1960). Dashed lines in the low magnification images **(A)** show the maximum dorsal extent of the claustrum, which is difficult to appreciate in most histological preparations. The rectangular outlines in **(a,b)** indicate areas shown at high magnification in **(c,d)**. Panels **(c,d)** show the difficulty of accurate estimation of the ventromedial boundary of the claustrum in standard histological preparations. Red arrowheads show a small cluster of cells separated from the putative claustrum boundary by a portion of the external capsule white matter. Small arrows in **(d)** show the approximate boundary between the dorsal endopiriform nucleus and the insular claustrum as estimated from the histological characteristics of the marmoset (Paxinos et al., 2012). Detailed cytoarchitectonic information is not currently available for *Cebus*, so this parcellation should be considered provisional, pending identification of reliable markers of internal and external claustrum boundaries in this species. Scale bars = 1 mm in **(b)**; 0.2 mm in **(d)**. **(B)** shows frontal (left) and lateral (right) views of case FR01, modeled as described in Materials and Methods. The lateral view was used as the template for heat mapping of tracer distribution in subsequent figures. Red and yellow asterisks provide common points of reference for the rotated views.

RESULTS

GENERAL FINDINGS

The cytoarchitectonic and myeloarchitectonic characteristics of the *Cebus* monkey claustrum have not been previously described in detail. The appearance of the claustrum in frontal sections is generally consistent with that of other commonly used laboratory primate species, including the macaque (Pearson et al., 1982; Kowianski et al., 1999), vervet monkey (Kowianski et al., 1999), and marmoset (Burman et al., 2011a; Paxinos et al., 2012). One morphological difference between the *cebus* monkey and the marmoset is the dorsolateral extension of the insular claustrum into the white matter of the parietal operculum overlying the lateral sulcus, as shown in **Figure 1**. This is not observed in marmosets, but is present in macaques (Baizer, 2014) and humans, though the functional significance and cortical connectivity of this region remain poorly characterized.

Definition of claustrum borders with respect to the adjacent white matter tracts was clearest in myelin-stained sections (**Figures 1Aa,c**), with the claustrum appearing as a region of lightly myelinated tissue between the external and extreme capsules. The dorsolateral extension of the claustrum was evident in both Nissl and myelin stains, although it was faint (**Figures 1Aa,b**, upper dotted lines). In addition, precise determination of the rostral and ventral boundaries of the claustrum was difficult, especially at the rostral-caudal level, where it converges with the anterior insula, consistent with findings from both rodent and other primate species (**Figure 1**; Mathur et al., 2009; Paxinos et al., 2012). In several sections, small clusters of cells were located away from the apparent medial boundary of the claustrum (**Figures 1Ac,d**; red arrows). In caudal sections, the boundary between the dorsal endopiriform nucleus and insular claustrum was best appreciated in Nissl stained sections (dark arrowheads in **Figures 1Ad**). The general location of this boundary is consistent with the demarcation reported for the marmoset (Paxinos et al., 2012), but the presence of detached cell clusters (green arrowheads in **Figures 1Ac,d**) precluded volumetric measurement or direct comparisons between species. Cytochrome oxidase was not particularly useful for delineation of either boundaries or internal compartments of the claustrum (data not shown).

Tracer injections were deemed successful if the main tracer deposit was predominantly confined to an area of cortical gray

matter which could be clearly localized by cytoarchitectonic and myeloarchitectonic characteristics, and for which long range transport of the tracer material could be definitively established by the presence of labeled cells in thalamic nuclei, cortical areas far removed from prefrontal cortex, or the homotopic contralateral cortical hemispheres. Nine successful tracer injections were placed in three monkeys. The majority of tracer deposits targeted the frontal pole (area 10). One deposit was placed in the rostral dorsolateral prefrontal cortex (area 9). Two injections were placed in area 12, one in the orbital subdivision (area 12o; case FR04-DY) near the border with the lateral subdivision of area 11, and one in ventrolateral prefrontal area 12 (FR02-DY). Double-labeled neurons were not observed, although it is still possible that these exist in small numbers.

As viewed from the lateral aspect, the *Cebus* claustrum is shaped like a distended rhomboid, slightly elongated on the rostral-caudal axis. Because of the undulating structure of the claustrum, this view has been used to demonstrate topography of cortical projections in previous studies (Pearson et al., 1982), and we employed it in this study to map the distribution of retrogradely labeled neurons, as detailed in the Materials and Methods.

FRONTAL POLE CONNECTIONS

Six injections were placed in the frontal pole region of two monkeys. The resulting distribution of labeled neurons in the ipsilateral claustrum is shown for a representative case (FR02) in **Figure 2**, which received two injections within area 10. Both injections resulted in patches of retrogradely labeled cells in the claustrum, which occupied a ventral position across multiple levels of the rostral-caudal axis. Areas of particularly dense clustering of labeled neurons were observed in the rostral and middle levels of the claustrum. However, no labeled cells were observed in the dorsal part the claustrum. The medial FE injection yielded far fewer labeled cells than the central FB injection, with the cells clustered into smaller areas (**Figures 2B,C**); these were completely encompassed within the area containing FB label. This pattern

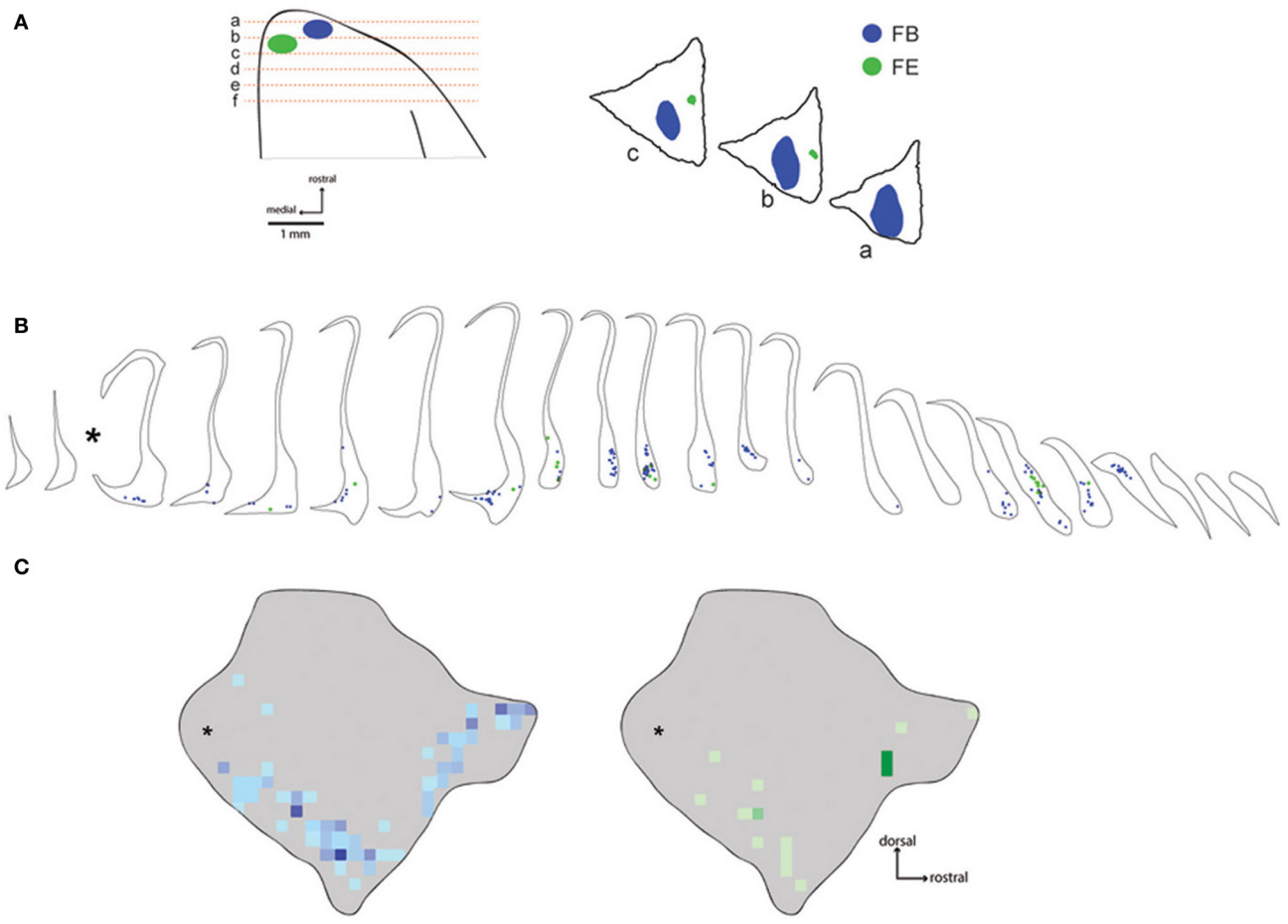

FIGURE 2 | Distribution of labeled neurons following injections in area 10. The placements of fast blue and fluoroemerald injections into the frontal pole are shown in **(A)**. Coronal section locations are shown schematically on the left, while the positions of the main tracer deposits are shown in the digitized tracings on the right. Note that the fluid volume of the fluoro emerald (FE) injection in this case (FR02) was quite large (1 μl, **Table 1**), but the largest fraction of the deposit was located in the histologically stained sections between the unstained fluorescence sections plotted in this figure. Panel **(B)** shows the location of each of the labeled neurons from these injections in coronal sections of the claustrum. The corresponding heat maps are shown in **(C)**, illustrating the overall distribution of labeled cells overlaid on the lateral view of the 3-D model of the *Cebus* claustrum. Asterisks indicate the position of approximately 2 sections lost at the interface of the rostral and caudal tissue blocks during tissue cutting.

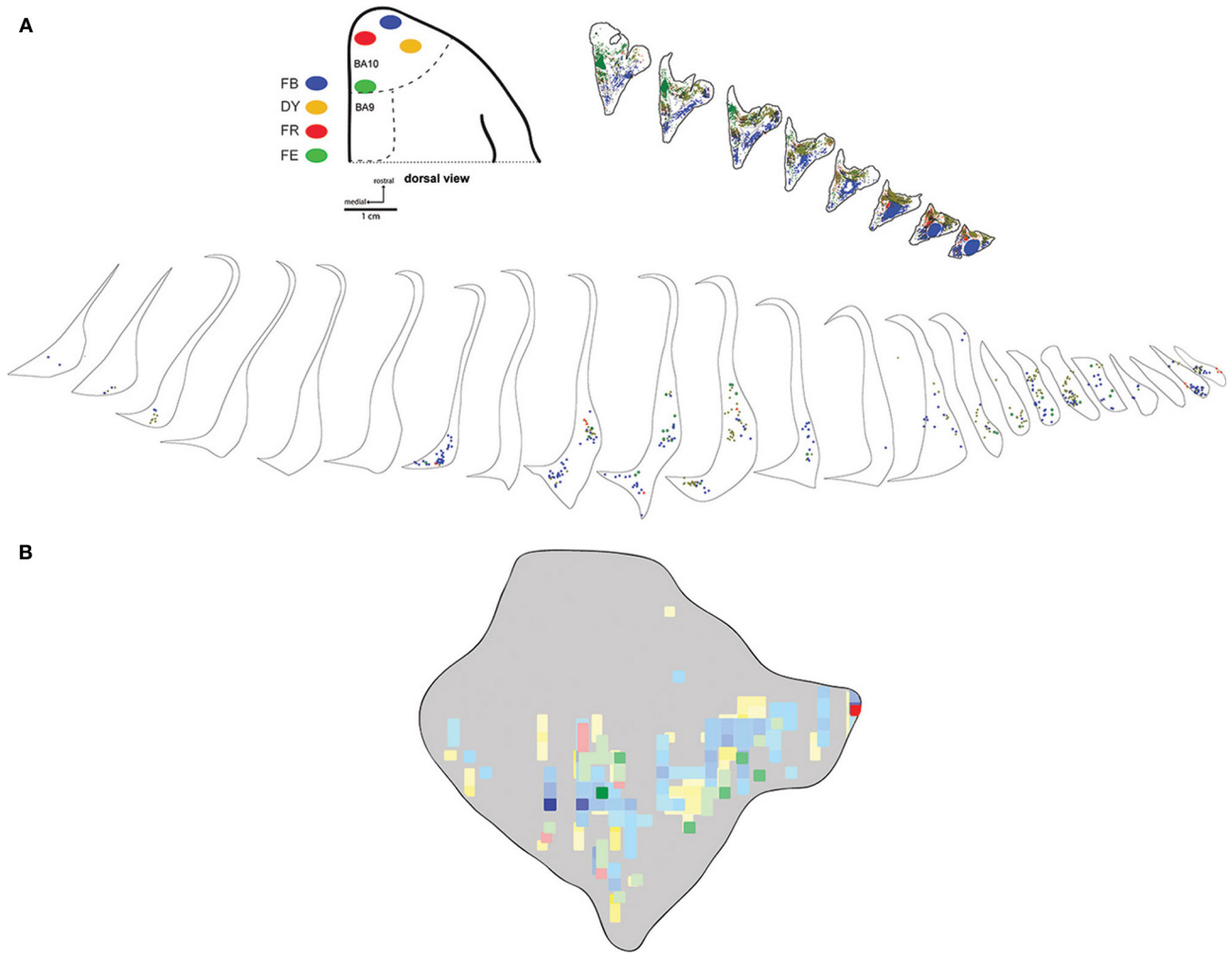

FIGURE 3 | Medial-lateral gradient of claustrum projections. Locations of 4 tracer injections in area 10 of case FR01 are shown schematically in **(A)**. The distributions of labeled neurons for each tracer are overlaid in the heatmap format in panel **(B)**. Scale bars = 1 cm in **(A)**; 1 mm in **(B)**. FB, fast blue; DY, diamidino yellow; FR, fluoro ruby; FE, fluoro emerald.

of increased claustrum label density following tracer injections in more rostral and lateral portions of area 10 was also evident in the second case, in which three of the injections were well contained within area 10 (FR01- FB, FR, DY), and one injection was located near the boundary with area 9 (FR01-FE). The distributions of tracer resulting from those injections are summarized in the heat map in **Figure 3**. The central and lateral injections (FB and DY, respectively) labeled a much broader area of ventral and medial claustrum than the medial injections (FE and FR), both in terms of overall tissue area and density of labeled neurons. Both medial injections yielded only isolated labeled cells in the claustrum. Whether this trend reflects functional differences within area 10, or different transport properties of the dextran-based tracers (FR and FE) will require further study. However, both of the medial area 10 injections resulted in long-range transport of tracer, confirmed by the presence of labeled neurons in various thalamic nuclei (data not shown).

DORSAL PREFRONTAL CONNECTIONS

The dorsal prefrontal region includes areas 8, 9, and 46 (Petrides and Pandya, 1999; Sallet et al., 2013). In this study, a large fast blue injection was deposited in area 9 of one animal (case FR04-FB), which yielded patches of retrogradely labeled neurons in a band which closely tracked the distribution of label observed following injections into the frontal pole, although in a slightly more dorsal position within the claustrum. A discrete, longitudinal patch centered in the rostral part of the claustrum was the dominant pattern, with isolated cells and scattered small patches extending along the ventral border to the caudal terminus (**Figure 4**). Consistent with the pattern observed following injections in area 10, the dorsal and dorsolateral parts of the claustrum were devoid of label, and no interhemispheric projections from the contralateral claustrum were evident. A single isolated cell body was observed in the mid-dorsal region of the contralateral claustrum following this area 9 injection.

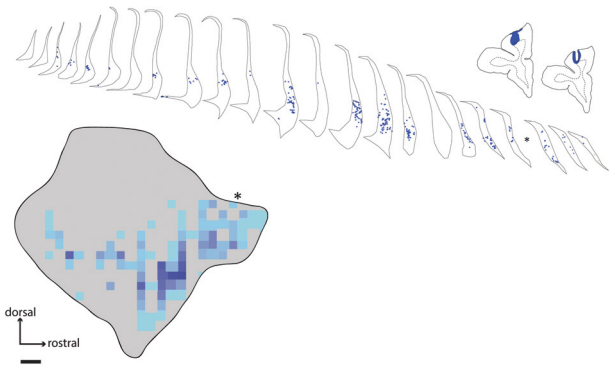

FIGURE 4 | Distribution of labeled neurons in claustrum following tracer injection in area 9. Line drawings show placement of fast blue injection in case FR04, along with the resulting retrogradely labeled cell bodies in the ipsilateral claustrum. Asterisk indicates the position of a single tissue section lost due to slide damage during coverslipping. Scale bar = 1 mm.

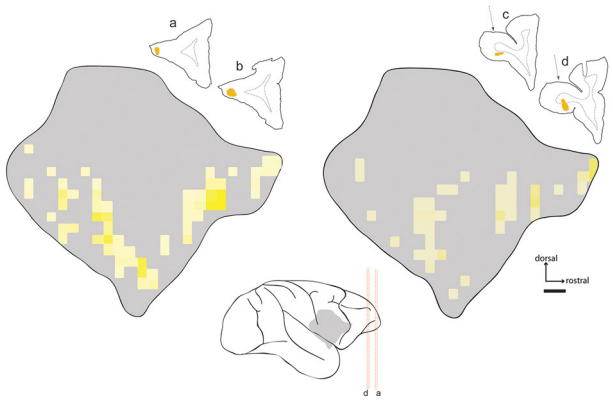

FIGURE 5 | Distribution of labeled neurons in claustrum following injections in area 12. Heat map projections for two injections of diamidino yellow (DY) in area 12 (cases FR02- left; FR04- right). Line drawings show injection locations in frontal sections. Center schematic image shows location of claustrum relative to tissue sections and major sulci of the *Cebus* brain (gray silhouette). Red dashed lines correspond to tissue sections as marked. The dotted arrows on the right indicate the approach used for injection of area 12o, which traversed the cortical white matter overlying that area. Implications of this approach for interpretation of the data are described in the text.

VENTRAL LATERAL PREFRONTAL AND LATERAL ORBITOFRONTAL CONNECTIONS

Two injections were placed in subdivisions of area 12. One DY injection was deposited in the ventral lateral prefrontal cortex (rostrolateral area 12; case FR02-DY), while the other was predominantly in orbital area 12 (case FR04-DY). In the latter case, the injection site obscured the likely cytoarchitectural boundary with area 11, so we cannot definitively exclude the possibility that some of the tracer was deposited in this area. However, the distribution of labeled neurons from both injections was qualitatively similar, as shown in **Figure 5**. As observed following prefrontal injections in areas 9 and 10, the majority of labeled cells were observed in a band running along the ventral part of the claustrum, with no cells in the dorsal or dorsolateral insular claustrum.

SUMMARY OF CONNECTIONS

The full extent of claustrum projections to prefrontal cortex is summarized in **Figures 6A–C**, which shows the relative position of the claustrum in lateral view (**Figure 6A**), as well as some of its proposed subdivisions (frontal- fCl, middle- mCl, and ventral- vCl; see Gattass et al.; this volume) within which prefrontal connections originated (**Figure 6B**). A smoothed representation of the extent of labeled cells originating from each case is shown in **Figure 6C**, which indicates the degree of homogeneity observed from injections into specific prefrontal areas.

DISCUSSION

The claustrum in most mammals has been broadly divided into a dorsal compartment, the "insular claustrum" or simply "claustrum," and the endopiriform nucleus, which is in turn divided into dorsal and ventral components (Paxinos et al., 2012). In other primate species, as well as in cats, the majority of connections from sensory and association cortex are confined to the insular region of the claustrum, while the endopiriform nucleus is largely connected with olfactory and entorhinal cortex, along with limbic subcortical nuclei. Our data in the *Cebus* conform to this pattern, with the overwhelming majority of projections to frontal pole and dorsolateral prefrontal areas arising from insular claustrum.

ORGANIZATION OF CLAUSTRUM-PREFRONTAL CONNECTIONS

The distribution of retrograde label in the claustrum following prefrontal injections in *Cebus* was largely consistent with our previous findings in the marmoset (Burman et al., 2011a), and with the topography of claustrum-prefrontal projections reported in macaques (Pearson et al., 1982). In particular, labeled neurons following injections in areas 9 and 10 were concentrated in a band located along the ventral portion of the claustrum. While the injection in area 9 labeled cells primarily in the rostral part of the claustrum, those in area 10 resulted in strong label in a second, more caudal cluster (compare **Figures 2**, **4**). Claustrum projections to area 12 originated from a similar territory. Labeled neurons were largely absent from the narrow dorsal region of the claustrum, medial to insular cortex, and were completely absent from the extreme dorsal and dorsolateral regions, which have been reported to contain the bulk of claustral neurons projecting to somatomotor cortex in the macaque (Pearson et al., 1982; Minciacchi et al., 1991). It should be noted that the injection of area 12o (Case FR04-DY) likely involved the white matter dorsal to this area, as the injection needle passed through the overlying tissue. However, we are confident that this did not affect the validity of our observations to an appreciable extent, given the lack of non-specific label in both cerebral hemispheres, which is generally observed in cases of significant white matter intrusion, and the similarity of the pattern of claustrum label resulting from this injection to the other area 12 case (case FR02-DY), in which the white matter was not involved.

With the exception of an isolated FB neuron from an injection in area 9 (case FR04-FB), retrogradely labeled neurons were

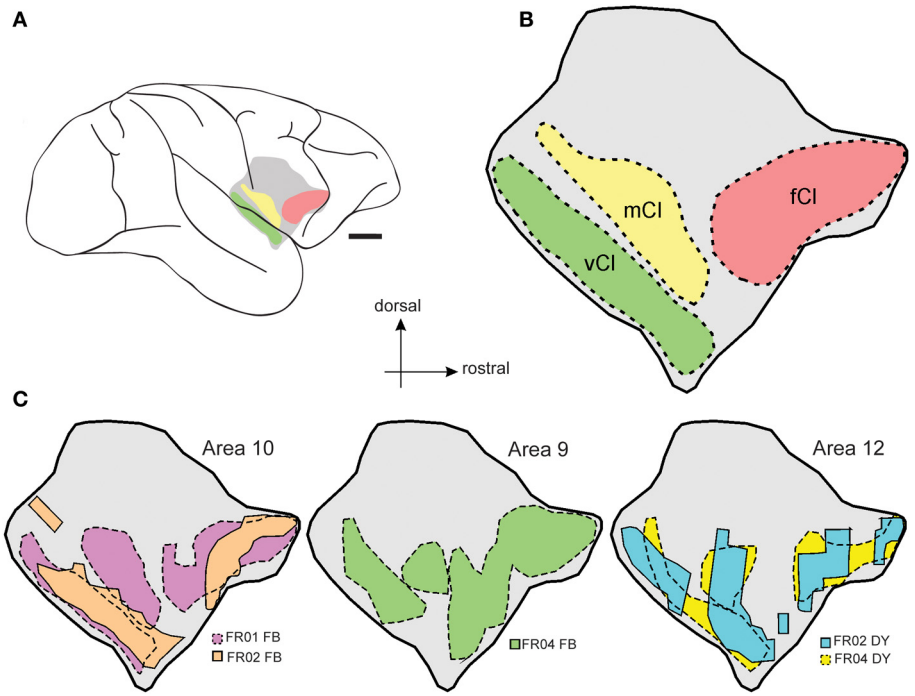

FIGURE 6 | Summary of claustrum-prefrontal projections. Regions of the *Cebus* claustrum as defined by Gattass et al. (this volume) are schematically displayed as color coded regions in **(A,B)**. **(C)** illustrates the smoothed outline of the maximum extent of each patch of labeled cells within the claustrum for each of the prefrontal cortex injections included in this study. Scale bar = 4 mm in **(A)**.

restricted to the ipsilateral claustrum. This is inconsistent with the pattern of interhemispheric connections observed in the rat, e.g., between claustrum and the frontal eye field (Smith and Alloway, 2014), and other prefrontal areas (Sloniewski et al., 1986; Smith and Alloway, 2010). This difference is unlikely to be related to the directionality of the tracers employed, as both FB and DY were employed by Slownieski et al., and resulted in bilateral labeling. In primates, interhemispheric claustral connections have been reported in the mouse lemur (Park et al., 2012), using high resolution diffusion tensor imaging, and in humans, using constrained spherical deconvolution tractography (Milardi et al., 2013). However, the nature of these methods does not allow disambiguation between projections to or from the cortex (see also Kunzle, 1975). Our data suggest that the interhemispheric claustrum-prefrontal projections in primates are qualitatively weaker than those of the rodent.

Consistent with results in the marmoset (Burman et al., 2011a), tracer injections into medial area 10 of *Cebus* yielded far fewer labeled cell bodies in the claustrum than injections in the dorsal and lateral portions of area 10. Whereas that result is to be considered preliminary based on the small number of injections and potential variation in transport of different tracer types, these results are in line with the hypothesis that differences in connectivity with the claustrum are related to other functional differences described between the lateral and medial subregions of area 10 (Ongur et al., 2003; Burman et al., 2011a,b). Area 10 is a cortical region that has expanded significantly across primate species, including humans (Semendeferi et al., 2001), and interestingly, the lateral portion of area 10 undergoes considerably greater postnatal expansion in humans than does the medial portion (Hill et al., 2010). A systematic review of the area 10 literature by Gilbert et al. (2006) found evidence for a significant difference in activation of medial vs. lateral area 10, with the lateral region exhibiting greater responses to tasks involved in episodic retrieval of non-emotional content. Whether the apparent difference in claustrum connectivity with the lateral vs. medial area 10 is present in humans and potentially correlated with the functionality of this area is an open question, which may be addressable using high definition tractography or similar approaches. Somewhat curiously, no double labeled neurons were observed in the claustrum in FR04 or any of the other cases examined, suggesting that projections from individual claustrum neurons to prefrontal areas in *Cebus* are restricted to relatively small cortical populations. The apparent absence of double labeled cells is especially surprising in case FR04, in which the tracers were placed in close proximity within a relatively small cortical area. It will be interesting to see if this pattern holds among tracer injections in widely disparate cortical areas, e.g., simultaneous tracer placement in PFC and cingulate or parietal areas, for instance. In the macaque, Selemon and Goldman-Rakic (1988) reported overlapping fields of terminal label from simultaneous parietal and prefrontal injections using anterograde tracer injections.

The distribution of labeled neurons in claustrum following the area 9 injection was largely consistent with previous studies of the macaque (Pearson et al., 1982; Saleem et al., 2014) and marmoset. Damage or hypoactivation of this area is often reported

in association with schizophrenia and impaired working memory (Barch et al., 2003). The dense projection we observed from the rostral and ventral claustrum to area 9 suggests a possible focus for future investigations of claustrum involvement in prefrontal function in both normal and pathological function, and the similar topography of this projection across primate species suggests that widely used laboratory primate species could be effective models of both of these states.

Activity in ventrolateral prefrontal cortex, which includes area 12 (according to Carmichael and Price, 1996; note that this region overlaps with area 47 in other nomenclatures Petrides and Pandya, 2002; Paxinos et al., 2012), is also associated with retrieval of information from memory, but not with maintenance or monitoring of that information post-retrieval, which is associated with areas 9 and 9/46 (Cadoret et al., 2001). Thus it is likely that the functional interaction between the claustrum and prefrontal cortex overlaps both working memory- and retrieval- dependent processes.

RELATIONSHIP OF CLAUSTRUM-PREFRONTAL PROJECTIONS TO CLAUSTRUM CONNECTIONS WITH SENSORY AND ASSOCIATION AREAS

Previous tracing studies of claustral projections in primates have shown localized sensory cortical connections within the body of the claustrum (Reviewed in Druga, 2014; visual cortex- Tigges et al., 1982; Doty, 1983; Baizer et al., 1997; Gattass et al., 2014; somatosensory cortex- Pearson et al., 1982; Minciacchi et al., 1991; auditory cortex- Pearson et al., 1982; Smiley et al., 2007; Reser et al., 2009). As mentioned above, it is currently impossible to draw complete homologies of the claustrum anatomy of primate species, though some general patterns have emerged. Projections to visual areas are largely confined to the caudal and mid-dorsal regions of the claustrum. In contrast, motor and somatosensory projections are heavily concentrated in the dorsal and dorsolateral portions of the claustrum, with virtually no overlap between the areas of somato-motor connectivity (Pearson et al., 1982; Minciacchi et al., 1991) and the distribution of prefrontal label we observed. Auditory connections are somewhat more difficult to characterize. We have observed sparse auditory cortex connections in the marmoset (Reser et al., 2009), and other groups have reported claustrum projections to auditory areas in the macaque (Smiley et al., 2007). Where topographic information has been provided, auditory connections were restricted to the ventral claustrum (Pearson et al., 1982). Thus, it appears that there is relatively little overlap among the major sensory cortical areas and PFC projections. This roughly concords with the description of claustrum connections in the human as reported by Fernandez-Miranda et al. (2008), allowing for differences in claustrum topology across species. Pearson et al. (1982) reported that labeled cells from injections in area 22 (non-primary auditory cortex) in the macaque were concentrated along the ventral portion of the middle and caudal claustrum. Based on the demarcation of the injection zone in that report, it is likely that the target tissue included part of the temporal lobe polymodal association cortex. The precise relationship of claustrum projections to association areas and respectively, auditory and visual sensory areas along the primate temporal lobe, remains to be determined.

HYPOTHESIS: POSSIBLE CLAUSTRUM INVOLVEMENT IN SWITCHING BETWEEN RESTING STATE NETWORKS

As discussed below, there are intriguing parallels between the observed anatomical connectivity of the claustrum and the prefrontal components of several of the known cortical resting state networks. Here we introduce the hypothesis that one function of the primate claustrum may involve mediation or modulation of resting state network activity.

The identification of synchronously oscillating patterns of regional blood flow and synaptic activity across cortico-cortical and subcortical-cortical networks in recent years has forced a re-examination of what occurs in the brain during periods of presumed inactivity. Approximately a dozen resting state cortical networks (Mantini et al., 2011; Van Den Heuvel and Sporns, 2013) have been identified in primates, including: the default mode network (DMN; Greicius et al., 2003; reviewed in Buckner et al., 2008); the central executive network (Damoiseaux et al., 2008); the fronto-parietal control network (Dosenbach et al., 2007; Vincent et al., 2008); and the salience network (Downar et al., 2002; Seeley et al., 2007).

Our data show that prefrontal areas which are part of the salience network (area 12) and areas which are not (9, 10) receive input from the same region of the claustrum (the rostral and ventral region), though the precise topography of inputs requires more detailed investigation. Specifically, it will be necessary in future studies to determine if individual claustrum cells project to multiple areas of prefrontal or other cortex, i.e., whether they could provide input to multiple cortical functional networks. The overlap in topography of input from the claustrum to these areas suggests to us that the circuitry of the claustrum-prefrontal connection would ideally position the claustrum as a modulator or "switch" that could desynchronize or terminate correlated activation of DMN-related areas when external cues require activation of the various task-positive networks. Indeed, the time-series analysis of Seeley et al. (2007) showed that the component cortical areas of the salience network exhibited weak correlation over time, suggesting that the temporal structure of network activity could be dictated by one or a very small number of hub areas. The claustrum is ideally positioned, in terms of connectivity and anatomy, to act in this capacity. Additional anatomical data which would be required to assess this hypothesis includes mapping of claustrum connections with other known network hubs, which include (for the DMN) ventromedial prefrontal (Damoiseaux et al., 2008) and subgenual anterior cingulate cortex (Mantini et al., 2011), the precuneus, and especially posterior cingulate cortex (Damoiseaux et al., 2008; Belcher et al., 2013). Extensive study will be required to assess the hypothesized involvement of the claustrum in DMN and/or other cortical networks, and to determine whether the claustrum acts in isolation or in concert with other cortical or subcortical structures.

POSSIBLE LIMITATIONS OF THIS STUDY

There are several aspects of this study which must be considered in evaluation of our results and conclusions. First, the homology between brain areas of different primate species is difficult to establish, especially as the size and function of the various regions is known to have changed across primate evolution (Semendeferi

et al., 2001; Chaplin et al., 2013), with a general trend toward segregation between areas and networks with increasing cortical size (Changizi and Shimojo, 2005). In both body mass and brain volume, the *Cebus* monkey is at least 10 times larger than the species we have studied most recently, the marmoset, so it is reasonable to assume that some functional changes across prefrontal areas have occurred. A second key consideration is our poor understanding of the functional architecture of the claustrum itself, especially in primates. Although recent advances have been made in identification of anatomical and neurochemical markers of the claustrum (Arimatsu et al., 2009; Mathur et al., 2009), this approach has not yet yielded reliable results in primates. Thus, it remains difficult to infer claustrum functions from compartmentalization or topographic organization of cortical connections. Finally, testing hypotheses regarding claustrum involvement in cortical functional networks will require a more precise survey of which cortical areas are components of specific networks, and reconciliation of the anatomical definitions of those areas with areas of increased or decreased activity in functional studies, which will likely require intensive future study and revisitation of existing datasets.

ACKNOWLEDGMENTS

The authors gratefully acknowledge the assistance of Edil Saturato and Liliane Pontes in surgical and histological preparations, and Dr. Elizabeth Zavitz for proofreading and editorial suggestions regarding the manuscript. This work was funded by grants from the Australian Research Council (DP110101200) and National Health and Medical Research Council (APP1068140), and by grants from FAPERJ and CNPq.

REFERENCES

Arimatsu, Y., Nihonmatsu, I., and Hatanaka, Y. (2009). Localization of latexin-immunoreactive neurons in the adult cat cerebral cortex and claustrum/endopiriform formation. *Neuroscience* 162, 1398–1410. doi: 10.1016/j.neuroscience.2009.05.060

Baizer, J. (2014). "The neurochemical organization of the claustrum," in *The Claustrum: Structural, Functional, and Clinical Neuroscience*, eds J. Smythies, L. Edelstein, and V. Ramachandran (San Diego, CA: Elsevier), 85–118.

Baizer, J. S., Lock, T. M., and Youakim, M. (1997). Projections from the claustrum to the prelunate gyrus in the monkey. *Exp. Brain Res.* 113, 564–568. doi: 10.1007/PL00005607

Barch, D. M., Sheline, Y. I., Csernansky, J. G., and Snyder, A. Z. (2003). Working memory and prefrontal cortex dysfunction: specificity to schizophrenia compared with major depression. *Biol. Psychiatry* 53, 376–384. doi: 10.1016/S0006-3223(02)01674-8

Belcher, A. M., Yen, C. C., Stepp, H., Gu, H., Lu, H., Yang, Y., et al. (2013). Large-scale brain networks in the awake, truly resting marmoset monkey. *J. Neurosci.* 33, 16796–16804. doi: 10.1523/JNEUROSCI.3146-13.2013

Buckner, R. L., Andrews-Hanna, J. R., and Schacter, D. L. (2008). The brain's default network: anatomy, function, and relevance to disease. *Ann. N.Y. Acad. Sci.* 1124, 1–38. doi: 10.1196/annals.1440.011

Burman, K. J., Palmer, S. M., Gamberini, M., and Rosa, M. G. (2006). Cytoarchitectonic subdivisions of the dorsolateral frontal cortex of the marmoset monkey (*Callithrix jacchus*), and their projections to dorsal visual areas. *J. Comp. Neurol.* 495, 149–172. doi: 10.1002/cne.20837

Burman, K. J., Reser, D. H., Richardson, K. E., Gaulke, H., Worthy, K. H., and Rosa, M. G. (2011a). Subcortical projections to the frontal pole in the marmoset monkey. *Eur. J. Neurosci.* 34, 303–319. doi: 10.1111/j.1460-9568.2011.07744.x

Burman, K. J., Reser, D. H., Yu, H. H., and Rosa, M. G. (2011b). Cortical input to the frontal pole of the marmoset monkey. *Cereb. Cortex* 21, 1712–1737. doi: 10.1093/cercor/bhq239

Burman, K. J., and Rosa, M. G. (2009). Architectural subdivisions of medial and orbital frontal cortices in the marmoset monkey (*Callithrix jacchus*). *J. Comp. Neurol.* 514, 11–29. doi: 10.1002/cne.21976

Cadoret, G., Pike, G. B., and Petrides, M. (2001). Selective activation of the ventrolateral prefrontal cortex in the human brain during active retrieval processing. *Eur. J. Neurosci.* 14, 1164–1170. doi: 10.1046/j.0953-816x.2001.01737.x

Carmichael, S. T., and Price, J. L. (1996). Connectional networks within the orbital and medial prefrontal cortex of macaque monkeys. *J. Comp. Neurol.* 371, 179–207. doi: 10.1002/(SICI)1096-9861(19960722)37

Changizi, M. A., and Shimojo, S. (2005). Parcellation and area-area connectivity as a function of neocortex size. *Brain Behav. Evol.* 66, 88–98. doi: 10.1159/000085942

Chaplin, T. A., Yu, H. H., Soares, J. G., Gattass, R., and Rosa, M. G. (2013). A conserved pattern of differential expansion of cortical areas in simian primates. *J. Neurosci.* 33, 15120–15125. doi: 10.1523/JNEUROSCI.2909-13.2013

Crick, F. C., and Koch, C. (2005). What is the function of the claustrum? *Philos. Trans. R. Soc. Lond. B Biol. Sci.* 360, 1271–1279. doi: 10.1098/rstb.2005.1661

Cruz-Rizzolo, R. J., De Lima, M. A., Ervolino, E., De Oliveira, J. A., and Casatti, C. A. (2011). Cyto-, myelo- and chemoarchitecture of the prefrontal cortex of the Cebus monkey. *BMC Neurosci.* 12:6. doi: 10.1186/1471-2202-12-6

Damoiseaux, J. S., Beckmann, C. F., Arigita, E. J., Barkhof, F., Scheltens, P., Stam, C. J., et al. (2008). Reduced resting-state brain activity in the "default network" in normal aging. *Cereb. Cortex* 18, 1856–1864. doi: 10.1093/cercor/bhm207

Dosenbach, N. U., Fair, D. A., Miezin, F. M., Cohen, A. L., Wenger, K. K., Dosenbach, R. A., et al. (2007). Distinct brain networks for adaptive and stable task control in humans. *Proc. Natl. Acad. Sci. U.S.A.* 104, 11073–11078. doi: 10.1073/pnas.0704320104

Doty, R. W. (1983). Nongeniculate afferents to striate cortex in macaques. *J. Comp. Neurol.* 218, 159–173. doi: 10.1002/cne.902180204

Downar, J., Crawley, A. P., Mikulis, D. J., and Davis, K. D. (2002). A cortical network sensitive to stimulus salience in a neutral behavioral context across multiple sensory modalities. *J. Neurophysiol.* 87, 615–620. doi: 10.1152/jn.00636.2001

Druga, R. (2014). "The structure and connections of the claustrum," in *The Claustrum: Structural, Functional, and Clinical Neuroscience*, eds J. Smythies, L. Edelstein, and V. Ramachandran (San Diego, CA: Academic Press, Elsevier), 29–84.

Eidelberg, E., and Saldias, C. A. (1960). A stereotaxic atlas for cebus monkeys. *J. Comp. Neurol.* 115, 103–123. doi: 10.1002/cne.901150202

Fernandez-Miranda, J. C., Rhoton, A. L. Jr., Alvarez-Linera, J., Kakizawa, Y., Choi, C., and De Oliveira, E. P. (2008). Three-dimensional microsurgical and tractographic anatomy of the white matter of the human brain. *Neurosurgery* 62, 989–1026. doi: 10.1227/01.neu.0000333767.05328.49

Gallyas, F. (1979). Silver staining of myelin by means of physical development. *Neurol. Res.* 1, 203–209.

Gattass, R., Soares, J. G., Desimone, R., and Ungerleider, L. G. (2014). Connectional subdivision of the claustrum: two visuotopic subdivisions in the macaque. *Front. Syst. Neurosci.* 8:63. doi: 10.3389/fnsys.2014.00063

Gilbert, S. J., Spengler, S., Simons, J. S., Steele, J. D., Lawrie, S. M., Frith, C. D., et al. (2006). Functional specialization within rostral prefrontal cortex (area 10): a meta-analysis. *J. Cogn. Neurosci.* 18, 932–948. doi: 10.1162/jocn.2006.18.6.932

Greicius, M. D., Krasnow, B., Reiss, A. L., and Menon, V. (2003). Functional connectivity in the resting brain: a network analysis of the default mode hypothesis. *Proc. Natl. Acad. Sci. U.S.A.* 100, 253–258. doi: 10.1073/pnas.0135058100

Hill, J., Dierker, D., Neil, J., Inder, T., Knutsen, A., Harwell, J., et al. (2010). A surface-based analysis of hemispheric asymmetries and folding of cerebral cortex in term-born human infants. *J. Neurosci.* 30, 2268–2276. doi: 10.1523/JNEUROSCI.4682-09.2010

Hoover, W. B., and Vertes, R. P. (2007). Anatomical analysis of afferent projections to the medial prefrontal cortex in the rat. *Brain Struct. Funct.* 212, 149–179. doi: 10.1007/s00429-007-0150-4

Kowianski, P., Dziewiatkowski, J., Kowianska, J., and Morys, J. (1999). Comparative anatomy of the claustrum in selected species: a morphometric analysis. *Brain Behav. Evol.* 53, 44–54. doi: 10.1159/000006581

Kunzle, H. (1975). Bilateral projections from precentral motor cortex to the putamen and other parts of the basal ganglia. an autoradiographic study in *Macaca fascicularis*. *Brain Res.* 88, 195–209. doi: 10.1016/0006-8993(75)90384-4

Mantini, D., Gerits, A., Nelissen, K., Durand, J. B., Joly, O., Simone, L., et al. (2011). Default mode of brain function in monkeys. *J. Neurosci.* 31, 12954–12962. doi: 10.1523/JNEUROSCI.2318-11.2011

Mathur, B. N., Caprioli, R. M., and Deutch, A. Y. (2009). Proteomic analysis illuminates a novel structural definition of the claustrum and insula. *Cereb. Cortex* 19, 2372–2379. doi: 10.1093/cercor/bhn253

Milardi, D., Bramanti, P., Milazzo, C., Finocchio, G., Arrigo, A., Santoro, G., et al. (2013). Cortical and subcortical connections of the human claustrum revealed *in vivo* by constrained spherical deconvolution tractography. *Cereb. Cortex* doi: 10.1093/cercor/bht231. [Epub ahead of print].

Minciacchi, D., Granato, A., and Barbaresi, P. (1991). Organization of claustrocortical projections to the primary somatosensory area of primates. *Brain Res.* 553, 309–312. doi: 10.1016/0006-8993(91)90840-R

Ongur, D., Ferry, A. T., and Price, J. L. (2003). Architectonic subdivision of the human orbital and medial prefrontal cortex. *J. Comp. Neurol.* 460, 425–449. doi: 10.1002/cne.10609

Park, S., Tyszka, J. M., and Allman, J. M. (2012). The claustrum and insula in *microcebus murinus*: a high resolution diffusion imaging study. *Front. Neuroanat.* 6:21. doi: 10.3389/fnana.2012.00021

Paxinos, G., Watson, C., Petrides, M., Rosa, M., and Tokuno, H. (2012). *The Marmoset Brain in Stereotaxic Coordinates*. London: Academic Press, Elsevier.

Pearson, R. C., Brodal, P., Gatter, K. C., and Powell, T. P. (1982). The organization of the connections between the cortex and the claustrum in the monkey. *Brain Res.* 234, 435–441. doi: 10.1016/0006-8993(82)90883-6

Petrides, M., and Pandya, D. N. (1999). Dorsolateral prefrontal cortex: comparative cytoarchitectonic analysis in the human and the macaque brain and corticocortical connection patterns. *Eur. J. Neurosci.* 11, 1011–1036. doi: 10.1046/j.1460-9568.1999.00518.x

Petrides, M., and Pandya, D. N. (2002). Comparative cytoarchitectonic analysis of the human and the macaque ventrolateral prefrontal cortex and corticocortical connection patterns in the monkey. *Eur. J. Neurosci.* 16, 291–310. doi: 10.1046/j.1460-9568.2001.02090.x

Reser, D. H., Burman, K. J., Richardson, K. E., Spitzer, M. W., and Rosa, M. G. (2009). Connections of the marmoset rostrotemporal auditory area: express pathways for analysis of affective content in hearing. *Eur. J. Neurosci.* 30, 578–592. doi: 10.1111/j.1460-9568.2009.06846.x

Saleem, K. S., Miller, B., and Price, J. L. (2014). Subdivisions and connectional networks of the lateral prefrontal cortex in the macaque monkey. *J. Comp. Neurol.* 522, 1641–1690. doi: 10.1002/cne.23498

Sallet, J., Mars, R. B., Noonan, M. P., Neubert, F. X., Jbabdi, S., O'Reilly, J. X., et al. (2013). The organization of dorsal frontal cortex in humans and macaques. *J. Neurosci.* 33, 12255–12274. doi: 10.1523/JNEUROSCI.5108-12.2013

Seeley, W. W., Menon, V., Schatzberg, A. F., Keller, J., Glover, G. H., Kenna, H., et al. (2007). Dissociable intrinsic connectivity networks for salience processing and executive control. *J. Neurosci.* 27, 2349–2356. doi: 10.1523/JNEUROSCI.5587-06.2007

Selemon, L. D., and Goldman-Rakic, P. S. (1988). Common cortical and subcortical targets of the dorsolateral prefrontal and posterior parietal cortices in the rhesus monkey: evidence for a distributed neural network subserving spatially guided behavior. *J. Neurosci.* 8, 4049–4068.

Semendeferi, K., Armstrong, E., Schleicher, A., Zilles, K., and Van Hoesen, G. W. (2001). Prefrontal cortex in humans and apes: a comparative study of area 10. *Am. J. Phys. Anthropol.* 114, 224–241. doi: 10.1002/1096-8644(200103)114:3

Sloniewski, P., Usunoff, K. G., and Pilgrim, C. (1986). Retrograde transport of fluorescent tracers reveals extensive ipsi- and contralateral claustrocortical connections in the rat. *J. Comp. Neurol.* 246, 467–477. doi: 10.1002/cne.902460405

Smiley, J. F., Hackett, T. A., Ulbert, I., Karmas, G., Lakatos, P., Javitt, D. C., et al. (2007). Multisensory convergence in auditory cortex, I. cortical connections of the caudal superior temporal plane in macaque monkeys. *J. Comp. Neurol.* 502, 894–923. doi: 10.1002/cne.21325

Smith, J. B., and Alloway, K. D. (2010). Functional specificity of claustrum connections in the rat: interhemispheric communication between specific parts of motor cortex. *J. Neurosci.* 30, 16832–16844. doi: 10.1523/JNEUROSCI.4438-10.2010

Smith, J. B., and Alloway, K. D. (2014). Interhemispheric claustral circuits coordinate sensory and motor cortical areas that regulate exploratory behaviors. *Front. Syst. Neurosci.* 8:93. doi: 10.3389/fnsys.2014.00093

Smythies, J., Edelstein, L., and Ramachandran, V. (2014). *The Claustrum: Structural, Functional, and Clinical Neuroscience*. San Diego, CA: Academic Press, Elsevier.

Tanne-Gariepy, J., Boussaoud, D., and Rouiller, E. M. (2002). Projections of the claustrum to the primary motor, premotor, and prefrontal cortices in the macaque monkey. *J. Comp. Neurol.* 454, 140–157. doi: 10.1002/cne.10425

Tigges, J., Tigges, M., Cross, N. A., McBride, R. L., Letbetter, W. D., and Anschel, S. (1982). Subcortical structures projecting to visual cortical areas in squirrel monkey. *J. Comp. Neurol.* 209, 29–40. doi: 10.1002/cne.902090104

Van Den Heuvel, M. P., and Sporns, O. (2013). An anatomical substrate for integration among functional networks in human cortex. *J. Neurosci.* 33, 14489–14500. doi: 10.1523/JNEUROSCI.2128-13.2013

Van Essen, D. C., Drury, H. A., Dickson, J., Harwell, J., Hanlon, D., and Anderson, C. H. (2001). An integrated software suite for surface-based analyses of cerebral cortex. *J. Am. Med. Inform. Assoc.* 8, 443–459. doi: 10.1136/jamia.2001.0080443

Vertes, R. P. (2004). Differential projections of the infralimbic and prelimbic cortex in the rat. *Synapse* 51, 32–58. doi: 10.1002/syn.10279

Vincent, J. L., Kahn, I., Snyder, A. Z., Raichle, M. E., and Buckner, R. L. (2008). Evidence for a frontoparietal control system revealed by intrinsic functional connectivity. *J. Neurophysiol.* 100, 3328–3342. doi: 10.1152/jn.90355.2008

Wong-Riley, M. (1979). Changes in the visual system of monocularly sutured or enucleated cats demonstrable with cytochrome oxidase histochemistry. *Brain Res.* 171, 11–28. doi: 10.1016/0006-8993(79)90728-5

Conflict of Interest Statement: The authors declare that the research was conducted in the absence of any commercial or financial relationships that could be construed as a potential conflict of interest.

Received: 15 March 2014; accepted: 10 June 2014; published online: 03 July 2014.
Citation: Reser DH, Richardson KE, Montibeller MO, Zhao S, Chan JMH, Soares JGM, Chaplin TA, Gattass R and Rosa MGP (2014) Claustrum projections to prefrontal cortex in the capuchin monkey (Cebus apella). Front. Syst. Neurosci. ***8****:123. doi: 10.3389/fnsys.2014.00123*
This article was submitted to the journal Frontiers in Systems Neuroscience.

frontiers in
SYSTEMS NEUROSCIENCE

METHODS ARTICLE
published: 14 May 2014
doi: 10.3389/fnsys.2014.00078

Exploitation of puddles for breakthroughs in claustrum research

John-Irwin Johnson[1,2]*, Brian A. Fenske[1], Amar S. Jaswa[1] and John A. Morris[3]

[1] *Division of Anatomy, Department of Radiology-Anatomy, Michigan State University, East Lansing, MI, USA*
[2] *Neuroscience Program, Michigan State University, East Lansing, MI, USA*
[3] *SNBL USA, Ltd., Everett, WA, USA*

Edited by:
Brian N. Mathur, University of Maryland School of Medicine, USA

Reviewed by:
Paul Manger, University of the Witwatersrand, South Africa
Roger Reep, University of Florida, USA

****Correspondence:***
John-Irwin Johnson, Division of Anatomy, Department of Radiology, Michigan State University, 965 Fee Road—A519, East Lansing, MI 48824, USA
e-mail: johnij@aol.com

Since its first identification as a thin strip of gray matter enclosed between stretches of neighboring fiber bundles, the claustrum has been considered impossible to study by many modern techniques that need a certain roominess of tissue for their application. Known as the front wall, *vormauren* in German from 1822, and still called *avant-mur* in French, we here propose a means for breaking into and through this wall, by utilizing the instances where the claustral tissue itself has broken free into more spacious dimensions. This has occurred several times in the evolution of modern mammals, and all that needs be done is to exploit these natural expansions in order to take advantage of a great panoply of technological advances now at our disposal. So here we review the kinds of breakout "puddles" that await productive exploitation, to bring our knowledge of structure and function up to the level enjoyed for other more accessible regions of the brain.

Keywords: minipig, mammal brain diversity, proteomic labeling, multiprobe microelectrode arrays, large mammal gene expression studies

WHAT IS A PUDDLE?

The simplest and canonical notion of the claustrum, dating from its discovery by Vicq d'Azyr (1786), has it a thin subcortical layer of gray matter extending from superior to inferior in the white matter between the insular cerebral cortex and the underlying putamen. Looking a bit further, virtually all mammalian claustrums do indeed show such a lamina, and at one point in its inferior reach, the layer curls around the fundus of the rhinal sulcus that separates insular and other meso- and neocortex above from the olfactory allocortex below.

In their seminal 2009 work, Mathur, et al. detail many of the details of the difficulties encountered in attempts to learn the functioning and organization of a thin laminar entity, and the limitations this has posed on learning much about what the claustrum is and does. In this article we have a pregnant suggestion about how to overcome this inherent difficulty, by utilizing natural biodiversity that is seen in the claustrum in a variety of species.

The curling claustral lamina descends beneath the rhinal sulcus fundus then spreads out a bit into a more diffuse group of subcortical cells internal to those of the trilaminar olfactory allocortex that has become known as the endopiriform region or "nucleus." This bridge from suprarhinal to infrarhinal regions shows no consistent break or marker between the claustral and endopiriform cell groups. We will hereafter term this consistent connection, frequent among the mammals that we have observed, the "root of the claustrum" and it may indeed be the region from which cells have migrated in opposite directions to grow into the adult claustrum and endopiriform regions.

SUPERIOR PYRAMIDOID PUDDLES

Figure 1 presents a clear illustration of this root region, with endopiriform below the sulcal fundus. And then, extending in a long thin and straight lamina, this claustrum of a Red Fox, *Vulpes vulpes*, spills out at its top, as seen in two dimensions, into an elegant triangular formation encompassing large accumulation of apparently claustral cells, in what we call the superior pyramidoid puddle. This graceful vulpine display introduces our notion of claustral puddles.

The puddle fills the wider space occasioned by the ending of the top of the putamen, which at anterior and lower levels may block the expansion of the claustrum medialward, and laterally by the folding of cerebral cortex opening a space in the middle of the fold, allowing the claustrum to "invade" the core of the gyrus. The space is bounded laterally by U fibers traveling between the tops of the neighboring gyri and accounting for most of the triangular appearance of the cell mass. This invasion, by points of claustrum entering cores of overlying gyri, was first depicted by Vicq d'Azyr (1786) in the first published description of a claustrum, and was shown in a human brain. This remarkable painting can be viewed directly at http://www2.biusante.parisdescartes.fr/livanc/?p=22&cote=00519x02&do=page We will see this gyrus invasion phenomenon repeated in many diverse animals.

At the posterior end of the fox claustrum, there is another enlarged region, constituting a Posterior Puddle, and we will take up that topic after further consideration of Superior Pyramidoid Puddles.

A superior pyramidoid puddle has been the site of a major breakthrough in understanding claustral structure and function

In the domestic cat, a superior pyramidoid puddle was the occasion of a major advance in the understanding of structure and function of the claustrum, in several articles by LeVay and Sherk (LeVay and Sherk, 1981a,b; Sherk and LeVay, 1981a,b, 1983; LeVay, 1986), and additional contributions by

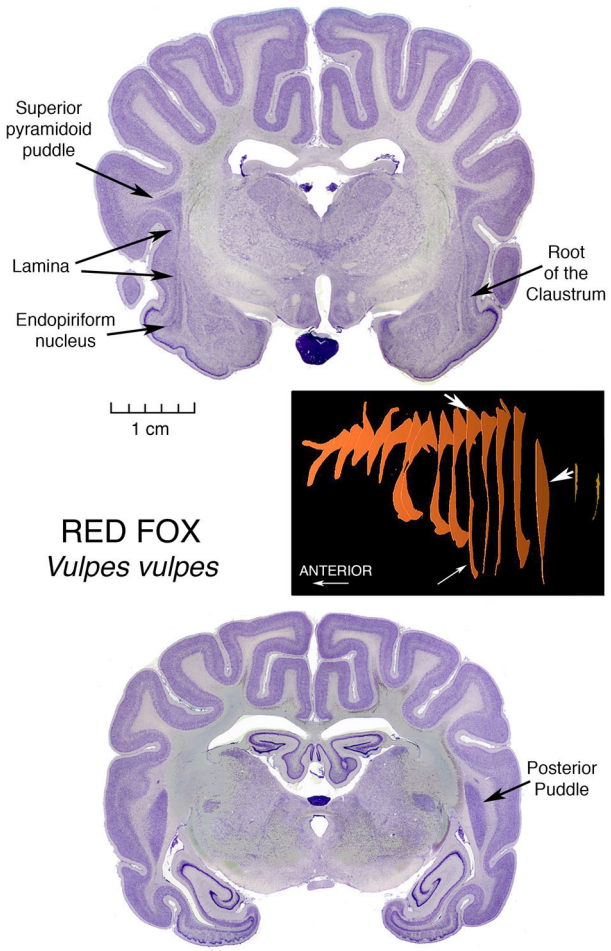

FIGURE 1 | Nissl stained coronal sections through the brain of a Red Fox, illustrating the morphology of the Superior Pyramidoid Puddle, the Root of the Claustrum, the Endopiriform Nucleus and the Posterior Puddle. Accompanying these histological images is a three-dimensional diagram, constructed from outlines of the Claustrum in these sections in series with those of other sections forming an evenly spaced sampling of the entire claustrum. The reconstructions were obtained using the ImageJ program. White arrows on the reconstruction denote the 3-dimensional localization of the features labeled in the section images by black arrows. The specimen in this Figure, as are those in all but the last **Figure 7**, is from the Welker Wisconsin Comparative Collection of Mammalian Brains, as scanned and displayed on the website at http://brainmuseum.org.

Olson and Graybiel (1980), and by Irvine and Brugge (1980). This series of studies was made possible by the wider expanse of the puddle compared with the lamina, enabling the location of arrays of projections inside the claustrum in somatotopic order. Analysis of the posterior end of this region of claustral expansion, using a coordinated panoply of anatomical and physiological techniques, yielded the knowledge that this restricted claustral region has extensive reciprocal connections with cortical sensory association regions in visual, somatic sensory, and auditory pathways, and suggested the concept well expressed by Olson and Graybiel (1980), that claustrum functions as something of a servicing satellite aiding these cortical regions in the dynamic regulation of receptive field properties of somatotopically organized sensory circuits in cerebral cortex. Earlier findings by Graybiel (1978), and Sherk (1979) had suggested that the small parabigeminal nucleus in the midbrain served the much larger superior colliculi as just such a satellite processor.

Of further interest is that these three claustral sensory regions are located in somatotopic parallel with the arrangement of their corresponding (in many senses of the word) cortical areas, with the visual area caudalmost, the somatic sensory area superiormost and the auditory area inferiormost. Furthermore, just as the cortical areas are located in roughly the posterior region of the hemisphere, while motor regions are in the anterior portion, so the posterior location of the sensory regions leads to speculation that the substantial more anterior remainder of this great puddle is devoted to relationships with motor cortical regions.

A somewhat similar arrangement is seen in the larger cortical-reciprocally-active brain part: the dorsal thalamus.

Similar superior pyramidoid puddles (see **Figure 3**) are seen in other, but not all, carnivores, as well as in perissodactyl zebras and artiodactyl llamas, zebus (representative of cattle or oxen), and pigs (Buchanan and Johnson, 2011).

POSTERIOR PUDDLES

A giant among puddles, and among research opportunities?

But in the pig, proceeding caudalward, the pyramid rather suddenly explodes into the "mother of all" puddles, a giant oblong mass of claustral tissue that separates into parallel lobules for a considerable distance caudalwards. This giant posterior puddle is a prime candidate for contemporary investigations. It will accommodate large injections that will remain completely within the claustrum, and multiprobe microelectrode arrays for recording simultaneously from several different intraclaustral active loci. It will provide large numbers of neurons, interneurons, possibly glia and other structures for quantitative assessments without contamination from neighboring fiber bundles. Here can be large concentrations of claustral neurotransmitters, and large populations of receptive synapses.

The dimensions of the puddle render possible the advantages of punch techniques for determining levels of chemical contents, and isotropic optical fractionation methods for cell counting (Herculano-Houzel and Lent, 2005).

Furthermore, small varieties of this species of artiodactyl are being well-developed as convenient and informative subjects for mammalian biological experimentation. That they have large and complex gyrencephalic brains adds to their potential for studies of functions that may not exist in small, simple, and perhaps vestigial brain regions in the murine rodent populations that have become the overwhelmingly dominant subject population at this time in the course of neuroscientific research. It is of particular interest that the same four lobules appear in a figure from a section of a minipig brain (Guidi et al., 2011, p. 173 **Figure 2** Frame 17.28), published to show something quite different—it was quite by chance that this section occurred right at the lobulating point in the minipig Posterior Puddle, leading to speculation that there could be functional significance to this peculiar organization of claustral tissue, such that it is replicated

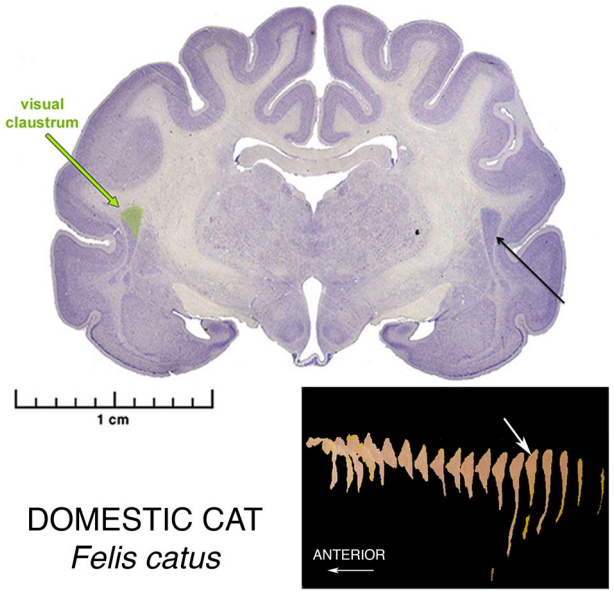

FIGURE 2 | Nissl stained coronal section the brain of a Domestic Cat, illustrating the morphology of the Superior Pyramidal Puddle. Within the puddle, the green color shows the location of the Visual Sensory Area of the claustrum. The Somatosensory Area is located just rostral, and the Auditory Area just rostro-inferior to the Visual Area. The Visual Area is the largest of the three. The white arrow in the three-dimensional reconstructions shows the location of this section in the whole claustrum. These sensory areas are found in only the posteriormost part of this Puddle.

in individuals of very different size. That such a local feature is reproduced from individual to individual marks this puddle as an opportunity to study local organization within the claustral tissue.

As a further bonus, as seen in the middle section in **Figure 4**, pigs possess the "mother of all" endopiriform regions, an unusually large and homogeneous region underpinning an expansive olfactory cortex that actually becomes gyrencephalic, folding its expanse into the space available in the front of the brain case. These animals thus become subjects of choice in an additional challenging task: determining just what is the endopiriform nuclear region and what does it do?

This becomes particularly important with the disappearance of the traditional cats and dogs from experimental laboratories. The current fad that permits only small murine rodents as suitable experimental subjects may be reaching its rate-limiting condition in brain study. Tiny brains can reveal only so much that is relevant to the operations of large brains, and the pigs with their large enough brains, and particularly available claustrums (and endopiriform too as a fortunate lagniappe) may well represent the avenue to rapid advancement in the study of claustrum and related structures. The olfactory cortex in pigs is unusual in that it has gyri and sulci, and the endopiriform cells extend up into the core of the upper gyrus, much as the claustral cells extend into the white matter of insular and other neocortical and mesocortical regions.

INFERIOR PUDDLES

The Inferior Puddles of anthropoid primates

Another large puddle of particular interest, since we humans possess this one, is the large Inferior Puddle seen in anthropoid primates. In the array in **Figure 5** it can be seen as a prominent and constant feature in the largest of the New World platyrrhines, the Mantled Howler monkey, and representing the Old World catarrhines, a Mandrill.

On the cover of the carefully detailed human brain atlas of Mai et al. (2008), and also on pp. 127–153, the Inferior Puddle, prominent and in the standard shape, contains five different subdivisions of the claustrum.

See the article by Baizer in this issue, to see the Gorilla version of the Inferior puddle.

In a macaque, Ribeiro Gomes et al. (2013) showed in a poster at the 2013 meetings of the Society for Neuroscience, early results of an extensive study identifying regions of claustrum with reciprocal connections with contrasting pairs of restricted regions of cerebral cortex. Regions were selected to be far from one another both spatially and functionally. Most of the cortical regions were connected with a stripe of claustral cells running for some distance across the diagonal extent of most of the claustrum, much as Mathur (2008) described for the cortical connections of a local region of cortex in a stripe of claustral cells running across the whole claustrum in rats. But in one case, a region of visual association area, V4, had its connections instead with a tight ball of cells located right in the center of the inferior puddle. To have an occipital region of cortex connected to the inferiormost extension of claustrum may point to a specialization of the puddle as something different than the usual long stripe of connections with a particular cortical area.

ANTERIOR PUDDLES

Prominent anterior puddles in marsupials

We have seen superior, posterior, and inferior puddles thus far. To complete the spatial possibilities, there are the large anterior puddles seen in all of the marsupials we have examined. They are shown in the brain of a wombat and a kangaroo, two of the largest of marsupial brains, in **Figure 6**. Very small marsupials also exhibit them, see them in brains of bandicoots and antechinuses. This taxon-wide commonality could be related to the arrangement of interhemispheric connections in marsupials. In place of a corpus callosum, the hemispheres communicate mainly through a greatly enlarged anterior commissure, and this structure forms a wall beyond which claustral cells cannot go. Therefore, they pile up at the front end of the corpus striatum. This condition is also seen in anteaters and sloths of the order Xenarthra, although these animals do have the normal placental large corpus callosum.

WHAT IS A CLAUSTRUM?

Debate over categorization of cellular groupings in the brain likely began immediately after the second examination of a specimen. Nuclear groupings have commonly been sorted by descriptions of apparent shapes and location, resorting to nomenclatures that often use prepositional modifiers relative to the few unambiguous landmarks that are argued least. So the literature contains

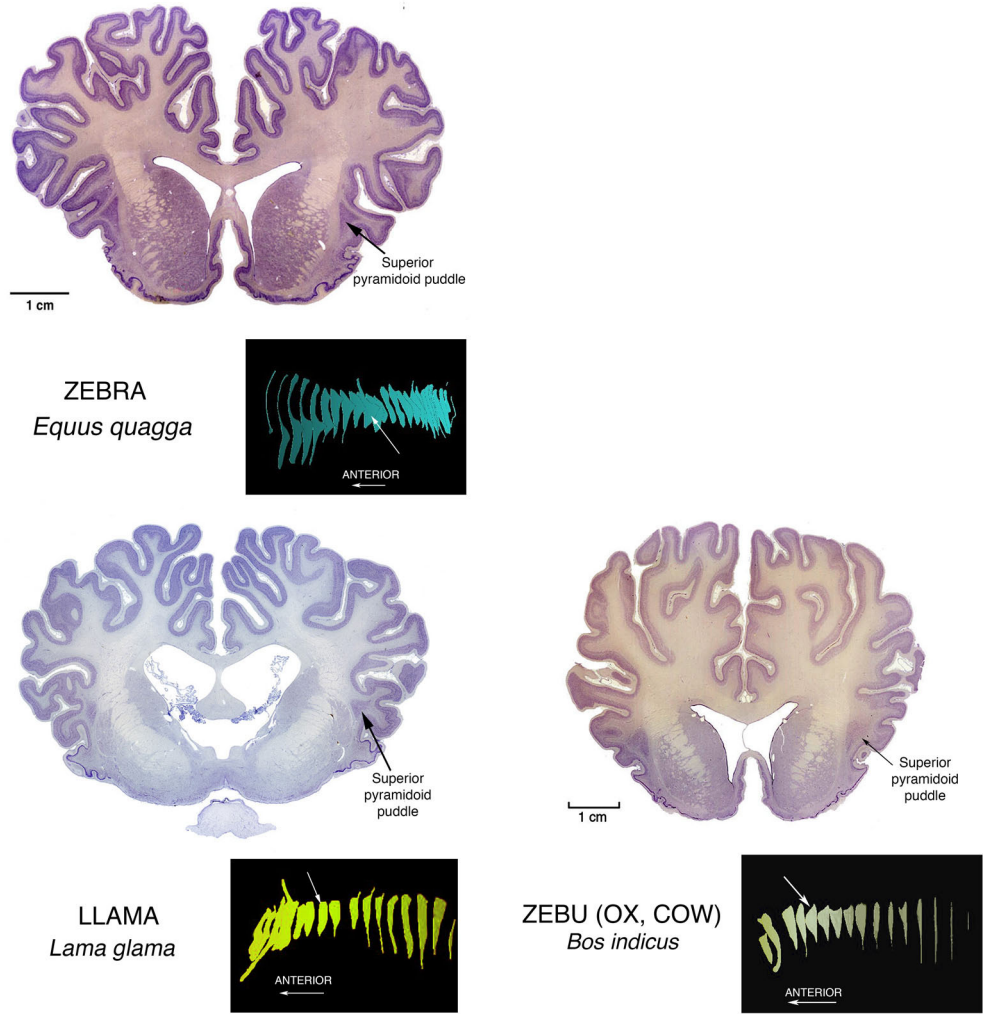

FIGURE 3 | Nissl stained coronal sections through the brains of perissodactyl Zebra, and artiodactyl Llama and Zebu (Ox, Cow) illustrating other instances of Superior Pyramidoid puddles. The white arrows in the reconstructions mark the positions of the illustrated sections in the anterior-posterior extents of the claustrums. This puddle shape along the superior aspect of the claustrum can occur anywhere from front to back. Its appearance may depend more upon the proximity of a relatively open overlying gyral core rather than to any consistent functional or genetic reason. This in turn may mean that the claustral mass can assume any convenient shape, and this in turn suggests that internal connections inside the claustrum are rare, and not of general functional significance.

examples such as the posterodorsal medial amygdala which translates as the top, back part, of the part nearer the midline, of a grouping that exhibits a vaguely almond-like shape, which results from a human brain cut just so, presumably from a vantage of sufficient distance to highlight the subject with appropriate contrast given the ambient light source and viewer acuity. Such is the practical convention that largely supplanted regional designations from the name of an initial publicist; with a few exceptions such as the Nucleus of Darkschewitz, a name that may persist purely on enigmatic connotation.

Careful research and means of observation have come about that give hope to a functional nomenclature, often more behavioral than purely physiological, such as ascribing a portion of the cortex found to primarily be involved in motor function, as "motor cortex," (and not "uniform high amplitude discharge zone"). Yet even there, consideration of various inputs and nearby areas of similar but not redundant function, results in a parcellation that yields primacy, where premotor and secondary motor areas then arise. Functional nomenclature is useful, but ultimately just another layer of metadata describing the brain, and not overly awkward, even when the motor cortex is idle. Of course regions of the brain do many different things together in varying concert, and the coordination and conduct of these areas must be measured to be understood.

Furthermore, the variation of brains is as immense as speciation, and even within a species, individual variance frustrates the logical desire to impose a Cartesian coordinate grid and retire the names. So in order to measure parts of the brain and communicate these findings, two questions must be answered together, both of which may vary considerable depending on

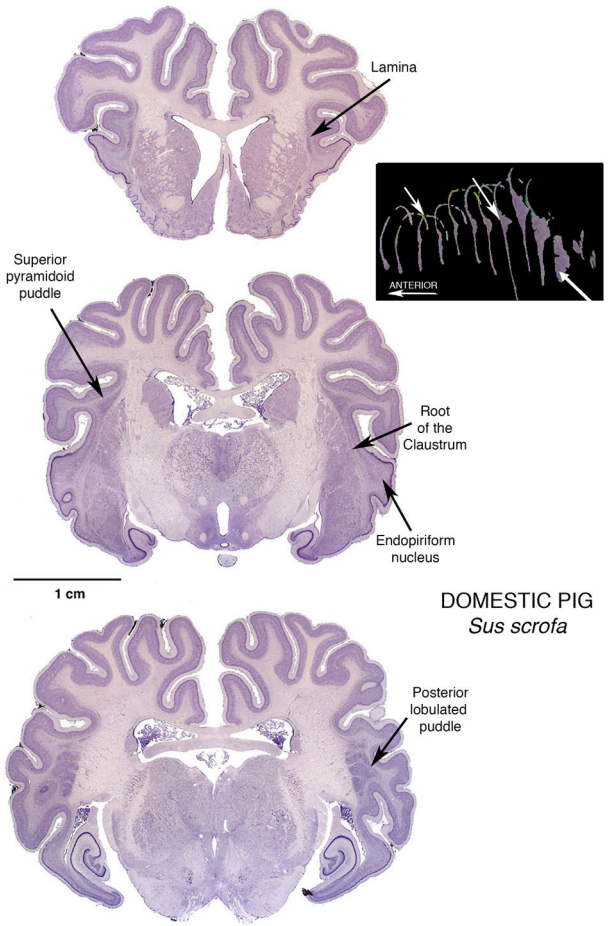

FIGURE 4 | Three Nissl stained coronal sections through the brain of a Domestic Pig, showing a modest Superior Pyramidoid Puddle that abruptly expands, posterior to the caudal limit of the putamen, to form a very large Posterior Puddle. This puddle, seen in this specimen and other published sections from other pigs, has a distinct lobulations into what appear to be four bars of cells, more or less separated from one another. This interesting arrangement is just one of many reasons for further investigation: if the claustral mass is sufficiently large, are there internal structural or functional reasons for assuming a particular shape? The 3-dimensional reconstruction in this figure is by Kenneth Buchanan.

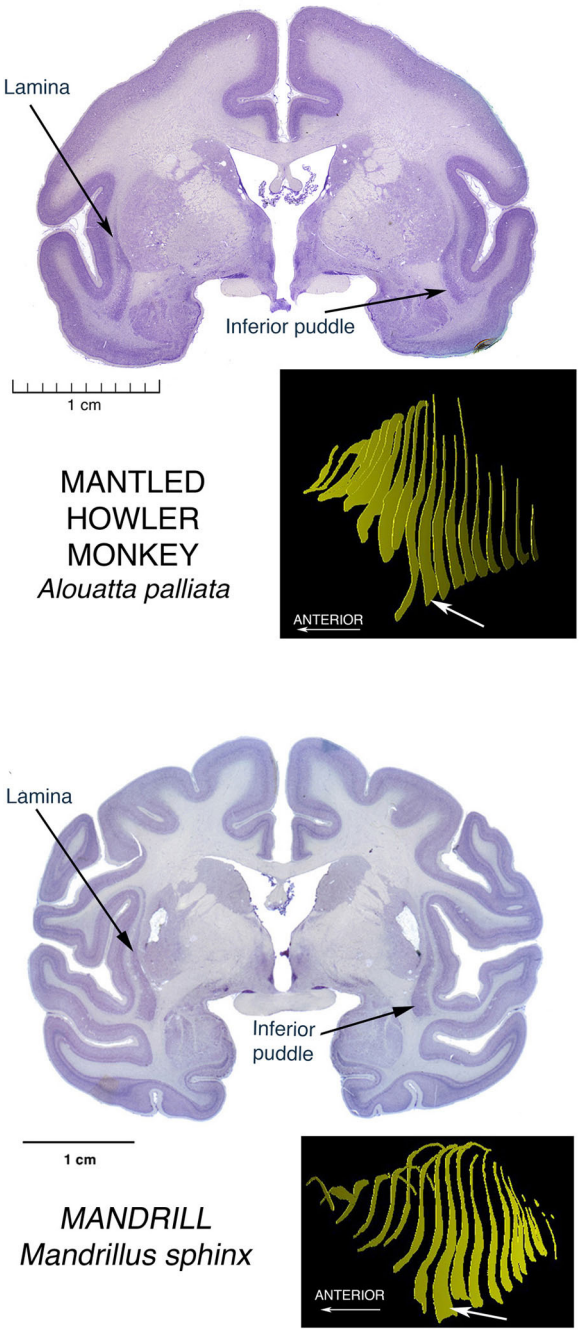

FIGURE 5 | Nissl stained coronal sections through the brains of two anthropoid primates, showing the Inferior Puddle seen in all members of this group that have been investigated, including humans. The New World Platyrrhine monkeys are represented here by the largest of these species, the Mantled Howler Monkey. The other major monkey radiation, the Old World Catarrhine monkeys, is represented here by the brain of a Mandrill.

definition; where precisely, are the limits of the claustrum, and what characteristics at its location are robust yet stable.

In the case of the claustrum, the convenience of being a bolt of cells enclosed by a barrier of white matter allows for a literal naming that serves as a unique reference, yet a lingering presumption is still implied, that the subject matter at hand is human or other sizable brain and sampled as its namesake, avoiding variability at the bulbous margins. It remains to be determined whether homogeneity of claustral elements is sufficient to keep its name.

DIRECT PROTEOMIC MARKING

Mathur et al. (2009), have revolutionized conceptualization of what claustrum is and does, and they have done it using a fashionable small murine rodent. They did this by recognizing a first principle, that one must be able to identify claustral cells as such, and to this end developed a proteomic marking technique that specifically would identify claustral cells, particularly as contrasted with cells of cerebral cortex. Their results demonstrated, in

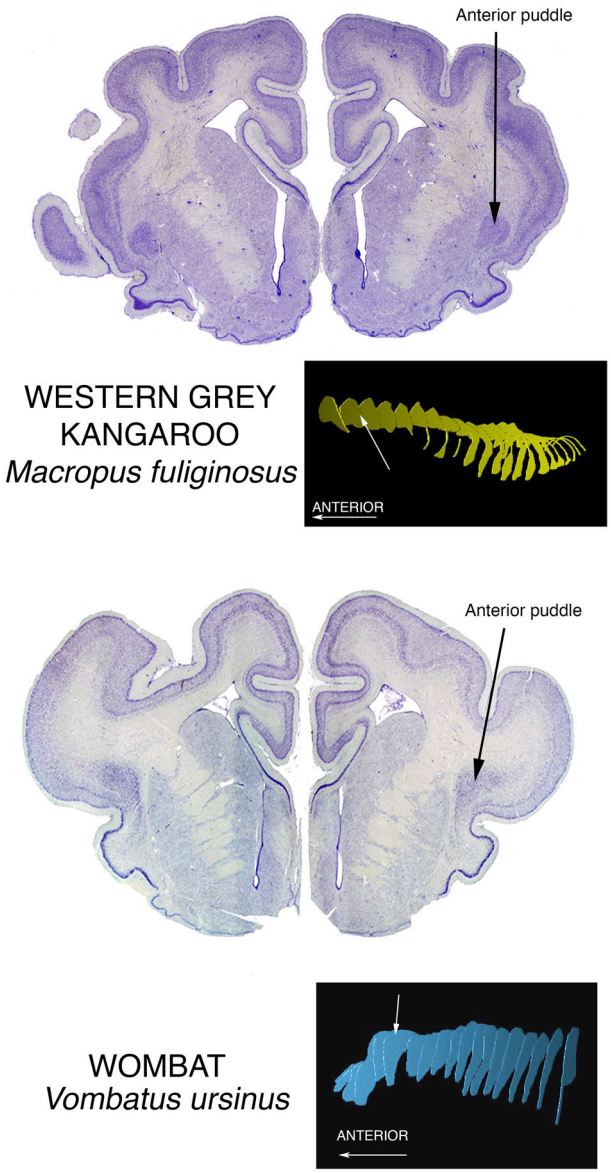

FIGURE 6 | Nissl stained coronal sections through the brains of two large marsupials show the Anterior Puddle seen in all marsupials of whatever body size.

the claustrum of rats, that the claustrum is really not a different place than cortex, but rather a region that has a number of cells that are different from the standard cells of cerebral cortex, particularly in their shape and arrangement relative to their neighbors. It is this distinctive shape and arrangement that led early debaters, chiefly Santiago Ramón y Cajal (1900), to decide that claustrum is a different kind of entity rather than just being another layer within or adjacent to cortex as proposed by, prominently, Meynert (1885) and Brodmann (1909).

Mathur et al. (2009) demonstrated that both opinions are true, but that the distinctive claustral cells in fact are intermingled with, and submerged into, a layer of cortex.

A major question now demanding resolution is whether this situation of submersion in cortex is a general feature of all claustrums, or is it a condition of a regressive vestige of a once robust claustrum in a species that is divesting itself of claustral function in the course of its evolution, just as arboreal primates jettisoned most of their olfactory systems in the course of their evolutionary adaptations.

We believe that a great deal can be learned by application of current proteomic identification techniques to each of the major puddles that we have described, beginning with the giant posterior puddle of the pig. This will provide almost instant answers to the questions whether the Mathur et al. picture of the claustrum as an internal cortical mechanism represents a general depiction of claustrum structure and function across mammals, or is it a portrait of a degenerate structure on the point of disappearing from the brain mechanisms of the small murine rodents?

One currently popular indirect method of proteomic identification is the use of markers of gene expression.

STUDIES OF GENE EXPRESSION. WHAT CAN THE GENES REVEAL ABOUT THE CLAUSTRUM AND THE PUDDLES? WHAT CAN THE CLAUSTRUM AND THE PUDDLES REVEAL ABOUT THE GENES?

Fortunately, a level of study that both controls for and accepts variation may yield understanding that neither attempt could achieve alone. In the laboratory, size, fecundity, and hardiness are the essential requirements that led to the selection of rodents as a research model. Substantial inbreeding allowed for the control of genetic variation, and hence brain variation, but the fortuitous susceptibility of mice to gene manipulation drove the consolidation of research, in only two decades, decisively to this species. Such control over genetic variation allows for precise measures of cellular organization and functional localization. This has provided for surprising discoveries that would have been lost, or not even considered, due to background variation in neural characteristics.

For example, because of their olfactory centered ethology and diminutive brain size, mice were overlooked as a model for the study of vision. Yet the anatomical precision afforded by consistency in genotype, quickly allowed for a number of subdivisions to be uncovered in the mouse visual cortex based on cortico-cortico connections and cytoarchitecture revealed by neurofilament protein, first by Wang and Burkhalter (2007) and van der Gucht et al. (2007), and then the subsequent functional verification of these subdivisions by Marshel et al. (2011). Similarly, gene expression can guide further studies of function by showing where brain areas subtly differ. The claustrum puddles in different locations by species, but if it does not in mouse, it could be due to an egress toward a "vestigial" state, or alternatively because it has not been examined closely.

An exploration of gene expression patterns

To more closely examine the claustrum of *Mus musculus* C57/B6 mouse (hereafter called just mouse) using gene expression as the categorical metric, we conducted gene expression experiments. For this we used a published resource presenting gene expression experiments for all brain areas and all known genes, from the Allen Brain Atlas (Lein et al., 2007) (brain-map.org). These

are made available online for public interrogation. We examined these experiments in a non-systematic way for gene expression patterns around the adult male mouse claustrum in order to inform whether claustrum (a) could be isolated from the deepest layers of cortex, (b) disambiguated from an endopiriform region, and (c) separated into a shell and core or beyond. These are questions that will persist until more data is compiled. It may be that protein expression, electrophysiological characteristics, cellular morphology, or cell type composition can distinguish these features in this region of the brain. In our case, we used gene expression to test these suggestions and compare findings.

The overall prediction was that gene expression experiments would confirm previous findings, but that careful attention could reveal subtle distinctions in the mouse brain, which might then lead to similar findings in a primate brain. Expected as well was organizational conformation in general between the species, but it would be good to uncover any exceptions that reveal species differences in gene expression or structural composition, or both. Therefore, we concurrently searched the Allen Atlas subset of gene expression experiments in the brain of the monkey *Macaca mulatta* (hereafter called macaque) for similar features, including differentiation of the Inferior Puddle of the claustrum.

Differential expression patterns found in mouse were compared in macaque where available. Our list included *Nr4a2* (nuclear receptor subfamily 4, group A, member 2), *Ntng2* (netrin G2), *Synpr* (synaptoporin), *Ctgf* (connective tissue growth factor), *Rgs4* (regulator of G-protein signaling 4), *Slc17a8* (solute carrier family 17 (sodium-dependent inorganic phosphate cotransporter, member 8), *Crym* (crystalline, mu), and *Rorb* (RAR-related orphan receptor beta).

Our findings. Segregation of brain subdivisions. We found the mouse claustrum to be compartmentalized loosely into a core and shell pattern, as suggested by previous studies (Dávila et al., 2005; Legaz et al., 2005). Genes were found that show expression, or lack thereof, mostly within the Nissl-defined claustrum of the Allen Reference Atlas, in a discrete, dense pocket of cells. The most distinctive of these (*Nr4a2*, *Ntng2*, *Synpr*) showed positive expression in a dense core of the claustrum (**Figures 7A–C**). This is distinctly reminiscent of the Mathur et al. (2009) findings, in rats, of a bolt of claustrum cells ensconced in a "shell" of cortical cells, which also appear different from cortex.

In addition to the shell-core, the separation of the mouse claustrum from deep cortical areas, in particular the insular and gustatory cortices, could be discerned from reciprocal expression patterns such as *Crym* and *Ntng2* (**Figures 7G,B**).

Genes specific to the endopiriform area were more difficult to identify, as expected, due to the more common sharing of expressing cells between regions. While it may be noted in other figures to show apparent differential expression from the deepest layer of piriform cortex, layer 3, it is difficult to show a clear distinction from the claustrum, with the exception of *Rorb* (**Figure 7H**) that labeled a possible more superficial aspect, and *Ctgf* (**Figure 7D**) that appeared biased toward a deeper aspect of the endopiriform nucleus. Overlapping expression patterns enriched or diminished in each respective area could reveal on average a separation, but the evidence presented is that the two areas show variation, but substantial comingling of cells.

Findings between genes. We then examined expression patterns that discriminated the mouse claustrum from the deepest cortical layer, 6b, and found that *Ctgf* and *Crym* reveal the claustrum, if slightly separating it from the external capsule (**Figures 7D,G**). Likewise, positive expression of *Nr4a2* in the claustrum was found that seemingly avoided marking layer 6b in the claustrum (**Figure 7A**), while marking 6b for cortex in general. Another observation arose from 6b positive expression of *Ctgf* that revealed deep cortex underlying the claustrum, but then continued to reveal enrichment of the endopiriform area (**Figure 7D**). Further work will be required to characterize the cells underneath the claustrum, if such results are repeated in additional genes. The expression patterns examined revealed the claustrum concurrent with several different cortical patterns, in that definition of the claustrum coincided with restricted cortical layer 6b (*Nr4a2*), 6a (*Ntng2*), and a general scattered pattern across all layers (*Synpr*) as seen in **Figures 7A–C**, respectively. Cells that expressed clearly in all layers but 6b of cortex, avoided the claustrum in the case of *Rgs4* expression.

In the macaque claustrum, while gene expression largely occurred throughout the extent of the claustrum along with deeper cortical expression, a few expression patterns suggested heterogeneity, both within and between the lamina and inferior puddle. The deepest region of the lamina that abuts the putamen at the external capsule, appeared differentially enriched with *RGS4* expression, yet less so with *NTNG2* expression. Moreover, the opposite pattern was found in the inferior puddle, with *NGNG2* revealing it along with the superficial lamina, while *RGS4* labeled less intensely in the puddle and superficial lamina (**Figures 7B′,E′**, respectively). The inferior puddle was compartmentalized by *CRYM* expression in the deepest corner, along with the deep lamina (**Figure 7G′**). *RORB* labeled the superficial gyral corner of the inferior puddle only, without notable expression in the remaining extent of the claustrum.

Our data indicates that gene expression reveals differential expression within the claustrum, suggesting various developmental backgrounds and functions. As an example, the claustrum of both species is not labeled by *Ctgf* expression, yet the deepest nearby cortex shows strong labeling. That the deepest cortical layer of the mouse, 6b (layer VII), is quite compact whereas in the macaque labeling appears more broadly in layer 6, may be understood as an effect of development, where differential rates and periods between species of sub-plate apoptosis and white matter encroachment, produce a more distributed appearance in the primate (Reep, 2000). That same hypothesis also implies that various parts of cortex may experience differing developmental effects, as suggested by *Nr4a2* expression in layer 6b of mouse that, unlike *Ctgf*, diminishes or disappears under the claustrum. Whether these neighboring cells are homologous requires additional examination and instances, and subtle pattern differences in deepest monkey cortex do present intrigue. The inferior puddle also showed some interesting variance at the margins, but likewise will require additional data to fully uncover a consistent pattern.

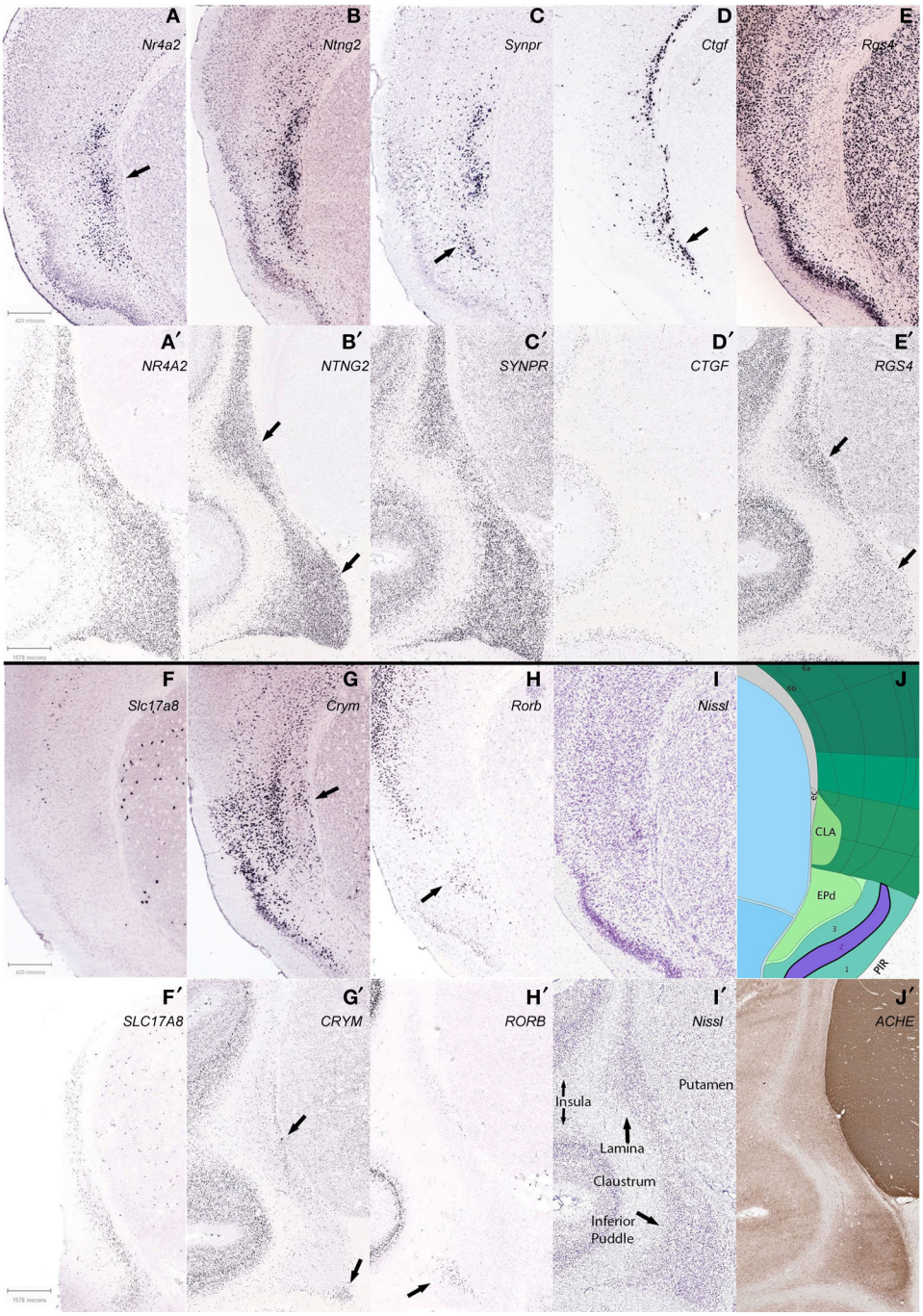

FIGURE 7 | Differential claustrum expression patterns within and between species, C57/B6 mice in 1st and 3rd panels (A–J), Macaque monkey *Macaca mulatta* in 2nd and 4th panels (A′–J′). (A) *Nr4a2* expression forms a dense core (arrow) surrounded by diffuse staining, with another dorsal cluster that is also found with *Ntng2* and *Synpr* labeling **(B,C)** and reciprocally in *Crym* **(G)**. **(D,D′)** *Ctgf* labeling of cortical layer 6b and deeper endopiriform nucleus (EPd), with a stream of cells that subtend the claustrum in mouse (arrow), and only deep cortex and non-neuronal appearing cells lightly labeled in macaque. **(E,E′)** *Rgs4* labeling avoids the mouse claustrum yet labels most other regions, but staining in macaque shows a species difference. **(F,F′)** *Slc17a8* shows another stark species difference in claustral expression, with no apparent expression in mouse and many cells expressing in macaque. **(G,G′)** *Crym* expression in mouse largely avoids the claustrum but the arrow shows a wedge of cells that together with the more superficial labeling, surrounds the claustrum, while in the macaque labeling also avoids the claustrum, but reveals a deep stream of cells in the lamina and the deep corner of the inferior puddle (arrows). **(H,H′)** Arrows show that *Rorb* expression marks the superficial EPd in mouse, and labels only the gyral portion of the inferior puddle in macaque. **(B′,E′)** Apparent reciprocal expression of *NTNG2* and *RGS4* in the macaque (arrows), in particular the inferior puddle. All macaque sections were from the same specimen except **(F′)**, and mouse experiments were from different specimens. Gene names are indicated (top right) of panels. See text for gene names. **(I,J)** Matching Nissl stain and atlas plate from Allen Mouse Brain atlas. **(I′,J′)** Two representative sections from the macaque brain are shown, stained for Nissl and acetylcholinesterase, respectively.

Findings between species. Species differences were noted in many expression patterns across genes. The most conspicuous, *Slc17a8*, was completely absent in the mouse claustrum, while appearing throughout the macaque claustrum; yet the putamen of both species showed a similar pattern (**Figures 7F,F′**). *Ctgf* clearly labels deepest cortex in both species, but the stream of cells that subtends the mouse claustrum was not apparent in the macaque claustrum (**Figures 7D,D′**). *Synpr* was similar in claustral expression, yet general cortical expression was scattered in mouse while all layers were abundantly labeled in macaque (**Figures 7C,C′**). As mentioned above, *Rgs4* labels the cortex of both species, and reveals the macaque claustrum, without labeling that of the mouse (**Figures 7E,E′**). *Crym* and *Rorb* largely have negligible expression in the majority of both species' claustrums, but *Crym* reveals deepest cells in both (**Figures 7G,G′**) and *Rorb* reveals the putative superficial enndopiriform cluster of cells only in mouse and a gyral pocket of cells in the macaque inferior puddle (**Figures 7H,H′**). *Nr4a2* and *Ntng2* expression was similar between both species, both in claustral and overall cortical patterns (**Figures 7A,A′,B,B′**). These many variations were unexpected and suggest complex gene regulation that differs between species. Thus, the intriguing possibility for using the claustrum for the study of gene regulation emerges, with the concomitant inference that additional species need to be studied as well.

Future studies. This sampling of gene expression in the claustrum informs that both species and structural variation in labeling occur, but that to understand either, will require both more genes, and more claustrums. Within these two species, it appears that gene expression in the claustrum is mostly uniform, but selected examples show sufficient variation to establish regionalization important to consider when interpreting other data derived from other modalities. While it is tempting to suggest then that the claustrum could provide an anchor to study brain function based on its simple appearance and cortical affiliation, a more careful comparison will be needed first in order to establish this assertion, such as methods more quantitatively sensitive to gene or protein expression levels, and obviously more species and more areas within the claustrum.

However, one might use this limited knowledge to more quickly isolate exemplar genes and species that showcase conformity or derivation across a particular parameter. For example, online resources that "lump" all of the claustral components together spatially, may still suggest differential anatomical gene expression, by searching for expression levels that show more variation relative to other genes. This approach requires at least a few separate samples to provide possible variation, and the same reasoning could uncover genetic contributions based on known functional variation across species. Such approaches have probed mouse expression databases to find genes that mark cell types, such as Von Economo cells, thought only to occur in larger brains (Allman et al., 2011).

More careful studies, across modalities, would need to be pursued before redrawing of any current brain maps, and as always, borders should be regarded as ultimately probabilistic. However, the efficiency of taking publically available data to find exemplar genes that specifically mark the claustrum with those that suggest intraclaustral subdivision, and then probe other species and confirm and expand these results, is appealing in its simplicity.

It may be that the puddles are genetically and functionally homogenous, and thus make for prime targets of understanding brain/structure relationships. Or, it may be that mouse brains exhibit a vestigial claustrum. And it might be likely, that expanding the gene markers in non-human primates and human experiments would reveal subtle distinctions that underpin functional differences.

The null hypothesis in this case is that variation in claustral function does not reside in expression patterns of single genes, but that combinatorial patterns will need to be analyzed. Even then, it is unlikely that there are many genes that can exhibit an undue influence on a particular brain area. But those few make for powerful targets and the means of isolating them more efficient.

If the claustrum were molecularly homogenous, it would be unusual, and thus would provide a brain region where physiology and connectivity may be probed more accurately. With the claustrum as presently studied in typical laboratory species appearing mostly uniform, with some elaboration in larger brains, it is in that respect, like many other cortical brain regions. But any unusual uniformity remains to be shown, and gene markers are available to test predictions, and so some resolution could be forthcoming.

A scenario. The ideas presented by Reep (2000) led us to the following speculative line of thought about the specific direction for research. Layer 7, in those few taxa where it is seen, consists of remnants of the Subplate, that did not apoptose as subplate cells usually do, after they have initiated and supervised the organization of the cells migrating through the plate and forming the cerebral cortex. The presence of Layer 7 could signify a "half-baked" brain: finishing the cortex was abandoned in favor of shorter gestation period, quick reproduction, and reduced brain size and energy use. So the cortical details may have been left undone and since it did not interfere with survival, the layer persisted in its paedomorphic state.

The Subplate and Layer 7 are between the claustrum and the external capsule. Therefore, they might direct the puddling of claustrum along with the organization of the overlying cortex. The presence of layer 7 in rats and mice could mean that claustrum and puddles, as well as cortex, did not have a chance to completely develop. One undone feature may be the location of cortical cells scattered through the claustrum (Mathur et al., 2009) In the absence of Subplate instructions, their segregation might not have been accomplished.

Rats and mice belong to one of the few taxa where Layer 7 is found (Reep, 2000). Others include some bats and insectivores, all of whom could have profited by reducing brain size, weight, and energy cost. This raises questions about their suitability as models for the study of "complete" mammalian brains.

All of these questions need developmental studies to solve the riddles not only of claustrum, but also those of Layer 7 and the endopiriform regions. These developmental studies need proteomic analysis including that using gene expression, along with the array of other methods that can be used in large accumulations of specialized cells, including the advanced

electrophysiological, neurochemical, and imaging techniques now available.

The Posterior Puddle of the Pig claustrum may be the optimal subject for such a comprehensive approach toward solution of all of these open questions. Along with its other advantages, the minipig brain has recently been shown to be suitable for transfection studies (Glud et al., 2011), and they have a suitably sized puddle for doing them.

REFERENCES

Allman, J. M., Tetreault, N. A., Hakeem, A. Y., and Park, S. (2011). The von Economo neurons in apes and humans. *Am. J. Hum. Biol.* 23, 5–21. doi: 10.1002/ajhb.21136

Brodmann, K. (1909). *Vergleichende Lokalisationslehre der Grosshirnrinde*. Leipzig: Johann Ambrosius Bart; as presented in translation in Garey L. J. (2006). *Brodmann's Localisation in the Cerebral Cortex.* New York, NY: Springer.

Buchanan, K. J., and Johnson, J. I. (2011). Diversity of spatial relationships of the claustrum and insula in branches of the mammalian radiation. *Ann. N.Y. Acad. Sci.* 1225(Supp. 1), E30–E63. doi: 10.1111/j.1749-6632.2011.06022.x

Dávila, J. C., Real, M. Á., Olmos, L., Legaz, I., Medina, L., and Guirado, S. (2005). Embryonic and postnatal development of GABA, calbindin, calretinin, and parvalbumin in the mouse claustral complex. *J. Comp. Neurol.* 481, 42–57 doi: 10.1002/cne.20347

Glud, A. N., Hedegaard, C., Nielsen, M. S., Søorensen, J. C., Bendixen, C., Jensen, P. H., et al. (2011). Direct MRI-guided stereotaxic viral mediated gene transfer of alpha-synuclein in the Göttingen minipig CNS. *Acta Neurobiol. Exp.* 71, 508–518.

Graybiel, A. M. (1978). A satellite system of the superior colliculus: the parabigeminal nucleus and its projections to the superficial collicular layers. *Brain Res.* 145, 365–374. doi: 10.1016/0006-8993(78)90870-3

Guidi, S., Bianchi, P., Olsen Alstrup, A. K., Henningsen, K., Smith, D. F., and Bartesaghi, R. (2011). Postnatal neurogenesis in the hippocampal dentate gyrus and subventricular zone of the Göttingen minipig. *Brain Res. Bull.* 85, 169–179. doi: 10.1016/j.brainresbull.2011.03.028

Herculano-Houzel, S., and Lent, R. (2005). Isotropic fractionator: a simple, rapid method for the quantification of total cell and neuron numbers in the brain. *J. Neurosci.* 25, 2518–2521. doi: 10.1523/JNEUROSCI.4526-04.2005

Irvine, D. R. F., and Brugge, J. F. (1980). Afferent and efferent connections between the claustrum and parietal association cortex in cat: a horseradish peroxidase and autoradiographic study. *Neurosci. Lett.* 20, 5–10. doi: 10.1016/0304-3940(80)90224-4

Legaz, I., García-López, M., and Medina, L. (2005) Subpallial origin of part of the calbindin-positive neurons of the claustral complex and piriform cortex. *Brain Res. Bull.* 66, 470–474. doi: 10.1016/j.brainresbull.2005.05.006

Lein, E. S., Hawrylycz, M. J., Ao, N., Ayres, M., Bensinger, A., Bernard, A., et al. (2007). Genome-wide atlas of gene expression in the adult mouse brain. *Nature* 445, 168–176. doi: 10.1038/nature05453

LeVay, S. (1986). Synaptic organization of claustral and geniculate afferents to the visual cortex of the cat. *J. Neurosci.* 6, 3564–3575.

LeVay, S., and Sherk, H. (1981a). The visual claustrum of the cat. I. Structure and connections. *J. Neurosci.* 1, 956–980.

LeVay, S., and Sherk, H. (1981b). The visual claustrum of the cat. II. The visual field map. *J. Neurosci.* 1, 981–992.

Mai, J. K., Paxinos, G. and Voss, T. (2008). *Atlas of the Human Brain, 3rd Edn.* Amsterdam: Elsevier Academic Press.

Marshel, J. H., Garrett, M. E., Nauhaus, I., and Callaway, E. M. (2011). Functional specialization of seven mouse visual cortical areas. *Neuron* 22, 72, 1040–1054. doi: 10.1016/j.neuron.2011.12.004

Mathur, B. N. (2008). *Unraveling The Seat Of Consciousness: Anatomical Redefinition and Molecular Characterization of the Claustrum*. Vanderbilt Univ: Ph. D. dissertation, Neuroscience.

Mathur, B. N., Caprioli, R. M., and Deutch, A. Y. (2009). Proteomic analysis illuminates a novel structural definitions of the claustrum and insula. *Cereb. Cortex* 19, 2372–2379. doi: 10.1093/cercor/bhn253

Meynert, T. (1885). Psychiatry. A Clinical Treatise on Diseases of the Forebrain Based upon a Study of Its Structure, Functions, and Nutrition. Part 1. The Anatomy, Physiology, and Chemistry of the Brain. New York, NY: G. P. Putnam's Sons. Reprinted by Ulan Press, Lexington KY, 2013.

Olson, C. R., and Graybiel, A. M. (1980). Sensory maps in the claustrum of the cat. *Nature* 288, 479–481. doi: 10.1038/288479a0

Ramón y Cajal, S. (1900). Estudios sobre la corteza cerebral humana. III. Estrutura de la corteza acustica. *Rev. Trim. Micrográf.* 5, 129–183.

Reep, R. L. (2000). Cortical layer VII and persistent subplate cells in mammalian brains. *Brain Behav. Evol.* 56, 212–234. doi: 10.1159/000047206

Ribeiro Gomes, A. R., Lamy, C., Misery, P., Dehay, C., Knoblauch, K., and Kennedy, H. (2013). A quantitative analysis of the topology of subcortical projections to the macaque cortex. SS*6 551.10 Poster, SFN* 2013.

Sherk, H. (1979). Connections and visual-field mapping in cat's tectoparabigeminal circuit. *J. Neurophysiol.* 42, 1656–1668.

Sherk, H., and LeVay, S. (1983). Contribution of the cortico-claustral loop to receptive field properties in area 17 of the cat. *J. Neurosci.* 3, 2121–2127.

Sherk, H., and LeVay, S. (1981a). Visual claustrum: topography and receptive field properties in the cat. *Science* 212, 87–89. doi: 10.1126/science.7209525

Sherk, H., and LeVay, S. (1981b). The visual claustrum of the cat. III. Receptive field properties. *J. Neurosci.* 1, 993–1002.

van der Gucht, E., Hof, P. R., Van Brussel, L., Burnat, K., and Arckens, L. (2007). Neurofilament protein and neuronal activity markers define regional architectonic parcellation in the mouse visual cortex. *Cereb. Cortex* 17, 2805–2819. doi: 10.1093/cercor/bhm012

Vicq d'Azyr, F. (1786). *Traité D'anatomie Et De Physiologie Avec Des Planches Coloriées Représentant Au Naturel Les Divers Organes De L'homme Et Des Animaux*. Vol. 1. Paris: François.

Wang, Q., and Burkhalter, A. (2007). Area map of mouse visual cortex. *J. Comp. Neurol.* 502, 339–357. doi: 10.1002/cne.21286

Conflict of Interest Statement: The authors declare that the research was conducted in the absence of any commercial or financial relationships that could be construed as a potential conflict of interest.

Received: 26 March 2014; accepted: 16 April 2014; published online: 14 May 2014.
*Citation: Johnson J-I, Fenske BA, Jaswa AS and Morris JA (2014) Exploitation of puddles for breakthroughs in claustrum research. Front. Syst. Neurosci. **8**:78. doi: 10.3389/fnsys.2014.00078*
This article was submitted to the journal Frontiers in Systems Neuroscience.

frontiers in
SYSTEMS NEUROSCIENCE

ORIGINAL RESEARCH ARTICLE
published: 02 July 2014
doi: 10.3389/fnsys.2014.00117

Comparative organization of the claustrum: what does structure tell us about function?

Joan S. Baizer[1]*, Chet C. Sherwood[2], Michael Noonan[3] and Patrick R. Hof[4]

[1] *Department of Physiology and Biophysics, University at Buffalo, Buffalo, NY, USA*
[2] *The Department of Anthropology, The George Washington University, Washington, DC, USA*
[3] *Animal Behavior, Ecology and Conservation, Canisius College Buffalo, Buffalo, NY, USA*
[4] *Fishberg Department of Neuroscience and Friedman Brain Institute, Icahn School of Medicine at Mount Sinai, New York, NY, USA*

Edited by:
Brian N. Mathur, University of Maryland School of Medicine, USA

Reviewed by:
Giorgio Innocenti, Karolinska Institutet, Sweden
Kathleen S. Rockland, Boston University School Medicine, USA
Muhammad A. Spocter, Des Moines University, USA

****Correspondence:***
Joan S. Baizer, Department of Physiology and Biophysics, University at Buffalo, 106 Sherman Hall, Buffalo, NY 14206, USA
e-mail: baizer@buffalo.edu

The claustrum is a subcortical nucleus present in all placental mammals. Many anatomical studies have shown that its inputs are predominantly from the cerebral cortex and its outputs are back to the cortex. This connectivity thus suggests that the claustrum serves to amplify or facilitate information processing in the cerebral cortex. The size and the complexity of the cerebral cortex varies dramatically across species. Some species have lissencephalic brains, with few cortical areas, while others have a greatly expanded cortex and many cortical areas. This evolutionary diversity in the cerebral cortex raises several questions about the claustrum. Does its volume expand in coordination with the expansion of cortex and does it acquire new functions related to the new cortical functions? Here we survey the organization of the claustrum in animals with large brains, including great apes and cetaceans. Our data suggest that the claustrum is not always a continuous structure. In monkeys and gorillas there are a few isolated islands of cells near the main body of the nucleus. In cetaceans, however, there are many isolated cell islands. These data suggest constraints on the possible function of the claustrum. Some authors propose that the claustrum has a more global role in perception or consciousness that requires intraclaustral integration of information. These theories postulate mechanisms like gap junctions between claustral cells or a "syncytium" to mediate intraclaustral processing. The presence of discontinuities in the structure of the claustrum, present but minimal in some primates, but dramatically clear in cetaceans, argues against the proposed mechanisms of intraclaustral processing of information. The best interpretation of function, then, is that each functional subdivision of the claustrum simply contributes to the function of its cortical partner.

Keywords: gorilla, whale, dolphin, calcium-binding proteins, visual cortex

The claustrum is a subcortical nucleus described in all placental mammals. Its structure, physiology, connections and neurochemistry have been studied in multiple species (references in Sherk, 1986; Buchanan and Johnson, 2011; Baizer, 2014). Classification schemes vary, but the claustrum is typically divided into two subdivisions, a dorsal and a ventral part, sometimes called the endopiriform nucleus (summary in Baizer, 2014). This paper will focus on the dorsal claustrum. Many studies show that the dorsal claustrum is functionally linked to the cerebral cortex, but the fundamental question of the function of the claustrum is still unanswered. We will consider first what is known about the organization and function of the claustrum from anatomical and electrophysiological studies in the cat and the macaque monkey. We will then ask what the comparative literature on the claustrum suggests about its function. We will supplement existing studies with data on the size and shape of the claustrum in a great ape, the western lowland gorilla, and from two cetaceans, the bottlenose dolphin and the humpback whale. Finally, we will summarize the implications of the comparative neuroanatomy of the claustrum for hypotheses about its function.

THE DORSAL CLAUSTRUM IN THE CAT AND THE MACAQUE MONKEY

Many anatomical studies in cat and monkey have shown that the cerebral cortex projects to the claustrum and the claustrum projects back to the cerebral cortex (Druga, 1966, 1968, 1971; Künzle, 1975; Riche and Lanoir, 1978; Turner et al., 1980; LeVay and Sherk, 1981a; Macchi et al., 1981, 1983; Mizuno et al., 1981; Pearson et al., 1982; Bullier et al., 1984; Ungerleider et al., 1984; Weber and Yin, 1984; Kennedy and Bullier, 1985; Guldin et al., 1986; LeVay, 1986; McCourt et al., 1986; Perkel et al., 1986; Sloniewski et al., 1986; Hinova-Palova et al., 1988; Minciacchi et al., 1991, 1995; Boussaoud et al., 1992; Clascá et al., 1992; Morecraft et al., 1992; Baizer et al., 1993, 1997; Tokuno and Tanji, 1993; Tanne-Gariepy et al., 2002; Miyashita et al., 2005;

Smith and Alloway, 2010). While there have been suggestions of subcortical connections of the claustrum, data from different studies are inconsistent and contradictory. For example, LeVay and Sherk (1981a), performed extensive experiments using both retrograde and anterograde tracers in the cat, and concluded that "no subcortical projections from the claustrum could be identified". In contrast, Amaral and Cowan (1980) reported a projection from the claustrum to the hippocampus in the macaque monkey. Similarly, Arikuni and Kubota (1985) reported a projection from claustrum to the caudate nucleus in the macaque monkey, while Saint-Cyr et al. (1990) did not find such a projection. Furthermore, in the most detailed anatomical study of the claustrum LeVay and Sherk (1981a) found that a large injection of retrograde tracer in visual cortex labeled 87% of the cells in the visual claustrum. The unlabeled cells were argued, on the basis of cell size, to represent local interneurons (LeVay and Sherk, 1981a). The weight of the evidence, at present, argues that the major, and possibly only, target of claustral projections is the cortex, and that the major input to the claustrum is from the cortex.

The connections between cortex and claustrum are topographic, with different cortical functional regions connected to dedicated claustrum territories (reviews in Sherk, 1986; Baizer, 2014). The cerebral cortex is characterized by both cytoarchitectural and neurochemical subdivisions, many of which correlate with functional regions (examples and references in Von Bonin and Bailey, 1947; Felleman and Van Essen, 1991; Geyer et al., 1996). However, cytoarchitectural and neurochemical analysis of the claustrum shows structural uniformity with no evidence of structurally- defined subdivisions (LeVay and Sherk, 1981a; Reynhout and Baizer, 1999; Baizer, 2001; Rahman and Baizer, 2007).

The claustrum of the cat extends over about 11 mm rostrocaudally (Snider and Niemer, 1961). **Figure 1** illustrates the claustrum of the cat on three sections showing its very different configuration at different rostro-caudal levels. **Figure 1A** shows a section at about the center of the claustrum, the locus of the large dorsal enlargement in which the visual region is found (LeVay and Sherk, 1981a,b). **Figure 1B** shows that neurons in the triangular part of the cat claustrum have round or oval somata. **Figures 1C,D** illustrate the shape of the claustrum at its caudal and rostral limits.

Anatomical data suggest that there is also a visual region of the macaque monkey claustrum that may contain more than one map of the visual field (Baizer et al., 1993, 1997). **Figures 2A–C** shows three sections at different rostral-levels of the macaque monkey claustrum. As in the cat, the shape of the claustrum changes with rostro-caudal level. **Figure 3** shows the neurons in the claustrum of the macaque monkey at different dorso-ventral levels. **Figures 3C,D** show that in the long, thin ascending stem of the claustrum many neurons have cell bodies elongated parallel to the long axis of the claustrum (**Figure 3D**), whereas in wider regions neurons have oval/polymorphic somata (**Figure 3B**). These differences in soma shape are presumably mirrored by differences in the shapes and extents of dendritic arbors. Further, the long dorsal stem of the claustrum can be discontinuous, with cell sparse regions (**Figure 3C**, large arrowhead). Interestingly, there is a major difference in the organization of the claustrum between macaque monkey and cat. In both species, the claustrum

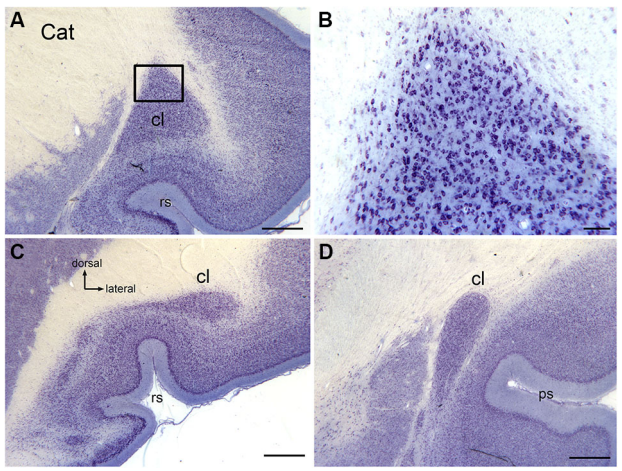

FIGURE 1 | The claustrum in the cat shown on cresyl violet-stained celloidin-embedded sections. (A) The claustrum at about its rostro-caudal center. The rectangle shows the location of the image in **(B)**. **(B)** Cells in the claustrum. **(C)** The claustrum at its rostral limit. **(D)** The claustrum at its caudal limit. Scale bars: **A, C, D** = 1 mm; **B** = 100 μm . Abbreviations: cl, claustrum; ps, pseudosylvian sulcus; rs, rhinal sulcus.

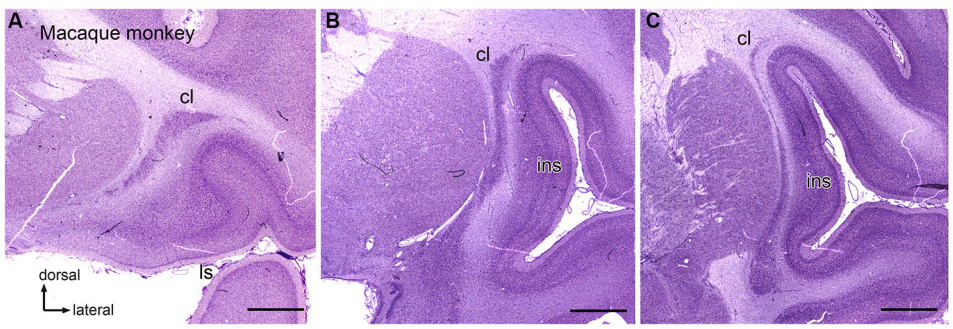

FIGURE 2 | The claustrum in the macaque monkey. (A) Rostral claustrum. **(B)** The claustrum at about its rostro-caudal center. **(C)** The caudal claustrum. Note the long, thin vertical stem and the ventral enlargement in **(B)**, **(C)**. Scale bars: **A, B, C** = 2 mm. Abbreviations: cl, claustrum; ls, lateral sulcus; ins, insula.

consists of a long thin stem with an enlargement but this enlargement is dorsally in the cat and ventrally the monkey. In both cat and macaque monkey, the visual claustrum is found within the enlarged region (LeVay and Sherk, 1981a,b; Baizer et al., 1993, 1997).

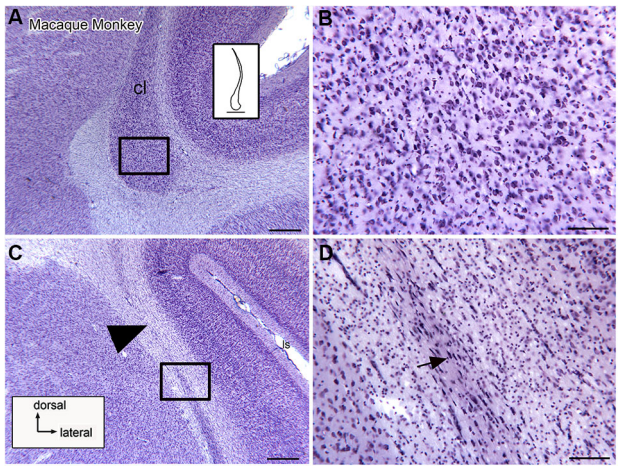

FIGURE 3 | Neuronal organization of the claustrum in the macaque monkey shown on higher magnification images. (A) The ventral expansion of the claustrum in the macaque monkey. The rectangle shows the location of the image in **(B)**. The inset shows an outline drawing of the entire claustrum. **(B)** Neurons in the ventral enlargement of the monkey have round or polygonal somata. **(C)** Cells in the long ascending stem of the claustrum. The arrowhead indicates a cell-sparse region. The rectangle shows the location of the image in **(D)**. **(D)** Many neurons in the thin ascending stem have somata that are elongated parallel to the borders of the structure (arrow). Scale bars: **A, C** = 500 μm; **A**, inset = 2 mm; **B, D** = 100 μm.

CELLULAR ORGANIZATION OF THE CLAUSTRUM

Studies in several species identify a population of projection neurons in the claustrum; these neurons are also the targets of descending projections from the neocortex (LeVay and Sherk, 1981a). In addition, there are populations of local interneurons. These were first identified by Golgi impregnation studies (LeVay and Sherk, 1981a; Mamos et al., 1986). Later studies showed that different populations of interneurons are immunoreactive for different calcium-binding proteins (Reynhout and Baizer, 1999; Rahman and Baizer, 2007; Baizer, 2014). **Figures 4A–C** shows neurons immunoreactive for calbindin (CB; **A**), calretinin (CR, **B**) and parvalbumin (PV, **C**) in the claustrum of the cat. **Figures 4D–F** show neurons in the claustrum of the macaque monkey immunoreactive for CB (**D**), CR (**E**) and PV (**F**). These interneurons provide a substrate for local information processing within the claustrum.

THEORIES OF THE FUNCTION OF THE CLAUSTRUM

There are two very different views of the function of the claustrum. One is that the claustrum is divided into independent functional zones defined by cortical connections and that each zone then influences only its cortical partner. This view derives from anatomical and physiological studies of the visual claustrum of the cat (Olson and Graybiel, 1980; LeVay and Sherk, 1981a,b; Macchi et al., 1981; Sherk and Levay, 1981; Boyapati and Henry, 1985; LeVay, 1986; Updyke, 1993; Minciacchi et al., 1995; Pérez-Cerdá et al., 1996). There is a visuotopic map of the contralateral visual hemifield in the

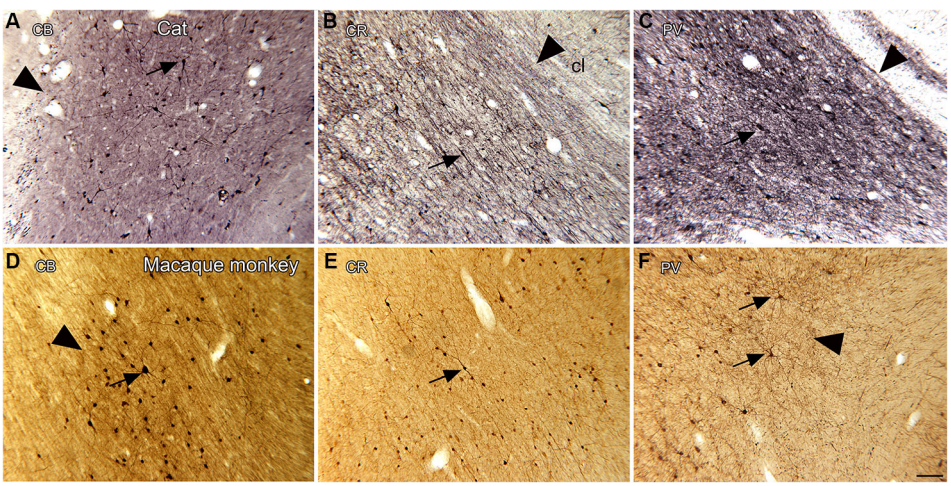

FIGURE 4 | Spacing and density of neurons in the claustrum of the cat (A, B, C) and macaque monkey (D, E, F) claustrum that are immunoreactive for the calcium-binding proteins. (A) CB, cat. The arrowhead indicates the medial border of the claustrum; the arrow indicates a labeled cell. **(B)** CR, cat. The arrowhead shows the border of the claustrum and the arrow a cell with a fusiform soma. **(C)** PV, cat. The claustrum is darkly stained; the border (arrowhead) is very clear. The arrow shows a PV-ir neuron. **A, B, C** glucose oxidase modification of DAB for visualization of immunoreactivity. **(D)** CB, monkey. The arrowhead shows the border of the claustrum, the arrow a labeled neuron. **(E)** CR, monkey. The arrow shows a neuron with an elongated soma. **(F)** PV, monkey. The arrowhead shows the edge of the claustrum. The arrows show two large neurons and their dendrites. **D, E, F**, standard DAB visualization of immunoreactivity. Scale bar: **F** = 100 μm; same magnification for all other panels. Abbreviations: CB, calbindin; CR, calretinin; PV, parvalbumin.

part of the claustrum connected with visual cortex (LeVay and Sherk, 1981a,b; Sherk and Levay, 1981). Neurons in this region have exclusively visual responses and receptive field properties similar to those of cells in V1 (LeVay and Sherk, 1981b; Sherk and Levay, 1981). By this view, it is not possible to define a single function for the claustrum, each functional subdivision would affect the function of its cortical counterpart, which could be sensory or motor or cognitive or affective. Other authors, however, have proposed a more integrative and global role for the claustrum, envisioning that it mediates consciousness (Crick and Koch, 2005) or perceptual integration across sensory modalities (Smythies et al., 2012). These ideas require the integration of information across different functional subdivisions of the claustrum. Anatomical studies did not find evidence for projections among subdivisions of the claustrum (LeVay and Sherk, 1981a), leading to the suggestion of novel mechanisms for intraclaustral information processing. Interneurons in the claustrum are critical for these mechanisms, which include gap junctions among interneurons (Crick and Koch, 2005), and/or dendrodendritic chemical synapses among claustral cells (Crick and Koch, 2005). A related proposal is that the interneurons of the claustrum form an "interactive gap-junction syncytium" (Smythies et al., 2014). These mechanisms require that the claustrum is a continuous structure with neurons in close proximity to each other, that "a densely packed amorphous syncytium [that] constitutes the interior of the claustrum (Smythies et al., 2014). This idea of the interior structure of the claustrum also implies a uniformity of arrangements of dendritic trees and spacing of neurons throughout the claustrum. Examination of the fine structure of the claustrum should allow some evaluation of the plausibility of these mechanisms.

Another implication of the more global theories of claustral function is that the claustrum should increase in importance over evolution. This hypothesis could be examined by quantitative comparative analysis of the relative sizes of claustrum and the cerebral cortex.

EVOLUTION, THE CLAUSTRUM, AND THE CORTEX

Because of the anatomical interdependence of cerebral cortex and claustrum, phylogenetic variation in the organization of the claustrum must be considered in the context of the organization of the cortex. The configuration of the cerebral cortex varies widely among mammals (images of the brains of many different species are shown at http://www.brainmuseum.org). There are many species-specific functional specializations of cortical areas. For example, the maps of the body in sensory and motor cortex adapt to reflect functional specializations in different species, e.g., a representation of the trunk in the somatosensory and motor cortex of the elephant or of high frequency sounds in the auditory cortex of bats (representative studies Edamatsu and Suga, 1993; Fitzpatrick et al., 1993, 1998; Esser et al., 1997; Xiao and Suga, 2004). The size and the complexity of the cerebral cortex change dramatically over evolution. Many rodents are lissencephalic with a relatively small number of cortical areas. By contrast, many anthropoid primates, including humans, have a greatly expanded cerebral cortex with considerable gyrification and an increased number of cortical areas (Agulhon et al., 1998).

Species differences in cortical organization are mirrored in differences in the size and shape of the claustrum. Buchanan and Johnson (2011) illustrate the shape and size of both cortex and claustrum in 26 different species. Kowiański et al. (1999) illustrated the shape of the claustrum in different species. They recognized five different morphological types; the shape of the dorsal claustrum in 8 different species is illustrated in **Figure 5** (modified from Kowiański et al., 1999). It is important to note, however, that while all of these drawings show the claustrum as a continuous structure, examination of Nissl sections from the macaque monkey at higher magnification (as in **Figure 3C**) shows discontinuities. **Figures 6A,B** supplement the drawings of the human claustrum with photomicrographs of the human claustrum (at arrows) in Nissl-stained coronal sections of the human brain. The image in A shows a hint of a ventral enlargement as seen in macaque monkey; the image in B supports dorsal-ventral symmetry. A ventral enlargement is present in small-brain lissencephalic New World anthropoid primates such as owl monkeys, squirrel monkeys, titi monkeys, tamarins and marmosets, although it is not as pronounced in the strepsirrhine primates, the lemurs and lorises. However, while illustrations can show species variability in the form of the claustrum, they cannot relate the differences in the shape and size of the claustrum to differences in the numbers or organization or specializations of cortical areas.

In addition to illustrating the species differences in the appearance of the claustrum, Kowiański et al. (1999) asked a critical question: do the claustrum and the cerebral cortex expand in parallel? They calculated the ratio of the volume of the claustrum to the volume of the cerebral hemispheres in several species; the data showed that the volume of the claustrum does not increase proportionately at the same rate to the volume of the cerebral cortex (Kowiański et al., 1999). Of the species they examined, the ratio of the volume of the claustrum to the volume of the isocortex was highest in mice (6.5%) and lowest in humans (0.45%). These data suggest that as the cerebral cortex expands the relative size of the claustrum actually decreases.

Both the qualitative and quantitative analyses of the claustrum in human raise questions about the similarity of its organization to that of other species. The shape of the claustrum in the human is strikingly different from that of the rodents, the cat and most primate species. Does the claustrum in human connect only with the "older" cortical structures, i.e., the primary sensory and motor areas or are there parts of the claustrum that are more related to association cortical areas and their functions? Is the claustrum in humans structurally uniform as it is in animals? In humans, there is lateralization of both language and handedness and this lateralization is also mirrored by structural asymmetries (Steinmetz et al., 1989; Jäncke et al., 1994; Steinmetz, 1996; Westbury et al., 1999; Pujol et al., 2002). Might this lateralization be reflected in left-right asymmetries in the claustrum? Another characteristic of cerebral cortex in humans, great apes and other primates with gyrified brains is individual variability in the pattern of cortical sulci and gyri (Steinmetz, 1996; Westbury et al., 1999). Is this individual variability mirrored in individual differences in claustrum morphology?

There are thus many questions about the organization and function of the claustrum in humans. How may these questions

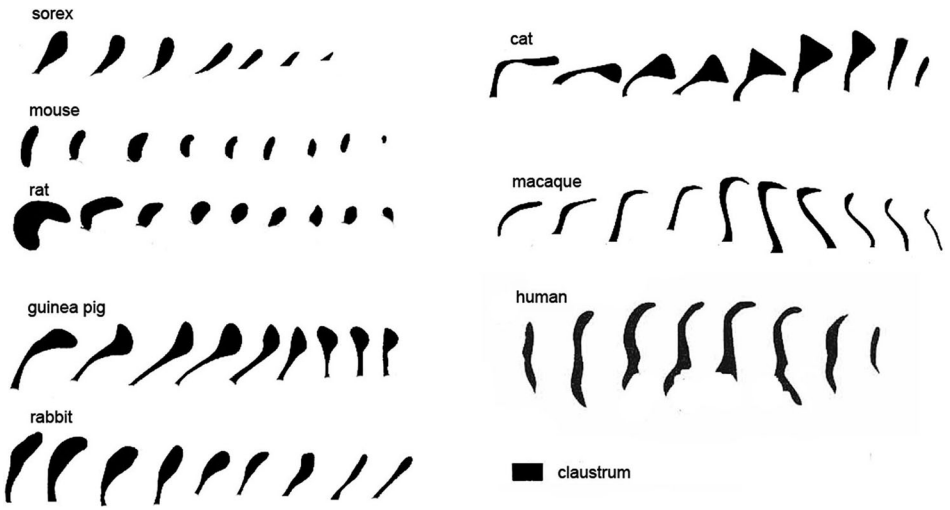

FIGURE 5 | Variations in the shape of the dorsal claustrum in eight different species. Modified from Figure 7 in Kowiański et al. (1999). The different drawings are not to scale. Note the presence of a dorsal enlargement and thin stem in sorex, cat and guinea pig compared to the dorsal-ventral symmetry seen in the mouse and the rat and, at some levels, human. In all species the images are arranged with the most rostral on the left.

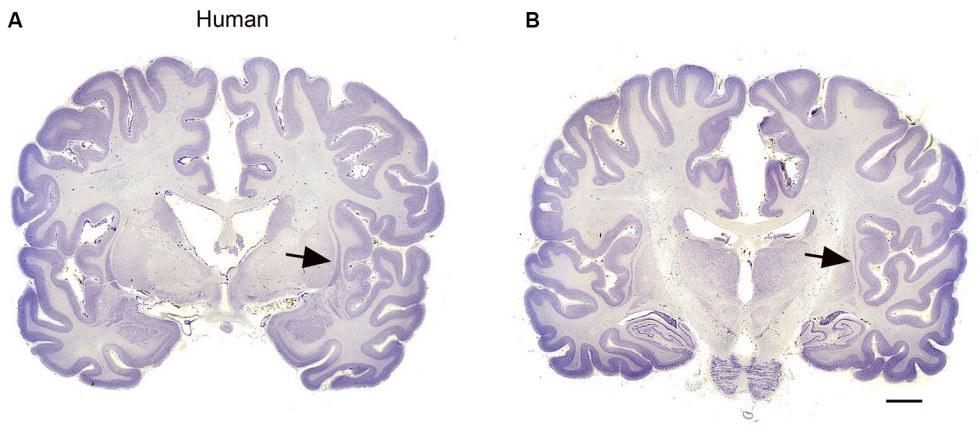

FIGURE 6 | (A, B) The claustrum in the human brain. The claustrum is shown on two coronal sections through the human brain about 17 mm apart. **A** is the more rostral. The arrows show the claustrum, which is quite small relative to the total size of the section. The images were downloaded from http://www.brains.rad.msu.edu and, http://brainmuseum.org sites supported by the US National Science Foundation, and used with permission. The brain had been embedded in celloidin and sectioned at 35 μm. Scale bar = 10 mm.

be addressed? Direct studies of connections and function using invasive techniques cannot be undertaken in humans or other great apes. However, descriptive anatomy based on postmortem tissue, as well as imaging studies, are powerful techniques that can be used in human.

There are studies of the cell types in the human claustrum (Braak and Braak, 1982; Spahn and Braak, 1985; Hinova-Palova et al., 2013). The anatomical data in general support the idea of the presence of both projection neurons and interneurons, and overall structural uniformity within the claustrum.

There are also imaging studies of the human claustrum using a variety of techniques. One study suggests that the claustrum in humans, as in other species, is interconnected with many regions of the cerebral cortex (Milardi et al., 2013). That study also showed both individual variability and left-right differences in claustral volumes, in keeping with findings for the human cerebral cortex. There were also sex differences in claustral volume, with males having a larger volume than females. This may reflect overall sex differences in brain size (Leonard et al., 2008; Luders et al., 2009) (One caution about the results of this study: a pathway between claustrum and basal ganglia was also found, such a pathway was not described in the most detailed experimental study of the connections of the claustrum (LeVay and Sherk, 1981a)).

There are many imaging studies that suggest a role of the claustrum in rather diverse functions. At this point, these studies

must be interpreted with caution, as the imaging resolution may not yet be sufficient to distinguish activation of the claustrum, which in humans is very thin, from that in surrounding brain regions like the cerebral cortex and the putamen. Imaging resolution is certainly not yet able to resolve activation differences within different functional zones of the claustrum itself. For example, Wegiel et al. (2014, p. 227) list 10 functions in which the claustrum has been implicated including "experiential dread" and "suppression of natural urges". In addition to the studies listed by Wegiel et al. (2014) there is a PET imaging study that suggested a role for the claustrum in sexual function (Redouté et al., 2000; **Figure 3**), an fMRI study linked the claustrum to ADHD (Wang et al., 2013), another to aesthetic judgment (Ishizu and Zeki, 2013) and yet another suggested pathology of the claustrum in bipolar disorder (Selvaraj et al., 2012). Increased resolution of imaging techniques may clarify the role of the claustrum in these, and other, as yet unstudied, functions.

THE CLAUSTRUM IN THE GORILLA

The drawings in **Figure 5** suggest that the human claustrum has more dorsal-ventral symmetry than seen in other species. In order to see if this is unique to humans or is a general feature of the brains of great apes, we examined the claustrum in the gorilla. **Figure 7F** shows a lateral view of the gorilla brain; its rostro-caudal extent is about 130 mm. There is a more complex pattern of sulci and gyri than seen in the macaque monkey. Examination of cresyl violet-stained sections showed that the claustrum was present over about 33 mm in the rostro-caudal direction. **Figures 7A–E** show five outline drawings of the claustrum at different rostro-caudal levels. The claustrum is very elongated in the dorso-ventral direction, extending as far as 20 mm (**Figure 7D**); it is also very thin. Comparison of the claustrum in the gorilla (**Figure 7**) and the human (**Figures 5**, **6**) shows that the claustrum in the gorilla is much longer and narrower than in the human. Strikingly, at some levels, the claustrum is not a continuous structure; **Figure 7A** shows an isolated cluster of neurons in the dorsal part of the claustrum. **Figures 8A,C** show lower magnification photomicrographs of the claustrum on two different sections, one at a more dorsal level and the other at a more ventral level. Again the isolated clusters of cells are apparent (**Figure 8A**). The shapes of the somata also vary with location in the claustrum. **Figures 8B,D** shows higher magnification images showing the numbers, shape, and density of stained neurons. **Figure 8B** shows somata that are elongated roughly parallel to the dorso-ventral axis. **Figure 8D** shows larger stained somata that are polygonal with no preferred orientation. These differences in soma shape probably correlate with differences in the shape and extent of the dendritic trees, differences not considered in the "gap junction syncytium" hypothesis. Since the brains for the cat and monkey were not prepared in the same way (celloidin vs. frozen sections) meaningful comparisons of neuronal size or neuronal packing density among these species cannot be made.

THE CLAUSTRUM IN CETACEANS

The drawings in **Figure 5** do not include all of the forms that the claustrum can take. In the elephant, the claustrum is elongated toward the frontal pole of the cortex and appears as cell islands just under the cortex (see Figure 2 in Hakeem et al., 2009). Cell islands are also found in cetaceans, animals with well developed and highly folded cerebral cortices. **Figure 9A** shows the highly folded cortex in the brain of the bottlenose dolphin; arrows indicate the locations of cell islands comprising the claustrum. **Figure 9B** shows claustral islands at higher magnification and **Figure 9C** shows the cellular organization of one such island. It

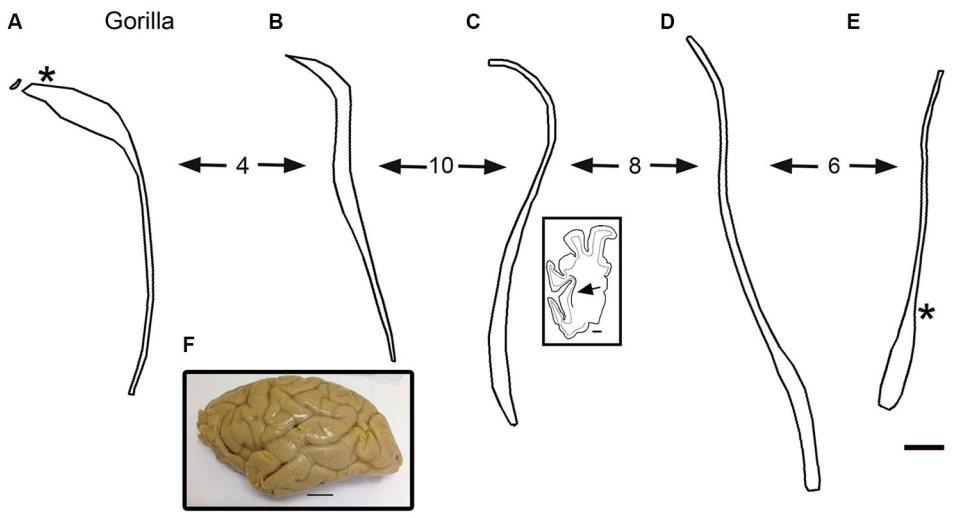

FIGURE 7 | (A–E) Outline drawings of the claustrum of the gorilla from five coronal cresyl-violet stained sections. **A** is the most rostral. The spacing of the sections (mm) is indicated by the numbers between the arrows. **(A)** The asterisk shows the approximate location of the image in **Figures 8A,C**. The inset shows an outline drawing of the left half of the cerebral cortex on the section for the level of the claustrum shown; the arrow indicates the location of the claustrum on this section. **(E)** The asterisk shows the approximate location of the image in **Figure 8C**. **(F)** Lateral view of the left hemisphere of a gorilla showing the sulci and gyri. Caudal is to the right. Scale bars: **E** = 2 mm, same scale for **A–D**; **C**, inset = 5 mm; **F** = 2 cm.

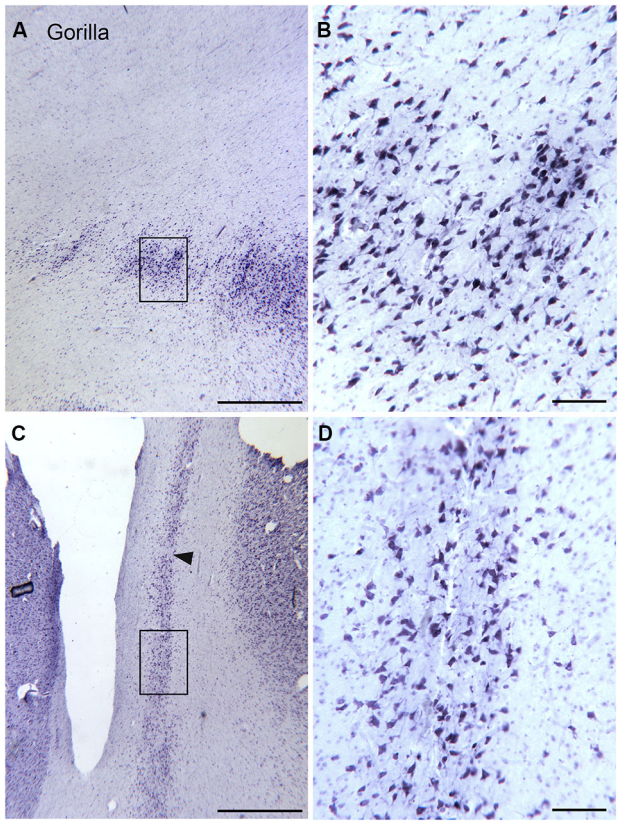

FIGURE 8 | Size shape and density of neurons in the claustrum of the gorilla at different rostro-caudal and dorso-ventral levels. (A) Cell islands in the dorsal claustrum (section outlined on **Figure 7A**). The rectangle shows the location of the image in **(B)**. **(B)** Stained somata in the claustrum; many somata are multipolar. Scale bar = 100 μm. **(C)** Image of the more ventral and caudal claustrum; the section was outlined in **Figure 7E**. The rectangle shows the location of the image in **(D)**. The arrowhead indicates a cell-sparse region. **(D)** Somata in the ventral and caudal claustrum; many are multipolar. Scale bars: **A, C** = 1 mm; **B, D** = 100 μm.

is not clear from the anatomy, of course, if the islands represent fragmented functional subdivisions (as would be the case, for example, if the the visual claustrum of the cat were broken up into isolated cell clusters) or if each island is a self-contained unit. **Figure 10A** shows the highly folded cerebral cortex of the whale on a parasagittal section; the arrows show the very scattered islands of claustral cells. **Figures 1B,C** show these cell clusters in more detail.

CONCLUSIONS: WHAT IS THE FUNCTION OF THE CLAUSTRUM?

The comparative data summarized here argue against the hypothesis that the claustrum has an important role in global perceptual integration and/or consciousness. First, examination of the shape of the claustrum in different species shows considerable variability, with several species having very long, thin claustral "stems" that would seem to impose constraints on the proposed mechanisms of intraclaustral processing. These notions of intraclaustral processing also require that the claustrum is a continuous structure, and that clearly is not the case in a number of species. We have shown sections in both macaque monkey and gorilla in which the claustrum is characterized by separated cell clusters. Claustral fragmentation is seen even more dramatically in the bottlenose dolphin and humpback whale. Another argument against a major integrative role for the claustrum, however, comes from the quantitative analysis showing its decreased relative size (as indicated by the ratio of volumes) as cerebral cortex expands (Kowiański et al., 1999). Rather than suggesting a global role for the claustrum, the comparative data reinforce the early view that each functional division of the claustrum is independent from the others, and works with the cortical area with which it is interconnected. By this view, the function of each subdivision would be to enhance or modulate the function of its cortical partner. Thus, the anatomical data do not support a more global role of the claustrum. The fact that expansion of the claustrum does not parallel cortical expansion suggests that the function of amplifying or adjusting cortical excitability was of greater importance in lissencephalic animals, and that the importance of claustrum for cortical operations has decreased as cortical complexity has increased.

MATERIALS AND METHODS

TISSUE AND HISTOLOGY

Cat, macaque monkey

We photographed archival celloidin-embedded cresyl violet stained sections of the cat and macaque monkey claustrum. These slides had been prepared in the laboratory of Dr. Mitchell Glickstein, then at Brown University. We also photographed archival immunostained sections that had been prepared in the course of earlier studies (Reynhout and Baizer, 1999; Rahman and Baizer, 2007).

Gorillas

We obtained the brains of two western lowland gorillas from the Buffalo Zoo. Gorilla 1 was a female, age at death 6 years, cause of death unknown. Gorilla 2 was a male, age at death 20 years; the cause of death was cancer. The brains were removed and stored in 10% formalin. No data on the postmortem intervals of this tissue were available. The brains were cryoprotected in 15% then 30% sucrose in 10% formalin. The brain of Gorilla 1 was blocked to include the claustrum; the brain of Gorilla 2 was divided into four equal size blocks. Frozen sections 40 μm thick were cut in the coronal plane on an American Optical sliding microtome fitted with a custom-built copper freezing platform. All sections were collected and stored in large plastic compartment boxes, 5 sections/compartment in 5% formalin in a cold room. Series of sections 2 mm apart were mounted onto gelled slides (Brain Research Laboratories, Newton, MA) and stained for Nissl substance with cresyl violet (following the protocol of LaBossiere and Glickstein, 1976).

Cetaceans

We photographed archival celloidin-embedded cresyl-violet stained sections of a bottlenose dolphin brain that had been used in earlier projects (Hof et al., 2005). We also photographed slides

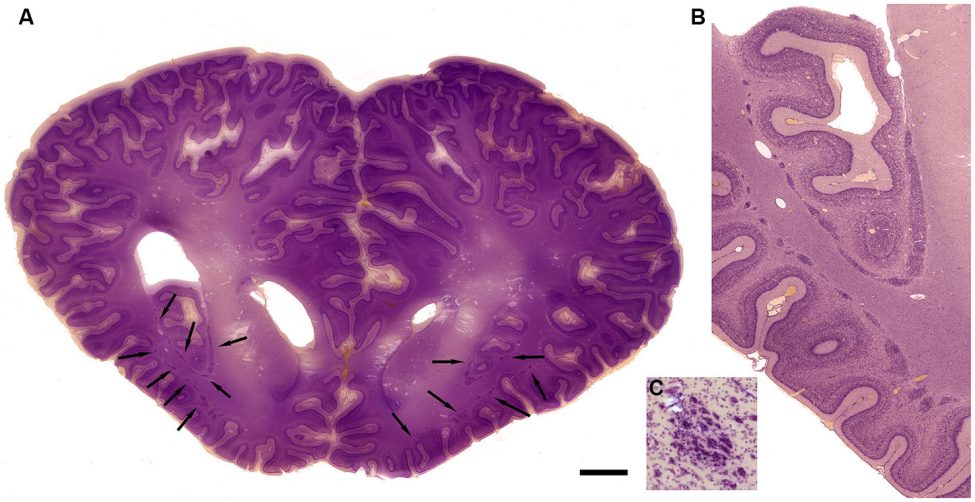

FIGURE 9 | Morphology of the claustrum in the bottlenose dolphin (*Tursiops truncatus*). (A) Coronal section through the brain of a 4 year old *Tursiops*. The arrows point to the location of the claustrum around the anterior portion of the insular pocket and to the highly unusual distribution of many claustral island along cortical gyri in the prefrontal cortex, shown at higher magnification in **(B)**. **(C)** Cellular details of one island of claustral neurons in the anterior portion of the ectosylvian gyrus. Scale bars = 1 cm **(A)**, 4 mm **(B)**, and 100 μm **(C)**.

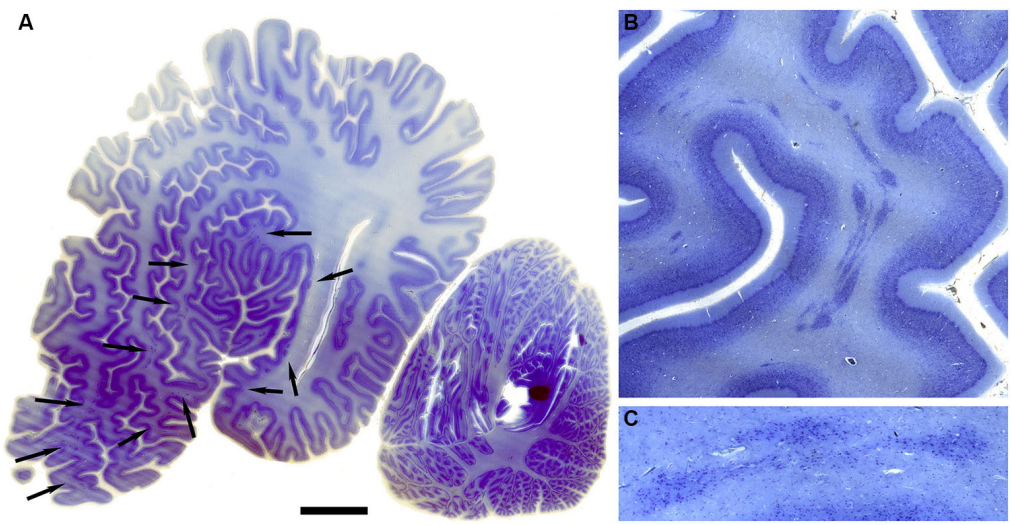

FIGURE 10 | Morphology of the claustrum in the humpback whale (*Megaptera novaeangliae*). (A) Parasagittal section through one hemisphere of an adult humpback whale. There are a very large number of claustral islands dispersed in the white matter underlying the perisylvian, ectosylvian, and suparsylvian cortex, as well as in the frontal pole (arrows). **(B)** Higher magnification image of a large cluster of these claustral neurons in the white matter of the suprasylvian gyrus. **(C)** Shows cellular details. Note that as in the bottlenose dolphin, these claustral island are completely separate from the neocortex. Scale bars = 2 cm **(A)**, 6 mm **(B)**, and 1.5 mm **(C)**.

of the brain of a stranded humpback whale; the cerebral cortex of that animal was described in an earlier report (Hof and Van der Gucht, 2007).

Outline drawings

The outlines of the gorilla claustrum in **Figure 7** were drawn from sections using MDplot software (Accustage, Shoreview, MN) with stage encoders mounted on a Leitz Dialux 20 microscope. These drawings were saved as .bmp files using the screen capture function of the software and then assembled into figures with Adobe Photoshop (Adobe, San Jose, CA).

Photography

Images (1600 × 1200 pixels) were captured with a SPOT Insight Color Mosaic camera (Diagnostic Imaging, Sterling Heights, MI) mounted on the Leitz microscope. We used Adobe Photoshop to adjust the brightness and contrast of images and to assemble and label the figures.

ACKNOWLEDGMENTS

Supported in part by grants from the James S. McDonnell Foundation to Patrick R. Hof and Chet C. Sherwood and by the Department of Physiology and Biophysics, University at Buffalo (Joan S. Baizer). Kathryn Callan provided technical support in the analysis of the gorilla brain.

REFERENCES

Agulhon, C., Charnay, Y., Vallet, P., Abitbol, M., Kobetz, A., Bertrand, D., et al. (1998). Distribution of mRNA for the alpha4 subunit of the nicotinic acetylcholine receptor in the human fetal brain. *Mol. Brain Res.* 58, 123–131. doi: 10.1016/s0169-328x(98)00113-2

Amaral, D. G., and Cowan, W. M. (1980). Subcortical afferents to the hippocampal formation in the monkey. *J. Comp. Neurol.* 189, 573–591. doi: 10.1002/cne.901890402

Arikuni, T., and Kubota, K. (1985). Claustral and amygdaloid afferents to the head of the caudate nucleus in macaque monkeys. *Neurosci. Res.* 2, 239–254. doi: 10.1016/0168-0102(85)90003-3

Baizer, J. S. (2014). "The neurochemical organization of the claustrum," in *The Claustrum. Structural, Functional and Clinical Neuroscience*, eds J. R. Smythies, L. R. Edelstein and V. S. Ramachandran (Amsterdam: Elsevier), 85–118.

Baizer, J. S. (2001). Serotonergic innervation of the primate claustrum. *Brain Res. Bull.* 55, 431–434. doi: 10.1016/s0361-9230(01)00535-4

Baizer, J. S., Desimone, R., and Ungerleider, L. G. (1993). Comparison of subcortical connections of inferior temporal and posterior parietal cortex in monkeys. *Vis. Neurosci.* 10, 59–72. doi: 10.1017/s0952523800003229

Baizer, J. S., Lock, T. M., and Youakim, M. (1997). Projections from the claustrum to the prelunate gyrus in the monkey. *Exp. Brain Res.* 113, 564–568. doi: 10.1007/pl00005607

Boussaoud, D., Desimone, R., and Ungerleider, L. G. (1992). Subcortical connections of visual areas MST and FST in macaques. *Vis. Neurosci.* 9, 291–302. doi: 10.1017/s0952523800010701

Boyapati, J., and Henry, G. H. (1985). The character and influence of the claustral pathway to the striate cortex of the cat. *Exp. Brain Res.* 61, 141–152. doi: 10.1007/bf00235629

Braak, H., and Braak, E. (1982). Neuronal types in the claustrum of man. *Anat. Embryol.* 163, 447–460. doi: 10.1007/bf00305558

Buchanan, K. J., and Johnson, J. I. (2011). Diversity of spatial relationships of the claustrum and insula in branches of the mammalian radiation. *Ann. N Y Acad. Sci.* 1225(Suppl. 1), E30–E63. doi: 10.1111/j.1749-6632.2011.06022.x

Bullier, J., Kennedy, H., and Salinger, W. (1984). Bifurcation of subcortical afferents to visual areas 17, 18 and 19 in the cat cortex. *J. Comp. Neurol.* 228, 309–328. doi: 10.1002/cne.902280303

Clascá, F., Avendaño, C., Román-Guindo, A., Llamas, A., and Reinoso-Suárez, F. (1992). Innervation from the claustrum of the frontal association and motor areas: axonal transport studies in the cat. *J. Comp. Neurol.* 326, 402–422. doi: 10.1002/cne.903260307

Crick, F. C., and Koch, C. (2005). What is the function of the claustrum? *Philos. Trans. R. Soc. Lond. B Biol. Sci.* 360, 1271–1279. doi: 10.1098/rstb.2005.1661

Druga, R. (1966). Cortico-claustral connections. I. Fronto-claustral connections. *Folia Morphol. (Praha)* 14, 391–399.

Druga, R. (1968). Cortico-claustral connections. II. Connections from the parietal, temporal and occipital cortex to the claustrum. *Folia Morphol. (Praha)* 16, 142–149.

Druga, R. (1971). Projection of prepyriform cortex into claustrum. *Folia Morphol. (Praha)* 19, 405–410.

Edamatsu, H., and Suga, N. (1993). Differences in response properties of neurons between two delay-tuned areas in the auditory cortex of the mustached bat. *J. Neurophysiol.* 69, 1700–1712.

Esser, K. H., Condon, C. J., Suga, N., and Kanwal, J. S. (1997). Syntax processing by auditory cortical neurons in the FM-FM area of the mustached bat *Pteronotus parnellii*. *Proc. Natl. Acad. Sci. U S A* 94, 14019–14024. doi: 10.1073/pnas.94.25.14019

Felleman, D. J., and Van Essen, D. C. (1991). Distributed hierarchical processing in the primate cerebral cortex. *Cereb. Cortex* 1, 1–47. doi: 10.1093/cercor/1.1.1

Fitzpatrick, D. C., Kanwal, J. S., Butman, J. A., and Suga, N. (1993). Combination-sensitive neurons in the primary auditory cortex of the mustached bat. *J. Neurosci.* 13, 931–940.

Fitzpatrick, D. C., Olsen, J. F., and Suga, N. (1998). Connections among functional areas in the mustached bat auditory cortex. *J. Comp. Neurol.* 391, 366–396. doi: 10.1002/(sici)1096-9861(19980216)391:3<366::aid-cne6>3.3.co;2-3

Geyer, S., Ledberg, A., Schleicher, A., Kinomura, S., Schormann, T., Burgel, U., et al. (1996). Two different areas within the primary motor cortex of man. *Nature* 382, 805–807. doi: 10.1038/382805a0

Guldin, W. O., Markowitsch, H. J., Lampe, R., and Irle, E. (1986). Cortical projections originating from the cat's insular area and remarks on claustrocortical connections. *J. Comp. Neurol.* 243, 468–487. doi: 10.1002/cne.902430404

Hakeem, A. Y., Sherwood, C. C., Bonar, C. J., Butti, C., Hof, P. R., and Allman, J. M. (2009). Von Economo neurons in the elephant brain. *Anat. Rec.* 292, 242–248. doi: 10.1002/ar.20829

Hinova-Palova, D. V., Edelstein, L., Landzhov, B. V., Braak, E., Malinova, L. G., Minkov, M., et al. (2013). Parvalbumin-immunoreactive neurons in the human claustrum. *Brain Struct. Funct.* doi: 10.1007/s00429-013-0603-x. [Epub ahead of print].

Hinova-Palova, D. V., Paloff, A. M., Usunoff, K. G., Dimova, R. N., Yossifov, T. Y., and Ivanov, D. P. (1988). Reciprocal connections between the claustrum and the auditory cortical fields in the cat. An experimental study using light- and electron microscopic anterograde degeneration methods and the horseradish peroxidase retrograde axonal transport. *J. Hirnforsch.* 29, 255–278.

Hof, P. R., Chanis, R., and Marino, L. (2005). Cortical complexity in cetacean brains. *Anat. Rec.* 287, 1142–1152. doi: 10.1002/ar.a.20258

Hof, P. R., and Van der Gucht, E. (2007). Structure of the cerebral cortex of the humpback whale, *Megaptera novaeangliae* (Cetacea, Mysticeti, Balaenopteridae). *Anat. Rec.* 290, 1–31. doi: 10.1002/ar.20407

Ishizu, T., and Zeki, S. (2013). The brain's specialized systems for aesthetic and perceptual judgment. *Eur. J. Neurosci.* 37, 1413–1420. doi: 10.1111/ejn.12135

Jäncke, L., Schlaug, G., Huang, Y., and Steinmetz, H. (1994). Asymmetry of the planum parietale. *Neuroreport* 5, 1161–1163. doi: 10.1097/00001756-199405000-00035

Kennedy, H., and Bullier, J. (1985). A double-labeling investigation of the afferent connectivity to cortical areas V1 and V2 of the macaque monkey. *J. Neurosci.* 5, 2815–2830.

Kowiański, P., Dziewiatkowski, J., Kowiańska, J., and Moryś, J. (1999). Comparative anatomy of the claustrum in selected species: a morphometric analysis. *Brain. Behav. Evol.* 53, 44–54. doi: 10.1159/000006581

Künzle, H. (1975). Bilateral projections from precentral motor cortex to the putamen and other parts of the basal ganglia. An autoradiographic study in *Macaca fascicularis*. *Brain Res.* 88, 195–209. doi: 10.1016/0006-8993(75)90384-4

LaBossiere, E., and Glickstein, M. (1976). *Histological Processing for the Neural Sciences.* Springfield, IL: Charles C. Thomas.

Leonard, C. M., Towler, S., Welcome, S., Halderman, L. K., Otto, R., Eckert, M. A., et al. (2008). Size matters: cerebral volume influences sex differences in neuroanatomy. *Cereb. Cortex* 18, 2920–2931. doi: 10.1093/cercor/bhn052

LeVay, S. (1986). Synaptic organization of claustral and geniculate afferents to the visual cortex of the cat. *J. Neurosci.* 6, 3564–3575.

LeVay, S., and Sherk, H. (1981a). The visual claustrum of the cat. I. Structure and connections. *J. Neurosci.* 1, 956–980.

LeVay, S., and Sherk, H. (1981b). The visual claustrum of the cat. II. The visual field map. *J. Neurosci.* 1, 981–992.

Luders, E., Gaser, C., Narr, K. L., and Toga, A. W. (2009). Why sex matters: brain size independent differences in gray matter distributions between men and women. *J. Neurosci.* 29, 14265–14270. doi: 10.1523/jneurosci.2261-09.2009

Macchi, G., Bentivoglio, M., Minciacchi, D., and Molinari, M. (1981). The organization of the claustroneocortical projections in the cat studied by means of the HRP retrograde axonal transport. *J. Comp. Neurol.* 195, 681–695. doi: 10.1002/cne.901950411

Macchi, G., Bentivoglio, M., Minciacchi, D., and Molinari, M. (1983). Claustro-neocortical projections studied in the cat by means of multiple retrograde fluorescent tracing. *J. Comp. Neurol.* 215, 121–134. doi: 10.1002/cne.902150202

Mamos, L., Narkiewicz, O., and Morys, J. (1986). Neurons of the claustrum in the cat; a Golgi study. *Acta Neurobiol. Exp. (Wars)* 46, 171–178. doi: 10.1007/bf00239531

McCourt, M. E., Boyapati, J., and Henry, G. H. (1986). Layering in lamina 6 of cat striate cortex. *Brain Res.* 364, 181–185. doi: 10.1016/0006-8993(86)91001-2

Milardi, D., Bramanti, P., Milazzo, C., Finocchio, G., Arrigo, A., Santoro, G., et al. (2013). Cortical and subcortical connections of the human claustrum revealed in vivo by constrained spherical deconvolution tractography. *Cereb. Cortex* doi: 10.1093/cercor/bht231. [Epub ahead of print].

Minciacchi, D., Granato, A., and Barbaresi, P. (1991). Organization of claustro-cortical projections to the primary somatosensory area of primates. *Brain Res.* 553, 309–312. doi: 10.1016/0006-8993(91)90840-r

Minciacchi, D., Granato, A., Antonini, A., Tassinari, G., Santarelli, M., Zanolli, L., et al. (1995). Mapping subcortical extrarelay afferents onto primary somatosensory and visual areas in cats. *J. Comp. Neurol.* 362, 46–70. doi: 10.1002/cne.903620104

Miyashita, T., Nishimura-Akiyoshi, S., Itohara, S., and Rockland, K. S. (2005). Strong expression of NETRIN-G2 in the monkey claustrum. *Neuroscience* 136, 487–496. doi: 10.1016/j.neuroscience.2005.08.025

Mizuno, N., Uchida, K., Nomura, S., Nakamura, Y., Sugimoto, T., and Uemura-Sumi, M. (1981). Extrageniculate projections to the visual cortex in the macaque monkey: an HRP study. *Brain Res.* 212, 454–459. doi: 10.1016/0006-8993(81)90477-7

Morecraft, R. J., Geula, C., and Mesulam, M. M. (1992). Cytoarchitecture and neural afferents of orbitofrontal cortex in the brain of the monkey. *J. Comp. Neurol.* 323, 341–358. doi: 10.1002/cne.903230304

Olson, C. R., and Graybiel, A. M. (1980). Sensory maps in the claustrum of the cat. *Nature* 288, 479–481. doi: 10.1038/288479a0

Pearson, R. C., Brodal, P., Gatter, K. C., and Powell, T. P. (1982). The organization of the connections between the cortex and the claustrum in the monkey. *Brain Res.* 234, 435–441. doi: 10.1016/0006-8993(82)90883-6

Pérez-Cerdá, F., Martinez-Millán, L., and Matute, C. (1996). Anatomical evidence for glutamate and/or aspartate as neurotransmitters in the geniculo-, claustro- and cortico-cortical pathways to the cat striate cortex. *J. Comp. Neurol.* 373, 422–432. doi: 10.1002/(sici)1096-9861(19960923)373:3<422::aid-cne7>3.0.co;2-4

Perkel, D. J., Bullier, J., and Kennedy, H. (1986). Topography of the afferent connectivity of area 17 in the macaque monkey: a double-labelling study. *J. Comp. Neurol.* 253, 374–402. doi: 10.1002/cne.902530307

Pujol, J., López-Sala, A., Deus, J., Cardoner, N., Sebastián-Gallés, N., Conesa, G., et al. (2002). The lateral asymmetry of the human brain studied by volumetric magnetic resonance imaging. *Neuroimage* 17, 670–679. doi: 10.1006/nimg.2002.1203

Rahman, F. E., and Baizer, J. S. (2007). Neurochemically defined cell types in the claustrum of the cat. *Brain Res.* 1159, 94–111. doi: 10.1016/j.brainres.2007.05.011

Redouté, J., Stoléru, S., Grégoire, M. C., Costes, N., Cinotti, L., Lavenne, F., et al. (2000). Brain processing of visual sexual stimuli in human males. *Hum. Brain Mapp.* 11, 162–177. doi: 10.1002/1097-0193(200011)11:3<162::aid-hbm30>3.0.co;2-a

Reynhout, K., and Baizer, J. S. (1999). Immunoreactivity for calcium-binding proteins in the claustrum of the monkey. *Anat. Embryol. (Berl)* 199, 75–83. doi: 10.1007/s004290050211

Riche, D., and Lanoir, J. (1978). Some claustro-cortical connections in the cat and baboon as studied by retrograde horseradish peroxidase transport. *J. Comp. Neurol.* 177, 435–444. doi: 10.1002/cne.901770306

Saint-Cyr, J. A., Ungerleider, L. G., and Desimone, R. (1990). Organization of visual cortical inputs to the striatum and subsequent outputs to the pallido-nigral complex in the monkey. *J. Comp. Neurol.* 298, 129–156. doi: 10.1002/cne.902980202

Selvaraj, S., Arnone, D., Job, D., Stanfield, A., Farrow, T. F., Nugent, A. C., et al. (2012). Grey matter differences in bipolar disorder: a meta-analysis of voxel-based morphometry studies. *Bipolar Disord.* 14, 135–145. doi: 10.1111/j.1399-5618.2012.01000.x

Sherk, H. (1986). "The claustrum and the cerebral cortex," in *Cerebral Cortex*, eds E. G. Jones and A. Peters (New York: Plenum), 467–499.

Sherk, H., and Levay, S. (1981). The visual claustrum of the cat. III. Receptive field properties. *J. Neurosci.* 1, 993–1002.

Sloniewski, P., Usunoff, K. G., and Pilgrim, C. (1986). Retrograde transport of fluorescent tracers reveals extensive ipsi- and contralateral claustrocortical connections in the rat. *J. Comp. Neurol.* 246, 467–477. doi: 10.1002/cne.902460405

Smith, J. B., and Alloway, K. D. (2010). Functional specificity of claustrum connections in the rat: interhemispheric communication between specific parts of motor cortex. *J. Neurosci.* 30, 16832–16844. doi: 10.1523/jneurosci.4438-10.2010

Smythies, J. R., Edelstein, L. R., and Ramachandran, V. S. (2012). Hypotheses relating to the function of the claustrum. *Front. Integr. Neurosci.* 6:53. doi: 10.3389/fnint.2012.00053

Smythies, J., Edelstein, L., and Ramachandran, V. (2014). Hypotheses relating to the function of the claustrum II: does the claustrum use frequency codes? *Front. Integr. Neurosci.* 8:7. doi: 10.3389/fnint.2014.00007

Snider, R. S., and Niemer, W. T. (1961). *A Stereotaxic Atlas of the Cat Brain.* Chicago: University of Chicago Press.

Spahn, B., and Braak, H. (1985). Percentage of projection neurons and various types of interneurons in the human claustrum. *Acta Anat. (Basel)* 122, 245–248. doi: 10.1159/000146023

Steinmetz, H. (1996). Structure, functional and cerebral asymmetry: in vivo morphometry of the planum temporale. *Neurosci. Biobehav. Rev.* 20, 587–591. doi: 10.1016/0149-7634(95)00071-2

Steinmetz, H., Rademacher, J., Huang, Y. X., Hefter, H., Zilles, K., Thron, A., et al. (1989). Cerebral asymmetry: MR planimetry of the human planum temporale. *J. Comput. Assist. Tomogr.* 13, 996–1005. doi: 10.1097/00004728-198911000-00011

Tanne-Gariepy, J., Boussaoud, D., and Rouiller, E. M. (2002). Projections of the claustrum to the primary motor, premotor and prefrontal cortices in the macaque monkey. *J. Comp. Neurol.* 454, 140–157. doi: 10.1002/cne.10425

Tokuno, H., and Tanji, J. (1993). Input organization of distal and proximal forelimb areas in the monkey primary motor cortex: a retrograde double labeling study. *J. Comp. Neurol.* 333, 199–209. doi: 10.1002/cne.903330206

Turner, B. H., Mishkin, M., and Knapp, M. (1980). Organization of the amygdalopetal projections from modality-specific cortical association areas in the monkey. *J. Comp. Neurol.* 191, 515–543. doi: 10.1002/cne.901910402

Ungerleider, L. G., Desimone, R., Galkin, T. W., and Mishkin, M. (1984). Subcortical projections of area MT in the macaque. *J. Comp. Neurol.* 223, 368–386. doi: 10.1002/cne.902230304

Updyke, B. V. (1993). Organization of visual corticostriatal projections in the cat, with observations on visual projections to claustrum and amygdala. *J. Comp. Neurol.* 327, 159–193. doi: 10.1002/cne.903270202

Von Bonin, G., and Bailey, P. (1947). *The Neocortex of Macaca Mulatta.* Urbana, IL: The University of Illinois Press.

Wang, X., Jiao, Y., Tang, T., Wang, H., and Lu, Z. (2013). Altered regional homogeneity patterns in adults with attention-deficit hyperactivity disorder. *Eur. J. Radiol.* 82, 1552–1557. doi: 10.1016/j.ejrad.2013.04.009

Weber, J. T., and Yin, T. C. (1984). Subcortical projections of the inferior parietal cortex (area 7) in the stump-tailed monkey. *J. Comp. Neurol.* 224, 206–230. doi: 10.1002/cne.902240204

Wegiel, J., Morys, J., Kowianski, P., Ma, S., Kuchna, I., Nowici, K., et al. (2014). "Delayed development of the claustrum in autism," in *The Claustrum. Structural, Functional and Clinical Neuroscience*, eds J. R. Smythies, L. R. Edelstein and V. S. Ramachandran (Amsterdam: Elsevier), 225–235.

Westbury, C. F., Zatorre, R. J., and Evans, A. C. (1999). Quantifying variability in the planum temporale: a probability map. *Cereb. Cortex* 9, 392–405. doi: 10.1093/cercor/9.4.392

Xiao, Z., and Suga, N. (2004). Reorganization of the auditory cortex specialized for echo-delay processing in the mustached bat. *Proc. Natl. Acad. Sci. U S A* 101, 1769–1774. doi: 10.1073/pnas.0307296101

Conflict of Interest Statement: The authors declare that the research was conducted in the absence of any commercial or financial relationships that could be construed as a potential conflict of interest.

Received: 27 March 2014; accepted: 02 June 2014; published online: 02 July 2014.
Citation: Baizer JS, Sherwood CC, Noonan M and Hof PR (2014) Comparative organization of the claustrum: what does structure tell us about function? Front. Syst. Neurosci. ***8****:117. doi: 10.3389/fnsys.2014.00117*
This article was submitted to the journal Frontiers in Systems Neuroscience.

frontiers in
SYSTEMS NEUROSCIENCE

ORIGINAL RESEARCH ARTICLE
published: 27 May 2014
doi: 10.3389/fnsys.2014.00096

Topographical distribution and morphology of NADPH-diaphorase-stained neurons in the human claustrum

Dimka V. Hinova-Palova[1], Lawrence Edelstein[2]*, Boycho Landzhov[1], Minko Minkov[3], Lina Malinova[1], Stanislav Hristov[4], Frank J. Denaro[5], Alexandar Alexandrov[4], Teodora Kiriakova[4], Ilina Brainova[4], Adrian Paloff[1] and Wladimir Ovtscharoff[1]

[1] Department of Anatomy, Histology, and Embryology, Medical University, Sofia, Bulgaria
[2] Medimark Corporation, Del Mar, CA, USA
[3] Department of Anatomy and Histology, Medical University, Varna, Bulgaria
[4] Department of Forensic Medicine and Deontology, Medical University, Sofia, Bulgaria
[5] Department of Biology, Morgan State University, Baltimore, MD, USA

Edited by:
Brian N. Mathur, University of Maryland School of Medicine, USA

Reviewed by:
Antonio Pereira, Federal University of Rio Grande do Norte, Brazil
Marco Aurelio M. Freire, Edmond and Lily Safra International Institute for Neurosciences of Natal, Brazil

***Correspondence:**
Lawrence Edelstein, Medimark Corporation, PO Box 2316, Del Mar, CA 92014, USA
e-mail: larry.edelstein@claustrum.com

We studied the topographical distribution and morphological characteristics of NADPH-diaphorase-positive neurons and fibers in the human claustrum. These neurons were seen to be heterogeneously distributed throughout the claustrum. Taking into account the size and shape of stained perikarya as well as dendritic and axonal characteristics, Nicotinamide adenine dinucleotide phosphate-diaphorase (NADPHd)-positive neurons were categorized by diameter into three types: large, medium and small. Large neurons ranged from 25 to 35 μm in diameter and typically displayed elliptical or multipolar cell bodies. Medium neurons ranged from 20 to 25 μm in diameter and displayed multipolar, bipolar and irregular cell bodies. Small neurons ranged from 14 to 20 μm in diameter and most often displayed oval or elliptical cell bodies. Based on dendritic characteristics, these neurons were divided into spiny and aspiny subtypes. Our findings reveal two populations of NADPHd-positive neurons in the human claustrum—one comprised of large and medium cells consistent with a projection neuron phenotype, the other represented by small cells resembling the interneuron phenotype as defined by previous Golgi impregnation studies.

Keywords: human claustrum, NADPH-diaphorase, nitric oxide, nitric oxide synthase, projection neurons, interneurons

INTRODUCTION

The claustrum is a telencephalic structure present in nearly all mammalian brains (Guirado et al., 2003; Real et al., 2003; Ashwell et al., 2004; Edelstein and Denaro, 2004). In humans, it is situated between the insular cortex and putamen, and bordered by the external and extreme capsules. The claustrum was first depicted by the noted French physician/anatomist Felix Vicq d' Azyr in his historic treatise (Vicq d'Azyr, 1786) and described as: "*Tractus cortical très délié qui se trouve entre le sillon de Sylvius et les corps striés* ['*Separated cortical tract between the Sylvian fissure and the corpus striatum*']" It is generally believed that the German physiologist Karl Burdach first ascribed the name "claustrum" to this nucleus (Burdach, 1822). The size of the claustrum varies by species (Berlucchi, 1927; Brockhaus, 1940; Macchi, 1948; Rae, 1954; Berke, 1960; Narkiewicz, 1964; Filimonoff, 1966; Druga, 1974, 1975; Zilles et al., 1980; Paxinos and Watson, 1998; Kowianski et al., 2004). The gross anatomical subdivisions of the claustrum are generally accepted as being dorsal (insular) and ventral (endopiriform) (Guirado et al., 2003; Ashwell et al., 2004; Edelstein and Denaro, 2004). Morys et al. (1996) further divided the claustrum into four parts: dorsal, orbital, temporal, and paraamygdalar. Namavar et al. (2005) distinguished three parts in the dorsoventral plane; cap, dorsal, and ventral.

The dorsal claustrum is connected with the neocortex (Narkiewicz, 1964; Druga, 1966a,b, 1968, 1975; Narkiewicz, 1972; Norita, 1977; Kunzle, 1978; Riche and Lanoir, 1978; Edelstein and Denaro, 1979, 1980; Olsen and Graybiel, 1980; Neal et al., 1986; Sloniewski et al., 1986a,b; Tanne-Gariepy et al., 2002). The ventral claustrum is situated just beneath the piriform cortex, well-interconnected with prepiriform and entorhinal cortices (Druga, 1971; Witter et al., 1988; Dinopoulos et al., 1992). Braak and Braak (1982) distinguished five types of neurons in the human claustrum: Type I representing spiny neurons varying in size and shape, Type II are large aspiny neurons, Type III are large aspiny neurons devoid of pigment deposits, Type IV are small pigment-laden aspiny neurons, and Type V are small aspiny neurons devoid of lipofuscin granules. The functional significance of the claustrum continues to be the subject of debate (Edelstein and Denaro, 2004; Crick and Koch, 2005; Smythies et al., 2012, 2014a,b). A recent comprehensive review by Sherk (2014) on the physiology of the claustrum offers considerable insight into this structures complex interplay with both sensory and motor cortices, while discussing hypotheses as to its function.

Nicotinamide adenine dinucleotide phosphate-diaphorase (NADPHd)-positive neurons and fibers are present in many parts of the nervous system in a variety of species, including

humans (Mizukawa et al., 1989; Mizukawa, 1990; Vincent and Kimura, 1992; Druga and Syka, 1993; Valtschanoff et al., 1993; Yan et al., 1996; Hinova-Palova et al., 1997; Paloff and Hinova-Palova, 1998; Moreno-Lopez et al., 1998; Saxon and Beitz, 2000; Lysakowski and Singer, 2000; Holstein et al., 2001; Martinelli et al., 2002; Papantchev et al., 2005, 2006; Edelstein et al., 2012a,b). Histochemical mapping studies of the mammalian brain reveal either neuronal nitric oxide synthase (NOS) or NADPHd activity in the claustrum (Vincent and Kimura, 1992; Paloff et al., 1994; Rodrigo et al., 1994; Switka et al., 1994; Hinova-Palova et al., 1997, 2013; Paloff and Hinova-Palova, 1998; Paxinos and Watson, 1998; Vincent, 2000; Edelstein et al., 2012a,b).

Under specific fixation conditions, NADPHd is routinely used as a histochemical marker for NOS (Mizukawa et al., 1989; Dawson et al., 1991; Hope et al., 1991; Bredt and Snyder, 1992; Vincent and Hope, 1992; Vincent and Kimura, 1992; Druga and Syka, 1993; Paloff et al., 1994; Switka et al., 1994). According to Matsumoto et al. (1993), paraformaldehyde adversely impacts NADPHd labeling, thus negating any observable correlation between NADPHd staining and NOS immunocytochemistry (Dun et al., 1992). In contrast to these studies, efforts by Terenghi et al. (1993) in humans and rats, as well as those by Artero et al. (1995) in the crested newt, have demonstrated a good correlation in similarly fixed tissue.

The demonstration that NADPHd staining is due to the activity of NOS (Hope et al., 1991) quickly facilitated the detailed anatomical analysis of NO-producing cells throughout the nervous system (Vincent and Hope, 1992; Vincent and Kimura, 1992). The direct relationship between NADPHd staining and NOS expression has been well-documented (Bredt et al., 1991; Dawson et al., 1991). The absence of neuronal expression of NADPHd and NOS activity in knockout mice lacking NOS provided definitive evidence for the specificity of this simple histochemical procedure (Huang et al., 1993). The results obtained with NADPHd histochemistry have been confirmed and extended using antibodies against the various NOS isoforms (Bredt et al., 1990) as well as with *in situ* hybridization (Bredt et al., 1991). Of particular importance has been the description of alternatively-spliced forms of NOS expressed in certain brain regions (Brenman et al., 1997; Eliasson et al., 1997). Freire et al. (2004, 2005, 2010) used NADPHd histochemistry to study cortical fields in several different animals, including barrel cortical fields in the rat and mouse, and V1, V2, V3 in the common agouti.

Recently, there has been an increasing focus on nitric oxide (NO), which participates in many physiological and pathological processes. In the brain, NO is an important messenger molecule involved in such diverse functions as transsynaptic transmission, neuronal development, plasticity, the release of neurotransmitters, as well as long-term synaptic modulation (Garthwaite, 1991; Schuman and Madison, 1991; Sibuki and Okada, 1991; Lorrian and Hull, 1993; Zhuo et al., 1993; Bredt and Snyder, 1994). With respect to the peripheral nervous system, NO serves as a transmitter in non-adrenergic and non-cholinergic neurons (Bult et al., 1990). NO is also produced in the cardiovascular, renal and lymphatic systems, thus playing an important role in hemodynamics, and vasodilatation (Palmer et al., 1987; Nathan and Nibs, 1991; Nathan, 1992; Romero et al., 1992). It also plays a role in various neurodegenerative disorders such as Parkinson's disease, Alzheimer's disease, and Huntington's disease (Ferrante et al., 1985, 1987; Koh et al., 1986; Boegman and Parent, 1988; Halliwell, 1989; Dawson et al., 1991; Mufson and Brandabur, 1994; Hunot et al., 1996; Tao et al., 1999; Freire et al., 2007). According to Aoki et al. (1995), NO controls a number of critical physiological processes. In this regard its actions run the gamut, from signal transduction to apoptosis, with its synthesis catalyzed by NOS (Bredt et al., 1990).

NOS has been localized to a variety of other organs in rats and humans (Bredt and Snyder, 1990; Bredt et al., 1990; Dun et al., 1992; Springall et al., 1992), including the central nervous system (CNS) of the crested newt (Artero et al., 1995). Using immunocytochemical procedures, Rodrigo et al. (1994) detailed the mapping of NOS in the adult rat brain.

Mizukawa et al. (1989) and Vincent and Kimura (1992) did not report on the topographical distribution of NO immunoreactive neurons in the claustrum, in the context of their CNS studies. The existence of NOS neurons in the claustrum has previously been noted, but in limited scope (Paloff et al., 1994; Rodrigo et al., 1994; Switka et al., 1994). To the best of our knowledge, ours is the first detailed assessment of the topographical distribution and morphological characteristics of NADPHd-positive neurons and fibers in the human claustrum.

The investigations of our laboratory have been focused on the cytoarchitecture, ultrastructure, immunocytochemistry, and connections of the claustrum for over 30 years (Hinova-Palova et al., 1979, 1980a,b, 1988, 1997, 2001, 2007, 2008, 2012a,b; Hinova-Palova, 1981, 1986; Hinova-Palova and Usunoff, 1981; Hinova-Palova and Christova, 1988a,b; Hinova-Palova and Braak, 1993; Edelstein et al., 2011a,b, 2012a,b). The internal complexity and intricate cortical interrelationships of this broad and sheet-like telencephalic mass comes as no surprise, given its diverse neuronal composition and intrinsic functional heterogeneity. Its topographical and functional relations with most if not all cortical and adjacent brain areas make it an especially interesting and challenging area for investigation (Edelstein and Denaro, 2004; Smythies et al., 2012, 2014a,b). It is the intention of this study to describe and depict the topographical distribution and morphology of NADPHd-positive neurons and fibers in the human claustrum.

MATERIALS AND METHODS

Brains were removed at 4–10 h post-mortem from four male patients (28, 42, 58, and 61 years of age) and three female patients (40, 52, and 68 years of age) with no known neurological disorders. The brains were blunt cut in the coronal plane into 1–2 cm slabs, then fixed for 2 days under gentle agitation in a mixture of 4% paraformaldehyde, 2% glutaraldehyde, 1% picric acid, and 10% glucose.

Next, the slabs were blocked to the area of interest, washed in 0.01 M phosphate-buffered saline (PBS) and sectioned at 40 μm on a freezing microtome (Reichert-Jung). All sections were treated with sodium borohydride for 45 min followed by three consecutive 2-min rinses in 0.01 M PBS. The slices were then incubated in a solution containing 0.2 mg/ml nitro blue tetrazolium chloride (NBT), 1 mg/ml NADPH tetrasodium salt and

0.5% Triton X-100 diluted in 0.1 M Tris-HCl buffer with pH 7.4 at 37°C for 30–60 min. The reaction was completed with 0.1 M Tris-HCl, pH 7.6. Afterwards, sections were rinsed three times for 5 min each in the same phosphate buffer, air-dried for 24 h and cover-slipped with Entellan (Merck Millipore). NADPHd staining was visualized as a blue reaction product within the neuronal cytoplasm.

For quantitative analysis, 40 slides containing sections of NADPHd-positive neurons were examined using an image analyzer (CUE-2, Olympus) and a 40× objective. The analysis began with capturing and storing images of the area of interest. Afterwards, we performed standard planar morphometry and linear analysis (i.e., line length and width). Next, we measured the maximum diameter of 700 neurons, and the cells were then divided into groups. A mean was then calculated for the minimum and maximum diameter of all neurons in each group. A Mann-Whitney analysis was performed to determine whether the special distribution and size differences were statistically significant. Subsequent to quantitative analysis, explanatory markers were added to all images using Adobe Photoshop 7.0.

RESULTS

Our results revealed a heterogeneous distribution and density of NADPHd-reactive neurons throughout the claustrum (**Figure 1**), often seen as clusters of 10–15 neurons (**Figure 2A**). Preparations through the caudal pole displayed 1–3 positive neurons per section (**Figure 2B**). A large number of stained cells were found in the posterior half of the rostral third of the claustrum. Conversely, positive neurons were only occasionally seen as one nears the anterior aspect of the rostral pole, and rarely in clusters. The ventral claustrum exhibited numerous NADPHd-positive neurons (**Figures 2C,D**), in particular, a large number (20–25 per section) within its caudal third (**Figure 3A**).

NADPHd-positive neurons were also observed within the external and extreme capsules proximal to the claustrum. As a rule, these neurons were oriented parallel to the capsular fibers (**Figures 3A–C**), but in some cases their projections ran perpendicular (**Figure 3D**). NADPHd-reaction product diffusely filled the cytoplasm (**Figure 4A**), while the nucleus remained stain-free. In the medial third of the claustrum a great number of neurons were lightly stained, while others resembled the intensity of a Golgi impregnation (**Figures 4B–D**).

A number of highly branched NADPHd-positive fibers were seen throughout the claustrum. They were readily seen to have traversed the claustrum in all of directions. This network of branching varicose fibers stood in stark contrast to the comparatively modest number of observable NADPHd-positive cells.

We were able to distinguish three NADPHd-positive neuronal types and four subtypes in the human claustrum with regard to the size and shape of their perikarya and dendritic morphology. Based on our quantitative analysis, these neurons were divided into three types, as depicted in **Diagram 1**: large (comprising 65.5% of the total sample), medium (22%), and small (12.5%).

The population density of the 700 sampled NADPHd-positive neurons in the dorsal, ventral and central zones of claustrum (**Diagram 2**)—two-thirds of which were of the large cell type—showed a statistically significant difference between the dorsal and central areas ($p < 0.001$), ventral and central areas ($p < 0.01$), and dorsal and ventral areas ($p < 0.005$). The population density of large NADPHd-positive neurons was shown to be representative of the overall sampled population in two of the three comparators (**Diagram 3**): dorsal and central ($p < 0.001$) and ventral and central ($p < 0.01$). No statistically significant differences in population density was noted for medium and small neurons between dorsal and ventral areas ($p < 0.05$).

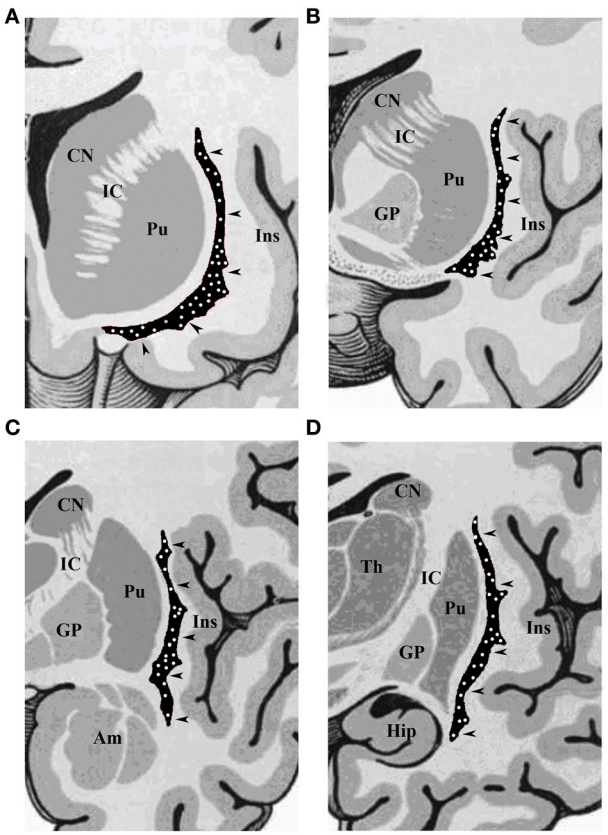

FIGURE 1 | Schematic drawings of coronal sections of human brain, from rostral to caudal through the (A) olfactory tract, (B) anterior commissure, (C) amygdaloid body, and (D) hippocampus. CN, caudate nucleus; IC, internal capsule; Pu, putamen; Ins, insular cortex; GP, globus pallidus; Am, amygdala; Hip, hippocampus; Th, thalamus. The arrowheads indicate the claustrum, with white dots depicting the topographical distribution of NADPHd-positive neurons.

LARGE NADPHD-POSITIVE NEURONS

Large NADPHd-positive neurons represented 65.5% of the total sampled (459/700). They ranged from 25 to 35 μm in diameter and were seen throughout the claustrum, though predominantly in its dilated rostroventral aspect (**Figure 2C**). Not unlike what has been seen in other species their shape varied widely, most commonly: multipolar (**Figure 5A**), pyramidal (**Figure 5B**), bipolar (**Figure 5C**), oval and pear (**Figure 5D**). Further, the large neurons could be divided into two subtypes by virtue of their dendritic morphology: spiny and aspiny.

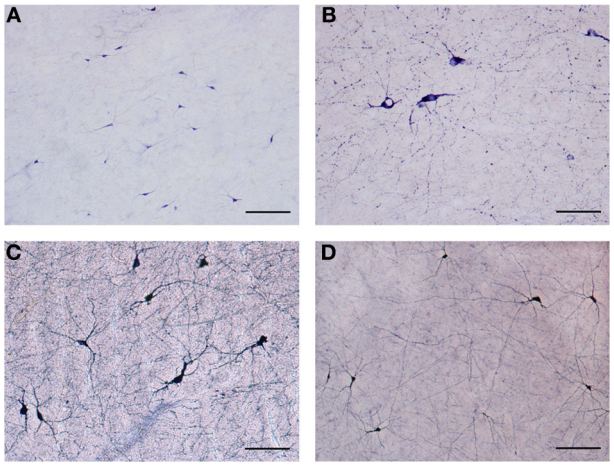

FIGURE 2 | (A) Low magnification of NADPHd-positive neurons in the claustrum. Note the heterogeneity of size and shape. Scale bar = 300 μm. **(B)** NADPHd-positive neurons and fibers in the caudal pole of the claustrum. Cell bodies are few, but the fibers and their varicose nature are quite evident. Scale bar = 100 μm. **(C)** NADPHd-positive neurons in the ventral claustrum. Scale bar = 100 μm. **(D)** NADPHd-positive neurons and fibers in the caudal third of the ventral claustrum. Scale bar = 200 μm.

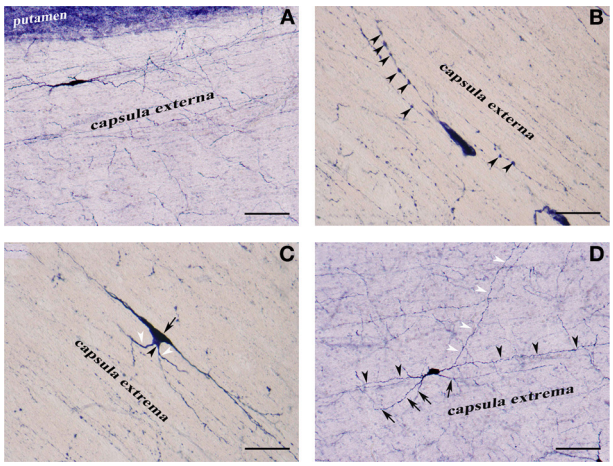

FIGURE 3 | (A) NADPHd-positive neuron located within the extreme capsule bordering the putamen. Scale bar = 100 μm. **(B)** NADPHd-positive neuron located within the extreme capsule. Note the prominent dendritic varicosities (arrowheads). Scale bar = 40 μm. **(C)** Two NADPHd-positive neurons located within the extreme capsule, one fusiform in shape (black arrow), the second, a smaller neuron, closely abutting the first (black arrowhead). Note the short dendrites on the smaller neuron (white arrowheads). Scale bar = 40 μm. **(D)** Multipolar NADPHd-positive neuron located within the extreme capsule. Some of the secondary dendrites can be seen running parallel to the capsular fibers of the white matter (black arrowheads), while other are traversing the white matter to enter the claustrum (white arrowheads). Still other secondary dendrites are seen crossing the extreme capsule toward the putamen (black arrows). Scale bar = 100 μm.

Large spiny neuron subtype

The NADPHd-positive neurons in this subtype were commonly found in the dilated rostroventral claustrum (**Figure 2C**), but could also be seen in its dorsal aspect. They ranged from 25 to 35 μm in diameter and displayed elliptical or multipolar perikarya, from which emanated 4–6 thick primary dendrites, each in turn producing secondary and tertiary branches covered with spines (**Figures 6A,B**). These secondary and tertiary dendrites took a wavy course and radiated 700–800 μm from the cell body in all directions, as well as seen crossing the capsules. In all instances, the dendrites were spiny, with axons arising from perikarya with a distinct axon hillock (**Figure 6A**), or from the primary dendrite as can be the case with dopaminergic neurons (**Figures 6A–D**). The characteristics of the dendritic tree were very much dependent upon the shape of the cell body.

Large aspiny neuron subtype

The NADPHd-positive neurons in this second subtype measured 25–30 μm, slightly smaller than the first. Most of these cells had a pear-shaped or irregular cell body producing a small number of far-reaching multidirectional dendrites from a cone-shaped proximal stem (**Figures 7A–D**). The dendritic diameter remained fairly constant along its length. The dendritic arbor bore a close resemblance to that of claustral stellate cells. The axon emerged from the cell body with a readily distinguishable axon hillock and initial segment while giving off a few thin collaterals, and was occasionally seen emanating from the trunk of the primary dendrite (**Figures 7B,D**).

MEDIUM NADPHD-POSITIVE NEURONS

These cells varied from 20 to 25 μm in diameter and comprised 22% (154/700) of sampled NADPHd-positive neurons. As with the large-type neurons, they too were observed throughout the claustrum. Though far fewer in number relative to the large neurons, clear differences in their somatodendritic morphology allowed for the distinction of two subtypes: spiny and aspiny.

Medium spiny neuron subtype

These NADPHd-positive neurons displayed multipolar, bipolar or irregular cell bodies (**Figures 8A–D**). Their perikarya typically gave rise to 3 or 4 dendrites (on rare occasion, five). The primary dendrites bifurcated (or trifurcated) into secondary branches which often took a markedly divergent course. As a rule, the dendrites in this subclass were spiny, especially along the secondary and tertiary branches. The secondary and tertiary dendrites were wavy in form, with the most distal branches extending 400–500 μm from the cell body. The axon was noted to emanate directly from the cell body (**Figures 8B,C**), with a somewhat thin initial segment that could be followed for 100–200 μm, at which point the labeling abruptly ended.

Medium aspiny neuron subtype

The second subtype of medium NADPHd-positive neurons is based on shape, prominent varicosities and a paucity of dendritic spines. Multipolar, oval, irregular, or bipolar cells were observed (**Figures 9A,B**). Two to four considerably thin and short beaded dendrites were noted originating from the cell body, radiating in all directions. Rarely were they seen to branch more than once, while giving rise to equally fine caliber and divergent secondaries with prominent varicosities. In some cases, parts of the dendrite

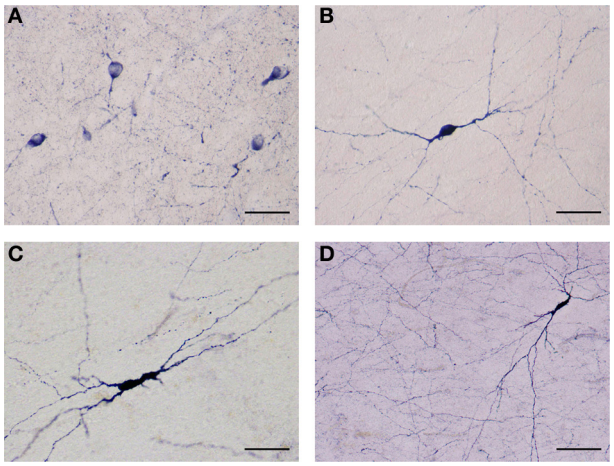

FIGURE 4 | (A) Several NADPHd-positive neurons located in the dorsal claustrum. Reaction product can be seen filling the cytoplasm, fills the cytoplasm, while the nucleus remains stain-free. Stained puncta and fibers are also clearly visible. Scale bar = 40 μm. **(B)** Densely stained NADPHd-positive neuron with an ovoid cell body. Primary dendrites can be seen bifurcating into secondaries within a short distance, subsequently branching into tertiary dendrites coursing in many directions over a long distance. Scale bar = 40 μm. **(C)** Densely stained NADPHd-positive neuron with an irregular shaped cell body. Scale bar = 40 μm. **(D)** Large NADPHd-positive spiny neuron. The dendritic arborization is quite extensive within the claustral neuropil. Scale bar = 100 μm.

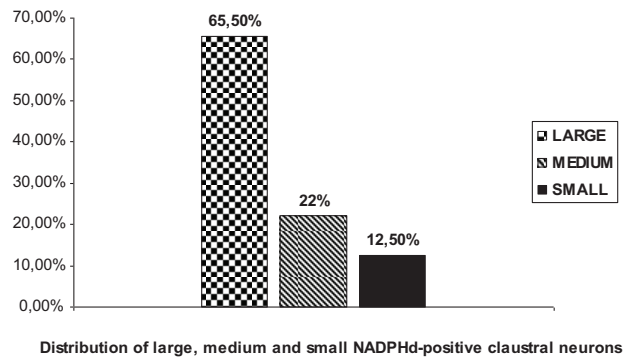

Diagram 1 | Percent distribution of NADPHd-positive claustral neurons by diameter.

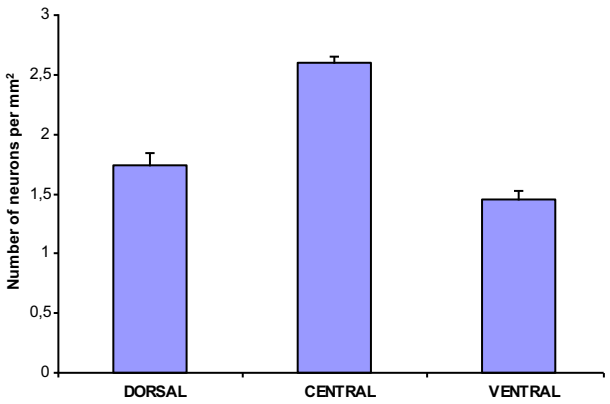

Diagram 2 | Density of NADPHd-positive claustral neurons.

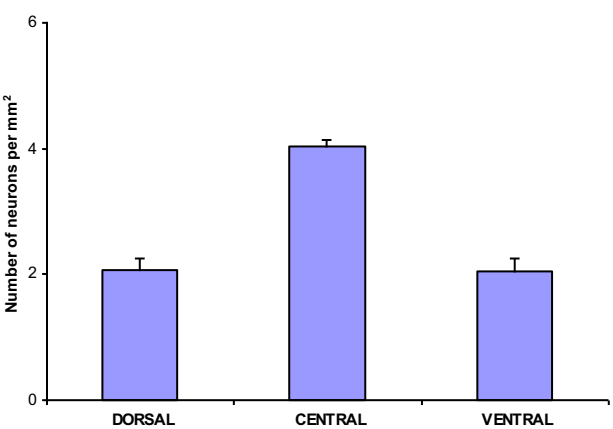

Diagram 3 | Density of large NADPHd-positive claustral neurons.

were dilated into large elongated bulbs (**Figures 9A,B**). The most distal dendritic branches could be tracked 250–400 μm from the cell body.

Small NADPHd-positive neurons

The third type of NADPHd-positive claustral neuron consists of small cells ranging from 14 to 20 μm in diameter, representing 12.5% (87/700) of all those sampled. Their shape was most often seen as either oval or elliptical, with an axon and 2–3 dendrites extending from the cell body (**Figures 9C,D**). Primary dendrites were usually thin in caliber with marked varicosities, rarely branching, and typically extending no more than 100–150 μm from the cell body, in rare instances 200–250 μm (**Figure 9C**). The axons were rarely seen as being stained. In principle, only the axon hillock and a short portion of the initial segment could be labeled.

DISCUSSION

The present study provides for the first detailed investigation of the distribution, size, characteristics, and morphology of NADPHd-positive neurons in the human claustrum. Our results confirm and extend the findings of the existence of such neurons in the human (Edelstein et al., 2012a,b), cat (Switka et al., 1994; Hinova-Palova et al., 1997), and rat (Vincent and Kimura, 1992). Generally speaking, our findings do not fully support the results of earlier investigations by Mizukawa et al. (1989) and Vincent and Kimura (1992) on the distribution of NADPHd-reactive neurons in the human claustrum. Moreover, we confirm the findings drawn by many investigators, in particular, that claustrocortical connections are distributed differently in the cortical areas (Norita, 1977; Divac, 1979; Macchi et al., 1981, 1983; Druga, 1984; Minciacchi et al., 1985; Guildin et al., 1986; Hinova-Palova, 1986; Druga et al., 1990; Dinopoulos et al., 1992). These findings have demonstrated that there is a tendency toward

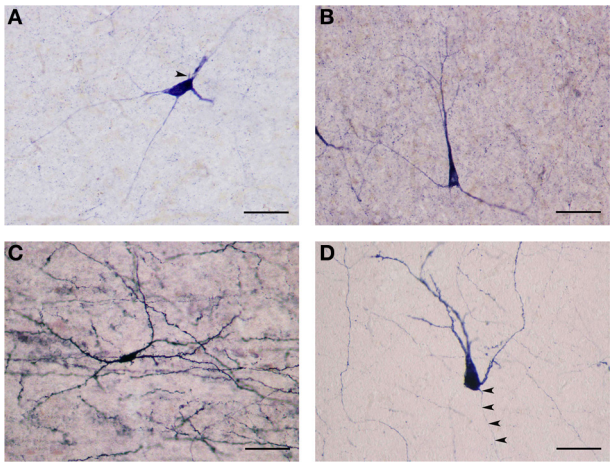

Figure 5 | (A) Large NADPHd-positive neuron with a multipolar cell body. Four dendrites are seen leaving the cell body, coursing in different directions. The axon hillock can be seen emerging from the cell body, neighboring the primary dendritic trunk (arrowhead). Scale bar = 40 μm. **(B)** Large NADPHd-positive neuron with a pyramidal cell body. Note the stain-free nucleus. Scale bar = 100 μm. **(C)** Large NADPHd-positive spiny neuron with bipolar cell body and spine-covered dendrites. Scale bar = 100 μm. **(D)** Large NADPHd-positive spiny neuron with a pear-shaped cell body. Two closely situated dendrites can be seen emerging from its apex, a third leaving its base along with a thin axon initial segment (arrowheads). Scale bar = 40 μm.

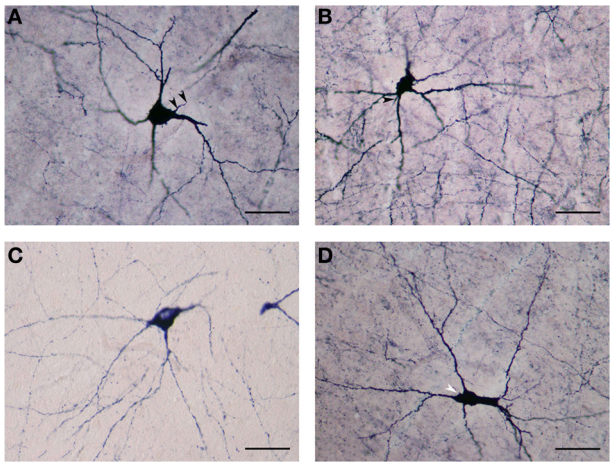

Figure 6 | (A) Large NADPHd-neuron with a pear-shaped cell body and four thick primary dendrites. The axon can be seen emerging from the base of the apical dendrite (arrowheads). Secondary and tertiary dendrites are rich with spines. Scale bar = 40 μm. **(B)** Large NADPHd-positive spiny neuron with a multipolar cell body and spine-covered dendrites. The axon is seen leaving the base of one of the dendritic trunks (arrowhead). Scale bar = 40 μm. **(C)** Large NADPHd-positive neuron with a tripolar cell body and three dendrites branching into secondary and tertiary spine-covered dendrites. Scale bar = 40 μm. **(D)** Large NADPHd-positive spiny neuron with an irregular shape and five spine-covered dendrites. The axon hillock is also visible (arrowhead). Scale bar = 40 μm.

topographic specificity, as reported by Macchi et al. (1981; 1983), and Minciacchi et al. (1985).

In comparing the observed distribution pattern of NADPHd-reactive neurons and the existence of cellular density gradients relative to their anteroposterior and dorsoventral locations, our data confirm the investigations of Druga (1984), Druga et al. (1990), Markowitsch et al. (1984), Guildin et al. (1986), Hinova-Palova et al. (1988), and Dinopoulos et al. (1992).

Based on our analysis of seven-hundred cells sampled from across the claustrum's dorsoventral and rostrocaudal continuum, we were able to categorize three types and four subtypes of NADPHd-positive neurons based on several defining characteristics, most notably, size: large (25–35 μm), medium (20–25 μm), and small (14–20 μm).

The present results confirm our previous study (Hinova-Palova, 1986), in which we had shown that the size and morphology of the large- and medium-sized NADPHd-positive cells correspond to spiny and aspiny type II and III neurons, which we viewed as projection neurons. This supposition was also confirmed by our use of HRP injections into various auditory fields in the cat and assessing retrograde labeling in the claustrum (Hinova-Palova et al., 1988). We found a heterogeneously distributed population of labeled projection neurons, demonstrating a similarly varied pattern.

There are contradictory data on the cellular composition, size and morphology of claustral efferents. According to the classification scheme of Brand (1981) there are three types of neurons in the primate claustrum, with only one type thought to be a projection neuron. Braak and Braak (1982) described five types of neurons in the human claustrum. In our previous Golgi investigation in the cat claustrum we defined four types of projection neurons (Hinova-Palova, 1986). Using the Golgi-Cox and HRP methods, Dinopoulos et al. (1992) described three subtypes of spiny projection neurons in the hedgehog claustrum on the basis of shape and the number of primary dendrites, as well as the presence of aspiny interneurons. In addition, numerous experiments have shown that claustral projection neurons are a heterogeneous neuronal population (Hinova-Palova, 1986; Neal et al., 1986; Hinova-Palova et al., 1988; Druga et al., 1990; Claska et al., 1992; Dinopoulos et al., 1992).

A significant variety of corticoclaustral and claustrocortical circuits of the claustrum is well known. Although the claustrum has also been shown to project to various subcortical nuclei, most notably the neostriatum, zona incerta, and sensory thalamic nuclei (Druga, 1972; Sloniewski et al., 1985; Carey and Neal, 1986; Hinova-Palova, 1986), defining the characteristics of those cells which target the cortex vs. subcortical efferents remains to be determined. The somatodendritic morphology of the labeled large and medium spiny neurons we have defined in this study leads to our belief that they are projection neurons.

It is our contention that NO plays an integral role in the function and regulation of claustrocortical connections. NO is colocalized with classical neurotransmitters and neuropeptides. In this regard, somatostatin and neuropeptide Y were observed in the striatum and cerebral cortex (Vincent et al., 1983; Bredt et al., 1990; Dawson et al., 1991), in the cat claustrum (Hinova-Palova and Christova, 1988a,b) and in the human claustrum (Hinova-Palova and Braak, 1993). Edelstein et al. (2010) reported

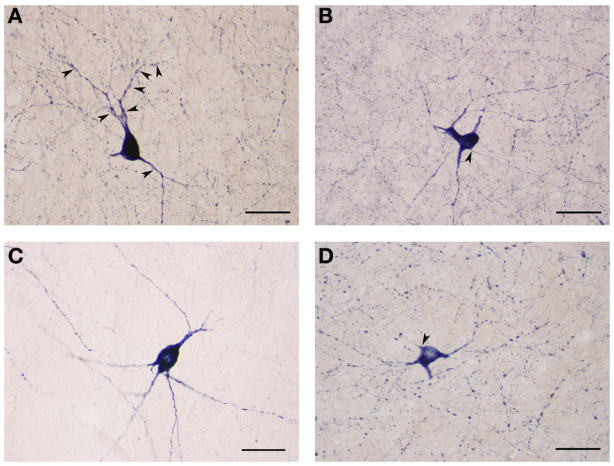

Figure 7 | (A) Large NADPHd-positive aspiny neuron with a pear-shaped cell body and varicose dendrites (arrowheads). Scale bar = 40 μm. **(B)** Large NADPHd-positive neuron with an irregular cell body and aspiny dendrites. The axon is seen leaving the cell body (arrowhead). Scale bar = 40 μm. **(C)** Large NADPHd-positive aspiny neuron with varicose dendrites. Scale bar = 40 μm. **(D)** Large NADPHd-positive aspiny neuron with varicose dendrites. The axon arises from the cell body with a clearly visible hillock (arrowhead). Scale bar = 40 μm.

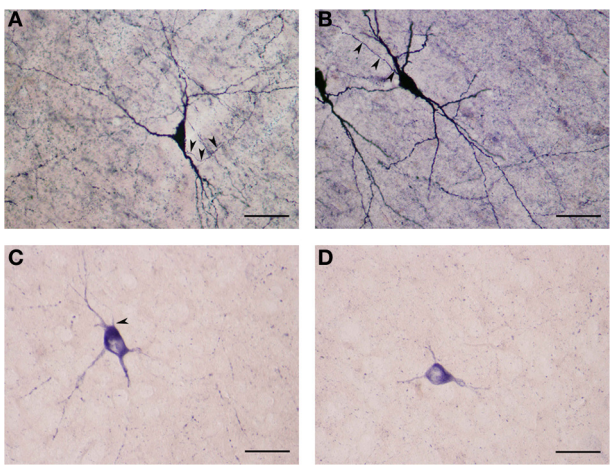

Figure 8 | (A) Medium NADPHd-positive spiny neuron with a tripolar cell body and three clearly visible spine-covered dendrites. The axon is seen arising from the initial segment of the dendritic trunk (arrowheads). Scale bar = 40 μm. **(B)** Medium NADPHd-positive spiny neurons with a bipolar cell bodies. The axon is seen emerging from the dendritic trunk of one cell (arrowheads). Scale bar = 40 μm. **(C)** Medium NADPHd-positive aspiny neuron with a multipolar cell body and thin dendrites. The axon is seen leaving the cell body (arrowhead). Scale bar = 30 μm. **(D)** Medium NADPHd-positive aspiny neuron with short varicose dendrites. Scale bar = 30 μm.

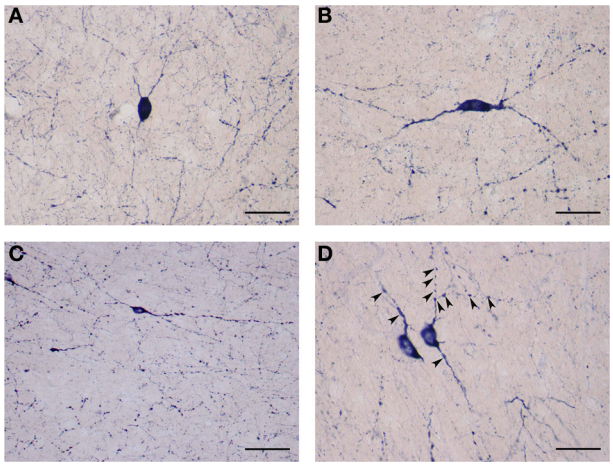

Figure 9 | (A) Medium NADPHd-positive aspiny neuron, densely stained with bulbous thin dendrites. Scale bar = 40 μm. **(B)** Medium NADPHd-positive aspiny neuron with a bipolar cell body and varicose dendrites. Scale bar = 40 μm. **(C)** Small NADPHd-positive aspiny neuron with elliptical cell body and two thin varicose dendrites. Numerous stained puncta and fibers are visible. Scale bar = 100 μm. **(D)** Small NADPHd-positive aspiny neurons with thin and varicose dendrites (arrowheads). Scale bar = 40 μm.

on neuropeptide Y-containing neurons in the cat claustrum, suggestive of an analogous colocalization. The third type of positive neuron we have seen in the present investigation is dispersed through the claustrum, morphologically resembling the small neurons seen in our earlier study of the cat claustrum (Hinova-Palova, 1986). Using the Golgi impregnation method we were able to divide the small neurons into two types: spiny and aspiny (Hinova-Palova, 1986). They were noted to have oval, round, or elliptical cell bodies with 3–5 markedly varicose dendrites. These cells closely resembled the small NADPHd-positive neurons characterized in the present study. As a result, we believe that it is accurate to state that the small NADPHd-positive neurons we have detailed in this study are morphologically if not functionally similar to the NOS-containing interneurons of the cerebral cortex as described by De Felipe (1993) and Rodrigo et al. (1994) in the rat.

Our findings of an extensive network of NADPHd-positive varicose and branching fibers in the claustrum prompt questions as to their etiology. The majority of these fibers represent dendrites and axons. Most likely, some of those fibers are snippets of afferents emanating from neurons in various topographically-linked areas (Hinova-Palova et al., 1984, 1988; Hinova-Palova, 1986; Druga et al., 1990). Indeed, a reasonable proportion of these fibers may well-arise from the neurons located in layer VI of cortex and the putamen which have traversed the external and extreme capsules.

Numerous investigations conducted over the past decade have led to a detailed understanding of the types of neurons which are capable of generating NO, and their distribution. NOS often colocalizes with classical neurotransmitters and neuropeptides (Vincent et al., 1986; Spike et al., 1993; Gabbot and Bacon, 1995; Rushlow et al., 1995; Feguerdo-Cardenas et al., 1996), and thus NO synthesis is often coupled to the release of these transmitters. In this regard, it is of interest to note that NOS is found in neurons using the excitatory neurotransmitter glutamate, as well as the inhibitory neurotransmitter GABA (Spike et al.,

1993; Gabbot and Bacon, 1995). The colocalization of NADPHd-reactive neurons and GABAergic neurons suggests that these interneurons are inhibitory. NOS is also found in cholinergic neurons and other aminergic cells. NOS is also present in the local circuit interneurons of many brain regions (Duchemin et al., 2012). However, in some areas it is found in principal neurons with lengthy projections. In addition, NOS is found in neurosecretory cells and in some circumventricular organs (Alm et al., 1997). Thus, as with other neurotransmitters, it is difficult to generalize regarding the role of NO in the nervous system. NOS is localized in cell bodies, axons, dendrites, and nerve terminals (Edelstein et al., 2012a,b). Therefore, it is reasonable to assume that NO production may be triggered by the activation of postsynaptic calcium channels and the release of intracellular calcium stores in dendrites and cell bodies, or by the opening of voltage-gated calcium channels in nerve terminals.

The clinical relevance of NADPHd is manifest in several ways with respect to neurodegenerative diseases. Extensive studies support the contention that NADPHd-positive neurons are spared from hypoxic-ischemic insults in several disorders, including Huntington's disease (Ferrante et al., 1985) and Parkinson's disease (Hunot et al., 1996). The selective sparing of NADPHd-positive neurons has been attributed to a resistance against N-methyl-D-aspartate or quinolinate toxicity (Koh et al., 1986; Koh and Choi, 1988). A distinct subset of striatal neurons—those containing NADPHd—was shown to be selectively resistant to the degenerative process that affects the striatum in Huntington's disease (Ferrante et al., 1985, 1987). Boegman and Parent (1988) injected the tryptophan metabolite quinolinic acid unilaterally into rat cerebral cortex and striatum in order to determine whether the neurotoxin would ablate neuropeptide Y-, somatostatin-, and NADPHd-containing neurons. Following intrastriatal injections of quinolinic acid, activity of all three were absent from the injection core area. In contrast, cortical neuropeptide Y-, somatostatin- and NADPHd-containing neurons proved resistant. These results suggest that, in contrast to striatal neurons, cortical somatostatin- and neuropeptide Y- containing neurons do not express NMDA receptors. Mufson and Brandabur (1994) reported that NADPHd-containing neurons within the striatum are spared in patients with Parkinson's disease and Alzheimer's disease. However, a number of these neurons in both diseases appeared shrunken or bulbous with shortened dendritic processes. Tao et al. (1999) studied the involvement of NADPHd-containing neurons in the cortex, subcortical white matter and striatum of Alzheimer's disease patients. Despite slight morphological changes in the cortex of the Alzheimer's patients, they found no significant difference in the number of NADPHd-positive neurons in either the cortex or the striatum when compared with the cortex of similarly aged controls. Their results provide further evidence for a selective preservation of NADPHd neurons in Alzheimer's disease. Freire et al. (2007) used NADPHd histochemistry to investigate the effects of mercury intoxication on the structure of the posteromedial barrel subfield in the primary somatosensory cortex of adult rats. It was found that NADPHd reactivity in the neuropil of barrel fields was drastically reduced in experimental animals, suggesting that the synthesis and transport of NOS can be altered during acute mercury intoxication. However, the cell bodies and dendrites of barrel neurons, also strongly reactive to the enzyme, were spared from mercury's deleterious effects.

This is the first detailed investigation of the light- and electron-microscopic features of the NADPHd-containing neurons and fibers in the human claustrum, a subcortical nucleus known to have reciprocal connectivity with nearly all cortical areas. It is hoped that a deeper understanding of the relationship between NADPHd and the sequelae of neurodegenerative disorders, as well as of NOS distribution and reasons for its colocalization with other neurotransmitters and neuropeptides, will help to better define the role of NO in the context of claustral function, the interplay between the claustrum and cerebral cortex, and of the nervous system proper.

REFERENCES

Alm, P., Skagerberg, G., Nylén, A., Larsson, B., and Andersson, K. E. (1997). Nitric oxide synthase and vasopressin in rat circumventricular organs. An immunohistochemical study. *Exp. Brain Res.* 117, 59–66. doi: 10.1007/s002210050199

Aoki, E., Takenchi, I. K., and Shoji, R. (1995). Nitric oxide: An attractive signalling molecule. *Acta Histochem. Cytochem.* 28, 97–106.

Artero, C., Mazzi, Y., Musucri, A., Barale, E., and Franzoni, M. F. (1995). Dihydronicotinamide adenine dinucleotide diaphorase in the central nervous system of the crested newt. *Eur. J. Histochem.* 39, 183–194.

Ashwell, K. W. S., Hardman, C., and Paxinos, G. (2004). The claustrum is not missing from all monotreme brains. *Brain Behav. Evol.* 64, 223–241. doi: 10.1159/000080243

Berke, J. J. (1960). The claustrum, the external capsule and the extreme capsule of *Macaca mulatta*. *Neurology* 115, 297–321.

Berlucchi, C. (1927). Richerche di fine anatomia sul claustrum e sull' insula dell gate [Microscopic anatomy of the claustrum and insula of the cat]. *Riv Sperim. Freniatria* 51, 125–157.

Boegman, R. J., and Parent, A. (1988). Differential sensitivity of neuropeptide Y, somatostatin and NADPH-diaphorase containing neurons in rat cortex and striatum to quinolinic acid. *Brain Res.* 445, 358–362. doi: 10.1016/0006-8993(88)91199-7

Braak, H., and Braak, E. (1982). Neuronal types in the claustrum of man. *Anat. Embryol.* 163, 447–460. doi: 10.1007/BF00305558

Brand, S. (1981). A serial section Golgi analysis of the primate claustrum. *Anat. Embyol.* 162, 475–488. doi: 10.1007/BF00301872

Bredt, D. S., and Snyder, S. H. (1990). Isolation of nitric oxide synthase, a calmodulin requiring enzyme. *Proc. Natl. Acad. Sci. U.S.A.* 87, 682–685. doi: 10.1073/pnas.87.2.682

Bredt, D. S., and Snyder, S. H. (1992). Nitric oxide, a novel neuronal messenger. *Neuron* 8, 3–11. doi: 10.1016/0896-6273(92)90104-L

Bredt, D. S., and Snyder, S. H. (1994). Transient nitric oxide synthase neurons in embryonic cerebral cortical plate, sensory ganglia and olfactory epithelium. *Neuron* 15, 301–331. doi: 10.1016/0896-6273(94)90348-4

Bredt, D. S., Glatt, C. E., Hwang, P. M., Fotuni, M., Dawson, D. M., and Snyder, S. H. (1991). Nitric oxide synthase protein and mRNA are discretely localized in neuronal populations of the mammalian CNS together with NADPH-diaphorase. *Neuron* 7, 615–124. doi: 10.1016/0896-6273(91)90374-9

Bredt, D. S., Hwang, P. M., and Snyder, S. H. (1990). Localization of nitric oxide synthase indicating a neural role for nitric oxide. *Nature* 347, 768–770. doi: 10.1038/347768a0

Brenman, J. E., Xia, H., Chao, D. S., Black, S. M., and Bredt, D. S. (1997). Regulation of neuronal nitric oxide synthase through alternative transcripts. *Dev. Neurosci.* 19, 224–231. doi: 10.1159/000111211

Brockhaus, H. (1940). Cytoarchitectural and myeloarchitectural study of claustral cortex and claustrum in man. *J. Psychol. Neurol.* 49, 249–348.

Bult, H., Boeckxtaens, G. E., Pelcumans, P. H., Jordaens, F. H., Van Maercke, J. M., and Herman, A. G. (1990). Nitric oxide as an inhibitory non-adrenergic non-cholinergic neurotransmitter. *Nature* 345, 346–347. doi: 10.1038/345346a0

Burdach, K. F. (1822). *Von Baue und Leben des Gehirns.* Leipzig: Dyk'schen Buchhandlung.

Carey, R. G., and Neal, T. L. (1986). Reciprocal connections between the claustrum and visual thalamus in the tree shrew (*Tupaia glis*). *Brain Res.* 386, 155–168. doi: 10.1016/0006-8993(86)90152-6

Claska, F., Avendano, C., Roman-Guindo, A., Llamas, A., and Reino-Suarez, F. (1992). Innervation from the claustrum of the frontal association and motor areas: axonal transport studies in the cat. *J. Comp. Neurol.* 326, 402–422.

Crick, F. C., and Koch, C. (2005). What is the function of the claustrum? *Philos. Trans. R. Soc. Lond. B Biol. Sci.* 360, 1271–1279. doi: 10.1098/rstb.2005.1661

Dawson, T. M., Bredt, D. S., Fotuhi, M., Huang, P. M., and Snyder, S. H. (1991). Nitric oxide synthase and neuronal NADPH-diaphorase are identical in brain and peripheral tissues. *Proc. Natl. Acad. Sci. U.S.A.* 88, 7797–7801. doi: 10.1073/pnas.88.17.7797

De Felipe, J. (1993). A study of NADPH-diaphorase-positive axonal plexuses in the human temporal cortex. *Brain Res.* 615, 342–346. doi: 10.1016/0006-8993(93)90047-Q

Dinopoulos, A., Papadopoulos, G. C., Michaloudi, H., Parnavelas, J. G., Uylings, H. B., and Karamanlidis, A. N. (1992). Claustrum in the Hedgehog (*Erinaceus europaeus*) brain: cytoarchitecture and connections with cortical and subcortical structures. *J. Comp. Neurol.* 1. 316, 187–205.

Divac, I. (1979). Patterns of subcorticocortical projections as revealed by somatopetal horseradish peroxidase tracing. *Neuroscience* 4, 455–461. doi: 10.1016/0306-4522(79)90123-4

Druga, R. (1966a). The claustrum of the cat (Felis domestica). *Folia Morphol. (Praha)* 14, 7–16.

Druga, R. (1966b). Cortico-claustral connections. I. Fronto-claustral connections. *Folia Morphol. (Praha)* 14, 391–399.

Druga, R. (1968). Cortico-claustral connections. II. Connections from the parietal, temporal and occipital cortex to the claustrum. *Folia Morphol. (Praha)* 16, 142–149.

Druga, R. (1971). Projection of prepyriform cortex into claustrum. *Folia Morphol. (Praha)* 19, 405–410.

Druga, R. (1972). Efferent projections from the claustrum (an experimental study using Nauta's method). *Fol. Morph. (Prague)* 20, 163–165.

Druga, R. (1974). The claustrum and the transitional neopaleocortical area of the hedgehog (Erinaceus europaeus). *Anat. Anz.* 135, 442–454.

Druga, R. (1975). *Claustrum (Struktura, Ontogenese a Spoje)*, Doctoral Dissertation, Charles University, Praha.

Druga, R. (1984). Reciprocal connections between the claustrum and the gyrus sigmoideus posterior in the rat. An experimental study using the anterograde de-generation methods and the HRP retrograde axonal transport. *Anat. Anz.* 156, 109–118.

Druga, R., Rokita, R., and Benes, V. (1990). Claustro-neocortical projections in the rhesus monkey (Projections to area 6). *J. Hirnforsch.* 31, 487–494.

Druga, R., and Syka, J. (1993). NADPH-diaphorase activity in the central auditory structures of the rat. *Neuro Report.* 4, 999–1002. doi: 10.1097/00001756-199308000-00001

Duchemin, S., Boily, M., Sadekova, N., and Girouard, H. (2012). The complex contribution of NOS interneurons in the physiology of cerebrovascular regulation. *Front. Neural Circuits*. 6:51. doi: 10.3389/fncir.2012.00051

Dun, N. J., Dun, S. L., Forstermann, U., and Tseng, L. F. (1992). Nitric oxide synthase immunireactivity in rat spinal cord. *Neurosci. Lett.* 147, 217–220. doi: 10.1016/0304-3940(92)90599-3

Edelstein, L., Denaro, F. J., Stamm, J. S., Landzhov, B., Malinova, L., Hinova-Palova, D., et al. (2011b). "Distribution of CB1 receptors in the claustrum of rats undergoing acute stress: an immunohistochemical study," in *Society for Neuroscience Annual Meeting* (Washington, DC).

Edelstein, L., Hinova-Palova, D., Denaro, F., Landzhov, B., Malinova, L., Minkov, M., et al. (2012a). "NADPH-diaphorase-positive neurons in the human claustrum," in *Society for Neuroscience Annual Meeting* (San Diego, CA).

Edelstein, L., Hinova-Palova, D., Landzhov, B., Malinova, L., Minkov, M., Paloff, A., et al. (2012b). "Neuronal nitric oxide synthase immunoreactivity in the human claustrum: light- and electron-microscopic investigation," in *Society for Neuroscience Annual Meeting* (San Diego, CA).

Edelstein, L., Hinova-Palova, D., Malinova, L., Papantchev, V., Landzhov, B., Paloff, A., et al. (2011a). "Distribution of neuropeptide Y in the dorsal claustrum of the cat. Light and electron-microscopic identification of distinct neuronal populations," in *Society for Neuroscience Annual Meeting* (Washington, DC).

Edelstein, L., Hinova-Palova, D., Paloff, A., Papantchev, V., and Ovtscharoff, W. (2010). "Leu-enkephalin immunoreactivity in the cat claustrum: a light-and electron-microscopic investigation," in *Society for Neuroscience Annual Meeting* (San Diego, CA).

Edelstein, L. R., and Denaro, F. J. (1979). The monkey claustrum: an electron-microscopic analysis. *Soc. Neurosci. Abstr.* 5:428.

Edelstein, L. R., and Denaro, F. J. (1980). The rat claustrum: a light and electron-microscopic analysis. *Soc. Neurosci. Abstr.* 6:735.

Edelstein, L. R., and Denaro, F. J. (2004). The claustrum: a historical review of its anatomy, physiology, cytochemistry and functional significance. *Cell. Mol. Biol.* 50, 675–702. doi: 10.1170/T558

Eliasson, M. J., Blackshow, S., Schell, M. J., and Snyder, S. H. (1997). Neuronal nitric oxide synthase alternatively spliced forms: prominent functional localization s in the brain. *Proc. Natl. Acad. Sci. U.S.A.* 94, 3396–3401. doi: 10.1073/pnas.94.7.3396

Feguerdo-Cardenas, G., Morello, M., Sancesario, G., Bernardi, G., and Reiner, A. (1996). Colocalization of somatostatine, neuropeptide Y, neuronal nitric oxide synthase and NADPH-diaphorase in striatal interneurons in rats. *Brain Res.* 735, 317–324. doi: 10.1016/0006-8993(96)00801-3

Ferrante, R. J., Kowall, N. W., Beal, M. F., Martin, J. B., and Bird, E. D., Richardson, E. P. Jr. (1987). Morphologic and histochemical characteristics of a spared subset of striatal neurons in Huntington's disease. *J. Neuropathol. Exp. Neurol.* 46, 12–27. doi: 10.1097/00005072-198701000-00002

Ferrante, R. J., Kowall, N. W., Beal, M. F., Richardson, E. P. Jr., Bird, E. D., and Martin, J. B. (1985). Selective sparing of a class of striatal neurons in Huntington's disease. *Science* 230, 561–563. doi: 10.1126/science.2931802

Filimonoff, I. N. (1966). The claustrum: its origin and development. *J. Hirnforsch.* 8, 503–528.

Freire, M. A., Franca, J. G., and Picanço-Diniz, C. W., Pereira, A. Jr. (2005). Neuropil reactivity, distribution and morphology of NADPH diaphorase type I neurons in the barrel cortex of the adult mouse. *J. Chem. Neuroanat.* 30, 71–81. doi: 10.1016/j.jchemneu.2005.04.006

Freire, M. A., Gomes-Leal, W., Carvalho, W. A., Guimarães, J. S., Franca, J. G., Picanço-Diniz, C. W., et al. (2004). A morphometric study of the progressive changes on NADPH diaphorase activity in the developing rat's barrel field. *Neurosci. Res.* 50, 55–66. doi: 10.1016/j.neures.2004.05.009

Freire, M. A., Oliveira, R. B., and Picanço-Diniz, C. W., Pereira, A. Jr. (2007). Differential effects of methylmercury intoxication in the rat's barrel field as evidenced by NADPH diaphorase histochemistry. *Neurotoxicology* 28, 175–181. doi: 10.1016/j.neuro.2006.06.007

Freire, M. A., Rocha, E. G., Oliveira, J. L., Guimarães, J. S., Silveira, L. C., Elston, G. N., et al. (2010). Morphological variability of NADPH diaphorase neurons across areas V1, V2, and V3 of the common agouti. *Brain Res.* 1318, 52–63. doi: 10.1016/j.brainres.2009.12.045

Gabbot, P. L., and Bacon, S. J. (1995). Co-localisation of NADPH-diaphorase activity and GABA immunoreactivity in local circuit neurons in the medial prefrontal cortex (mPFC) of the rat. *Brain Res.* 699, 321–328. doi: 10.1016/0006-8993(95)01084-9

Garthwaite, J. (1991). Glutamate, nitric oxide and Cell-cell signaling in the nervous system. *Trends Neurosci.* 14, 60–67. doi: 10.1016/0166-2236(91)90022-M

Guildin, W. O., Markowtsch, H. J., Lampe, R., and Irle, E. (1986). Cortical projections originating from the cat's insular area and remarks on claustrocortical Connections. *J. Comp. Neurol.* 243, 468–487.

Guirado, S., Real, M. A., Olmos, J. L., and Davila, J. C. (2003). Distinct types of nitric oxide-producing neurons in the developing and adult mouse claustrum. *J. Comp. Neurol.* 465, 431–444. doi: 10.1002/cne.10835

Halliwell, B. (1989). Oxidants and the central nervous system: some fundamental questions. Is oxidant damage relevant to Parkinson's disease, Alzheimer's disease, traumatic injury or stroke? *Acta Neurol. Scand. Suppl.* 126, 23–33.

Hinova-Palova, D., Christova, T., Yotovski, P. V., Logofetof, A. P., and Paloff, A. M. (2001). Somatostatin-like neurons and fibres in the cat claustrum. *Compt. Rend. Acad. Bulg. Sci.* 54, 81–84.

Hinova-Palova, D., Edelstein, L., Landzhov, B., Minkov, M., Malinova, L., Paloff, A., et al. (2012b). "Light microscopic immunocytochemical identification of Leukine Enkephaline in human claustrum," in *Jubilee Symposium "50 Years of the Department of Anatomy, Histology and Embriology* (Varna: Medical University).

Hinova-Palova, D., Edelstein, L., Landzhov, B., Minkov, M., Malinova, L., Paloff, A., et al. (2013). Light microscopic immunocytochemical identification of leucine enkephalin in human claustrum. *Scr. Sci. Med.* 45, (Suppl. 1), 23–28.

Hinova-Palova, D., Edelstein, L., Paloff, A., Hristov, S., Papantchev, V., and Ovtscharoff, W. (2007). Parvalbumin in cat claustrum: ultrastructure, distribution and functional implications. *Acta Histochem.* 109, 61–77. doi: 10.1016/j.acthis.2006.09.006

Hinova-Palova, D., Edelstein, L., Paloff, A., Hristov, S., Papantchev, V., and Ovtscharoff, W. (2008). Neuronal nitric oxide synthase immunopositive neurons in cat claustrum- a light and electron microscopic study. *J. Mol. Hist*. 39, 447–457. doi: 10.1007/s10735-008-9184-z

Hinova-Palova, D., Edelstein, L., Papantchev, V., Landzhov, B., Malinova, L., Minkov, M., et al. (2012a). Light and electron-microscopic study of leukine enkephalin immunoreactivity in the cat claustrum. *J. Mol. Histol*. 43, 641–649. doi: 10.1007/s10735-012-9448-5

Hinova-Palova, D. V. (1981). Identification of degenerated boutons in claustrum dorsale after lesion of visual cortex. *Compt. Rend. Acad. Bulg. Sci*. 34, 449–452.

Hinova-Palova, D. V. (1986). *Light Microscopic and Ultrastructural Organization of the Claustrum in the Cat. Afferent and Efferent Connections.* Ph.D Thesis, Medical Academy, Sofia.

Hinova-Palova, D. V., and Braak, E. (1993). "Somatostatin like immunoreactive neurons in the human claustrum," in *11th Congress of Anatomists, Histologists and Embryologists* (Sofia), Abstr. 29.

Hinova-Palova, D. V., and Christova, T. (1988a). "Immunohistochemical investigations of somatostatin (SRIF), vasoactive intestinal polypeptide (VIP) and glial fibrillary acidic protein (GFAP) in the claustrum of the cat," in *Third Symposium and School of Histochemistry and Cytochemistry* (Varna).

Hinova-Palova, D. V., and Christova, T. (1988b). Immunohistochemical investigation of somatostatin (SRIF), vasoactive intestinal polypeptyde (VIP) and glial fibrillary acidic protein (GFAP) in the claustrum of the cat. *Gegenbaurs Morphol. Jahrb. Leipzig.* 135, 320.

Hinova-Palova, D. V., Paloff, A., Christova, T., and Ovtscharoff, W. (1997). Topographical distribution of NADPH-diaphorase-possitive neurons in the cat's claustrum. *Eur. J. Morphol*. 35, 105–116. doi: 10.1076/ejom.35.2.0105

Hinova-Palova, D. V., Paloff, A. M., and Usunoff, K. G. (1980a). Identification of three types of degenerated boutons in claustrum dorsale in cat after lesion of the auditory cortex. *Compt. Rend. Acad. Bulg. Sci*. 33, 129–132.

Hinova-Palova, D. V., Paloff, A., and Penev, D. I. (1979). Synaptic organization of the claustrum in the cat. *Comp. Rend. Acad. Bulg. Sci*. 32, 831–834.

Hinova-Palova, D. V., Paloff, A. M., and Usunoff, K. G. (1980b). Identification of three types of degenerated boutons in claustrum dorsale in cat after lesion of the frontal cortex. *Compt. Rend. Acad. Bulg. Sci*. 33, 683–686.

Hinova-Palova, D. V., Paloff, A. M., and Usunoff, K. G. (1984). "Electron microscopic identification of thalamioclaustral axon terminals in the cat," in *2nd Symposium of Peripheral and Central Synapses* (Varna).

Hinova-Palova, D. V., Paloff, A. M., Usunoff, K. G., Dimova, R., Yossifov, T., and Ivanov, D. (1988). Reciprocal connections between the claustrum and the auditory cortical fields in the cat. An experimental study using light- and electron microscopic anterograde degeneration methods, and the horseradish peroxidase retrograde axonal transport. *J. Hirnforsch*. 29, 255–278.

Hinova-Palova, D. V., and Usunoff, K. (1981). Electron microscopic evidence for the existence of nigroclaustral projection in the cat. *Compt. Rend. Acad. Bulg. Sci*. 34, 729–732.

Holstein, G. R., Friedrich, V. L., and Martinelli, G. P. (2001). Monoclonal L-citrulline immunostaining reveals nitric oxide-producing vestibular neurons. *Ann. N.Y. Acad. Sci.* 942, 65–78. doi: 10.1111/j.1749-6632.2001.tb03736.x

Hope, B. T., Michael, G. J., Knigge, K. M., and Vincent, S. R. (1991). NADPH-diaphorase is a nitric oxide synthase. *Proc. Natl. Acad. Sci. U.S.A.* 88, 2811–2814. doi: 10.1073/pnas.88.7.2811

Huang, P. L., Dawson, T. M., Bredt, D. S., Snyder, S. H., and Fishman, M. C. (1993). Targeted disruption of the neuronal nitric oxide synthase gene. *Cell* 75, 1273–1286. doi: 10.1016/0092-8674(93)90615-W

Hunot, S., Boissière, F., Faucheux, B., Brugg, B., Mouatt-Prigent, A., Agid, Y., et al. (1996). Nitric oxide synthase and neuronal vulnerability in Parkinson's disease. *Neuroscience*. 72, 355–363. doi: 10.1016/0306-4522(95)00578-1

Koh, J. Y., and Choi, D. W. (1988). Vulnerability of cultured cortical neurons to damage by excitotoxins: differential susceptibility of neurons containing NADPH-diaphorase. *J. Neurosci.* 8, 2153–2163.

Koh, J. Y., Peters, S., and Choi, D. W. (1986). Neurons containing NADPH-diaphorase are selectively resistant to quinolinate toxicity. *Science* 234, 73–76. doi: 10.1126/science.2875522

Kowianski, P., Morys, J. M., Wojcik, S., Dziewiatkowski, J., and Luczynska, A., Spodnik, E. et al. (2004). Neuropeptide-containing neurons in the endopiriform region of the rat: morphology and colocalization with calcium-binding proteins and nitric oxide synthase. *Brain Res.* 996, 97–110. doi: 10.1016/j.brainres.2003.10.020

Kunzle, H. (1978). An autoradiographic analysis of the efferent connections from the premotor and adjacent prefrontal regions (area 6 and 9) in Macaca fascicularis. *Brain Behav. Evol.* 15, 185–234.

Lorrian, D. C., and Hull, E. M. (1993). Nitric oxide increases dopamine and serotonin re1ease in the medial preoptic area. *Neuroreport* 5, 87–89. doi: 10.1097/00001756-199310000-00024

Lysakowski, A., and Singer, M. (2000). Nitric oxide synthase localized in a subpopulation of vestibular efferents with NADPH diaphorase histochemistry and nitric oxide synthase immunohistochemistry. *J. Comp. Neurol.* 427, 508–521. doi: 10.1002/1096-9861(20001127)427:4<508::AID-CNE2>3.0.CO;2-L

Macchi, G. (1948). Morphology and structure of human claustrum. *Cervello* 24, 1–26.

Macchi, G., Bentivogli, M., Minciacchi, D., and Molinari, M. (1981). The organization of the claustroneocortical projections in the cat studied by means of the HRP retrograde axonal transport. *J. Comp. Neurol.* 195, 681–695.

Macchi, G., Bentivoglio, M., Minciacchi, D., and Molinari, M. (1983). Claustroneocortical projections studuied in the cat by means of multiple retrograde fiuorescent tracing. *J. Comp. Neurol.* 215, 121–134.

Markowitsch, H. J., Irle, E., Bang-Olsen, R., and Flindt-Egebak, P. (1984). Claustral efferents to the cat's limbic cortex studied with retrograde and anterograde tracing techniques. *Neuroscience* 12, 409–425. doi: 10.1016/0306-4522(84)90062-9

Martinelli, G., Fridrich, V., and Holstein, G. (2002). L-citrulline immunostaining identifies nitric oxide production sites within neurons. *Neuroscience* 114, 111–122. doi: 10.1016/S0306-4522(02)00238-5

Matsumoto, T., Nakane, M., Pollock, J. S., Kuk, J. E., and Forstermann, U. (1993). A correlation between soluble brain nitric oxide synthase and NADPH-diaphorase activity is only seen after exposure of the tissue to fixative. *Neurosci. Lett.* 155, 61–64. doi: 10.1016/0304-3940(93)90673-9

Minciacchi, D., Molinai, M., Bentivoglio, M., and Macchi, G. (1985). The organization of the ipsi- and contralateral claustrocortical system in rat with notes on the bilateral claustrocortical projections in cat. *Neuroscience* 16, 557–576. doi: 10.1016/0306-4522(85)90192-7

Mizukawa, K. (1990). Reduced nicotinamide-adenine-dinucleotide-phosphate-diaphorase histochemistry: light and electron microscopic investigations. *Meth. Neurosci.* 3, 457–472 doi: 10.1016/B978-0-12-185255-9.50031-6

Mizukawa, K., Vincent, S. R., McGreer, P. L., and McGreer, E. G. (1989). Distribution of reduced- nicotinamide- adenine- dinucleotide-phosphate-diaphorase positive cells and fibers in the cat central nervous system. *J. Comp. Neurol.* 279, 281–311. doi: 10.1002/cne.902790210

Moreno-Lopez, B., Estrada, C., and Escuero, M. (1998). Mechanisms of action and targets of nitric oxide in the oculomotor system. *J. Neurosci.* 18, 10672–10679.

Morys, J., Berdel, B., Maciejewska, B., Sadowski, M., Sidorowicz, M., Kowianska, J., et al. (1996). Division of the human claustrum according to its architectonics, morpho- metric parameters and cortical connections. *Folia. Morphol.* 55, 69–82.

Mufson, E. J., and Brandabur, M. M. (1994). Sparing of NADPH-diaphorase striatal neurons in Parkinson's and Alzheimer's diseases. *Neuroreport* 5, 705–708. doi: 10.1097/00001756-199402000-00011

Namavar, M. R., Sadeghi, Y., and Haghir, H. (2005). A new division of the human claustrum basis on the anatomical landmarks and morphological findings. *J. Iran. Anat. Sci.* 3, 57–66.

Narkiewicz, O. (1964). Degeneration in the claustrum after regional neocortical ablations in the cat. *J. Comp. Neurol.* 123, 335–336. doi: 10.1002/cne.901230304

Narkiewicz, O. (1972). Frontoclaustral interrelations in cats and dogs. *Acta Neurobiol. Exp.* 32, 141–150.

Nathan, C. P. (1992). Nitric oxide as a secretory product of mammalian cells. *FASEB J.* 6, 3051–3064.

Nathan, C. P., and Nibs, J. B. (1991). Role of nitric oxide synthasis in macrophage antimicrobial activity. *Curr. Opin. Immunol.* 3, 65–70. doi: 10.1016/0952-7915(91)90079-G

Neal, J. W., Pearson, R. C., and Powell, T. P. (1986). The relationship between the auditory cortex and the claustrum in the cat. *Brain Res.* 366, 145–151. doi: 10.1016/0006-8993(86)91289-8

Norita, A. M. (1977). Demonstration of bilateral claustrocortical connections in the cat with the method of retrograde axonal transport of horseradish peroxidase. *Arch. Histol. Jpn.* 40, 1–10. doi: 10.1679/aohc1950.40.1

Olsen, C. R., and Graybiel, A. M. (1980). Sensory maps in the claustrum of the cat. *Nature* 288, 479–481. doi: 10.1038/288479a0

Palmer, R. M., Ferrige, A. G., and Moncada, S. (1987). Nitric oxide release accounts for the biological activity of endothelium derived relaxing factor. *Nature* 327, 524–527. doi: 10.1038/327524a0

Paloff, A. M., Christova, T., Hinova-Palova, D., and Ovtscharoff, W. (1994). "Topographical distribution of NOS. Investigation with NADPH-diaphorase reaction in the cat's brain," in *National Conference of Anatomy, Histology and Embryology* (Stara Zagora), Abstr. 33.

Paloff, A. M., and Hinova-Palova, D. (1998). Topographical distribution of NADPH-diaphorase-positive neurons in the cat's inferior colliculus. *J. Brain Res.* 39, 231–243.

Papantchev, V., Paloff, A., Christova, T., Hinova-Palova, D., and Ovtscharoff, W. (2005). Light microscopical study of nitric oxide synthase I-positive neurons, including fibres in the vestibular nuclear complex of the cat. *Acta Histochem.* 107, 113–120. doi: 10.1016/j.acthis.2005.01.004

Papantchev, V., Paloff, A., Hinova-Palova, D., Hristov, S., Todorova, D., and Ovtscharoff, W. (2006). Neuronal nitric oxide synthase immunipositive neurons in the cat vestibular nuclear complex: a light and electron microscopic study. *J. Mol. Histol.* 37, 343–352. doi: 10.1007/s10735-006-9061-6

Paxinos, G., and Watson, C. (1998). *The Rat Brain in Stereotaxic Coordinates, 3rd Edn*. San Diego, CA: Academic Press.

Rae, A. S. L. (1954). The connections of the claustrum. *Confin. Neurol.* 14, 211–219. doi: 10.1159/000105714

Real, M. A., Davila, J. C., and Guirado, S. (2003). Expression of calcium- binding proteins in the mouse claustrum. *J. Chem. Neuroanat.* 25, 151–160. doi: 10.1016/S0891-0618(02)00104-7

Riche, D., and Lanoir, J. (1978). Some claustrocortical connections in the cat and baboon as studied by retrograde HRP transport. *J. Comp. Neurol.* 177, 435–444. doi: 10.1002/cne.901770306

Rodrigo, J., Springall, D. R., Uttenthal, O., Bentura, M. L., Abadia-Molina, F., Riveros-Moreno, V., et al. (1994). Localization of nitric oxide synthase in the adult rat brain. *Philos. Trans. R. Soc. Lond. B Biol. Sci.* 345, 175–221. doi: 10.1098/rstb.1994.0096

Romero, J. C., Lahera, V., Salom, M. G., and Biondi, M. L. (1992). Role of the endothelium-dependent relaxing factor nitric oxide on renal function. *J. Am. Soc. Neurol.* 2, 1371–1387.

Rushlow, F., Flumerfelt, B. A., and Naus, C. C. (1995). Colocalization of somatostatin, neuropeptide Y, and NADPH-diaphorase in the caudate-putamen of the rat. *J. Comp. Neurol.* 351, 499–508. doi: 10.1002/cne.903510403

Saxon, D. W., and Beitz, A. J. (2000). "Neuropeptides associated with the vestibular nuclei. In: Neurichemistry of the Vestibular System," in *Neurochemistry of the Vestibular System*, eds A. J. Beitz and J. H. Anderson (Boca Raton, FL: CRC Press), 183–196.

Schuman, E. M., and Madison, D. V. (1991). A requirement for the intercellular messenger nitric oxide in long- term potentiation. *Science* 254, 1503–1506. doi: 10.1126/science.1720572

Sherk, H. (2014). "The physiology of the claustrum," in *The Claustrum: Structural, Functional and Clinical Neuroscience. Chapter 5*, eds J. R. Smythies, L. R. Edelstein, and V. S. Ramachandran (Oxford: Elsevier), 177–191. doi: 10.1016/B978-0-12-404566-8.00005-2

Sibuki, K., and Okada, D. (1991). Endogenous nitric oxide release required for long-term synaptic depression in the cerebellum. *Nature* 349, 326–328. doi: 10.1038/349326a0

Sloniewski, P., Usunoff, K. G., and Pilgrim, C. (1986a). Diencephalic and mesencephalic afferents of the rat claustrum. *Anat. Embryol.* 173, 401–411. doi: 10.1007/BF00318925

Sloniewski, P., Usunoff, K. G., and Pilgrim, C. (1986b). Retrograde transport of fluorescent tracers reveals extensive ipsi- and contralateral claustrocortical connections in the rat. *J. Comp. Neurol.* 246, 467–477. doi: 10.1002/cne.902460405

Sloniewski, P., Usunoff, K. G., and Pilgrim, C. H. (1985). Efferent connections of the claustrum to the posterior thalamic and pretectal region in the rat. *Neurosci. Lett.* 60, 195–199. doi: 10.1016/0304-3940(85)90243-5

Smythies, J., Edelstein, L., and Ramachandran, V. (2014a). Hypotheses relating to the function of the claustrum II: instructional oscillations and dendritic integration. *Front. Integr. Neurosci.* 8:7. doi: 10.3389/fnint.2014.00007

Smythies, J., Edelstein, L., and Ramachandran, V. S. (2012). Hypotheses relating to the function of the claustrum. *Front. Integr. Neurosci.* 6:53. doi: 10.3389/fnint.2012.00053

Smythies, J. R., Edelstein, L. R., and Ramachandran. V. S. (eds.). (2014b). *The Claustrum: Structural, Functional and Clinical Neuroscience*. Oxford: Elsevier.

Spike, R. C., Todd, A. J., and Johnston, H. M. (1993). Coexistence of NADPH-diaphorase with GABA, glycine and acetylcholine in rat spinal cord. *J. Comp. Neurol.* 335, 320–333. doi: 10.1002/cne.903350303

Springall, D. R., Riveros-Moreno, V., Buttery, L., Suburo, A., Bishop, A. E., Merrett, M., et al. (1992). Immunological detection of nitric oxide synthase(s) in human tissues using heterologous antibodies suggesting different isoforms. *Histochemistry* 98, 259–266. doi: 10.1007/BF00271040

Switka, A., Schenermann, D. W., Adriaensen, D., Timmermans, J. P., and Narkiewicz, O. (1994). "NADPH diaphorase enzyme activity, serotonin and tyrosine hydroxylase immunocytochemistry in the claustrum of the domestic cat," in *Verhandlungen der Anatomischen Gosellschaft*, ed W. Kühnel (Stuttgart: Gustav Fischer Verlag Jena), 182.

Tanne-Gariepy, J., Boussaoud, D., and Rouiller, E. M. (2002). Projections of the claustrum to the primary motor, premotor, and prefrontal cortices in the macaque monkey. *J. Comp. Neurol.* 454, 140–157. doi: 10.1002/cne.10425

Tao, Z., Van Gool, D., Lammens, M., and Dom, R. (1999). NADPH-diaphorase-containing neurons in cortex, subcortical white matter and neostriatum are selectively spared in Alzheimer's disease. *Dement. Geriatr. Cogn. Disord.* 10, 460–468. doi: 10.1159/000017190

Terenghi, G., Riveros-Moreno, V., Hudson, L. D., Ibrahim, N. B., and Polak, J. M. (1993). Immunohistochemistry of nitric oxide synthase demonstrates immunoreactive neurons in spinal cord and dorsal root ganglia of man and rat. *J. Neurol. Sci.* 118, 34–37. doi: 10.1016/0022-510X(93)90242-Q

Valtschanoff, J. G., Weiberg, R. J., Kharazia, V. N., Schmidt, H. H., Nakane, M., and Rustioni, A. (1993). Neurons in cerebral cortex that synthesize nitric oxide: NADPH diaphorase histochemistry, NOS immunocytochemistry and colocalization with GABA. *Neurosci. Lett.* 157, 157–161. doi: 10.1016/0304-3940(93)90726-2

Vicq d'Azyr, F. (1786). *Traité d'Anatomie et de Physiologie avec des Planches Coloriées Représentant au Naturel les Divers Organes de l'Homme et des Animaux*. Vol. II, plates X, XI, XXII and XXVI. Paris: François Didot l'aîné.

Vincent, S. R. (2000). "Histochemistry of nitric oxide synthase in the central nervous system," in *Functional Neuroanatomy of the Nitric Oxide System*, eds H. W. M. Steinbush, J. De Vente, and S. R. Vincent, (Amsterdam: Elsevier), 19–49. doi: 10.1016/S0924-8196(00)80056-1

Vincent, S. R., and Hope, B. T. (1992). Neurons that say NO. *Trends Neurosci.* 15, 108–113. doi: 10.1016/0166-2236(92)90021-Y

Vincent, S. R., Johansson, O., Hokfelt, T., Skirboll, L., Elde, R. P., Terenius, L., et al. (1983). NADPH-diaphorase: a selective histochemical marker for striatal neurons containing both somatostatin and avian pancreatic polypeptide (APP)- like immunoreactivities. *J. Comp. Nenrol.* 217, 252–263.

Vincent, S. R., and Kimura, H. (1992). Histochemical mapping of nitric oxide synthase in the rat brain. *Neuroscience* 46, 755–784. doi: 10.1016/0306-4522(92)90184-4

Vincent, S. R., Satoh, K., Armstrong, D. M., Paula, P., Vale, W., and Fibiger, H. S. (1986). Neuropeptides and NADPH-diaphorase activity in the ascending cholinergic reticulum system of the rat. *Neuroscience* 17, 167–182. doi: 10.1016/0306-4522(86)90234-4

Witter, M. P., Room, P., Groenewegen, H. J., and Lohman, A. H. (1988). Reciprocal connections of the insular and piriform claustrum with limbic cortex: an anatomical study in the cat. *Neuroscience* 24, 519–539. doi: 10.1016/0306-4522(88)90347-8

Yan, X. X., Jen, L. S., and Garey, L. J. (1996). NADPH-diaphorase-positive neurons in primate cerebral cortex colocalize with GABA and calcium-binding proteins. *Cereb. Cortex* 6, 524–529. doi: 10.1093/cercor/6.3.524

Zhuo, M., Small, S. A., Kandel, E. R., and Hawkins, R. D. (1993). Nitric oxide and carbon monoxide produce activity-dependent long-term synaptic enhancement in hippocampus. *Science* 260, 1946–1950. doi: 10.1126/science.8100368

Zilles, K., Zilles, B., and Schleicher, A. (1980). A quantitative approach to cytoarchitectonics. VI. The areal pattern of the cortex of the albino rat. *Anat. Embryol.* 159, 335–360. doi: 10.1007/BF00317655

Conflict of Interest Statement: The authors declare that the research was conducted in the absence of any commercial or financial relationships that could be construed as a potential conflict of interest.

Received: 29 January 2014; accepted: 06 May 2014; published online: 27 May 2014.
Citation: Hinova-Palova DV, Edelstein L, Landzhov B, Minkov M, Malinova L, Hristov S, Denaro FJ, Alexandrov A, Kiriakova T, Brainova I, Paloff A and Ovtscharoff W (2014) Topographical distribution and morphology of NADPH-diaphorase-stained neurons in the human claustrum. Front. Syst. Neurosci. ***8****:96. doi: 10.3389/fnsys.2014.00096*
This article was submitted to the journal Frontiers in Systems Neuroscience.

frontiers in
SYSTEMS NEUROSCIENCE

ORIGINAL RESEARCH ARTICLE
published: 26 May 2014
doi: 10.3389/fnsys.2014.00099

Expression of calcium-binding proteins and selected neuropeptides in the human, chimpanzee, and crab-eating macaque claustrum

Andrea Pirone[1], Maura Castagna[2], Alberto Granato[3], Antonella Peruffo[4], Francesca Quilici[2], Laura Cavicchioli[4], Ilaria Piano[5], Carla Lenzi[1] and Bruno Cozzi[4]*

[1] Department of Veterinary Sciences, University of Pisa, Pisa, Italy
[2] Department of Translational Resource on New Technologies in Medicine and Surgery, University of Pisa, Pisa, Italy
[3] Department of Psychology, Catholic University, Milan, Italy
[4] Department of Comparative Biomedicine and Food Science, University of Padova, Padova, Italy
[5] Department of Pharmacy, University of Pisa, Pisa, Italy

Edited by:
Brian N. Mathur, University of Maryland School of Medicine, USA

Reviewed by:
Ariel Y. Deutch, Vanderbilt University Medical Center, USA
Michael Bubser, Vanderbilt University Medical Center, USA

Correspondence:
Bruno Cozzi, Department of Comparative Biomedicine and Food Science, University of Padova, Viale dell'Università 16, 35020 Legnaro (PD), Padova, Italy
e-mail: bruno.cozzi@unipd.it

The claustrum is present in all mammalian species examined so far and its morphology, chemoarchitecture, physiology, phylogenesis and ontogenesis are still a matter of debate. Several morphologically distinct types of immunostained cells were described in different mammalian species. To date, a comparative study on the neurochemical organization of the human and non-human primates claustrum has not been fully described yet, partially due to technical reasons linked to the postmortem sampling interval. The present study analyze the localization and morphology of neurons expressing parvalbumin (PV), calretinin (CR), NPY, and somatostatin (SOM) in the claustrum of man (# 5), chimpanzee (# 1) and crab-eating monkey (# 3). Immunoreactivity for the used markers was observed in neuronal cell bodies and processes distributed throughout the anterior-posterior extent of human, chimpanzee and macaque claustrum. Both CR- and PV-immunoreactive (ir) neurons were mostly localized in the central and ventral region of the claustrum of the three species while SOM- and NPY-ir neurons seemed to be equally distributed throughout the ventral-dorsal extent. In the chimpanzee claustrum SOM-ir elements were not observed. No co-localization of PV with CR was found, thus suggesting the existence of two non-overlapping populations of PV and CR-ir interneurons. The expression of most proteins (CR, PV, NPY), was similar in all species. The only exception was the absence of SOM-ir elements in the claustrum of the chimpanzee, likely due to species specific variability. Our data suggest a possible common structural organization shared with the adjacent insular region, a further element that emphasizes a possible common ontogeny of the claustrum and the neocortex.

Keywords: claustrum, calretinin, parvalbumin, somatostatin, NPY, human, chimpanzee, monkey

INTRODUCTION

The word claustrum comes from the Latin term that indicates a hidden place, here referred to the position of the structure that is placed between the inner surface of the insular cortex and the outer surface of the putamen. The claustrum is a symmetrical, thin, and irregular sheet of gray matter present in all mammalian species examined so far, including man (Kowianski et al., 1999). Its phylogenesis and ontogenesis are still a matter of debate (Edelstein and Denaro, 2004; Pirone et al., 2012). Projections to the primary somatosensory cortex have been demonstrated in the monkey claustrum (Minciacchi et al., 1991) and reciprocal diffuse connections with the cortex have been shown in several species (Carman et al., 1964; LeVay and Sherk, 1981; Carey and Neal, 1985; Dinopoulos et al., 1992). However the existence of functional subunits of the claustrum, based on topography of cortical projections or segregation of neural cell types, remains uncertain.

Calbindin-28 KD (CB), parvalbumin (PV), and calretinin (CR) belong to the EF-hand family of the calcium binding proteins (CBPs; Baimbridge et al., 1992). The CBPs are involved in many cellular physiological processes mediated by Ca^{2+} (Miller, 1991) and these neural markers are widely expressed also in the brain of vertebrates (Jande et al., 1981; Parmentier et al., 1987; Baimbridge et al., 1992; Andressen et al., 1993; Crespo et al., 1999; Dávila et al., 2000; Díaz-Regueira and Anadón, 2000; Milán and Puelles, 2000; Castro et al., 2003; Morona and González, 2008). The immunohistochemical distribution of the CBPs is an excellent tool to highlight the relationship between function and structure most notably in the thalamus (Jones and Hendry, 1989; Rausell and Jones, 1991; Rausell et al., 1992; Cusick et al., 1993)

and in the brainstem (Parvizi and Damasio, 2003). A series of recent studies focused on the expression of CBPs in the claustrum of different species (Kowianski et al., 1999; Real et al., 2003; Wojcik et al., 2004; Rahman and Baizer, 2007). In particular, in the monkey claustrum, immunoreactivity to the CBPs revealed no functional segregation or structural heterogeneity (Reynhout and Baizer, 1999). Reactivity to PV has been reported in a recent detailed study in the human claustrum (Hinova-Palova et al., 2013).

CBPs and neuropeptides have been used as markers that distinguish among types of cortical interneurons (DeFelipe et al., 1989; Hendry et al., 1989; Rogers, 1989; DeFelipe, 1993, 1997; Cauli et al., 1997; Gonchar and Burkhalter, 1997; Somogyi and Klausberger, 2005; Ascoli et al., 2008). Moreover, it has been demonstrated that inhibitory neurons expressing CBPs contain also neuropeptides such as: somatostatin (SOM), vasoactive intestinal peptide (VIP), cholecystokinin (CCK), and neuropeptide Y (NPY; Xu et al., 2006).

The topography of immunoreactive interneurons is relevant for a better understanding of the chemoarchitecture of the claustrum and its functional role. Little is known about the function of the claustrum and specific systematic studies are sparse. For these reasons, the aim of the present study is to characterize the distribution of CBPs in neural cells of the human, chimpanzee and crab-eating monkey claustrum, and compare them with the distribution of NPY and SOM in the same species.

MATERIALS AND METHODS

TISSUE SAMPLES

In this study we used archival samples obtained from five patients of different sex and age, with no history of psychiatric or neurological disorder. The average age was 59.6 years and the average post-mortem delay was 26 h. The samples consisted of blocks approx. 5 cm thick, including the claustrum, surrounded by portions of the adjoining structures (extreme and external capsules, insular cortex, putamen). The samples were carefully dissected during post-mortem procedures performed by qualified pathologists at the S. Chiara Hospital, University of Pisa. The brain samples were removed within routine diagnostic scopes, following a procedure approved by the Ethic Committee of the University of Pisa (protocol number 3482). The blocks were fixed by immersion in buffered formalin, washed in phosphate saline buffer (PBS) 0.1 M, pH 7.4 and processed for paraffin embedding. Reference sections were stained either with Nissl or Luxol Fast Blue stains.

We also considered samples of primate brains. To this effect we examined the claustrum of an adult male chimpanzee (*Pan troglodytes*, Blumenbach, 1775) living in a zoological park, whose body was forwarded to the Department of Comparative Biomedicine and Food Science of the University of Padova for post-mortem diagnosis. The time interval between death and removal of the brain cannot be determined precisely, as the animal was found dead by the wardens on the morning round. The cause of death was not neurological. Samples from the chimpanzee brain were treated with the same protocol used for the human samples. The monkey claustrum was sampled from the brains of the three crab-eating macaques (*Macaca fascicularis*, Raffles, 1821) stored in the archives of the same Department. The brains were initially perfused with buffered formalin and removed from animals formerly employed for a translational transplant research authorized by the University Ethical Committee. Use of archival samples is encouraged based on the EU Directive 2010/63/ of 22 September 2010 on the protection of animals used for scientific purposes (Introduction section).[1] After repeated washings in PBS, perfusion-fixed samples from the crab-eating monkey brains were processed for paraffin embedding. Archival brain samples of the rat cortex stored at the Department of Veterinary Sciences of the University of Pisa were used as a positive control for CBPs immunostaining (see below).

IMMUNOHISTOCHEMISTRY

A rabbit polyclonal anti- CR antibody (H-45: sc-50453; Santa Cruz Biotech., Inc., Santa Cruz, CA; dilution 1:200), a mouse monoclonal anti-PV antibody (Clone PA-235, Cat. # P-3171, Sigma-Aldrich, St. Louis, MO, USA; dilution 1:3000), a mouse monoclonal anti-CB-D-28K antibody (Clone CB-955, Cat. # C9848, Sigma-Aldrich, St. Louis, MO, USA; dilution 1:3000) a rabbit polyclonal anti NPY antibody (ab30914, Abcam; dilution 1:3000), and a rabbit polyclonal anti-SOM antibody (ab103790, Abcam; dilution 1:700) were used in this study. Epitope retrieval was carried out at 120°C in a pressure cooker for 5 min using a Tris/EDTA buffer pH 9.0. Sections were rinsed in PBS and incubated in 1% H_2O_2-PBS for 10 min, then pre-incubated in PBS with 0.3% Triton X-100 (TX) (Sigma-Aldrich, St. Louis, MO, USA) and 5% normal goat serum (Vector Labs, Burlingame, CA) to reduce non-specific staining. Next, sections were incubated overnight in a humid chamber at 4°C with the primary antibody diluted in PBS with 0.3% TX and 1% normal goat serum. After several washings in PBS, sections were incubated for 1 h at room temperature in biotinylated goat anti-rabbit immunoglobulins (for CR, NPY and SOM) and biotinylated goat anti-mouse immunoglobulins (for PV and CB) (Vector Labs, Burlingame, CA), diluted 1:300 in PBS. Sections were then washed for 3 × 10 min in PBS, and incubated for 1 h at room temperature in avidin-biotin-horseradish peroxidase complex (ABC; Vector Labs, Burlingame, CA), diluted 1:125 in PBS. After washing for 3 × 10 min in Tris/HCl (pH 7.6), peroxidase activity was detected by incubation in a solution of 0.125 mg/ml diaminobenzidine (Sigma-Aldrich, St. Louis, MO, USA) and 0.1% H_2O_2 in the same buffer for 10 min.

CBPs PROTEIN SEQUENCES IN THE THREE SPECIES

The amino-acid composition of CR is highly preserved in mammals. The antibody that we used recognizes human epitope aa 123–167, with a minimal correspondence score of 99.43% considering clusta1W2,[2] or >98%[3] if considering *Macaca mulatta* instead of *Macaca fascicularis*. The PV amino-acid sequence is also maintained with a minimum of 97.27% correspondence between the species that we examined.[3] The antibody that we used was a

[1] "Member States should, where appropriate, facilitate the establishment of programmes for sharing the organs and tissue of animals that are killed".
[2] www.ebi.ac.uk
[3] www.ensembl.org

monoclonal raised against the segments of the protein sequence conserved in man and macaque and was extensively validated in man, monkey and rodents (for reference see Saleem et al., 2007). Conservation of the CB amino-acid sequence between the three primates is >98.85[3] and >98.47% with the sequence of the bovine kidney used to produce the antibody.

The specificity of the immunohistochemical staining was field tested in repeated trials as follows: substitution of either the antibody, the anti-rabbit IgG, or the ABC complex by PBS or non-immune serum. Under these conditions staining was abolished.

Moreover, cryostat sections (15–20 μm) of a rat brain perfused with 4% paraformaldehyde were employed as positive control.

PROCEDURE FOR PV AND CR-ir NEURONS COUNT

Three evenly spaced 3 μm thick coronal sections were cut through the claustral region (and including also parts of the insular cortex) of each brain and mounted on positively charged slides. In each section the whole area of the claustrum was analyzed at 10x. In all the microscope fields captured with 10x objective the number of positive cells was counted employing also a 25x objective to better detect positive neurons. To compare immunoreactive neuronal subpopulations containing PV and CR, the neuronal density as the number of cells per square millimeter was estimated. Additional coronal sections were also stained with Cresyl violet and Luxol Fast Blue for comparison. All photos were taken with a light microscope (Leitz Diaplan, Wetzlar, Germany) connected to a PC via a Nikon digital system (Digital Sight DS-U1).

IMMUNOFLUORESCENCE CO-LOCALIZATION

Two sections for each species (one rostral and one caudal) were washed 3 × 10 min in PBS, permeabilized and blocked with PBS + 1% bovine serum albumin (BSA) + 0.3% Triton X-100 in a humid chamber at room temperature for 45 min. Sections were then incubated overnight in a humid chamber at 4°C using a combination of rabbit polyclonal anti-CR antibody and a mouse monoclonal anti-PV antibody (1:200/1:2000), diluted in PBS + 1% BSA + 0.03% TritonX-100 (PBS-BT). After washing for 3 × 10 min in PBS, the slides were incubated in a combination of secondary antibodies: anti-mouse Alexa 488 (1:500) and anti-rabbit Rhodamin Red-x (1:1000) (Invitrogen, Carlsbad, CA, USA). The sections were washed for 3 × 10 min in PBS and mounted in Vectashield (Vector Labs). Slides were examined with a Leica TCS-NT confocal microscope equipped with a krypton–argon laser.

The specificity of the immunohistochemical staining was tested in repeated trials by replacing either the primary or the secondary antibody with PBS.

RESULTS

The planes of section represented in **Figure 1** were regularly applied to the analysis of the chemical neuroanatomy of the claustrum in man, chimpanzee and crab-eating macaque. The topography of the claustrum is consistent in the three primate species (**Figure 1**), including its well-established relationships with the adjacent structures (*capsulae*, basal ganglia, insular cortex, thalamus, ventro-lateral temporal cortex). The relative lesser development of the temporal lobe (and especially of the *gyri temporalis medius* and *inferior*) in the chimpanzee and crab-eating monkey places the claustrum of these two species topographically closer to the ventral surface of the brain than in man. The planes of section represented in **Figure 1** were regularly applied to the analysis of the chemical neuroanatomy of the claustrum in the three primate species. For cellular studies and practical purposes, in each plane of section the claustrum was furtherly

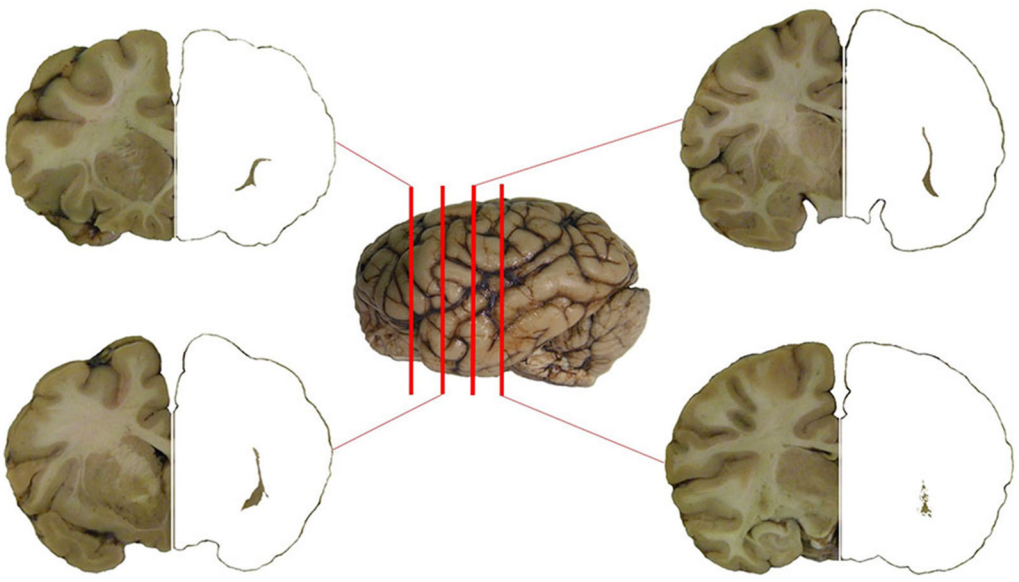

FIGURE 1 | The claustrum of the chimpanzee in four subsequent sections of the brain. Position of the section is represented against the left side of the brain. The claustrum has been isolated on the right side of the four sections.

Table 1 | Distribution and density pattern of CR-, PV-, SOM- and NPY-ir cells in the dorsal, central and ventral regions of the claustrum.

	Human			Chimpanzee			Crab-eating macaque		
	Dorsal	Central	Ventral	Dorsal	Central	Ventral	Dorsal	Central	Ventral
CR	+	+++	++	+	+++	++	+	+++	++
PV	+	+++	++	+	+++	++	+	+++	++
SOM	+	+	+	−−	−−	−−	+	+	+
NPY	++	++	++	++	++	++	++	++	++

+ Moderate; ++ Numerous; +++ Very numerous.

Table 2 | CR and PV neuronal density in the human, chimpanzee, and crab-eating macaque claustrum (count of labeled cells *per* mm^2).

	CR			PV		
	Cells	mm^2	Density (cells/mm^2)	Cells	mm^2	Density (cells/mm^2)
Human	1070	218	4.9	401	200	2
Chimpanzee	380	82.6	4.6	158	78.4	2
Crab-eating monkey	134	30.8	4.4	216	32.2	6.7

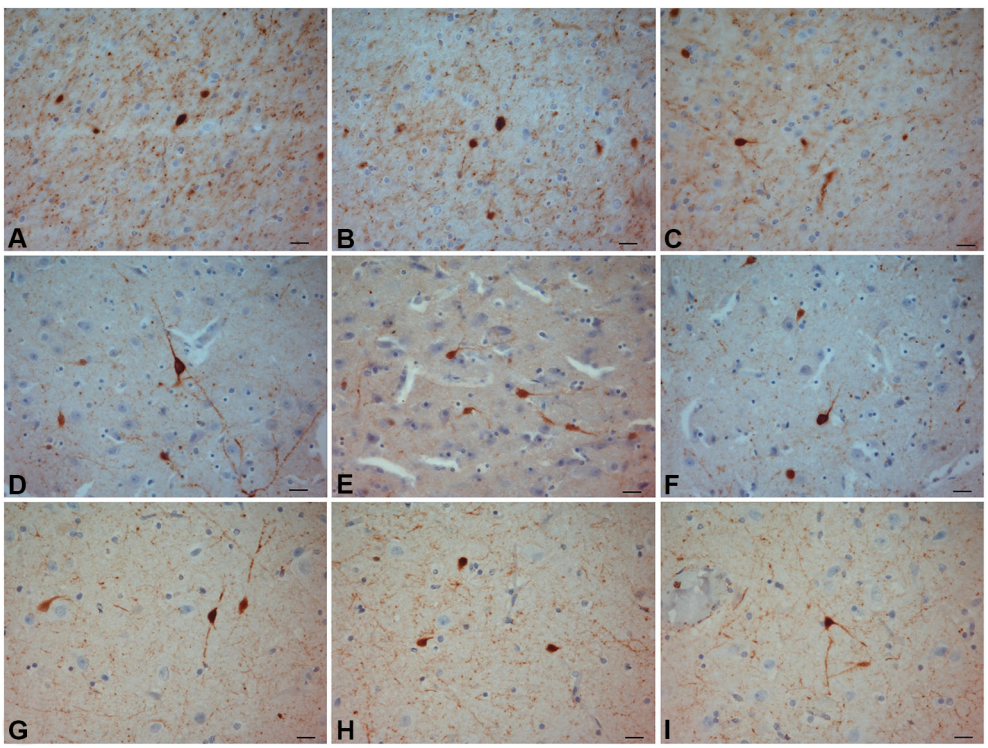

FIGURE 2 | CR-ir neurons. **(A–C)** crab-eating monkey; **(D–F)** chimpanzee; **(G–I)** human. Scale bars = 20 μm.

topographically subdivided into dorsal, central and ventral claustrum (for discussion on the possible subdivisions of the claustrum see Hinova-Palova et al., 2013).

The morphological features and the distribution pattern of the PV-ir, CR-ir, NPY-ir and SOM-ir neurons observed in the insular cortex and in the putamen in each section were considered the standard reference control (data not shown). CB immunoreactivity was not detected in our samples while CB-ir neurons were found (data not shown) in archival samples of the rat brain cortex used as positive controls. The relative density of the immunostained neurons is reported in **Table 1**. The cell density of the PV and CR immunostained neurons in the human, chimpanzee, and

crab-eating monkey claustrum, calculated as the total of cells per mm^2, is reported in **Table 2**.

We observed several morphologically distinct types of immunostained cells in the claustrum of the three species. CR-ir neurons were the most numerous CBP-type expressed, and represented a relatively uniform population. PV-ir neurons resulted more numerous in the crab-eating macaque and belonged to two distinct cell types according to the soma shape and diameter (see below). Immunoreactivity to CR, PV, NPY and SOM was observed in neuronal cell bodies and processes distributed throughout the anterior-posterior extent of the claustrum. Both CR- and PV-ir neurons exhibited a gradient pattern of increasing number from dorsal to ventral claustrum. Differently, NPY and SOM immunostained cells were evenly scattered all through the claustrum (**Figure 12**).

CALRETININ

The most frequently observed CR-ir neurons in human, chimpanzee and crab-eating monkey appeared to be darkly stained with 1–2 processes and a round or fusiform somata (**Figure 2**). The main diameter was inferior to 20 μm. Triangular somata were seldom observed in the human claustrum (**Figure 2I**). In the three species CR-ir neurons were more abundant in the central and ventral region, few CR-ir neurons were detected in the dorsal part of the claustrum. Positive fibers were localized in the neuropil, in particular they were numerous in the crab-eating monkey (**Figures 2A–C**).

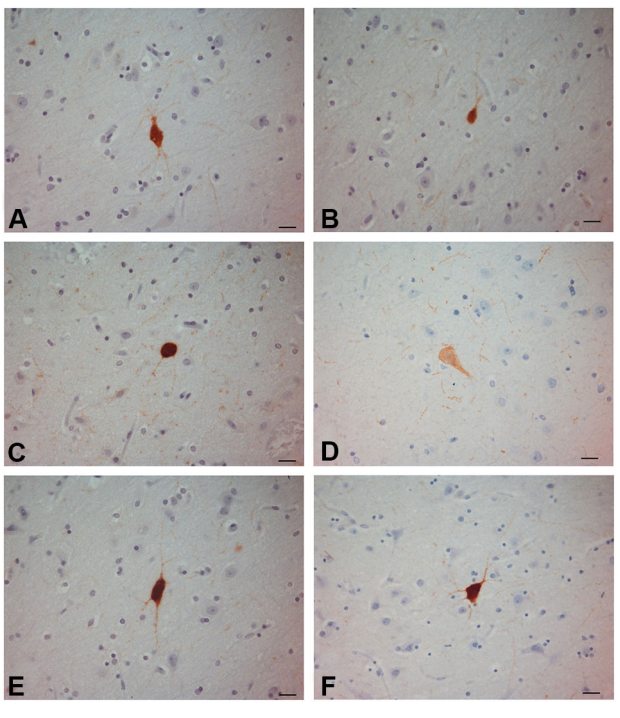

FIGURE 3 | PV-ir neurons in the human claustrum. (A–F) Scale bars = 20 μm.

PARVALBUMIN

PV-immunoreactive neurons of different sizes and shape were diffused in the claustrum of the three species (**Figures 3–5**). In the human and chimpanzee claustrum we described fusiform, round, triangular, polygonal and pear shaped cell bodies (**Figures 3**, **4**). In the crab-eating monkey, somata were mainly fusiform, round or pear shaped (**Figure 5**). As a rule, labeling in the processes was

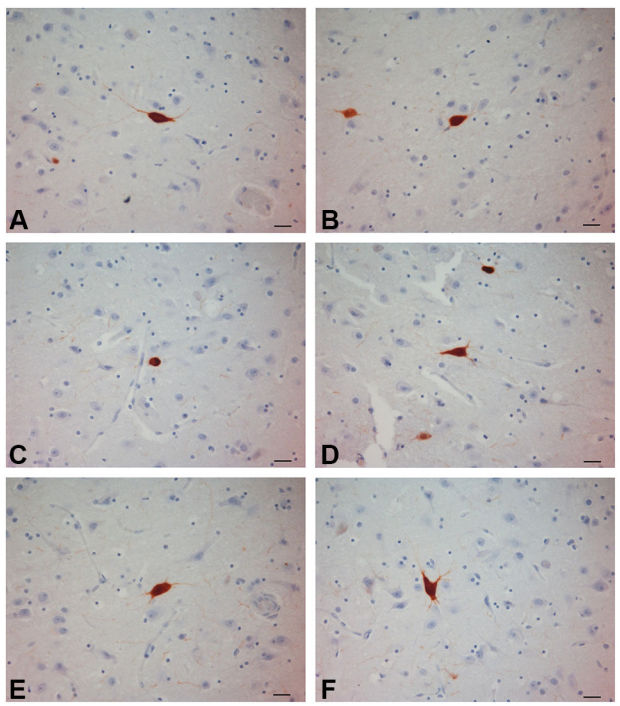

FIGURE 4 | PV-ir neurons in the chimpanzee claustrum. (A–F) Scale bars = 20 μm.

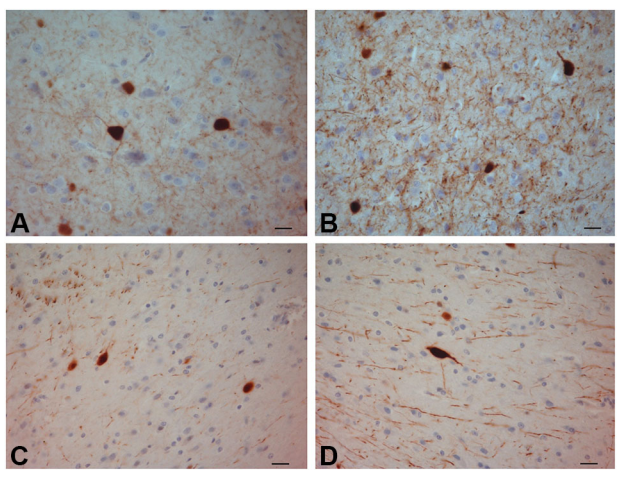

FIGURE 5 | PV-ir neurons in the crab-eating monkey claustrum. (A–D) Scale bars = 20 μm.

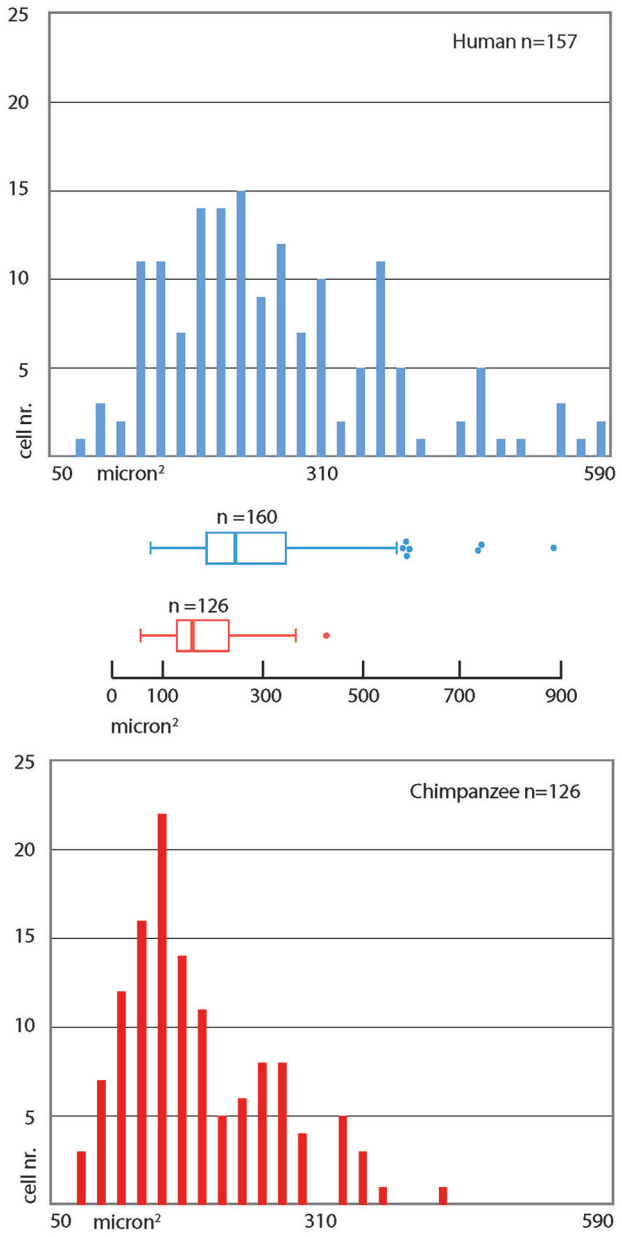

FIGURE 6 | Frequency distribution of cross-section areas of PV immunoreactive neurons in the human and chimpanzee claustrum. Bins = 20 μm^2. The box in the box plot shows the median and interquartile range. Left whiskers include low extreme values; the length of right whiskers is interquartile range × 1.5.

fainter than in the cell body. In the three species PV-ir neurons were particularly numerous in the central and ventral region. In the dorsal part PV-ir neurons were rarely seen. PV-ir fibers were found in the claustrum neuropil of the crab-eating monkey (**Figure 5**), but their presence was less conspicuous in the human and chimpanzee. The frequency distribution of cross-section areas of PV labeled neurons in the human and chimpanzee claustrum is shown in **Figure 6**. For the chimpanzee, there is a main population of cells with mean area around 190 μm^2, and a second population with a peak of frequency around 300 μm^2. The distribution of cross-section areas is more widespread in humans, compared to the chimpanzee.

Figure 7 contains low-magnification comparisons of the distribution of CR- (**Figure 7Aa-b**) and PV- (**Figure 7Cc-d**) immunoreactive neurons in the human claustrum.

SOMATOSTATIN

In the human and crab-eating monkey claustrum, SOM positive somata were identified (**Figure 8**). They presented a round or fusiform soma with faintly labeled processes. SOM immunoreactive fibers were rarely seen. These immunostained neurons were evenly scattered throughout the human and monkey claustrum. In the chimpanzee claustrum, SOM-ir neurons were not observed (**Figure 9**), but neurons clearly immunostained were detected in the putamen (**Figure 9A**) and in the insular cortex (**Figure 9B**).

NPY

NPY-ir neurons were found in the claustrum of the three species (**Figure 10**). Neurons with darkly stained somata and processes were uniformly diffused throughout the claustrum. The soma was round, fusiform or triangular. Many positive beaded fibers were localized in the neuropil.

CO-LOCALIZATION

The number of cells examined was approx. 8–12 for each slide (total 16–20 cells for each species), depending on the condition of the single tissue sections. No co-localization of PV with CR was found. PV- and CR-ir cells appeared to be organized into two different neuronal populations (**Figure 11**).

DISCUSSION

The present study describes the localization and the morphology of the PV-, CR-, NPY-, and SOM-ir neurons in the human, chimpanzee and crab-eating monkey claustrum. Data on the presence of selected CBPs in the human and monkey claustrum were already present in the literature (for general reference see the elegant study of Hinova-Palova et al., 2013 on PV in the human claustrum). However the present study describes for the first time the CBPs in three key primates. Furthermore, to our knowledge, this is the first time that the localization of CR, PV, SOM, and NPY has been studied in chimpanzee claustrum.

In general, the topography of the claustrum, the morphological feature and distribution of the labeled cells were similar in the three species, confirming their close phylogenetic relationship. Here we assume that the human and chimpanzee dorsal claustrum maintains the extensive relationship with the somatosensory and with the auditory cortical areas demonstrated in the Rhesus monkey (Minciacchi et al., 1991; Remedios et al., 2010). Moreover, the segregation of the visual modality in the ventrocaudal claustrum, as described in the macaque monkey (e.g., Remedios et al., 2010), is likely to be preserved also in the enlarged ventral part of the ape and human claustrum. It remains to be established whether the higher density of PV-ir neurons in the ventral claustrum, observed in the present study,

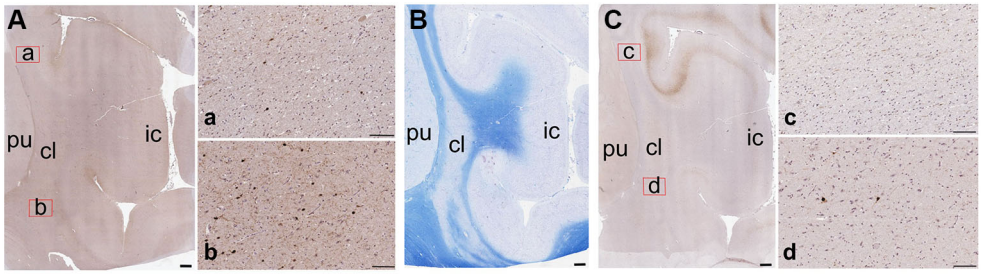

FIGURE 7 | Low-magnification images of the CBPs in the human claustrum. (A) CR-immunoreactive neurons; a and b are enlargements of the corresponding red rectangles in **A**; **(B)** Reference image stained with Luxol Fast Blue; **(C)** PV-immunoreactive neurons; c and d are enlargements of the corresponding red rectangles in **C**; pu; putamen; cl: claustrum; ic: insular cortex. Scale bars: A, B, C = 1 mm; a, b, c, d, = 100 μm.

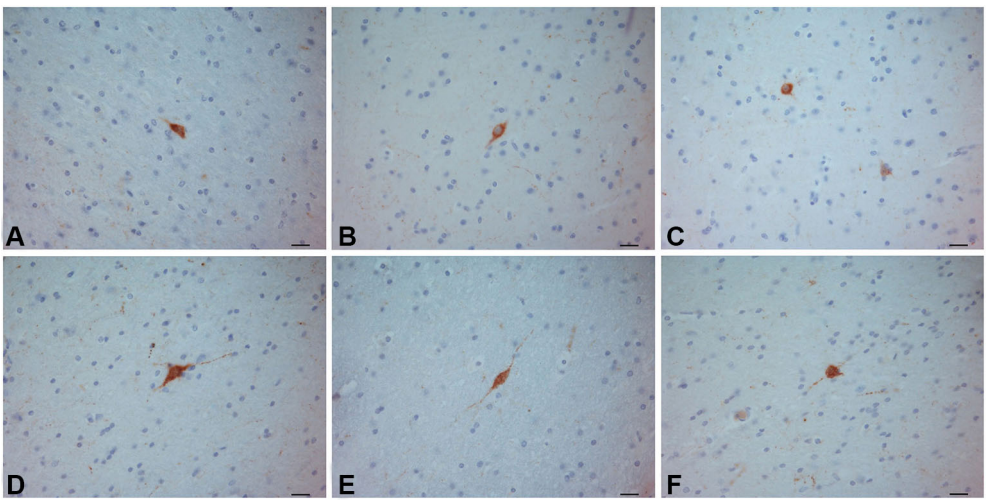

FIGURE 8 | SOM–ir neurons in the crab-eating monkey (A–C) and human (D–F) claustra. Scale bars = 20 μm.

is functionally related to the processing of visual (rather than somatosensory and auditory) information.

In our immunohistochemical characterization, as seen in coronal sections, ir-neural cells were always denser in the central part of the dorso-ventral extension of the claustrum, but we cannot presently pinpoint any specific function to these data, as classical projection studies obviously do not apply to apes and human. Interestingly, a novel approach to mapping claustral projections in living humans, using constrained spherical deconvolution tractography (Milardi et al., 2013), showed multiple and possibly multi-functional connections of the claustrum with cortical and subcortical structures. On the contrary, studies performed in rats by proteomic analysis combined with traditional tracing methods (Mathur et al., 2009) showed that claustral connections were limited to cortical structures, and no sub-cortical projection was identified.

The major difference that we found among the three species was the absence of SOM-ir neurons in the claustrum of the chimpanzee. Technical or fixation-related motives for the absence of SOM staining in the chimpanzee may be excluded, since SOM-ir neurons were clearly present in the adjacent structures: the putamen and the insular cortex. It is possible that this difference could be due to species-specific variability. On the other hand, neurochemical variations among closely related species are not uncommon, i.e., the expression of cortical chemical markers varies among rodents (Xu et al., 2006; Gonchar et al., 2008; Miyoshi et al., 2007).

On the whole, our data agree with those reported for the presence of PV-ir and CR-ir neurons in the claustrum of different species (Reynhout and Baizer, 1999; Real et al., 2003; Wojcik et al., 2004; Rahman and Baizer, 2007) including man (Hinova-Palova et al., 2013). In particular, our findings on the PV-ir neurons in the human claustrum were consistent with those previously reported by Hinova-Palova et al. (2013). The technique we employed (paraffin sections of 5 μm) did not allow us to describe the dendritic arborization but the PV-ir cell distribution agrees with what observed by these authors. We were not able to distinguish the existence of seven morphological subtypes of PV-ir neurons, but we identified the presence at least of five subtypes in the human claustrum: round, fusiform, triangular, polygonal and pear shaped. The morphology of the cells expressing CR was similar to that reported in the monkey (*Macaca fascicularis*)

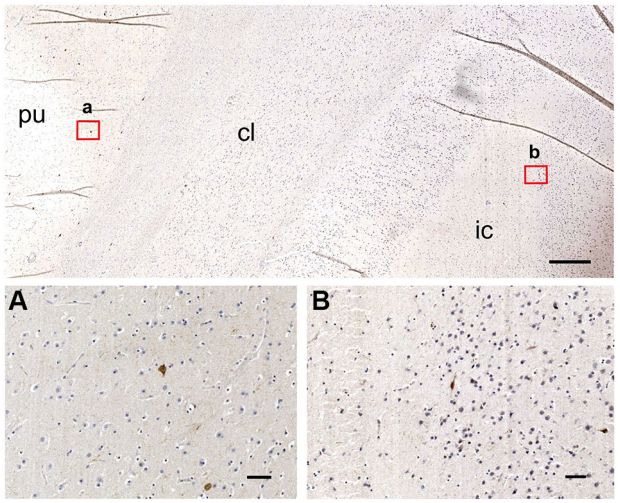

FIGURE 9 | SOM–ir neurons are absent from the chimpanzee claustrum (top), but present in putamen (A) and insular cortex (B). pu; putamen; cl: claustrum; ic: insular cortex. Scale bars; image at the top = 500 μm; a, b = 50 μm.

(Reynhout and Baizer, 1999). Both the PV- and CR-labeled were more abundant in the central and ventral part of the claustrum, as reported in **Table 1**.

Different neuronal types have been described in the human claustrum by Golgi stain (Braak and Braak, 1982). According to the soma size and shape, we can speculate that the PV-ir cells of our study may correspond—at least in part–to the large aspiny neurons described by Braak and Braak (1982) with Golgi stain. The CR-ir described in the present paper may match small aspiny cells of Golgi stain, even though our observations were not consistent with the dendrites radiating in all directions as reported in the cited study (Braak and Braak, 1982). The CR-ir cells may also represent interneurons not yet described by Golgi technique.

We note that CB immunoreactivity was not detected in our samples, but the rat brain cortex used as positive control (data not shown) tested positive. In addition, the CB monoclonal antibody used in the present study has been shown to immunoreact with primate retinal cells (Puthussery et al., 2011). Possible explanations for the lack of CB immunoreactivity in our samples include potential loss of signal due to post-mortem interval occurred before sampling or an hitherto undetermined specific factor influencing the presence of CB in the primate claustrum. CB is widely expressed by several classes of cortical interneurons, such as neurogliaform, double bouquet, and Martinotti cells (e.g., Gabbott and Bacon, 1996). The lack of CB-ir neurons can be explained by the absence of some claustral interneuron populations homologue to those of the cortex. However, we cannot rule out that the absence of CB can be due to the fact that its peculiar role in Ca^{2+} buffering and signaling (extensively discussed in Bastianelli, 2003) is not needed in the primate claustrum.

Calcium-binding proteins and neuropeptides have been used as markers that distinguish among cortical interneurons (Garcia-Segura et al., 1984; DeFelipe et al., 1989; Hendry et al., 1989; DeFelipe, 1993; Cauli et al., 1997; Gonchar and Burkhalter, 1997; Somogyi and Klausberger, 2005; Ascoli et al., 2008). Moreover, it has been demonstrated that inhibitory neurons expressing CBPs contain also neuropeptides such as: SOM, VIP, CCK, and NPY (Xu et al., 2006). In particular, PV, CR and SOM are considered informative markers because they have minimal overlap with other markers (DeFelipe, 1993; Kubota et al., 1994; Kawaguchi and Kubota, 1996, 1997; Gonchar and Burkhalter, 1997; Gonchar et al., 2008). In the present study we identified SOM and NPY labeled neurons in the investigated claustra with the exception of SOM in the chimpanzee. Former studies confirmed the presence of these two neuropeptides in the rat claustrum (Kowianski et al., 2001, 2009). The somewhat puzzling absence of SOM-ir elements in the claustrum of the chimpanzee (**Figure 9**) remains unexplained, considering also that SOM-ir neurons are present in the putamen and insular cortex (**Figures 9A–B**). We were not able to trace any former study on the expression of SOM in the chimpanzee brain. A study in the human (Mengod et al., 1992), failed to detect SOM mRNA-containing neurons in the claustrum, but described them in several locations, including the neocortex and putamen. Another study (Breder et al., 1992) reported the presence of SSTR2 (SOM receptor type 2) mRNA but not SSTR1 (SOM receptor type 1) mRNA in rats and humans, suggesting the existence of a complex network (for review see Møller et al., 2003). A study of the expression of the different SOM receptors in the chimpanzee may contribute to a better understanding of our data.

The presence of CBPs, SOM and NPY, along with the lack of PV-CR co-localization, suggests the existence of diverse neuronal subpopulations in the chimpanzee, crab-eating monkey and human claustrum. This scheme could indicate a similarity to the neocortex where different non-overlapping classes of GABAergic interneurons have been described (DeFelipe et al., 1989; Hendry et al., 1989; DeFelipe, 1993; Cauli et al., 1997; Gonchar and Burkhalter, 1997; Kawaguchi and Kubota, 1997; Somogyi and Klausberger, 2005; Ascoli et al., 2008). Similarly, several classes of claustral inhibitory interneurons can be distinguished on the basis of the differential expression of CBPs and neuropeptides (see also Kowianski et al., 2009; Smythies et al., 2012). However, we should also take into account that CBPs are not exclusively expressed by GABAergic interneurons of the claustrum, but are also found in spiny projection neurons (Hinova-Palova et al., 2007; Hendry et al., 1989).

Is the neurochemistry of the primate claustrum different form that of other mammals? Among the three species we noted a difference in the density of the neurons expressing the CaBPs (**Table 2**). In particular, in the human and in the chimpanzee the density of the CR-ir neurons was greater than that of the cells expressing PV while in the macaque there was an opposite situation. Several studies have been carried out in non-primate mammals. Real et al. (2003) investigated the CBPs expression in the dorsal and ventral (endopiriform nucleus, ED) division of the mouse claustrum. CR-ir neurons were very scarce in both divisions. In contrast, PV-ir cells were more numerous in the dorsal division than in the ED. These results were in line with the findings reported in the rat claustrum (Celio, 1990; Druga et al., 1993). Four neuronal types have been described in the rabbit claustrum based on CBPs immunohistochemistry (Wojcik

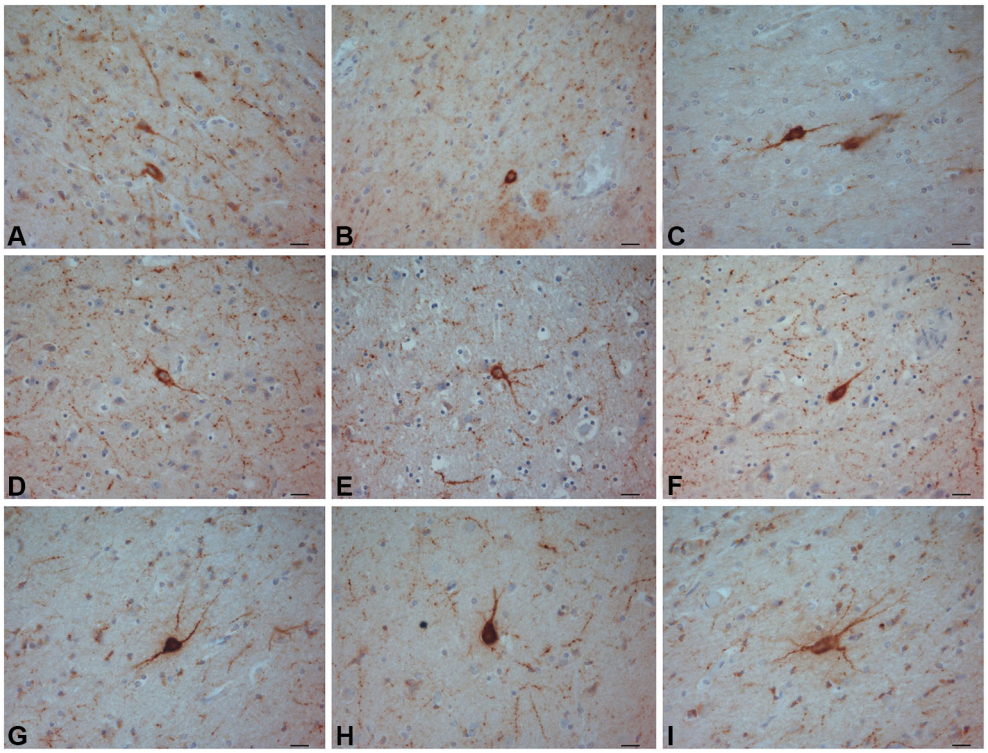

FIGURE 10 | NPY-ir neurons in the crab-eating monkey (A–C) chimpanzee (D–F) and human (G–I) claustra. Scale bars = 20 μm.

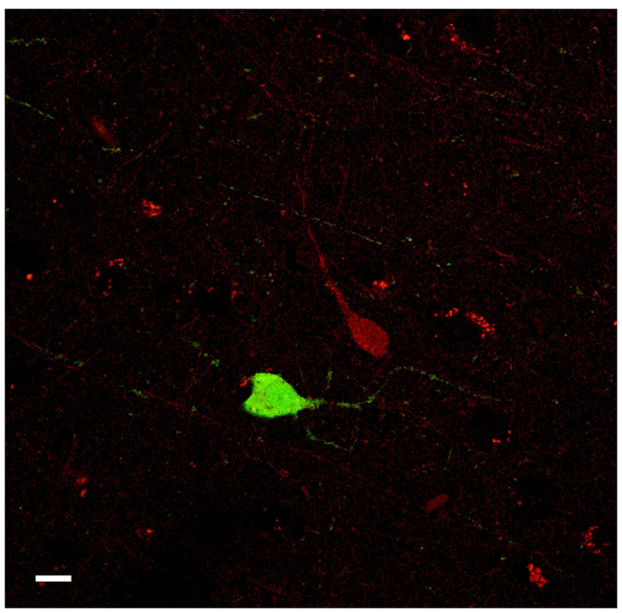

FIGURE 11 | Confocal microscope images of PV-ir (green), and CR-ir (red) neurons in the human claustrum. No co-localization was observed. Scale bar = 10 μm.

et al., 2004). In this latter species, PV immunoreactivity in the ED was lower than that observed in the dorsal claustrum while immunostain for CR was low in both divisions, similarly to what reported for the mouse (Real et al., 2003). As we reported in the crab-eating monkey, in the cat, cells immunoreactive to CR were less numerous than those positive to PV (Rahman and Baizer, 2007). Our results in the human and chimpanzee suggest the opposite, since, CR-ir neurons represented the most evident CBP-positive category. Furthermore, both PV- and CR-ir cells were more concentrated in the central and ventral part of the claustrum. Most likely, these differences were due to species-specific differences (Baimbridge et al., 1992), and possibly indicate a neurochemical organization peculiar of primates.

A comparison of the morphology and the cellular density observed in the human claustrum with that of the mammalian neocortex may yield important information and contribute to the understanding of the ontogenesis of this enigmatic structure. In the mammal neocortex, CR-ir neurons were mainly bipolar or bitufted, displayed a fusiform or oval soma, and localized in layers II and III (Barinka and Druga, 2010). Differently, the greatest density of PV-ir positive neurons of the first type with large round multipolar somata and of the second type with a small- to medium-sized multipolar soma has been described in layers III and IV. Besides, in the mammalian (and especially in the primate) neocortex the relative density of CR-ir cells was approximately twice that of PV-ir elements (Hof et al., 1999). In particular, the CR/PV ratio in the monkey was found to be about 1.8 (Barinka and Druga, 2010). These findings are in agreement with our results described in **Table 2**. As the former Authors reported in

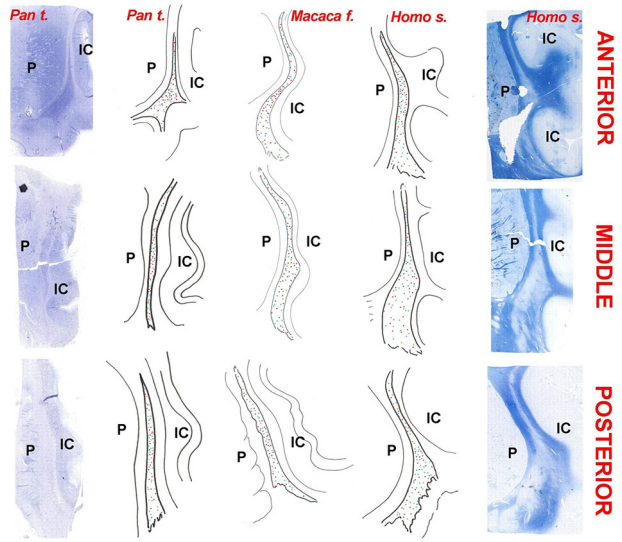

FIGURE 12 | Chartings of the claustrum of the chimpanzee (*Pan troglodytes*), crab-eating macaque (*Macaca fascicularis*), and man (*Homo sapiens*). Column of photographs on the left: Nissl stain of the neurons in the claustrum of the chimpanzee; Column of photographs on the far right: Luxol fast-blue stain of fibers in the human claustrum. The chartings are drawn from original sections. The species is indicated on the top. Red dots: PV; Blue dots: CR; Green dots: NPY; Indigo dots: SOM (absent in the chimpanzee); P = putamen; IC: insular cortex.

the neocortex, we described a single class of CR-ir cells and, at least in the chimpanzee, two types of PV-ir neurons, based on the size. Unlike the cortex, these cells were evenly distributed without a layered organization. Furthermore, we observed a higher density of the CR-ir in respect to PV-ir cells. The latter data is close to that indicated in the neocortex. Taken together these findings may give a further contribute to the pallial origin (and possibly function) of the human claustrum (for a comprehensive review see Park et al., 2012; Pirone et al., 2012). At least in the cortex, there is a considerable degree of CR-VIP overlap (e.g., Cauli et al., 1997) and VIP interneurons mediate the feedback input from higher-order cortical areas (reviewed in Karnani et al., 2014). Therefore, the prevalence of CR neurons in the primate cortex and claustrum is likely to be justified by the substantial increase of the associative network in the primate brain.

Based on neuronal morphology and present failure of co-localization, our study suggests that in the primate claustrum CR- and PV-containing neurons might be segregated into two distinct sub-populations. These findings agree with what previously reported for human and monkey cortical interneurons (del Rio and DeFelipe, 1996; Zaitsev et al., 2009, 2005). The importance of CBPs as a tool for interneuronal subpopulations sorting has been recently validated by gene cluster analysis (Toledo-Rodriguez et al., 2004). In the neocortex of rodents, 100% of CR-labeled neurons were GABAergic (Gonchar and Burkhalter, 1997; Gonchar et al., 2008). This does not fully apply to primates, in which approx 25% of CR-ir neurons are not GABAergic (del Rio and DeFelipe, 1996; Melchitzky et al., 2005). Moreover, PV is reported to be consistently localized in subpopulations of GABAergic neurons in the central nervous system (Bastianelli, 2003). Based on the studies mentioned above, we may suppose that in the human claustrum a large part of PV-ir and CR-ir neurons belong to the GABAergic system too. The presence of two different interneuronal sub-populations could indicate the existence of an inhibitory and a disinhibitory network able to modulate complex intra or extra-claustral interactions. This is consistent with the theory of the claustrum function proposed by Crick and Koch (2005) and with the findings reported by Rahman and Baizer (2007) in the cat. Although studies on the human and macaque claustrum were already present in the literature, the present investigation reports the first description of the claustrum of an ape, the chimpanzee. We also present evidence of PV- and CR-ir neurons in the chimpanzee claustrum, confirm the distribution of the CBPs in the human and offer for the first time direct comparisons in the three primates. Our findings suggest that these two CBPs are localized into two different sub-populations of PV- and CR-ir interneurons. The morphology and the density of distribution of the immunostained cells further support a possible common ontogeny of the claustrum and the neocortex (Pirone et al., 2012).

ACKNOWLEDGMENTS

The authors wish to thank Dr. Stefano Montelli and Dr. Mattìa Panin of the Department of Comparative Biomedicine and Food Science of the University of Padova for the useful insights into the revision of the present manuscript.

REFERENCES

Andressen, C., Blümcke, I., and Celio, M. R. (1993). Calcium-binding proteins: selective markers of nerve cells. *Cell Tissue Res.* 271, 181–208. doi: 10.1007/bf00318606

Ascoli, G. A., Alonso-Nanclares, L., Anderson, S. A., Barrionuevo, G., Benavides-Piccione, R., Burkhalter, A., et al. (2008). Petilla terminology: nomenclature of features of GABAergic interneurons of the cerebral cortex. *Nat. Rev. Neurosci.* 9, 557–568. doi: 10.1038/nrn2402

Baimbridge, K. G., Celio, M. R., and Rogers, J. H. (1992). Calcium-binding proteins in the nervous system. *Trends Neurosci.* 15, 303–308. doi: 10.1016/0166-2236(92)90081-i

Barinka, F., and Druga, R. (2010). Calretinin expression in the mammalian neocortex: a review. *Physiol. Res.* 59, 665–677.

Bastianelli, E. (2003). Distribution of calcium-binding proteins in the cerebellum. *Cerebellum* 2, 242–262. doi: 10.1080/14734220310022289

Braak, H., and Braak, E. (1982). Neuronal types in the claustrum of man. *Anat. Embryol. (Berl)* 163, 447–460. doi: 10.1007/bf00305558

Breder, C. D., Yamada, Y., Yasuda, K., Seino, S., Saper, C. B., and Bell, G. I. (1992). Differential expression of somatostatin receptor subtypes in brain. *J. Neurosci.* 12, 3920–3934.

Carey, R. G., and Neal, T. L. (1985). The rat claustrum: afferent and efferent connections with visual cortex. *Brain Res.* 329, 185–193. doi: 10.1016/0006-8993(85)90524-4

Carman, J. B., Cowan, W. M., and Powell, T. P. (1964). The cortical projection upon the claustrum. *J. Neurol. Neurosurg. Psychiatry* 27, 46–51. doi: 10.1136/jnnp.27.1.46

Castro, A., Becerra, M., Manso, M. J., and Anadón, R. (2003). Distribution and development of calretinin-like immunoreactivity in the telencephalon of the brown trout, *Salmo trutta fario*. *J. Comp. Neurol.* 467, 254–269. doi: 10.1002/cne.10923

Cauli, B., Audinat, E., Lambolez, B., Angulo, M. C., Ropert, N., Tsuzuki, K., et al. (1997). Molecular and physiological diversity of cortical nonpyramidal cells. *J. Neurosci.* 17, 3894–3906.

Celio, M. R. (1990). Calbindin D-28k and parvalbumin in the rat nervous system. *Neuroscience* 35, 375–475. doi: 10.1016/0306-4522(90)90091-h

Crespo, C., Porteros, A., Arévalo, R., Briñón, J. G., Aijón, J., and Alonso, J. R. (1999). Distribution of parvalbumin immunoreactivity in the brain of the tench (*Tinca tinca* L., 1758). *J. Comp. Neurol.* 413, 549–571. doi: 10.1002/(sici)1096-9861(19991101)413:4<549::aid-cne5>3.0.co;2-d

Crick, F. C., and Koch, C. (2005). What is the function of the claustrum? *Philos. Trans. R. Soc. Lond. B Biol. Sci.* 360, 1271–1279. doi: 10.1098/rstb.2005.1661

Cusick, C. G., Scripter, J. L., Darensbourg, J. G., and Weber, J. T. (1993). Chemoarchitectonic subdivisions of the visual pulvinar in monkeys and their connectional relations with the middle temporal and rostral dorsolateral visual areas, MT and DLr. *J. Comp. Neurol.* 336, 1–30. doi: 10.1002/cne.903360102

Dávila, J. C., Guirado, S., and Puelles, L. (2000). Expression of calciumbinding proteins in the diencephalon of the lizard *Psammodromus algirus*. *J. Comp. Neurol.* 427, 67–92. doi: 10.1002/1096-9861(20001106)427:1.0.co;2-2

DeFelipe, J. (1993). Neocortical neuronal diversity: chemical heterogeneity revealed by colocalization studies of classic neurotransmitters, neuropeptides, calcium-binding proteins and cell surface molecules. *Cereb. Cortex* 3, 273–289. doi: 10.1093/cercor/3.4.273

DeFelipe, J. (1997). Types of neurons, synaptic connections and chemical characteristics of cells immunoreactive for calbindin-D28K, parvalbumin and calretinin in the neocortex. *J. Chem. Neuroanat.* 14, 1–19. doi: 10.1016/s0891-0618(97)10013-8

DeFelipe, J., Hendry, S. H. C., and Jones, E. G. (1989). Visualization of chandelier cell axons by parvalbumin immunoreactivity in monkey cerebral-cortex. *Proc. Natl. Acad. Sci. U S A* 86, 2093–2097. doi: 10.1073/pnas.86.6.2093

del Rio, M. R., and DeFelipe, J. (1996). Colocalization of calbindin D-28k, calretinin and GABA immunoreactivities in neurons of the human temporal cortex. *J. Comp. Neurol.* 369, 472–482. doi: 10.1002/(sici)1096-9861(19960603)369:3.0.co;2-k

Díaz-Regueira, S., and Anadón, R. (2000). Calretinin expression in specific neuronal systems in the brain of an advanced teleost, the grey mullet (*Chelon labrosus*). *J. Comp. Neurol.* 426, 81–105. doi: 10.1002/1096-9861(20001009)426:1<81::AID-CNE6>3.0.CO;2-E

Dinopoulos, A., Papadopoulos, G. C., Michaloudi, H., Parnavelas, J. G., Uylings, H. B. N., and Karamanlidis, A. N. (1992). Claustrum in the hedgehog (Erinaceus europaeus) brain: cytoarchitecture and connections with cortical and subcortical structures. *J. Comp. Neurol.* 316, 187–205. doi: 10.1002/cne.903160205

Druga, R., Chen, S., and Bentivoglio, M. (1993). Parvalbumin and calbindin in the rat claustrum: an immunocytochemical study combined with retrograde tracing frontoparietal cortex. *J. Chem. Neuroanat.* 6, 399–406. doi: 10.1016/0891-0618(93)90014-u

Edelstein, L. R., and Denaro, F. J. (2004). The claustrum: a historical review of its anatomy, physiology, cytochemistry and functional significance. *Cell. Mol. Biol. (Noisy-le-grand)* 50, 675–702. doi: 10.1170/T558

Gabbott, P. L., and Bacon, S. J. (1996). Local circuit neurons in the medial prefrontal cortex (areas 24a,b,c, 25 and 32) in the monkey: I. Cell morphology and morphometrics. *J. Comp. Neurol.* 364, 567–608. doi: 10.1002/(sici)1096-9861(19960122)364:4.0.co;2-1

Garcia-Segura, L. M., Baetensa, D., Rotha, J., Normana, A. W., and Orcia, L. (1984). Immunohistochemical mapping of calcium-binding protein immunoreactivity in the rat central nervous system. *Brain Res.* 296, 75–86. doi: 10.1016/0006-8993(84)90512-2

Gonchar, Y., and Burkhalter, A. (1997). Three distinct families of GABAergic neurons in rat visual cortex. *Cereb. Cortex* 7, 347–358. doi: 10.1093/cercor/7.4.347

Gonchar, Y., Wang, Q., and Burkhalter, A. (2008). Multiple distinct subtypes of GABAergic neurons in mouse visual cortex identified by triple immunostaining. *Front. Neuroanat.* 1:3. doi: 10.3389/neuro.05.003.2007

Hendry, S. H. C., Jones, E. G., Emson, P. C., Lawson, D. E. M., Heizmann, C. W., and Streit, P. (1989). Two classes of cortical GABA neurons defined by differential calcium binding protein immunoreactivities. *Exp. Brain Res.* 76, 467–472. doi: 10.1007/bf00247904

Hinova-Palova, D. V., Edelstein, L., Landzhov, B. V., Braak, E., Malinova, L. G., Minkov, M., et al. (2013). Parvalbumin-immunoreactive neurons in the human claustrum. *Brain Struct. Funct.* doi: 10.1007/s00429-013-0603-x. [Epub ahead of print].

Hinova-Palova, D. V., Edelstein, L. R., Paloff, A. M., Hristov, S., Papantchev, V. G., and Ovtscharoff, W. A. (2007). Parvalbumin in the cat claustrum: ultrastructure, distribution and functional implications. *Acta Histochem.* 109, 61–77. doi: 10.1016/j.acthis.2006.09.006

Hof, P. R., Glezer, I. I., Conde, F., Flagg, R. A., Rubin, M. B., Nimchinsky, E. A., et al. (1999). Cellular distribution of the calcium-binding proteins parvalbumin, calbindin and calretinin in the neocortex of mammals: phylogenetic and developmental patterns. *J. Chem. Neuroanat.* 16, 77–116. doi: 10.1016/s0891-0618(98)00065-9

Jande, S. S., Maler, L., and Lawson, D. E. (1981). Immunohistochemical mapping of vitamin D-dependent calcium-binding protein in brain. *Nature* 294, 765–767. doi: 10.1038/294765a0

Jones, E. G., and Hendry, S. H. (1989). Differential calcium binding protein immunoreactivity distinguishes classes of relay neurons in monkey thalamic nuclei. *Eur. J. Neurosci.* 1, 222–246. doi: 10.1111/j.1460-9568.1989.tb00791.x

Karnani, M. M., Agetsuma, M., and Yuste, R. (2014). A blanket of inhibition: functional inferences from dense inhibitory connectivity. *Curr. Opin. Neurobiol.* 26, 96–102. doi: 10.1016/j.conb.2013.12.015

Kawaguchi, Y., and Kubota, Y. (1996). Physiological and morphological identification of somatostatin- or vasoactive intestinal polypeptide-containing cells among GABAergic cell subtypes in rat frontal cortex. *J. Neurosci.* 16, 2701–2715.

Kawaguchi, Y., and Kubota, Y. (1997). GABAergic cell subtypes and their synaptic connections in rat frontal cortex. *Cereb. Cortex* 7, 476–486. doi: 10.1093/cercor/7.6.476

Kowianski, P., Dziewiatkowski, J., Kowianska, J., and Morys, J. (1999). Comparative anatomy of the claustrum in selected species: a morphometric analysis. *Brain Behav. Evol.* 53, 44–54. doi: 10.1159/000006581

Kowianski, P., Dziewiatkowski, J., Morys, J. M., Majak, K., Wojcik, S., Edelstein, L. R., et al. (2009). Colocalization of neuropeptides with calciumbinding proteins in the claustral interneurons during postnatal development of the rat. *Brain Res. Bull.* 80, 100–106. doi: 10.1016/j.brainresbull.2009.06.020

Kowianski, P., Timmermans, J. P., and Morys, J. (2001). Differentiation in the immunocytochemical features of intrinsic and cortically projecting neurons in the rat claustrum — combined immunocytochemical and axonal transport study. *Brain Res.* 905, 63–71. doi: 10.1016/S0006-8993(01)02408-8

Kubota, Y., Hattori, R., and Yui, Y. (1994). Three distinct subpopulations of GABAergic neurons in rat frontal agranular cortex. *Brain Res.* 649, 159–173. doi: 10.1016/0006-8993(94)91060-x

LeVay, S., and Sherk, H. (1981). The visual claustrum of the cat. I. Structure and connections. *J. Neurosci.* 1, 956–980.

Mathur, B. N., Caprioli, R. M., and Deutch, A. Y. (2009). Proteomic analysis illuminates a novel structural definition of the claustrum and insula. *Cereb. Cortex* 19, 2372–2379. doi: 10.1093/cercor/bhn253

Melchitzky, D. S., Eggan, S. M., and Lewis, D. A. (2005). Synaptic targets of calretinin-containing axon terminals in macaque monkey prefrontal cortex. *Neuroscience* 130, 185–195. doi: 10.1016/j.neuroscience.2004.08.046

Mengod, G., Rigo, M., Savasta, M., Probst, A., and Palacios, J. M. (1992). Regional distribution of neuropeptide somatostatin gene expression in the human brain. *Synapse* 12, 62–74. doi: 10.1002/syn.890120108

Milán, F. J., and Puelles, L. (2000). Patterns of calretinin, calbindin, and tyrosine hydroxylase expression are consistent with the prosomeric map of the frog diencephalon. *J. Comp. Neurol.* 419, 96–121. doi: 10.1002/(sici)1096-9861(20000327)419:1.0.co;2-v

Milardi, D., Bramanti, P., Milazzo, C., Finocchio, G., Arrigo, A., Santoro, G., et al. (2013). Cortical and subcortical connections of the human claustrum revealed in vivo by constrained spherical deconvolution tractography. *Cereb. Cortex* doi: 10.1093/cercor/bht231. [Epub ahead of print].

Miller, R. J. (1991). The control of neuronal Ca2 homeostasis. *Prog. Neurobiol.* 37, 255–285. doi: 10.1016/0301-0082(91)90028-y

Minciacchi, D., Granato, A., and Barbaresi, P. (1991). Organization of claustrocortical projections to the primary somatosensory area of primates. *Brain Res.* 553, 309–312. doi: 10.1016/0006-8993(91)90840-r

Miyoshi, G., Butt, S. J., Takebayashi, H., and Fishell, G. (2007). Physiologically distinct temporal cohorts of cortical interneurons arise from telencephalic Olig2-expressing precursors. *J. Neurosci.* 27, 7786–7798. doi: 10.1523/jneurosci.1807-07.2007

Møller, N. L., Stidsen, E. C., Hartmann, B., and Holst, J. J. (2003). Somatostatin receptors. *Biochim. Biophys. Acta* 16, 1–84. doi: 10.1016/S0005-2736(03)00235-9

Morona, R., and González, A. (2008). Calbindin-D28k and calretinin expression in the forebrain of anuran and urodele amphibians: further support for newly identified subdivisions. *J. Comp. Neurol.* 511, 187–220. doi: 10.1002/cne.21832

Park, S., Tyszka, J. M., and Allman, J. M. (2012). The claustrum and insula in *microcebus murinus*: a high resolution diffusion imaging study. *Front. Neuroanat.* 6:21. doi: 10.3389/fnana.2012.00021

Parmentier, M., Ghysens, M., Rypens, F., Lawson, D. E. M., Pasteels, J. L., and Pochet, R. (1987). Calbindin in vertebrate classes: immuimmunohistochemical localization and Western blot analysis. *Gen. Comp. Endocrinol.* 65, 399–407. doi: 10.1016/0016-6480(87)90125-0

Parvizi, J., and Damasio, A. R. (2003). Differential distribution of calbindin D28k and parvalbumin among functionally distinct sets of structures in the macaque brainstem. *J. Comp. Neurol.* 462, 153–167. doi: 10.1002/cne.10711

Pirone, A., Cozzi, B., Edelstein, L., Peruffo, A., Lenzi, C., Quilici, F., et al. (2012). Topography of Gng2- and NetrinG2-expression suggests an insular origin of the human claustrum. *PLoS One* 7:e44745. doi: 10.1371/journal.pone.0044745

Puthussery, T., Gayet-Primo, J., Taylor, W. R., and Haverkamp, S. (2011). Immunohistochemical identification and synaptic inputs to the diffuse bipolar cell type DB1 in macaque retina. *J. Comp. Neurol.* 519, 3640–3656. doi: 10.1002/cne.22756

Rahman, F. E., and Baizer, J. S. (2007). Neurochemically defined cell types in the claustrum of the cat. *Brain Res.* 1159, 94–111. doi: 10.1016/j.brainres.2007.05.011

Rausell, E., and Jones, E. G. (1991). Histochemical and immunocytochemical compartments of the thalamic VPM nucleus in monkeys and their relationship to the representational map. *J. Neurosci.* 11, 210–225.

Rausell, E., Bae, C. S., Viñuela, A., Huntley, G. W., and Jones, E. G. (1992). Calbindin and parvalbumin cells in monkey VPL thalamic nucleus: distribution, laminar cortical projections and relations to spinothalamic terminations. *J. Neurosci.* 12, 4088–4111.

Real, M. A., Davila, J. C., and Guirado, S. (2003). Expression of calcium-binding proteins in the mouse claustrum. *J. Chem. Neuroanat.* 25, 151–160. doi: 10.1016/s0891-0618(02)00104-7

Remedios, R., Logothetis, N. K., and Kayser, C. (2010). Unimodal responses prevail within the multisensory claustrum. *J. Neurosci.* 30, 12902–12907. doi: 10.1523/jneurosci.2937-10.2010

Reynhout, K., and Baizer, J. S. (1999). Immunoreactivity for calcium-binding proteins in the claustrum of the monkey. *Anat. Embryol.* 199, 75–83. doi: 10.1007/s004290050211

Rogers, J. H. (1989). Two calcium-binding proteins mark many chick sensory neurons. *Neuroscience* 31, 697–709. doi: 10.1016/0306-4522(89)90434-x

Saleem, K. S., Price, J. L., and Hashikawa, T. (2007). Cytoarchitectonic and chemoarchitectonic subdivisions of the perirhinal and parahippocampal cortices in macaque monkeys. *J. Comp. Neurol.* 500, 973–1006. doi: 10.1002/cne.21141

Smythies, J., Edelstein, L., and Ramachandran, V. (2012). Hypotheses relating to the function of the claustrum. *Front. Integr. Neurosci.* 6:53. doi: 10.3389/fnint.2012.00053

Somogyi, P., and Klausberger, T. (2005). Defined types of cortical interneurone structure space and spike timing in the hippocampus. *J. Physiol.* 562, 9–26. doi: 10.1113/jphysiol.2004.078915

Toledo-Rodriguez, M., Blumenfeld, B., Wu, C., Luo, J., Attali, B., Goodman, P., et al. (2004). Correlation maps allow neuronal electrical properties to be predicted from single-cell gene expression profiles in rat neocortex. *Cereb. Cortex* 14, 1310–1327. doi: 10.1093/cercor/bhh092

Wojcik, S., Dziewiatkowski, J., Spodnik, E., Ludkiewicz, B., Domaradzka-Pytel, B., Kowianski, P., et al. (2004). Analysis of calcium binding protein immunoreactivity in the claustrum and the endopiriform nucleus of the rabbit. *Acta Neurobiol. Exp. (Wars)* 64, 449–460.

Xu, X., Roby, K. D., and Callaway, E. M. (2006). Mouse cortical inhibitory neuron type that coexpresses somatostatin and calretinin. *J. Comp. Neurol.* 499, 144–160. doi: 10.1002/cne.21101

Zaitsev, A. V., Gonzalez-Burgos, G., Povysheva, N. V., Kroner, S., Lewis, D. A., and Krimer, L. S. (2005). Localization of calcium-binding proteins in physiologically and morphologically characterized interneurons of monkey dorsolateral prefrontal cortex. *Cereb. Cortex* 15, 1178–1186. doi: 10.1093/cercor/bhh218

Zaitsev, A. V., Povysheva, N. V., Gonzalez-burgos, G., Rotaru, D., Fish, K. N., Krimer, L. S., et al. (2009). Interneuron diversity in layers 2-3 of monkey prefrontal cortex. *Cereb. Cortex* 19, 1597–1615. doi: 10.1093/cercor/bhn198

Conflict of Interest Statement: The authors declare that the research was conducted in the absence of any commercial or financial relationships that could be construed as a potential conflict of interest.

Received: 29 January 2014; accepted: 08 May 2014; published online: 26 May 2014.
Citation: Pirone A, Castagna M, Granato A, Peruffo A, Quilici F, Cavicchioli L, Piano I, Lenzi C and Cozzi B (2014) Expression of calcium-binding proteins and selected neuropeptides in the human, chimpanzee, and crab-eating macaque claustrum. Front. Syst. Neurosci. ***8****:99. doi: 10.3389/fnsys.2014.00099*
This article was submitted to the journal Frontiers in Systems Neuroscience.

frontiers in
SYSTEMS NEUROSCIENCE

ORIGINAL RESEARCH ARTICLE
published: 19 May 2014
doi: 10.3389/fnsys.2014.00093

Interhemispheric claustral circuits coordinate sensory and motor cortical areas that regulate exploratory behaviors

Jared B. Smith [1,2] ***and Kevin D. Alloway*** [2,3] ***

[1] *Department of Engineering Science and Mechanics, Penn State University, University Park, PA, USA*
[2] *Center for Neural Engineering, Penn State University, University Park, PA, USA*
[3] *Department of Neural and Behavioral Sciences, Penn State University, Hershey, PA, USA*

Edited by:
Brian N. Mathur, University of Maryland School of Medicine, USA

Reviewed by:
Preston E. Garraghty, Indiana University, USA
Helen Sherk, University of Washington, USA

****Correspondence:***
Kevin D. Alloway, Center for Neural Engineering, Millennium Science Complex, Pollock Road, University Park, PA 16802, USA
e-mail: kda1@psu.edu

The claustrum has a role in the interhemispheric transfer of certain types of sensorimotor information. Whereas the whisker region in rat motor (M1) cortex sends dense projections to the contralateral claustrum, the M1 forelimb representation does not. The claustrum sends strong ipsilateral projections to the whisker regions in M1 and somatosensory (S1) cortex, but its projections to the forelimb cortical areas are weak. These distinctions suggest that one function of the M1 projections to the contralateral claustrum is to coordinate the cortical areas that regulate peripheral sensor movements during behaviors that depend on bilateral sensory acquisition. If this hypothesis is true, then similar interhemispheric circuits should interconnect the frontal eye fields (FEF) with the contralateral claustrum and its network of projections to vision-related cortical areas. To test this hypothesis, anterograde and retrograde tracers were placed in physiologically-defined parts of the FEF and primary visual cortex (V1) in rats. We observed dense FEF projections to the contralateral claustrum that terminated in the midst of claustral neurons that project to both FEF and V1. While the FEF inputs to the claustrum come predominantly from the contralateral hemisphere, the claustral projections to FEF and V1 are primarily ipsilateral. Detailed comparison of the present results with our previous studies on somatomotor claustral circuitry revealed a well-defined functional topography in which the ventral claustrum is connected with visuomotor cortical areas and the dorsal regions are connected with somatomotor areas. These results suggest that subregions within the claustrum play a critical role in coordinating the cortical areas that regulate the acquisition of modality-specific sensory information during exploration and other behaviors that require sensory attention.

Keywords: motor cortex, neuronal tracing, sensorimotor, visuomotor, frontal eye fields, somatosensory cortex, claustrum, visual cortex

INTRODUCTION

The claustrum is present in nearly all mammalian lineages (Kowianski et al., 1999), but its behavioral functions have not been elucidated because of its unusual geometry. Relatively narrow with a long rostrocaudal extent, the claustrum is difficult to study with standard lesion or recording techniques in a behavioral paradigm. Neuronal tracing techniques, however, have revealed many aspects of claustral circuitry, and most views about claustral functions are based on its cortical connectivity (Edelstein and Denaro, 2004; Crick and Koch, 2005; Smythies et al., 2012), which include several unique interhemispheric projections (Minciacchi et al., 1985; Li et al., 1986; Sloniewski et al., 1986a; Sadowski et al., 1997).

Using physiology-based tracing techniques in rats, we recently reported that the M1-Wh region projects strongly to the contralateral claustrum, but only weakly to the ipsilateral claustrum (Alloway et al., 2009; Colechio and Alloway, 2009; Smith and Alloway, 2010; Smith et al., 2012b). While the M1-Wh region does not receive reciprocal feedback projections from the contralateral claustrum, it is strongly innervated by the ipsilateral claustrum. By contrast, claustral connections with the M1 forelimb regions are comparatively sparse and are exclusively ipsilateral. In addition, the whisker region in S1 barrel cortex is innervated by the ipsilateral claustrum even though S1 cortex does not project to the claustrum in either hemisphere.

These findings are significant because exploratory whisking is an active sensory process that requires attention and is bilaterally-coordinated for the purpose of acquiring tactile information about the spatial features of the local environment (Towal and Hartmann, 2006; Mitchinson et al., 2007). By comparison, rodent forelimb movements are rarely if ever used used to perceive the spatial features of three-dimensional space, but are mainly concerned with supporting and moving the body through space.

The discovery of an interhemispheric claustrum-based pathway that connects the cortical regions that process whisker-related information prompted us to hypothesize that the claustrum should have similar circuit connections with the visual system. Like whisking behavior, exploratory eye movements require attention and are concerned with actively acquiring visual information to perceive a broad spatial region (Chelazzi et al., 1989; Andrews and Coppola, 1999; Wallace et al., 2013). In rats the claustrum receives a few projections from visual area 18b, but

virtually none from area 17 (Miller and Vogt, 1984a; Carey and Neal, 1985). The ventral part of the rat claustrum projects to visual cortex (Li et al., 1986; Sadowski et al., 1997), but whether the claustrum has afferent or efferent connections with the FEF remains unknown. Indeed, no data indicate whether the rat claustrum is part of a disynaptic interhemispheric circuit that could coordinate the FEF and V1 areas.

Therefore, to test this hypothesis, we injected anterograde and retrograde tracers into physiologically-defined sites in FEF and V1. We compared the results, along with unreported data from our previous rat study (Smith and Alloway, 2010), to tracing data accessible from the Allen Mouse Brain Connectivity Atlas. Our findings indicate that the claustrum is part of an interhemispheric circuit that enables the FEF in one hemisphere to transmit the same information to the V1 and FEF cortical areas in the other hemisphere.

MATERIALS AND METHODS

Anatomical tracing experiments were performed on three adult male Sprague-Dawley rats (Charles River) weighing 300–350 g. All procedures conformed to National Institute of Health standards and were approved by Penn State University's Institutional Animal Care and Use Committee.

ANIMAL SURGERY

Rats were initially anesthetized via intramuscular (IM) injection of a mixed solution of ketamine HCl (40 mg/kg) and xylazine (12 mg/kg). Additional IM injections of atropine methyl nitrate (0.5 mg/kg) to limit bronchial secretions, dexamethasone sodium phosphate (5 mg/kg) to reduce brain swelling, and enrofloxacin (2.5 mg/kg) to prevent infection were given before intubating the trachea through the oral cavity and ventilating the rat with oxygen. After placing the animal in a stereotaxic instrument, its heart rate, respiratory rate, end-tidal carbon dioxide, and blood oxygen were monitored (Surgivet) throughout the experimental procedure. Body temperature was regulated by a rectal probe attached to a homeothermic blanket placed on the dorsal side of the animal; a hot water blanket was placed underneath the rat as well. Ophthalmic ointment was applied to prevent corneal drying. After injecting bupivicaine into the scalp, a midline incision was performed to visualize the cranium, and a ground screw was inserted into a craniotomy over the cerebellum. Craniotomies were also made over motor cortex (1–3 mm rostral, 0.5–3 mm lateral to bregma) and visual cortex (5–7 mm caudal, 3–5 mm lateral to bregma) in both hemispheres according to coordinates in Paxinos and Watson (2007).

INTRACRANIAL MICROSTIMULATION

Intracranial microstimulation (ICMS) was done in rats to map motor cortex. Microstimulation was performed under ketamine-xylazine anesthesia to produce forepaw, whisker, or eye movements. Following microstimulation mapping, the anesthetic state was maintained with ∼1% isoflurane.

Cortical stimulation was administered by ∼1 MΩ saline-filled glass pipettes. Both short (80-ms, 250 Hz) and long (1-s, 100 Hz) pulse trains were administered. A biphasic constant current source (Bak Electronics, BSI-2) was used to test current levels of 10–250 μA to identify the lowest threshold at each site capable of eliciting a movement. Stimulation was conducted at multiple sites in each animal so that tracer injections could be centralized within the target region to avoid tracer leakage into surrounding representations.

The stereotaxic coordinates that evoked movements were similar to previous reports (Hall and Lindholm, 1974; Neafsey et al., 1986; Hoffer et al., 2003; Brecht et al., 2004; Haiss and Schwarz, 2005). Electrodes were positioned orthogonal to the pial surface and inserted to depths (∼1 mm) that correspond to layer V, which contains corticobulbar and corticospinal neurons. The electrode was initially placed 2–3 mm lateral to the midline to identify the forepaw representation (M1-Fp). More medial sites (1–2 mm lateral) evoked brief whisker retractions (M1-Re) during 80-ms stimulation trains. At the most medial coordinates (∼1 mm lateral), the electrode was advanced deeper to determine the motor representations in the medial bank of frontal cortex. At sites located 1.5–3.0 mm rostral, stimulation at depths 1.5–2.5 mm below the pial surface evoked eye movements visible to the naked eye. Further caudally, 1-s long train stimulation evoked repetitive rhythmic whisker movements at M1 (M1-RW) sites located 0.5–1.7 mm rostral to bregma. Whisker movements at M1-RW sites were frequently bilateral (Haiss and Schwarz, 2005). Both FEF and M1-RW are located deep in the medial bank of frontal cortex, but they have distinct domains along the rostral and caudal axis.

EXTRACELLULAR NEURONAL RECORDINGS

To identify sites in primary visual cortex (V1), the same electrodes used for ICMS mapping were used to map visual cortex. After disconnecting the electrode from the constant current source, it was connected to the headstage of a Dagan amplifier (Model 2200) so that extracellular discharges could be amplified, bandpass filtered (300–3000 Hz), and monitored with an oscilloscope and acoustic speaker. Electrodes were placed at stereotaxic coordinates (5.0–7.0 mm caudal to bregma, 2.0–4.0 mm lateral) that correspond to V1 (Paxinos and Watson, 2007), and were advanced ∼400 μm into the brain to reach layer IV. Neuronal responses to visual stimulation were tested by manipulating a handheld blue LED in different directions over the ipsilateral and contralateral eyes to identify responsive areas corresponding to the monocular or binocular regions of V1. Because this procedure may not distinguish V1 from adjacent visual areas, injection sites in V1 were verified by cytoarchitectonic criteria (see Results).

TRACER INJECTIONS

Tracers were injected either iontophoretically or by pressure. For anterograde tracing, 15% solutions of FluoroRuby (FR; D-1817, Invitrogen) or biotinylated dextran amine (BDA; D-7135, Invitrogen) in 0.01 M phosphate buffered saline (PBS) were used. For retrograde tracing, 2% solutions of True Blue chloride (TB; T-1323, Invitrogen) or Fluorogold (FG; H-22845, Fluoro-Chrome) were used.

The FEF received iontophoretic injections of BDA or FG from glass pipettes (∼30 μm tip). A retention current (-7.0 μA) was used to limit tracer leakage while advancing the pipette to its injection depth, where the retention current was turned off and

positive current pulses of 2–5 μA (7 s on/off duty cycle) were applied for 10–20 min to eject the tracer at two depths separated by 300 μm. In one rat, a mixture of FG and BDA was iontophoretically ejected in FEF. Visual cortex received pressure injections of FR or TB from Hamilton syringes in which glass pipettes (∼50 μm diameter tips) were cemented on the end of the needle. A summary of the tracer injections is in **Table 1**.

Following tracer injections, the skin was sutured and treated with antibiotic ointment. Each animal received additional doses of atropine, dexamethasone, and enrofloxacin. Animals were returned to single housed cages for a 7–10 day survival period to allow for tracer transport.

HISTOLOGY

Rats were deeply anesthetized with IM injections of ketamine (80 mg/kg) and xylazine (18 mg/kg) and perfused transcardially with heparinized saline, 4% paraformaldehyde, and 4% paraformaldehyde with 10% sucrose. Brains were removed and stored in 4% paraformaldehyde and 30% sucrose at 4°C until saturated.

All brains were sectioned bilaterally into 60-μm slices using a freezing microtome with a slit in the left hemisphere (ventral to the rhinal fissure) to allow proper orientation when mounting. Serially-ordered sections were divided into three series. The first series was mounted on gelatin-coated slides, and then dried and stained with thionin acetate to reveal cytoarchitecture. The second series was processed to visualize BDA using a heavy metal enhanced horse radish peroxidase immunohistochemical reaction as previously described (Kincaid and Wilson, 1996; Smith et al., 2012a). Briefly, sections were first washed in 0.3% H_2O_2 to degrade endogenous enzyme activity, rinsed in two 0.3% Triton-X-100 (TX-100) washes, and then incubated for 2 h in avidin-biotin horse radish peroxidase solution mixed in 0.3% TX-100. Sections were then washed twice in 0.1 M PBS and incubated in 0.05% DAB, 0.0005% H_2O_2, 0.05% $NiCl_2$, and 0.02% $CoCl_2$ in 0.1 M tris buffer (pH = 7.2) for 10 min. Two subsequent washes in 0.1 M PBS stopped the reaction. Following immunohistochemistry to visualize BDA, sections were mounted on gelatin-coated slides, dried overnight, dehydrated in ethanol, cleared in xylene and coverslipped with Cytoseal. The third series was directly mounted, dried, dehydrated, defatted, and coverslipped to visualize fluorescent tracers alone.

Table 1 | Summary of tracer injections from current study and previously published data (Smith and Alloway, 2010).

Case	Left hemisphere		Right hemisphere	
	Motor region	Sensory region	Motor region	Sensory region
TI-14	–	V1 (FR)	FEF (FG/BDA)	V1 (TB)
TI-15	FEF (BDA)	V1 (FR)	FEF (FG)	V1 (TB)
TI-16	FEF (BDA)	V1 (FR)	FEF (FG)	V1 (TB)
CL-01	M1-Re (FR)	–	M1-Re (FG)	–
CL-02	M1-Re (FR)	–	M1-Re (FG)	–
CL-03	M1-Fp (FR)	–	M1-Fp (FG)	–
CL-04	M1-Fp (FR)	–	M1-Fp (FG)	–
CL-05	M1-Re (FR)	–	M1-Re (FG)	–
CL-06	M1-Fp (FR)	–	M1-Fp (FG)	–
CL-21	M1-RW (FR)	–	M1-RW (FG)	–
CL-22	M1-RW (FR)	–	M1-RW (FG)	–
CL-23	M1-RW (FR)	–	M1-RW (FG)	–

Anterograde tracers: BDA, biotinylated dextran amine; FR, FluoroRuby. Retrograde tracers: FG, FluoroGold; TB, True Blue Chloride.

ANATOMICAL ANALYSIS

All tissue was inspected with an Olympus BH-2 microscope equipped for both brightfield and fluorescent microscopy. Terminals labeled with BDA were visualized with brightfield, whereas TB and FG labeling were visualized with a near UV filter (11000v2; Chroma Technologies), and a TRITC filter (41002, Chroma Technologies) was used for FR labeling. Labeled soma and terminal synapses were plotted and digitally reconstructed using optical transducers attached to the microscope stage (MDPlot, Accustage). For anterograde tracers, beaded varicosities on the axonal terminals were plotted because they represent en passant synapses (Voight et al., 1993; Kincaid and Wilson, 1996). For retrograde tracers, only labeled cells with dendrites were plotted. Digital photomicrographs of brightfield and fluorescent labeling were acquired with a Retiga EX CCD digital camera mounted on the BH-2 microscope. Additional images were obtained with an Olympus FV1000 laser scanning confocal microscope using a 60× oil immersion objective. For TB (405 nm excitation, 410–460 nm emission) and FG (405 nm, excitation, 520–600 nm), sections were scanned sequentially to demonstrate both single and double labeled neurons and were then merged to produce a composite image.

Quantitative analysis of tracer reconstructions was performed using MDPlot software (version 5.1; Accustage). Analysis of the claustrum was confined to sections that contained the striatum because more rostral levels do not contain the claustrum-associated Gng2 protein (Mathur et al., 2009). After the sections were plotted, a grid of 50 μm^2 bins was superimposed on the reconstructions. Bins containing at least four labeled terminals and one labeled neuron were classified as containing overlapping tracer labeling. Analyses of BDA-FG and BDA-TB overlap were performed separately. The number of overlapping bins was expressed as a percentage of the total number of bins that contained tracer labeling. Statistical analysis was performed using Origin software (version 8.0; Origin Lab). Because BDA processing diminishes the intensity of fluorescence, the third series, which was processed for fluorescence but not BDA, was used to count FG- and TB-labeled and double-labeled neurons.

In addition to our own neuroanatomical tracing experiments, corticoclaustral connectivity in mice was analyzed by accessing data in the Allen Mouse Brain Connectivity Atlas. The analyzed cases were chosen based on the Allen Brain Institute's designation of cortical injection site area. We chose homologous cytoarchitectonic regions and confirmed the functional representation of these regions based on labeling patterns in subcortical structures (see Results).

RESULTS

To compare the claustral connections with FEF and V1, three rats received different anterograde and retrograde tracers in FEF

and V1 of the left and right hemispheres, respectively, (**Table 1**). Combining different tracer injections in the same animal allowed us to quantify tracer overlap in the claustrum bilaterally and determine the relative strength of corticoclaustral and claustrocortical connections with FEF and visual cortex.

In the first rat, a combined solution of FG and BDA was iontophoretically injected into FEF of the right hemisphere, whereas FR and TB were separately injected into V1 of the left and right hemispheres, respectively. In the other two rats, BDA and FR were separately injected into respective sites in FEF and V1 of the left hemisphere, whereas FG and TB were separately injected into respective sites in FEF and V1 of the right hemisphere.

PROJECTIONS FROM FEF

In agreement with previous reports (Neafsey et al., 1986; Brecht et al., 2004; Haiss and Schwarz, 2005), cortical sites that evoked eye movements were consistently found at coordinates in the cingulate (Cg) cortex. As shown by **Figures 1**, **2**, tracer injections at these sites were largely confined to CG cortex but some tracer occupied the most medial part of the medial agranular (med-AGm) cortex. While FEF is rostral to M1 sites that evoke rhythmic whisking movements, both FEF and M1-RW reside in Cg and, possibly, the most medial part of AGm (med-AGm) as defined by cytoarchitectonic criteria.

Many BDA-labeled projections from FEF terminated in visual cortex and brainstem regions such as the dorsomedial superior colliculus, periaqueductal gray, oculomotor complex, and the pontine reticular formation. These results corroborate studies that placed rodent FEF in the Cg/med-AGm region on the basis of its connections with oculomotor-related nuclei in the brainstem (Leichnetz et al., 1987; Stuesse and Newman, 1990; Bosco et al., 1994; Guandalini, 2003).

Labeled projections from FEF terminated in the contralateral Cg and other forebrain structures in both hemispheres, including the dorsomedial neostriatum, ventral claustrum (vCLA), and thalamus (see **Figure 1**). These patterns are similar, but not identical, to projections from the M1 whisker regions, (Alloway et al., 2008, 2009). While projections from FEF terminate more medially in neostriatum than those from M1-Wh, both motor regions project to numerous thalamic regions including the anteromedial (AM), interanteromedial (IAM), paracentral (PC), centrolateral (CL), parafasicular (Pf), reuniens (Re), ventral anterior (VA), and ventromedial (VM) nuclei. The FEF also projects to the ipsilateral mediodorsal (MD) nucleus and, to a lesser extent, to the contralateral MD (**Figures 1G'–J**), and these projections to MD appear homologous to the FEF projections in primates (Stanton et al., 1988; Sommer and Wurtz, 2004).

Inspection of the claustrum in both hemispheres revealed dense projections from the contralateral FEF. As seen in both **Figures 1**, **2**, BDA injections in FEF produced dense terminal labeling in a large part of the contralateral vCLA, but produced noticeably weaker labeling in a smaller area in the ipsilateral vCLA. These corticoclaustral projections from FEF are remarkably similar to the pattern of corticoclaustral projections that originate from the M1 whisker regions (Smith and Alloway, 2010).

PROJECTIONS FROM V1

We used physiology, cytoarchitecture, and demarcations in the Paxinos and Watson (2007) atlas to confirm the injections in V1. Cytoarchitecturally, V1 is characterized by a prominent granular layer IV, which is not present in surrounding medial and lateral secondary visual cortices, areas 18a and b (Miller and Vogt, 1984b). Substantial amounts of transported tracer in the lateral geniculate nucleus (LGN) of the thalamus further confirmed our injections into V1 (data not shown).

Examination of the claustrum in both hemispheres revealed very sparse projections from V1 cortex. In fact, as shown in **Figure 2**, the few labeled projections from V1 to the claustrum that were most noticeable were generally located in the ipsilateral hemisphere. By contrast, projections from V1 were observed in several subcortical structures, and many of these overlapped with the projections from FEF. Labeled projections from FEF and V1 overlapped ipsilaterally in the dorsomedial neostriatum, superior colliculus, PC, CL, and lateroposterior (LP) thalamic nuclei. Non-overlapping projections from V1 and FEF appeared in the laterodorsal (LD) thalamus, the dorsal zona incerta (ZI), and in the basal pontine nuclei, in which labeled projections from FEF were observed on both sides of this structure.

CLAUSTRAL PROJECTIONS TO FEF AND V1

Injections of FG in FEF and TB in V1 of the same hemisphere produced a dense population of labeled soma in the vCLA of the ipsilateral hemisphere. As shown in **Figure 3**, FG- and TB-labeled neurons were intermingled in the ipsilateral vCLA, but very few labeled neurons appeared in the contralateral vCLA. A small proportion ($7.0 \pm 1.2\%$, mean $\pm$ s.e.m.) of the labeled soma were double labeled as shown in confocal images (see **Figures 3C,E**). Because TB is not easily visualized and is not transported as efficiently as FG, this quantitative measurement of double labeled neurons probably underestimates the proportion of claustral neurons that project to both FEF and V1.

Nonetheless, our plotted reconstructions illustrate partial overlapping populations of FG- and TB-labeled neurons in vCLA. Double-labeled neurons dominated the center of the labeled population (see **Figure 3D**), and the presence of these neurons indicates that vCLA sends divergent projections to both FEF and V1 in the ipsilateral hemisphere, as reported previously in cats (Minciacchi et al., 1985). This result is similar to our previous observations indicating that the claustrum sends divergent projections to the S1 and M1 whisker regions in the ipsilateral hemisphere (Smith et al., 2012b).

The TB and FG injections also produced intermingled labeled neurons, including double-labeled cells, in several other subcortical regions. Populations of FG- and TB-labeled neurons were intermingled in the ipsilateral intralaminar nuclei (PC, CL, IAM, Pf) and bilaterally in the Re nucleus, which occupies the midline of the thalamus. Prominent labeling, including dual-labeled cells, also appeared in the lateral preoptic area.

CORTICO-CLAUSTRO-CORTICAL CIRCUIT CONNECTIONS

Tracer overlap in the claustrum was quantified for the two cases (TI15 and TI16) in which both FEF and V1 were bilaterally injected. In these cases, BDA (FEF) and FR (V1) were deposited

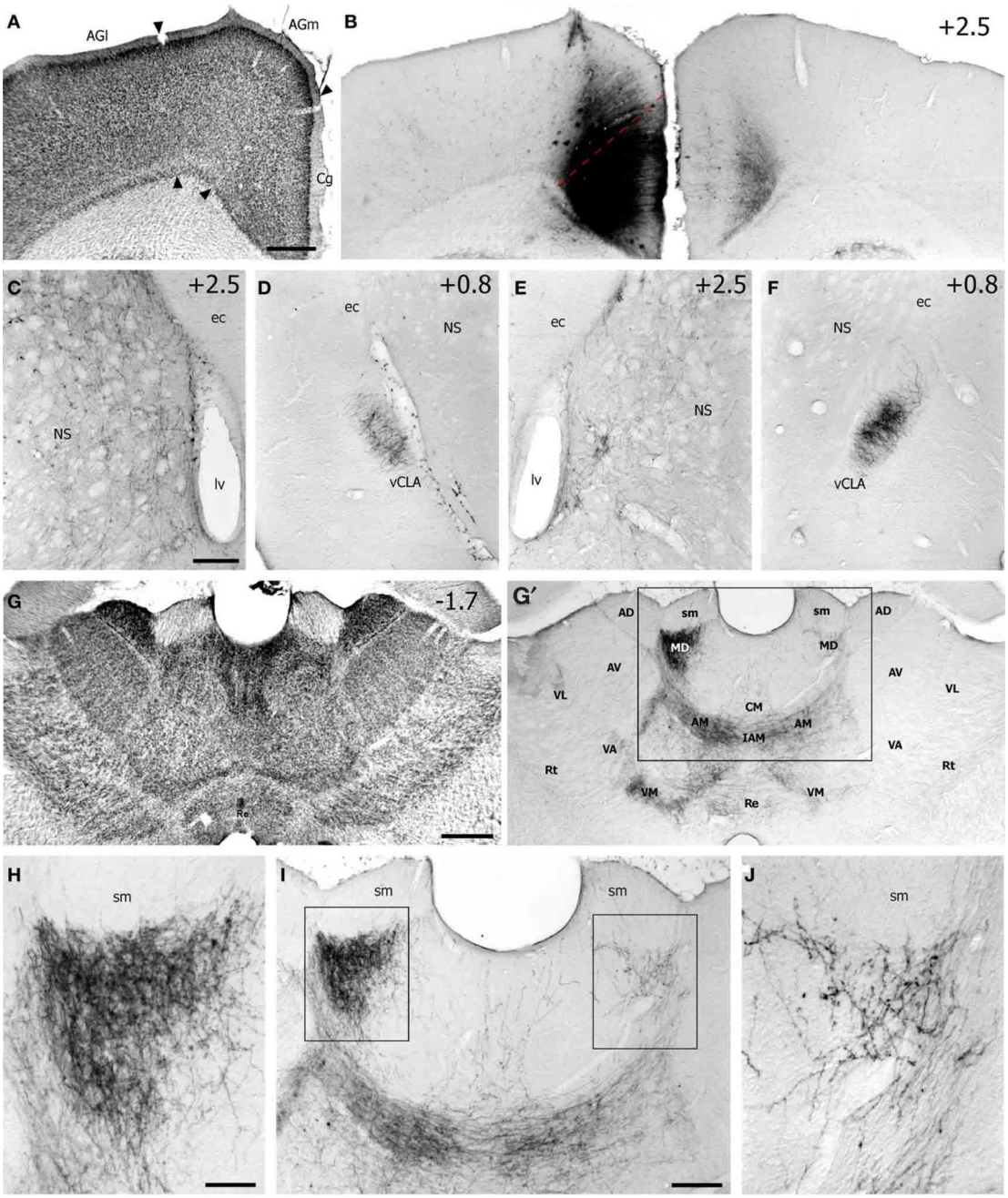

FIGURE 1 | Case TI-16 demonstrates that the FEF projects to claustrum and other forebrain regions. (A) Nissl-stained section through the lateral agranular (AGl), medial agranular (AGm), and cingulate (Cg) cortices. **(B)** Deposit of biotinylated dextran amine (BDA) at an M1 site in Cg cortex that evoked eye movements and produced labeled terminals in the contralateral Cg cortex. **(C–F)** The BDA deposit produced labeled terminals in the dorsomedial neostriatum (NS) and ventral claustrum (vCLA) in the left **(C,D)** and right **(E,F)** hemispheres. **(G)** Nissl-stained section of thalamus used to identify BDA-labeled projections **(G′)** in the anterior medial (AM), interanteromedial (IAM), mediodorsal (MD), reuniens (Re), ventromedial (VM), and ventroanterior (VA) nuclei. Box corresponds to **(I)**. **(H–J)** Terminal labeling was densest in the AM and MD nuclei. Boxes in **(I)** indicate **(H,J)**. ec, external capsule; lv, lateral ventricle; sm, stria medularis; AV, anteroventral; AD, anterodorsal; CM, centromedial; Rt, reticular nucleus; VL, ventrolateral. Numbers in **(B–G)** indicate distance from bregma in millimeters. Scale bars: 500 μm in **(A,G)**; 250 μm in **(C,I)**; 100 μm in **(H)**.

on the left side while FG (FEF) and TB (V1) were injected on the right side (**Table 1**). As shown in **Figure 4B**, labeling from all four tracers occupied a compact region in the vCLA, spanning no more than 500 μm^2 within each coronal section. Using 50-μm^2 bins, a bin had to contain at least four labeled varicosities and one labeled soma to be classified as terminal-soma overlap. This represents the same standard that we used previously to assess cortico-claustro-cortical connectivity (Smith and Alloway, 2010).

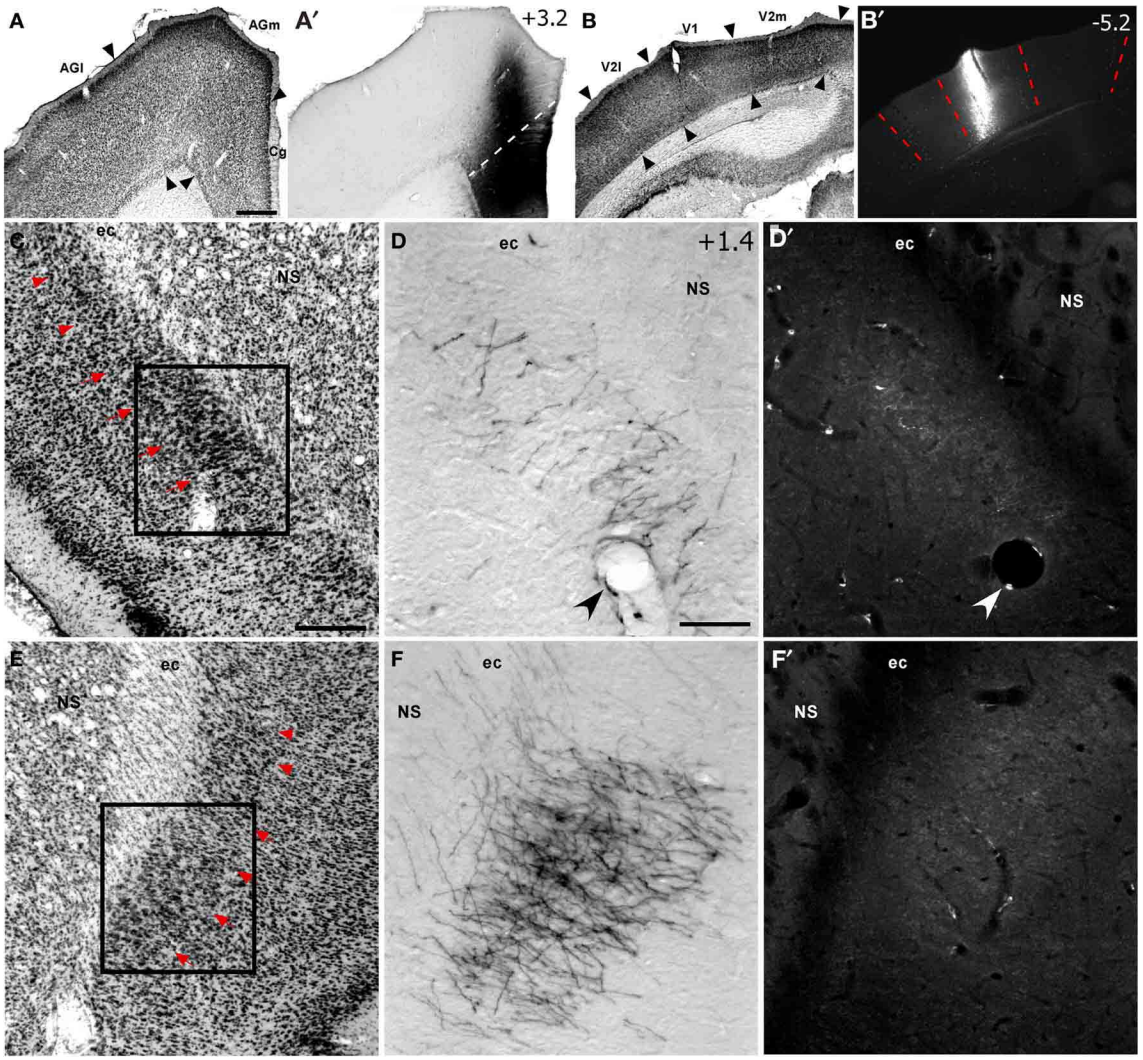

FIGURE 2 | Corticoclaustral projections from FEF and V1 in case TI-15. (A–B′) Left hemisphere injections of BDA in FEF **(A,A′)** and FluoroRuby (FR) in V1 **(B,B′)** of the same rat. BDA labeling appeared bilaterally in vCLA **(D,F)**, but was noticeably denser on the contralateral side **(F)**. Sparse FR labeling was apparent only in the ipsilateral vCLA **(D′)**. Boxes in **(C)** and **(E)** correspond to **(D,D′)** and **(F,F′)**, respectively. Red arrowheads demarcate the dorsal claustrum (dCLA) from the vCLA. Black and white arrowheads denote common blood vessels. Scale bars: 500 μm in **(A)**; 250 μm in **(C)**; 100 μm in **(D)**.

Anterograde tracer injections in the left FEF produced dense terminal labeling in the right claustrum. This terminal labeling surrounded the labeled soma produced by retrograde tracer injections in the right FEF. Our overlap analysis indicated that nearly half of the labeled bins in the right claustrum contained both tracers (see **Figure 4C**). By comparison, terminal-somal overlap in the left claustrum was virtually absent owing to a paucity of labeling from either tracer (**Figure 4A**). When terminal-soma overlap across all claustral sections was calculated, the proportion of all labeled bins that contained both BDA-labeled terminals and FG-soma (i.e., terminal-somal overlap) was much larger contralateral to the FEF-BDA injection (43.3 ± 4.6%) than ipsilaterally (5.3 ± 4.3%). Hence, the FEF projects mainly to the contralateral claustrum, which then projects to the FEF in that hemisphere to create an interhemispheric cortico-claustro-cortical circuit between the FEF regions in the two hemispheres.

A similar pattern was found for the connections between FEF and the contralateral V1 region. As shown by the section reconstructed in **Figures 4D,E**, terminal-somal overlap was 17.5% in the claustrum contralateral to the FEF-BDA injection but was 0% in the ipsilateral claustrum. When terminal-somal overlap was calculated for all sections through the claustrum that contained labeled bins, the proportion of bins that contained overlap was larger in the claustrum contralateral to the FEF-BDA injection (37.2 ± 3.0%) than in the ipsilateral claustrum (11.4 ± 1.2%). These findings clearly demonstrate the presence of an interhemispheric cortico-claustro-cortical circuit in which the FEF transmits information disynaptically to the

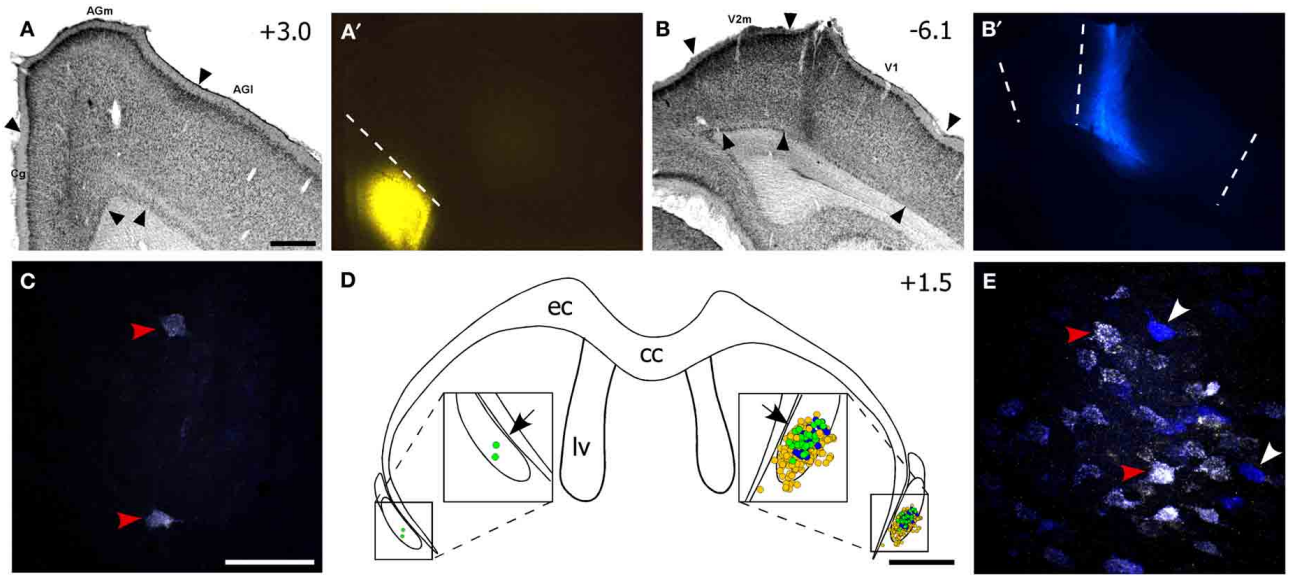

FIGURE 3 | The ventral claustrum projects to both FEF and V1. (A–B′) Fluorogold (FG) deposit in FEF and True Blue (TB) in V1 of the right hemisphere for the same case in **Figure 2**. **(C)** Confocal image of two faintly double-labeled neurons in the left vCLA. **(D)** Reconstruction of labeled soma in the vCLA. Yellow and blue dots are FG- and TB-labeled soma, respectively, and green dots are double-labeled neurons. Black arrows indicate areas in **(C,E)**. **(E)** Confocal image of multiple retrogradely-labeled neurons in the right CLA. Red arrowheads in **(C,E)** indicate double-labeled neurons, white arrowheads indicate TB-labeled neurons. Scale bars: 500 μm in **(A)**; 50 μm in **(C)**; 1 mm in **(D)**.

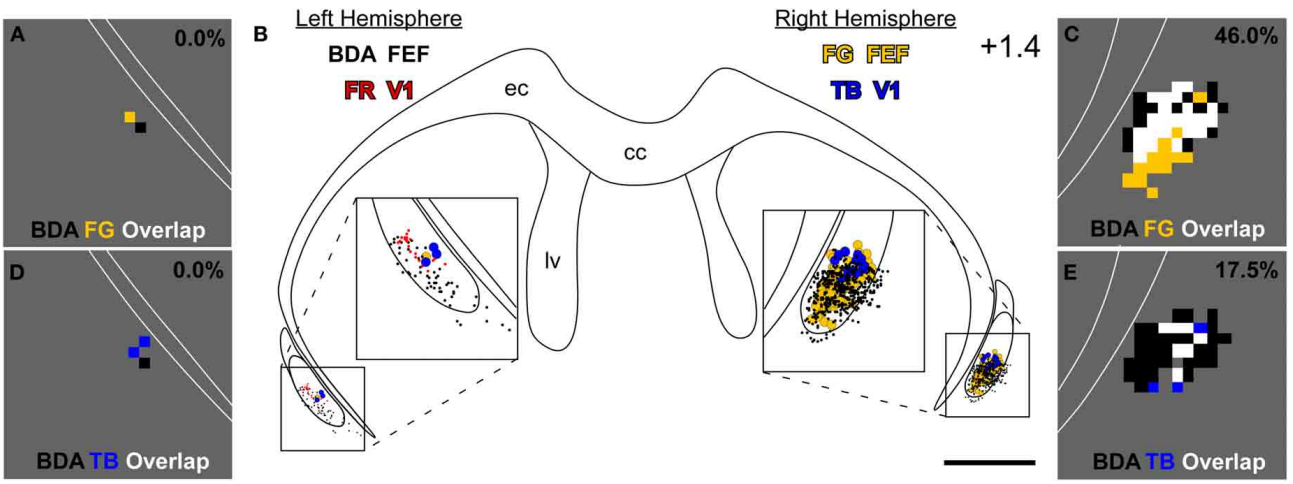

FIGURE 4 | Projections from the left M1-FEF terminate in the right claustrum, which projects to FEF and V1 in the right hemisphere. (B) Reconstructions of claustral labeling for the same case depicted in **Figures 2**, **3**. BDA- and FR-labeled terminals shown as black and red dots, respectively; TB- and FG-labeled soma shown as blue- and gold-filled circles, respectively. **(A,C)** Overlap analysis in the left **(A)** and right **(C)** claustrum shows black bins, which contain at least four BDA-labeled varicosities; gold bins, which contain at least one FG-labeled soma; and white bins, which contain both an FG-labeled soma and four BDA-labeled varicosities. **(D,E)** Overlap analysis of BDA-labeled terminals and TB-labeled soma using the same threshold criteria for the bins as in **(A,C)**. Percentages represent fraction of total bins that are colored white in the claustrum of this specific section (i.e., terminal-soma overlap). Scale bars: 1 mm in **(B)**. Bin sizes: 50 μm^2 in **(A,C–E)**.

contralateral V1 by means of its projections to the contralateral claustrum.

RETROGRADE CONFIRMATION OF CORTICOCLAUSTRAL PROJECTIONS

Our anterograde tracing results indicate that V1 sends very weak projections to the claustrum, whereas FEF sends dense projections to vCLA. To confirm this finding, we inspected data from our previous study in which we injected FG into the claustrum (see Figure 9 in Smith and Alloway, 2010). In that case, the contralateral frontal cortex contained many retrogradely-labeled neurons in the Cg and medial AGm regions (see Figures 10, 11 in Smith and Alloway, 2010), but no labeled neurons were

observed in the S1 barrel region of either hemisphere. In the occipital region, however, separate populations of FG-labeled neurons were found ipsilaterally (data not reported previously). As indicted by **Figure 5**, a few labeled neurons appeared in layer VI of primary visual cortex (V1) and lateral secondary visual cortex (V2l), but many more labeled neurons were observed in the medial part of the secondary visual cortex (V2m), which is consistent with previous reports (Miller and Vogt, 1984a; Carey and Neal, 1985).

FUNCTIONAL TOPOGRAPHY OF CLAUSTRAL CONNECTIONS WITH MOTOR CORTEX

The claustral connections with FEF in the present study were compared to the claustral connections for the M1 whisker (M1-RW, M1-Re) and M1 forepaw (M1-Fp) representations that we characterized previously (Smith and Alloway, 2010). **Figure 6** shows the rostrocaudal distribution of claustral labeling produced by injecting retrograde (**Figure 6A**) or anterograde (**Figure 6B**) tracers into these four motor regions (summary of injections in **Table 1**). Statistical analysis revealed significant effects for injection location and hemispheric labeling for both anterograde (Injected area: $F = 34.2$; $p < 0.00001$; Hemispheric labeling: $F = 25.1$; $p < 0.00001$) and retrograde injections (Injected area: $F = 10.5$; $p < 0.00001$; Hemispheric labeling: $F = 95.1$; $p < 0.00001$).

The FEF, M1-RW, and M1-Re regions all project significantly more strongly to the contralateral than to the ipsilateral claustrum (FEF, paired $t = 2.46$, $p < 0.05$; M1-RW, paired $t = 6.26$, $p < 0.000001$; M1-Re, paired $t = 5.59$, $p < 0.00001$). Following retrograde tracer injections into these motor regions, however, the number of labeled neurons is much larger ipsilaterally (FEF, paired $t = 7.34$, $p < 0.0000001$; M1-RW, paired $t = 6.46$, $p < 0.000001$; M1-Re, paired $t = 5.38$, $p < 0.00001$). By comparison, labeling produced by tracer injections in M1-Fp is extremely weak in both directions and is present almost entirely on the ipsilateral side (anterograde labeling, $t = 6.04$, $p < 0.000001$; retrograde labeling, $t = 5.60$, $p < 0.00001$).

The retrograde labeling patterns observed in the claustrum in the present study were compared with three cases of retrograde labeling in the claustrum (CL01, CL05, and CL21) that

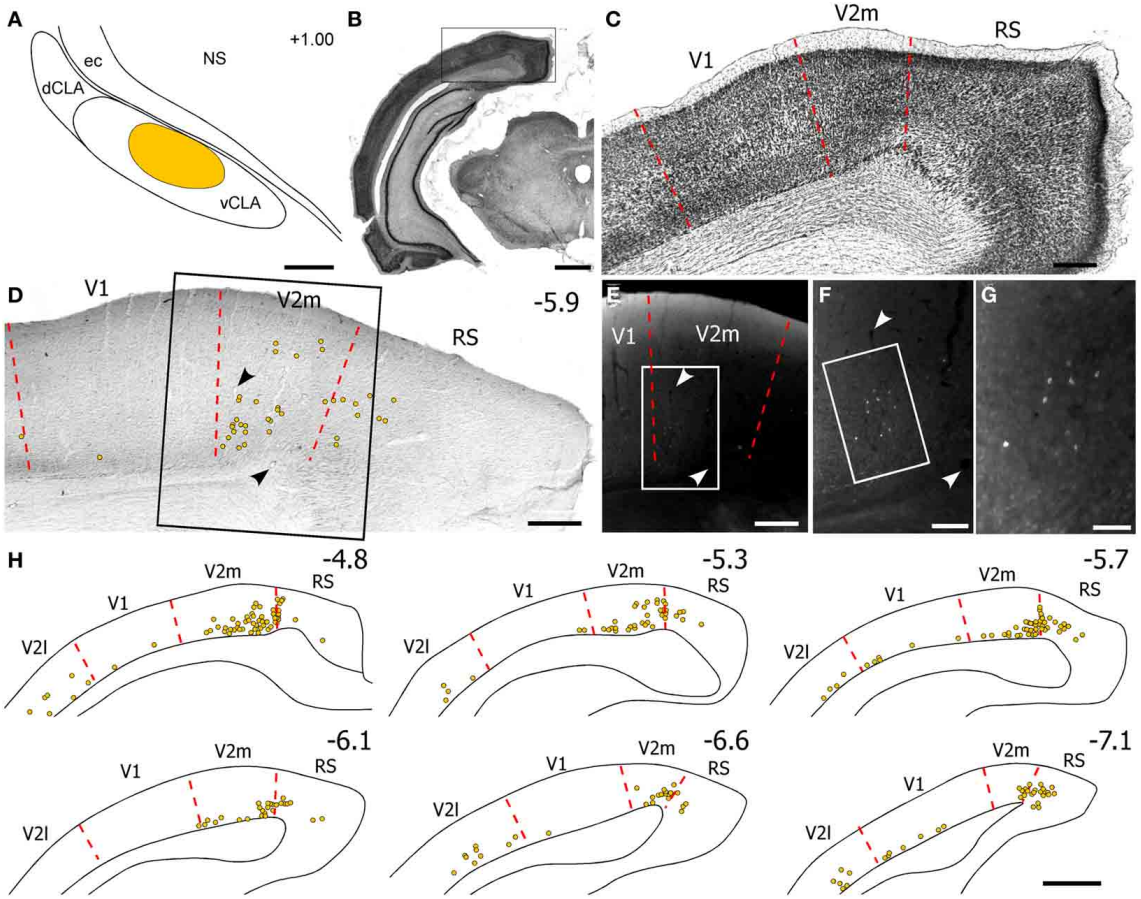

FIGURE 5 | Few neurons in visual cortex project to the claustrum. **(A)** Reconstruction of an FG deposit in claustrum depicted in Figure 9 of Smith and Alloway (2010). **(B,C)** Nissl-stained section through primary visual (V1), medial secondary visual (V2m), and retrosplenial cortices. **(D)** Plotted location of FG-labeled neurons in an adjacent section. Inset in **(D)** indicates location of **(E)**. **(F,G)** Successive magnifications of retrogradely-labeled soma in V2m. **(H)** Digital reconstructions of FG-labeled neurons in visual cortex. Numbers indicate caudal distance from bregma. Scale bars: 250 μm in **(A,C–E)**; 1 mm in **(B,H)**; 100 μm in **(F)**; 50 μm in **(G)**.

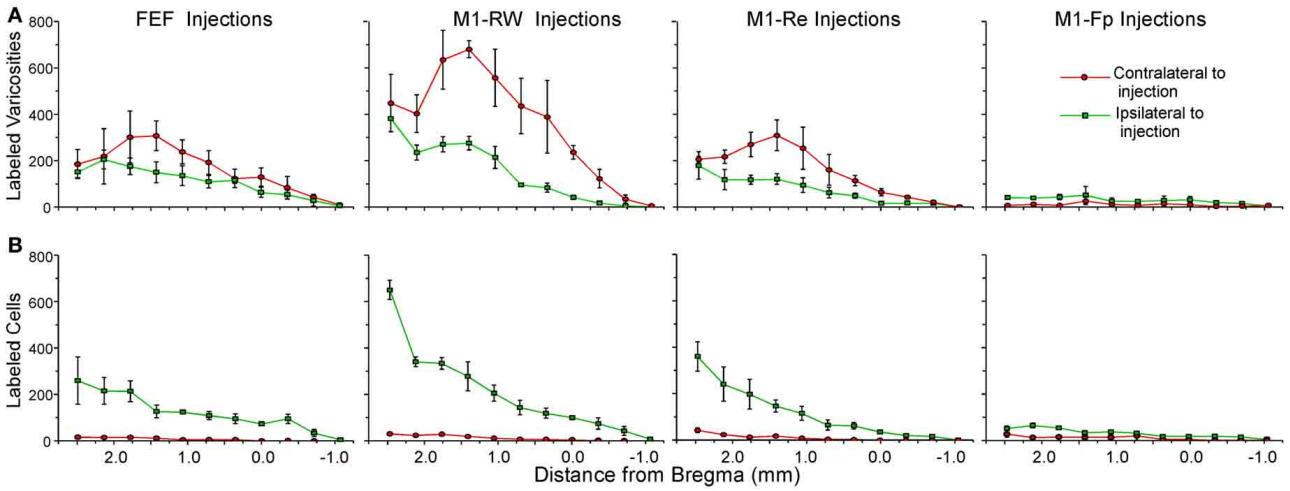

FIGURE 6 | Distribution of mean terminal and cell counts from tracer injections in different parts of rat motor cortex. (A) Labeled terminal counts in the ipsilateral and contralateral claustrum from BDA and FR injections in FEF and in the rhythmic whisking (M1-RW), whisker retraction (M1-Re), and forepaw (M1-Fp) regions from a previous study (Smith and Alloway, 2010). **(B)** Labeled cell counts in the claustrum of both hemispheres from FG injections in the same regions. Symbols in each line graph represent the mean counts per section from three tracer injection cases; error bars represent standard error of the mean.

were illustrated previously in Figures 1–3 of Smith and Alloway (2010). These comparisons indicate that the claustrum has a distinct functional topography. As shown in **Figure 7**, each ICMS-defined and tracer-injected motor region is linked to a specific part of the claustrum. The FG injections in FEF (case TI-15) and in M1-RW (case CL21), which occupy the Cg/med-AGm region, produced retrograde labeling in the deepest parts of the vCLA. The FG injection in M1-Re (case CL05), which is centered in AGm, produced labeling in the middle of vCLA. Finally, an FG injection in M1-Fp (case CL03), which occupies AGl, revealed labeled neurons mainly in the dCLA. These data indicate that the claustrum has a topographic organization in which the medial to lateral extent of M1 cortex is represented ventral to dorsal in the claustrum.

These claustrum subdivisions are defined not only by the specificity of their inputs from motor cortex, but also by their projections to different sensory regions. Comparison of the retrograde labeling in the present study with those from our previous report (Smith et al., 2012b), indicates that vCLA projects to both FEF and V1, whereas the middle of the claustrum projects to both M1-Re and S1-Wh.

CORTICOCLAUSTRAL PROJECTIONS IN MICE

We inspected the corticoclaustral connections in the Allen Mouse Brain Connectivity Atlas (2012), and focused on cases with tracer injections in S1, V1, Cg, AGm, and AGl. We examined mouse cases in which the tracers filled all cortical layers and the injection locations appeared equivalent to our injection sites as determined by the surrounding anatomical landmarks. Finally, we analyzed whether the terminal labeling patterns in the forebrain and brainstem matched the patterns seen in our rat experiments to assure functional homology with our data. We observed, for example, that Cg injections in mice produced labeling in the dorsomedial neostriatum, nucleus MD in the thalamus, dorsomedial superior colliculus, and the ocular motor complex in the midbrain. This pattern of labeling is completely consistent with the patterns that we observed when anterograde tracers were deposited in the FEF (Cg cortex) of rats. Likewise, tracer injections in AGm or AGl of mice produced subcortical labeling patterns that are consistent with our anterograde tracer injections at sites where ICMS evoked movements of the whiskers or forelimb (Alloway et al., 2008, 2009, 2010).

Qualitative inspection of the injections in the S1-Wh (Experiment#: 126908007, 127866392) region matched our previous finding that rat S1 does not project to the claustrum (Smith et al., 2012b). Mice that received injections in V1 showed sparse labeling in the ipsilateral claustrum (Experiment#: 113887162, 100141599), which corresponds to our findings when rat V1 region is injected. Finally, as shown in **Figure 8**, injections into Cg (**Figures 8A–C**; Experiment# 112514202), AGm (**Figures 8D–F**; Experiment# 141603190), and AGl (**Figures 8G–I**, Experiment# 141602484) display patterns of interhemispheric corticoclaustral labeling that are highly similar to our results in the rat. In mice, as in rats, the majority of coronal sections containing the claustrum indicate that the AGm and Cg regions project more strongly to the contralateral than to the ipsilateral claustrum (confirming findings by Mao et al., 2011), whereas AGl has sparse connections with the claustrum in either hemisphere.

DISCUSSION

By placing different anterograde and retrograde tracers in FEF and V1 of both hemispheres, this study revealed several new findings about the functional organization of the rat claustrum. Most significantly, rat FEF sends dense projections to the contralateral claustrum, but sends relatively weak projections to the ipsilateral claustrum. The claustrum receives weak projections

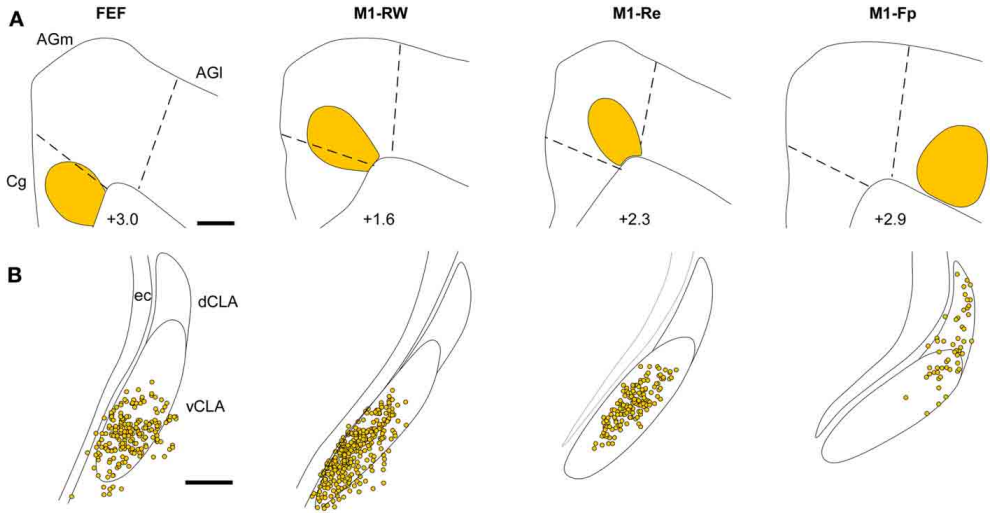

FIGURE 7 | Representative examples illustrating the topography of labeled neurons in the claustrum produced by tracer injections in FEF, M1-RW, M1-Re, and M1-Fp. (A) Reconstructions of the M1 tracer injections in the current study (case TI-15) and in cases CL-03, CL-05, and CL-21 illustrated in Figures 1–3 of Smith and Alloway (2010). **(B)** Reconstruction of FG-labeled neurons in the claustrum from each injection in **(A)**. Scale bars: 500 μm in **(A)**; 250 μm in **(B)**.

from ipsilateral V1 but is not innervated by the contralateral V1. When different retrograde tracers are injected into FEF and V1 of the same hemisphere, many intermingled and double-labeled neurons appear in the ipsilateral, but not the contralateral, claustrum.

These results indicate that the claustrum is part of an interhemispheric circuit for transmitting information from FEF to separate visuomotor regions in the other hemisphere. Our previous work shows that the claustrum has a parallel set of circuit connections with the M1 and S1 whisker regions (Smith and Alloway, 2010; Smith et al., 2012b). Collectively, these findings indicate that the claustrum has a role in the interhemispheric transmission of certain types of sensorimotor information.

While the claustrum receives dense interhemispheric projections from cortical motor regions that regulate movements of the whiskers and eyes, the M1 limb regions send very weak projections to the claustrum and only within the same hemisphere. These differences in the density of corticoclaustral projections from different parts of M1 are also apparent in the Allen Mouse Brain Connectivity Atlas. A summary of these functional differences in claustral connectivity is illustrated in **Figure 9**.

Our last major finding is that the claustrum has a well-defined functional topography along its dorsoventral axis. The M1 forepaw region projects to the dorsal claustrum, the M1 whisker region projects to the middle claustrum, and the FEF region projects to the vCLA. Likewise, the S1 forelimb, the S1 whisker, and the V1 regions receive projections from the dorsal, middle, and vCLA, respectively.

VISUOMOTOR CLAUSTRUM CIRCUITRY

Corticoclaustral projections from the frontal and occipital cortices differ both qualitatively and quantitatively. The FEF projects densely to the contralateral claustrum, but only weakly to the ipsilateral claustrum. Visual cortex sends some projections to the ipsilateral claustrum, but these originate mainly from V2m, which also projects to FEF and the ventral superior colliculus, regions known for controlling saccadic eye movements (Wang and Burkhalter, 2013; Wang et al., 2013). The corticoclaustral projections from both FEF and V2m originate from layer V, which is significant because this layer contains corticobulbar motor output neurons. These facts indicate that rat vCLA has a role in processing information concerned with eye movements.

The lack of reciprocal projections between certain cortical areas and the claustrum provides some clues about the function of the claustrum. While FEF projects strongly to the contralateral claustrum, the claustrum projects ipsilaterally to FEF but does not send feedback projections to the contralateral FEF. Likewise, the connections between the claustrum and primary visual cortex are not reciprocal. The claustrum projects strongly to ipsilateral V1, but reciprocal projections from V1 to the claustrum are practically nil (Miller and Vogt, 1984a; Carey and Neal, 1985). After placing different retrograde tracers in FEF and V1 of the same hemisphere, we observed many double-labeled neurons in the ventral part of the ipsilateral claustrum, and this indicates that identical information is transmitted from vCLA to both FEF and V1.

When these divergent claustral projections to V1 and FEF are considered with the relative weakness of corticoclaustral feedback projections in the same hemisphere, the emerging circuit suggests that the claustrum is important for coordinating V1 and FEF processing in the same hemisphere.

FUNCTIONAL TOPOGRAPHY IN THE CLAUSTRUM

Our studies demonstrate that rat claustrum has a well-defined functional topography. In a previous report we showed that the M1 forelimb region is linked to dCLA, whereas the M1 whisker region is connected to vCLA (Smith and Alloway, 2010). The present study extends this work by showing that visuomotor

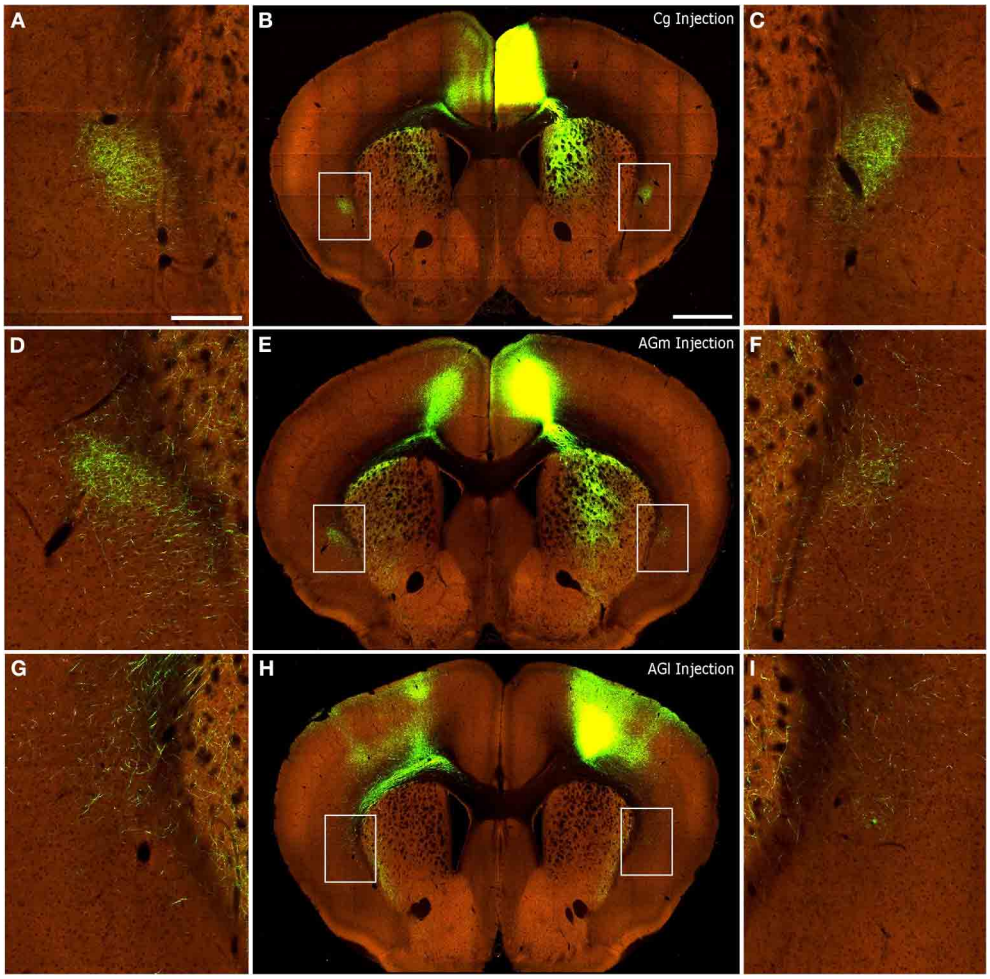

FIGURE 8 | Corticoclaustral projections from Cg, AGm, and AGl in mice. Images of AAV injections and subsequent labeling acquired from the Allen Mouse Brain Connectivity Atlas (2012). Center panels show images of labeling from representative AAV tracer injections in Cg **(B)**, AGm **(E)**, and AGl **(H)**. Hyperlinks connect to the complete data sets on the Allen Institute website. In each case, labeling appears in the contralateral cortex as well as bilaterally in the striatum and claustrum. **(A,D,G)** correspond to insets of the claustrum in the left hemisphere of center panels. **(C,F,I)** likewise correspond to insets of the claustrum in the right hemisphere of center panels. Scale bars: 250 μm in **(A)**; 1 mm in **(B)**.

cortical areas are connected to the most ventral part of vCLA. We have observed intraclaustral connections along the rostrocaudal, but not the dorsoventral axis (Smith and Alloway, 2010). This anisotropic organization of intraclaustral connectivity is consistent with the segregation of unimodal responses in different subregions of the primate claustrum (Remedios et al., 2010).

THEORETICAL FUNCTION OF INTERHEMISPHERIC SENSORIMOTOR CLAUSTRAL CIRCUITS

We recently injected different retrograde tracers into S1 and M1, and we observed many double-labeled neurons in the claustrum (Smith et al., 2012b). In the present study we observed many double-labeled claustral neurons after injecting different retrograde tracers into FEF and V1. These results are consistent with Type A and B claustral neurons that were previously reported in the brains of rats and cats (Minciacchi et al., 1985). Selective placement of different retrograde tracers in cortex of the same animals has revealed claustral neurons that innervate both ipsilateral and contralateral frontal regions (Type C neurons), and others that innervate the contralateral frontal and ipsilateral occipital regions (Type D neurons). Other studies on a variety of mammalian species have identified specific claustral regions that project to sensory and motor cortical areas, including divergent projections to the S1 and S2 cortices (Li et al., 1986; Sadowski et al., 1997; Jakubowaska-Sadowska et al., 1998).

The presence of double-labeled neurons demonstrates that the claustrum conveys the same information to separate, but functionally-related cortical areas. While the exact nature of the information that is transmitted to FEF and V1 (or to the M1 and S1 whisker regions) remains unknown, claustral divergence provides a mechanism for ensuring simultaneous processing of the same information in separate cortical regions.

Our findings in two different sensorimotor systems indicate that dense interhemispheric projections to the claustrum

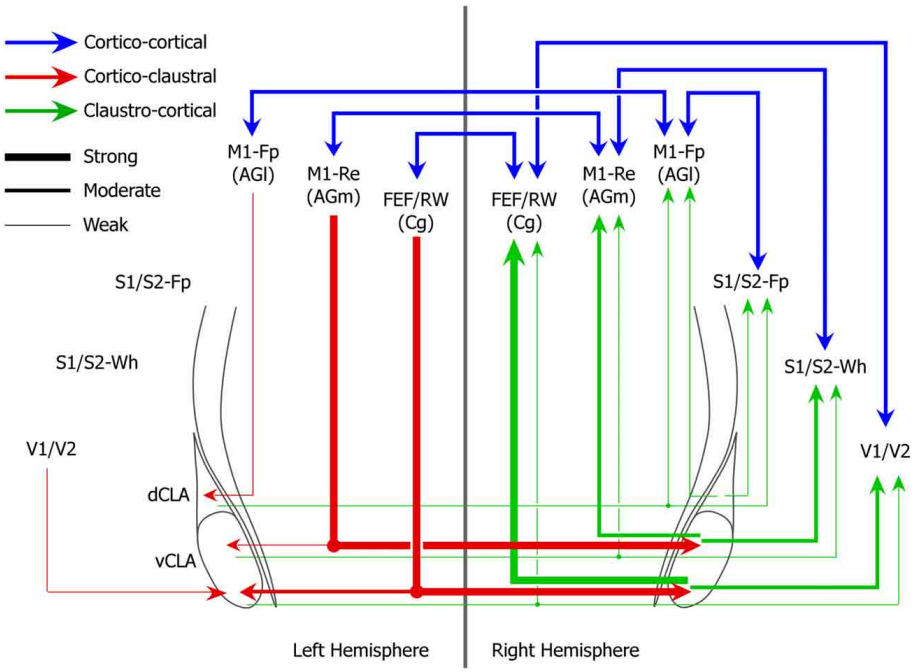

FIGURE 9 | Circuit diagram of interhemispheric sensorimotor cortico-claustro-cortical circuits in rats. Strength of projections are indicated by line thicknesses (see legend).

originate from motor regions in frontal cortex. Mounting evidence indicates that these frontal regions (Cg, AGm) in the rat are involved not only in motor control, but also in directed-attention and memory-guided orienting behaviors (Reep and Corwin, 2009; Erlich et al., 2011; Boly et al., 2013).

Transmission of attention-related motor signals to the claustrum is supported by the fact that the several intralaminar thalamic nuclei also have connections with the claustrum. Many tracing studies have reported that the claustrum receives non-reciprocal projections from the centromedial, CL, PC, and Pf nuclei (Kaufman and Rosenquist, 1985; Sloniewski et al., 1986b; Vertes et al., 2012; Alloway et al., 2014). Substantial evidence implicates these intralaminar nuclei with a critical role in attention and conscious perception, (Hudetz, 2012), and these connections suggest that the claustrum is involved in dispersing attention-dependent signals during the conscious state.

Consistent with our past work (Smith and Alloway, 2010; Smith et al., 2012b), the present study supports our hypothesis that claustral connections enable interhemispheric transmission of certain types of modality-specific information to widely-separated cortical areas. By transmitting information from the frontal cortex in one hemisphere to parietal and occipital regions in the other hemisphere, the claustrum provides an interhemispheric route that extends beyond the other callosal projections that interconnect corresponding sites in both hemispheres.

Ocular saccades and whisking are rapid movements involved in the active acquisition of visual and somesthetic information from both sides of the body. These movements are purposeful, they require a conscious state, and they are dynamically modulated by sensory inputs. In addition to callosal connections between corresponding cortical areas in the two hemispheres, the claustrum provides a node for transmitting attention-dependent sensorimotor signals from one frontal region to multiple sensorimotor regions in the other hemisphere. This is especially relevant when attention is directed toward improving the acquisition and interpretation of sensory inputs that may come from a broad expanse of extra-personal space. Indeed, studies in the human visual system have indicated that callosal connections and subcortical circuits are involved in interhemispheric visuomotor integration, "promoting a unified experience of the way we perceive the visual world and prepare our actions" (Schulte and Muller-Oehring, 2010). In our view, the claustrum facilitates interhemispheric corticocortical transmission so that multiple sensorimotor cortical regions can work together to produce a stable global percept out of the rapidly shifting sensory information coming in from sensors on both sides of the head.

ACKNOWLEDGMENTS

This work was supported by NIH grant NS37532 awarded to Kevin D. Alloway.

REFERENCES

Allen Mouse Brain Connectivity Atlas. (2012). *Allen Institute for Brain Science*. Available online at: http://connectivity.brain-map.org/

Alloway, K. D., Olson, M. L., and Smith, J. B. (2008). Contralateral corticothalamic projections from MI whisker cortex: potential route for modulating hemispheric interactions. *J. Comp. Neurol.* 510, 100–116. doi: 10.1002/cne.21782

Alloway, K. D., Smith, J. B., and Beauchemin, K. J. (2010). Quantitative analysis of the bilateral projections from the MI whisker and forepaw regions to the brainstem. *J. Comp. Neurol.* 518, 4546–4566. doi: 10.1002/cne.22477

Alloway, K. D., Smith, J. B., Beauchemin, K. J., and Olson, M. L. (2009). Bilateral projections from rat MI whisker cortex to the neostriatum, thalamus, and

claustrum: forebrain circuits for modulating whisker behavior. *J. Comp. Neurol.* 515, 548–564. doi: 10.1002/cne.22073

Alloway, K. D., Smith, J. B., and Watson, G. D. R. (2014). Thalamostriatal projections from the medial posterior and parafasicular nuclei have distinct topographic and physiologic properties. *J. Neurophysiol.* 111, 36–50. doi: 10.1152/jn.00399.2013

Andrews, T. J., and Coppola, D. M. (1999). Idiosyncratic characteristics of saccadic eye movements when viewing different visual environments. *Vision Res.* 39, 2947–2953. doi: 10.1016/S0042-6989(99)00019-X

Boly, M., Seth, A. K., Wilke, M., Ingmundson, P., Baars, B., Laureys, S., et al. (2013). Consciousness in humans and non-human animals: recent advances and future directions. *Front. Psychol.* 4:625. doi: 10.3389/fpsyg.2013.00625

Bosco, G., Giaquinta, G., Raffaele, R., Smecca, G., and Perciavalle, V. (1994). Projections from the cerebral cortex to the accessory oculomotor nuclei of the rat: a neuroanatomical and immunohistochemical study. *J. Hirnforsch.* 35, 521–529.

Brecht, M., Krauss, A., Muhammad, S., Sinai-Esfahani, L., Bellanca, S., and Margrie, T. W. (2004). Organization of rat vibrissa motor cortex and adjacent areas according to cytoarchitectonics, microstimulation, and intracellular stimulation of identified cells. *J. Comp. Neurol.* 479, 360–373. doi: 10.1002/cne.20306

Carey, R. G., and Neal, T. L. (1985). The rat claustrum: afferent and efferent connections with visual cortex. *Brain Res.* 329, 185–193. doi: 10.1016/0006-8993(85)90524-4

Chelazzi, L., Rossi, F., Tempia, F., Ghirardi, M., and Strata, P. (1989). Saccadic eye movements and gaze holding in the head-restrained pigmented rat. *Eur. J. Neurosci.* 1, 639–646. doi: 10.1111/j.1460-9568.1989.tb00369.x

Colechio, E. M., and Alloway, K. D. (2009). Differential topography of the bilateral cortical projections to the whisker and forepaw regions in rat motor cortex. *Brain Struct. Funct.* 213, 423–439. doi: 10.1007/s00429-009-0215-7

Crick, F. C., and Koch, C. (2005). What is the function of the claustrum? *Philos.Trans. R. Soc. Lond. B Biol. Sci.* 360, 1271–1279. doi: 10.1098/rstb.2005.1661

Edelstein, L. R., and Denaro, F. J. (2004). The claustrum: a historical review of its anatomy, physiology, cytochemistry and functional significance. *Cell. Mol. Biol (Noisy-le-grand)* 50, 675–702.

Erlich, J. C., Bialek, M., and Brody, C. D. (2011). A cortical substrate for memory-guided orienting in the rat. *Neuron* 72, 330–343. doi: 10.1016/j.neuron.2011.07.010

Guandalini, P. (2003). The efferent connections of the pupillary constriction area in the rat medial frontal cortex. *Brain Res.* 962, 27–40. doi: 10.1016/S0006-8993(02)03931-8

Haiss, F., and Schwarz, C. (2005). Spatial segregation of different modes of movement control in the whisker representation of rat primary motor cortex. *J. Neurosci.* 25, 1579–1587. doi: 10.1523/JNEUROSCI.3760-04.2005

Hall, R. D., and Lindholm, E. P. (1974). Organization of motor and somatosensory neocortex in the albino rat. *Brain Res.* 66, 23–38. doi: 10.1016/0006-8993(74)90076-6

Hoffer, Z. S., Hoover, J. E., and Alloway, K. D. (2003). Sensorimotor corticocortical projections from rat barrel cortex have an anisotropic organization that facilitates integration of inputs from whiskers in the same row. *J Comp. Neurol.* 466, 525–544. doi: 10.1002/cne.10895

Hudetz, A. G. (2012). General anesthesia and human brain connectivity. *Brain Connect.* 2, 291–302. doi: 10.1089/brain.2012.0107

Jakubowaska-Sadowska, K., Morys, J., Sadowski, M., Kowianski, P., Karwacki, Z., and Narkiewicz, O. (1998). Visual zone of the claustrum shows localization and organizational differences among rat, guinea pig, rabbit and cat. *Anat. Embryol. (Berl).* 198, 63–72. doi: 10.1007/s004290050165

Kaufman, E. F. S., and Rosenquist, A. C. (1985). Efferent projections of the thalamic intralaminar nuclei in the cat. *Brain Res.* 335, 257–279. doi: 10.1016/0006-8993(85)90478-0

Kincaid, A. E., and Wilson, C. J. (1996). Corticostriatal innervation of the patch and matrix in rat neostriatum. *J. Comp. Neurol.* 374, 578–592. doi: 10.1002/(SICI)1096-9861(19961028)374:4%3C578::AID-CNE7%3E3.0.CO;2-Z

Kowianski, P., Dziewiatkowski, J., Kowianska, J., and Morys, J. (1999). Comparative anatomy of the claustrum in selected species: a morphometric analysis. *Brain Behav. Evol.* 53, 44–54. doi: 10.1159/000006581

Leichnetz, G. R., Hardy, S. G., and Carruth, M. K. (1987). Frontal projections to the region of the oculomotor complex in the rat: a retrograde and anterograde HRP study. *J.Comp. Neurol.* 263, 387–399. doi: 10.1002/cne.902630306

Li, Z. K., Takada, M., and Hattori, T. (1986). Topographic organization and collateralization of claustrocortical projections in the rat. *Brain Res. Bull.* 17, 529–532. doi: 10.1016/0361-9230(86)90220-0

Mao, T., Kusefoglu, D., Hooks, B. M., Huber, D., Petreanu, L., and Svoboda, K. (2011). Long-range neuronal circuits underlying the interactions between sensory and motor cortex. *Neuron* 71, 111–123. doi: 10.1016/j.neuron.2011.07.029

Mathur, B. N., Caprioli, R. M., and Deutch, A. Y. (2009). Proteomic analysis illuminates a novel structural definition of the claustrum and insula. *Cereb. Cortex* 19, 2372–2379. doi: 10.1093/cercor/bhn253

Miller, M. W., and Vogt, B. A. (1984a). Direct connections of rat visual cortex with sensory, motor, and association cortices. *J. Comp. Neurol.* 226, 184–202. doi: 10.1002/cne.902260204

Miller, M. W., and Vogt, B. A. (1984b). Heterotopic and homotopic callosal connections in rat visual cortex. *Brain Res.* 297, 75–89. doi: 10.1016/0006-8993(84)90544-4

Minciacchi, D., Molinari, M., Bentivoglio, M., and Macchi, G. (1985). The organization of the ipsi- and contralateral claustrocortical system in rat with notes on the bilateral claustrocortical projections in cat. *Neuroscience* 16, 557–576. doi: 10.1016/0306-4522(85)90192-7

Mitchinson, B., Martin, C. J., Grant, R. A., and Prescott, T. J. (2007). Feedback control in active sensing: rat exploratory whisking is modulated by environmental contact. *Proc. Biol. Sci.* 274, 1035–1041. doi: 10.1098/rspb.2006.0347

Neafsey, E. J., Bold, E. L., Haas, G., Hurley-Gius, K. M., Quirk, G., Sievert, C. F., et al. (1986). The organization of rat motor cortex: a microstimulation mapping study. *Brain Res.* 396, 77–96. doi: 10.1016/0165-0173(86)90011-1

Paxinos, G., and Watson, C. (2007). *The Rat Brain in Stereotaxic Coordinates*, 6th Edn. New York, NY: Academic.

Reep, R. L., and Corwin, J. V. (2009). Posterior parietal cortex as part of a neural network for directed attention in rats. *Neurobiol. Learn. Mem.* 91, 104–113. doi: 10.1016/j.nlm.2008.08.010

Remedios, R., Logothetis, N. K., and Kayser, C. (2010). Unimodal responses prevail within the multisensory claustrum. *J. Neurosci.* 30, 12902–12907. doi: 10.1523/JNEUROSCI.2937-10.2010

Sadowski, M., Morys, J., Jakubowska-Sadowska, K., and Narkiewicz, O. (1997). Rat's claustrum shows two main cortico-related zones. *Brain Res.* 756, 147–152. doi: 10.1016/S0006-8993(97)00135-2

Schulte, T., and Muller-Oehring, E. M. (2010). Contribution of callosal connections to the interhemispheric integration of visuomotor and cognitive processes. *Neuropsychol. Rev.* 20, 174–190. doi: 10.1007/s11065-010-9130-1

Sloniewski, P., Usunoff, K. G., and Pilgrim, C. H. (1986a). Retrograde transport of fluorescent tracers reveals extensive ipsi- and contralateral claustrocortical connections in the rat. *J. Comp. Neurol.* 246, 467–477. doi: 10.1002/cne.902460405

Sloniewski, P., Usunoff, K. G., and Pilgrim, C. (1986b). Diencephalic and mesencephalic afferents of the rat claustrum. *Anat. Embryol. (Berl).* 173, 401–411. doi: 10.1007/BF00318925

Smith, J. B., and Alloway, K. D. (2010). Functional specificity of claustrum connections in the rat: interhemispheric communication between specific parts of motor cortex. *J. Neurosci.* 30, 16832–16844. doi: 10.1523/JNEUROSCI.4438-10.2010

Smith, J. B., Mowery, T. M., and Alloway, K. D. (2012a). Thalamic POm projections to the dorsolateral striatum of rats: potential pathway for mediating stimulus-response associations for sensorimotor habits. *J. Neurophysiol.* 108, 160–174. doi: 10.1152/jn.00142.2012

Smith, J. B., Radhakrishnan, H., and Alloway, K. D. (2012b). Rat claustrum coordinates but does not integrate somatosensory and motor cortical information. *J. Neurosci.* 32, 8583–8588. doi: 10.1523/JNEUROSCI.1524-12.2012

Smythies, J., Edelstein, L., and Ramachandran, V. (2012). Hypotheses relating to the function of the claustrum. *Front. Integr. Neurosci.* 6:53. doi: 10.3389/fnint.2012.00053

Sommer, M. A., and Wurtz, R. H. (2004). What the brain stem tells the frontal cortex. I. oculomotor signals sent from superior colliculus to frontal eye field via mediodorsal thalamus. *J. Neurophysiol.* 91, 1381–1402. doi: 10.1152/jn.00738.2003

Stanton, G. B., Goldberg, M. E., and Bruce, C. J. (1988). Frontal eye field efferents in the macaque monkey: I. Subcortical pathways and topography

of striatal and thalamic terminal fields. *J. Comp. Neurol.* 271, 473–492. doi: 10.1002/cne.902710402

Stuesse, S. L., and Newman, D. B. (1990). Projections from the medial agranular cortex to brain stem visuomotor centers in rats. *Exp. Brain Res.* 80, 532–544. doi: 10.1007/BF00227994

Towal, R. B., and Hartmann, M. J. (2006). Right-left asymmetries in the whisking behavior of rats anticipate head movements. *J. Neurosci.* 26, 8838–8846. doi: 10.1523/JNEUROSCI.0581-06.2006

Vertes, R. P., Hoover, W. B., and Rodriquez, J. J. (2012). Projections of the central medial nucleus of the thalamus in the rat: node in cortical, striatal and limbic forebrain circuitry. *Neuroscience* 219, 120–136. doi: 10.1016/j.neuroscience.2012.04.067

Voight, T., De Lima, A. D., and Bekmann, M. (1993). Synaptophysin immunohistochemistry reveals inside-out pattern of early synaptogenesis in ferret cerebral cortex. *J. Comp. Neurol.* 330, 48–64. doi: 10.1002/cne.903300105

Wallace, D. J., Greenberg, D. S., Sawinski, J., Rulla, S., Notaro, G., and Kerr, J. N. D. (2013). Rats maintain an overhead binocular field at the expense of constant fusion. *Nature* 498, 65–69. doi: 10.1038/nature12153

Wang, Q., and Burkhalter, A. (2013). Stream-related preferences of inputs to the superior colliculus from areas of dorsal and ventral streams of mouse visual cortex. *J. Neurosci.* 33, 1696–1705. doi: 10.1523/JNEUROSCI.3067-12.2013

Wang, Q., Sporns, O., and Burkhalter, A. (2013). Network analysis of corticocortical connections reveals ventral and dorsal processing streams in mouse visual cortex. *J. Neurosci.* 32, 4386–4399. doi: 10.1523/JNEUROSCI.6063-11.2012

Conflict of Interest Statement: The authors declare that the research was conducted in the absence of any commercial or financial relationships that could be construed as a potential conflict of interest.

Received: 28 January 2014; accepted: 30 April 2014; published online: 19 May 2014.
Citation: Smith JB and Alloway KD (2014) Interhemispheric claustral circuits coordinate sensory and motor cortical areas that regulate exploratory behaviors. Front. Syst. Neurosci. ***8****:93. doi: 10.3389/fnsys.2014.00093*
This article was submitted to the journal Frontiers in Systems Neuroscience.

frontiers in
SYSTEMS NEUROSCIENCE

ORIGINAL RESEARCH ARTICLE
published: 04 April 2014
doi: 10.3389/fnsys.2014.00044

A role of the claustrum in auditory scene analysis by reflecting sensory change

Ryan Remedios[1,2]*, Nikos K. Logothetis[1,3] and Christoph Kayser[1,4]*

[1] *Max Planck Institute for Biological Cybernetics, Tübingen, Germany*
[2] *Division of Biology, California Institute of Technology, Pasadena, CA, USA*
[3] *Division of Imaging Science and Biomedical Engineering, University of Manchester, Manchester, UK*
[4] *Institute of Neuroscience and Psychology, University of Glasgow, Glasgow, UK*

Edited by:
Brian N. Mathur, University of Maryland School of Medicine, USA

Reviewed by:
Francisco Clasca, Autonomous University of Madrid School of Medicine, Spain
James Bisley, University of California Los Angeles School of Medicine, USA

***Correspondence:**
Ryan Remedios, Max Planck Institute for Biological Cybernetics, Spemannstrasse 38, Tübingen, Germany
e-mail: ryan@caltech.edu
Christoph Kayser, Institute of Neuroscience and Psychology, University of Glasgow, 58, Hillhead Street, Glasgow, UK
e-mail: christoph.kayser@glasgow.ac.uk

The biological function of the claustrum remains speculative, despite many years of research. On the basis of its widespread connections it is often hypothesized that the claustrum may have an integrative function mainly reflecting objects rather than the details of sensory stimuli. Given the absence of a clear demonstration of any sensory integration in claustral neurons, however, we propose an alternative, data-driven, hypothesis: namely that the claustrum detects the occurrence of novel or salient sensory events. The detection of new events is critical for behavior and survival, as suddenly appearing objects may require rapid and coordinated reactions. Sounds are of particular relevance in this regard, and our conclusions are based on the analysis of neurons in the auditory zone of the primate claustrum. Specifically, we studied the responses to natural sounds, their preference to various sound categories, and to changes in the auditory scene. In a test for sound-category preference claustral neurons responded to but displayed a clear lack of selectivity between monkey vocalizations, other animal vocalizations or environmental sounds (Esnd). Claustral neurons were however able to detect target sounds embedded in a noisy background and their responses scaled with target signal to noise ratio (SNR). The single trial responses of individual neurons suggest that these neurons detected and reflected the occurrence of a change in the auditory scene. Given its widespread connectivity with sensory, motor and limbic structures the claustrum could play the essential role of identifying the occurrence of important sensory changes and notifying other brain areas—hence contributing to sensory awareness.

Keywords: claustrum, saliency, auditory response, sounds, vocalizations, insula

INTRODUCTION

The biological function of the claustrum as a brain structure remains speculative, despite many years of research. Past and present hypotheses (Edelstein and Denaro, 2004; Crick and Koch, 2005; Smythies et al., 2012) proposed a function based on the claustrum's most pronounced feature: its widespread anatomical connections throughout the brain. The claustrum reciprocally and topographically connects cortical areas and subcortical structures including both early sensory and higher association regions (Pearson et al., 1982; Sadowski et al., 1997; Tanné-Gariépy et al., 2002; Fernandez-Miranda et al., 2008; Park et al., 2012; Milardi et al., 2013). This connectivity suggests an integrative function utilizing the afferents from multiple brain regions. This notion of an integrative function was supported by findings of single neuron studies reporting that claustral neurons respond to sensory stimulation in visual, acoustic, and somatic modalities, hence based on experimental evidence for a convergence of afferent multisensory information (Segundo and Machne, 1956; Spector et al., 1970, 1974; Olson and Graybiel, 1980; Clarey and Irvine, 1986; Sherk, 1986). Similar conclusions were also drawn based on results in human functional imaging studies (Hadjikhani and Roland, 1998; Banati et al., 2000). Based on the overall anatomical and functional evidence, and by drawing analogies between claustrum and other integrative brain structures, it has been proposed that the claustrum serves as an integrator of sensory information (Edelstein and Denaro, 2004; Crick and Koch, 2005; Smythies et al., 2012).

Yet, alternatively, the strong connectivity of claustrum may in principle reflect its capacity to impact on multiple brain structures. Indeed, direct attempts to uncover claustral neural functions typically associated with multisensory processing or integration have failed. For example, we have previously studied claustral neurons during audio-visual stimulation (Remedios et al., 2010). Using established indices of non-trivial multisensory neural-response properties we systematically probed claustral neurons for typical signs of response enhancement or depression known from other multisensory structures (Kayser and Logothetis, 2007; Stein and Stanford, 2008). Surprisingly, we found that the vast majority of neurons responded only to visual or auditory stimuli and very few neurons exhibited statistically

significant multisensory response interactions. This data, on one hand, confirm the multisensory nature of the claustrum as a structure consisting of distinct and separated unisensory zones, and on the other hand refute the idea of claustrum being a direct sensory integrator; a notion also supported by more recent work (Smith et al., 2012). While these results do not necessarily rule out a role in handling or routing information from multiple sensory modalities in general (Smythies et al., 2012), they suggest that the primary function of the claustrum is a different one than the direct integration and merging of multisensory information.

Based on data obtained in a previous study we have suggested that the claustrum may serve as a detector for the occurrence of novel or salient sensory events—saliency here referring to an acoustic difference between a specific sound token and the background auditory scene (Remedios et al., 2010). This hypothesis is not only consistent with our observation of relatively transient responses to auditory stimuli in the primate claustrum (Remedios et al., 2010) but also fits well with reported properties of visual neurons in the claustrum. Early pioneering studies on the visual claustrum in the cat found an overrepresentation of the peripheral visual field, that claustral neurons are broadly tuned and respond best to large and moving, hence salient, visual stimuli (Olson and Graybiel, 1980; Sherk and Levay, 1981a). In addition, the claustrum has anatomical connections with parietal and frontal areas involved in saliency processing (Bogler et al., 2011). In a function as novelty or saliency detector the claustrum would be more involved in reporting the appearance of a new sensory events rather than encoding their specific configural attributes. It subsequently would report the occurrence of such events to a wide-spread network of cortical and subcortical areas to trigger additional sensory processing or guide immediate behavioral reactions.

The detection of novel sensory events is critical for behavior and survival, as suddenly appearing objects may require rapid and coordinated reactions. Sounds are of particular relevance in this regard, as they can carry warning signals that can be perceived regardless of state of vigilance or direction of gaze (Issa and Wang, 2008). We here elaborate on the still speculative hypothesis about a role of the claustrum in novelty detection based on experimental data that makes a step towards testing this hypothesis more directly. Specifically, we consider auditory responsive neurons in the auditory zone of the claustrum and study their response properties with regard to encoding sound categories and detecting novel sounds. Overall our data provide evidence that is more consistent with a role in sound onset detection than a role in encoding information about the detailed nature of the respective sensory event.

MATERIALS AND METHODS

Two adult male rhesus monkeys (*Macaca mulatta*) participated in these experiments. All procedures were approved by the local authorities (Regierungspräsidium Tübingen) and were in full compliance with the guidelines of the European Community (EUVD 86/609/EEC) for the care and use of laboratory animals. The animals were socially (group-) housed in an enriched environment under daily veterinary supervision. All surgical procedures were performed under aseptic and sterile conditions. Briefly, neural responses were recorded using a custom-made multi-electrode system from alert animals that were passively listening to acoustic stimuli in a dark and anechoic booth. Neural signals were amplified using an Alpha Omega system (Alpha Omega GmbH), filtered between 4 Hz and 9 kHz and digitized at 20.83 kHz. The general procedures used in this study have been previously published (Dahl et al., 2009; Remedios et al., 2009, 2010). To approach the claustrum recording chambers were positioned based on pre-operative magnetic resonance (MR) images and stereotaxic coordinates. In one animal the claustrum was targeted at an angle of 20° anterio-posterior (AP) and 45° dorso-ventrally (DV) so that recordings were centered about at AP +14 mm, DV +18 mm. In the other animal the claustrum was approached vertically, with recordings centered about at AP +18 mm, DV +17 mm. Details of claustral approach and assignment of recording sites to this structure can be found in previous work (Remedios et al., 2010). In general, we sampled many sites along multiple penetrations through the claustrum but here analyzed only those responding to acoustic stimuli. In addition, the neurons analyzed here were all recorded in the "auditory zone", located roughly half-way between the dorsal and ventral ends of the claustrum (see **Figure 1A**). However, it should be noted that this zone has been defined purely based on functional properties of the recorded neurons and not based on detailed histological maps. Hence, the recording locations in **Figure 1A** are only approximate; see (Remedios et al., 2010) for additional discussion.

In the present study we analyzed data from two experimental paradigms involving different acoustic stimuli. The first paradigm has been used previously to study the sound category preferences of neurons at different stages of auditory pathways (Remedios et al., 2009; Perrodin et al., 2011). This stimulus set consisted of 15 sounds each in three categories: (1) macaque vocalizations (Mvoc); (2) vocalizations and noises of other animals (Avoc); and (3) environmental sounds (Esnd) (45 different sounds in total). The Mvoc comprised five call types (coos, grunts, barks, pant-threats and screams), sounds of other animals ranged from birds to lions, horses and tigers and Esnd including noises such as produced by wind, water, doors or jungle background sound. All sounds were sampled at 22.1 kHz and lasted between 0.35 and 1 s and had an intensity of 65 dB root mean square (rms) value. These sounds were presented as a pseudo-random sequence with silent gaps of 1 s in between, and each sound was repeated at least twice. The second paradigm consisted of brief target sounds presented on a background of pink noise (65 dB rms). A pink noise background was used with a similar overall spectrum as the set of sounds used in the first paradigm. The target sounds were a brief white noise burst (80 ms duration), a naturalistic sound (monkey vocalization, grunt, a contextual call that facilitates non-aggressive encounters, 80 ms) or a 300 ms long white noise burst. As control condition, trials without target sound and only presenting the background were included (baseline condition). These targets were presented 500 ms after the onset of the background and were presented at three relative intensities (measured as rms) relative to the background (+0, +6, +12 dB). For each recording site each of these conditions

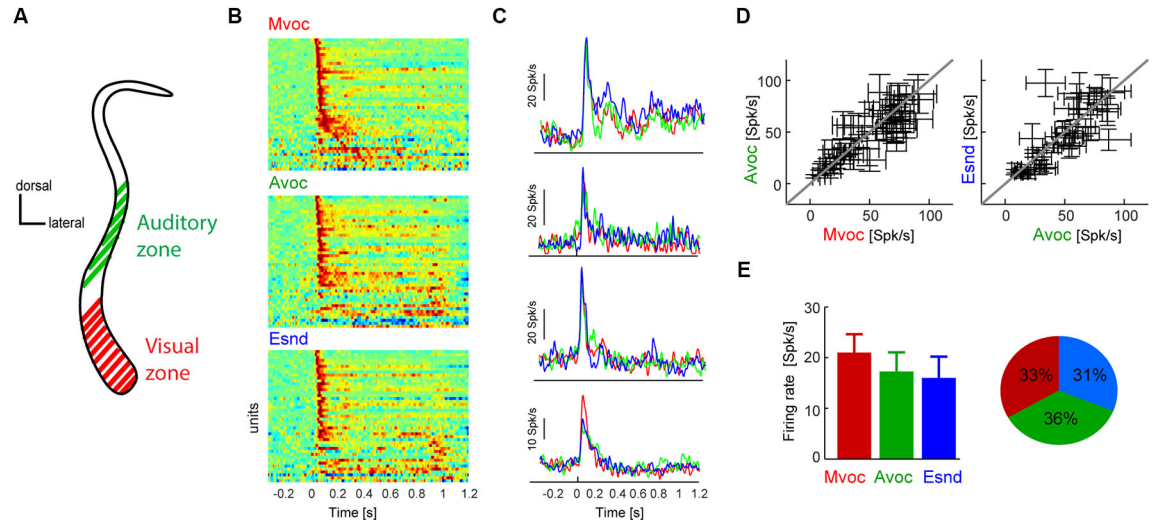

FIGURE 1 | (A) Schematic coronal section through the claustrum showing the putative location of the auditory and visual sensory zones. In previous work we have established a visually dominant and an auditory dominant zone along the dorso-ventral extend of the claustrum, the approximate locations of which are indicated in the figure. Please refer to previous work for an in-depth description of the anatomical localization of these regions (Remedios et al., 2010). The neurons analyzed here were all recorded in the auditory zone. **(B)** Diagram showing each units average response to each sound category. For display purpose each time course was scaled to within the same range, and red colors indicate periods of high response amplitude (n = 45 units). Sounds start at t = 0 and lasted between 0.3 and 1 s. **(C)** Example data from four units, showing the average response time course within each category. Except for the bottom example, responses were highly similar between sound categories. **(D)** Response amplitudes for all units and sound categories. Responses were calculated in 100 ms windows centered on the peak response for each individual sound. Errorbars indicate each units' average responses to each category and the standard error across sounds within each category. **(E)** Population averaged response amplitudes (mean and s.e.m.) and the fraction of units "preferring" each category (defined based on the maximal response amplitude). Sound categories: Mvoc: conspecific vocalizations; Avoc: sounds of other animals; Esnd: environmental sounds).

(target types × intensities, baseline) was repeated at least 8 times. We do not report results for the 300 ms noise target, as they were qualitatively and quantitatively very comparable to those obtained for the 80 ms noise target. All sounds were presented from two calibrated free field speakers (JBL Professional) positioned 70 cm from the head and 50° to left and right.

The data was analyzed in Matlab (MathWorks Inc.). Spike-sorted activity was extracted using commercial spike-sorting software (Plexon Offline Sorter, Plexon Inc.) after high-pass filtering the raw signal at 500 Hz. For the present analysis we did not distinguish between single and multi-unit sites. The use of multi-units may in principle influence some of the results on sound selectivity; e.g., individual neurons could be more acoustically selective than derived from our analysis. However, this seems unlikely given that individual responses were very transient, leaving little room for differential selectivity that would disappear in an aggregate response. In addition, the use of multi-unit responses would not affect the interpretation of the sound detection analysis, as mechanistically such a function would most likely be embodied by multiple neurons.

Significant responses were determined using a threshold of three standard deviations of the variability of baseline activity. Only those units were included for group analysis that responded significantly to at least one acoustic condition (Mvoc, Avoc or Esnd in paradigm 1; or that responded to the onset of the background noise in paradigm 2). This resulted in the inclusion of 45 units for paradigm 1 and 53 for paradigm 2 (out of 128 unit sampled with paradigm 1; 120 with paradigm 2). For further analysis the responses of each unit to each stimulus were adjusted for differences in spontaneous firing rate by subtracting the average spike count in pre-stimulus period (−400 to −50 ms). For paradigm 1 response amplitudes were calculated for each sound in a 100 ms window centered on the peak of the response time course to this specific sound (with the peak constrained to be within the stimulation period). Amplitudes were then averaged across sounds within each category. The preferred category was defined as that yielding the strongest response amplitude, as in previous work (Remedios et al., 2009). Using shorter windows (e.g., 75 ms) did not qualitatively affect the results. For paradigm 2 the response amplitude for target sounds (**Figure 2D**) was calculated in 80 ms time windows and with an average latency of 46 ms relative to target onset (derived from a separate latency analysis). Response latencies to target sounds (**Figure 2D**) were calculated as the first time point of the trial-averaged response crossing the 95% percentile of the distribution of response values in a (300 ms) pre-event period. For this analysis responses were smoothed with a Gaussian window of 10 ms (half-width at half-height).

The analysis for single-trial stimulus detection proceeded as follows. One analysis compared the response amplitudes during target presentation (pooling all signal to noise ratios (SNRs)) to those during a baseline condition provided by trials in which no target was presented. A second analysis compared the response

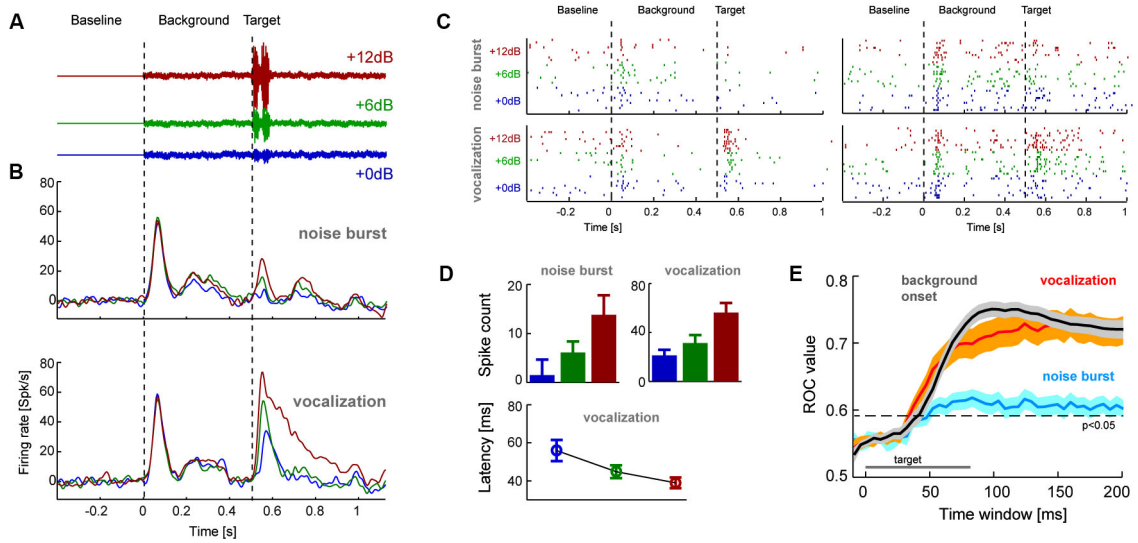

FIGURE 2 | (A) The second experiment presented target sounds embedded in a pink noise background sound. Targets had three relative signal to noise ratios (SNR) to the background and were either a short (80 ms) white noise burst or naturalistic sound (conspecific vocalization, 80 ms; shown here). **(B)** Population averaged response time course for each target type and SNR (n = 53 units; left). **(C)** Example single trial rasters from two units. Each tick denotes one action potential and different lines show different repeats of the same stimulus condition. **(D)** Average response amplitudes for the target sounds computed in 80 ms windows (shifted by the overall mean latency; 45 ms), and response latency for vocalization targets. Error-bars denote mean and s.e.m. **(E)** Results from a single trial sound detection analysis quantified by receiver operator characteristic (ROC) scores (area under the ROC curve). Lines denote the mean and shaded areas the s.e.m. across units for each target type and the onset of the background sound. Time is indicated relative to the event-onset (either background or target sound) and the ROC scores are based on the cumulative response amplitude in the respective window duration. The indicated significance level (relative to chance performance) was obtained from a randomization test.

amplitudes following background onset to a pre-stimulus baseline. The receiver operator characteristic (ROC) was calculated by applying a variable threshold to both sets of response amplitudes (targets, baseline) and computing the true and false positive rates for detecting a stimulus. The area under the ROC curve was then used as index to compare detection performance across target types. This analysis was performed based on responses in windows of progressively longer duration (starting at 10 ms pre-event and lasting up to 200 ms post-event onset). To test the statistical significance of ROC values against the null hypothesis of no systematic performance we performed a randomization test in which baseline and stimulus conditions were shuffled (500 permutations). Other statistical comparisons were mostly based on two-way ANOVAs or paired t-tests.

RESULTS

In previous work we have employed an audio-visual paradigm and identified two spatially separated populations of neurons within the claustrum: an auditory zone in which neurons predominantly respond to acoustic stimuli and a visual zone where neurons predominantly respond to visual stimuli (**Figure 1A**; Remedios et al., 2010). We here explore the response properties of the acoustically responsive zone in more detail. In the following we report findings from two experiments, one testing the general sound category selectivity and one more specifically testing the hypothesis that claustral neurons may function to report the onset of newly appearing sounds.

CLAUSTRAL NEURONS LACK SELECTIVITY TO SOUND CATEGORY

We first presented stimuli pertaining to three natural sound categories (Mvoc: conspecific vocalizations, Avoc: sounds of other animals, Ensd: environmental sounds) that have been used in previous studies to establish selectivity of neurons in anterior auditory regions (Perrodin et al., 2011), the posterior insula and caudal auditory cortex (Remedios et al., 2009). **Figure 1B** displays the responses of all responsive claustral units (both single- and multi-units were included in the same analysis) to the three sound categories and illustrates the general response features in this paradigm. As with most brain regions we expected the claustrum to be a heterogeneous structure comprising neurons with varying selectivity and response properties. The data show that most units exhibited a strong transient onset response within the first 200 ms, which was followed by a more transient response only for a few of the units (**Figure 1B**). Also, only a few units responded with longer latencies (>100 ms) during the stimulus period, but not at the immediate sound onset. **Figure 1C** shows the responses of four examples in more detail. Of these, all show a transient response to sound onset and three exhibited very comparable responses across sound categories, while one responded more strongly to the conspecific vocalizations.

This overall insensitivity to sound category was generally true for the entire population. To quantify the selectivity of each unit to the three sound categories we first calculated each unit's peak response to each individual sound and then averaged response amplitudes within each category. Using individual windows to quantify responses to different sounds ensures that this analysis is

insensitive to differences in response latency or time course and to differences in sound duration across stimuli. This result is shown in **Figure 1D** as scatter plots, which indicate each unit's average response to the different categories and the variability within each category (standard error across sounds). In general, there was considerably variability of response amplitude across sounds within each category, and the average coefficient of variation (standard deviation divided by mean) was 0.88 ± 0.04 (mean ± s.e.m.). Nevertheless, across units the data scatter along the diagonal, hence revealing differences in the overall response amplitude between units but no systematic effect of sound category. This is further substantiated in **Figure 1E**, which displays the population average responses (21 ± 3 Spk/s for Mvoc, 17 ± 3 for Avoc, 15 ± 4 for Esnd; mean ± s.e.m.). Statistical assessment revealed no effect of category (ANOVA $F_{(3,179)} = 0.8$, $p = 0.4$). In addition, the fraction of units preferring each of the three sound categories was very comparable (**Figure 1E**; chi-square test $\chi^2 = 0.9$, $p = 0.13$).

In sum, we found that claustral neurons exhibit strong transient responses to the onset of natural sounds, but as a population do not show a specific preference for any of the tested sound categories. This lack of selectivity differs from data obtained in the insula (Remedios et al., 2009) and anterior auditory regions (Perrodin et al., 2011), where a clear and significant preference for conspecific vocalizations was observed; it also differs from data obtained in primary auditory fields where responses to conspecific vocalizations were weaker than those for the other sounds (Remedios et al., 2009).

CLAUSTRAL NEURONS DETECT CHANGES IN THE AUDITORY SCENE AND SALIENT EVENTS

These neurons hence exhibit two properties that seem to argue against a primary function in representing acoustic features or sound identity. First, the responses show a lack of selectivity for a specific sound category, and second, responses are very transient even for sounds lasting several hundreds of milliseconds. This suggests that these neurons are more sensitive to the generic onset of new sounds rather than acoustic qualities. This prompted us to test the hypothesis that the claustrum may potentially function as a detector of newly occurring sounds within an auditory scene.

In a second experiment we recorded additional claustral neurons ($n = 53$ responsive units) in response to a paradigm involving the appearance of a target sound amidst continuous background noise (**Figure 2**). The target was either a short (80 ms duration) white noise burst or a naturalistic sound (monkey vocalization; 80 ms). We chose a vocalization because of its ethological and behavioral relevance. These targets were presented on a pink noise background at various relative SNR (+0, +6 or +12 dB, see **Figure 2A**). Analysis of response time courses showed that claustral neurons responded well to the onset of the background noise (at $t = 0$ s) and responded with variable amplitudes to the different targets (at $t = 0.5$ s; **Figure 2B**). **Figure 2C** furthermore displays the single trial responses of two example-units in this paradigm. Across units, target evoked responses scaled with SNR (computed in 80 ms windows; **Figure 2D**): an ANOVA (units and SNRs as factors) showed that the effect of SNR was significant for each target type (noise burst: $F_{(2,158)} = 7.2$, $p < 0.01$; vocalization: $F = 39$, $p < 10^{-10}$). In addition, target-evoked responses were overall higher for the vocalization compared to the noise (paired t-test $p < 10^{-5}$, responses averaged across SNRs). Closer inspection of the responses to the vocalization target also indicated a possible effect of response latency (c.f. **Figure 2B**). We hence analyzed response latencies in more detail. In the vocalization condition target-evoked response latencies could be obtained (for all SNRs) for 26 of the units. For this subset of units, latencies systematically decreased with SNR (56 ± 6 ms, 44 ± 3 ms and 38 ± 3 respectively; mean ± s.e.m.; **Figure 2D**) and an ANOVA returned a significant effect of SNR ($F_{(2,77)} = 6.2$, $p < 0.01$). Hence, target-evoked responses scale in amplitude and latency with the relative intensity of the target sound. This suggests that claustral neurons identified sounds in a noisy background and responded with firing rate and latency changes.

We predicted that one should be able to decode changes in the auditory scene above chance using claustral responses. A change in the auditory scene could here either be the onset of the background relative to silence or the onset of the target sound relative to background. Given that target-evoked responses were stronger for the vocalization compared to the noise burst, we predicted that this effect should be stronger for the vocalization. To test these hypotheses we performed a single trial detection analysis based on the spike count in a time window of interest. These windows were either aligned to the onset of the background (quantifying how well responses differentiate this from silence) or to the onset of a target (quantifying how well responses differentiate target onset from background noise). A threshold was applied to these response amplitudes to differentiate the condition of interest from responses sampled either during silence or the background. By varying this threshold we calculated the respective receiver operator characteristic (ROC; see Section Materials and Methods), which indicates how well the claustral neurons could serve to detect the onset of new sounds on a single trial basis. This analysis was performed based on responses in windows of variable length, providing an estimate of effect size and the stimulus period required to achieve above chance performance.

We first calculated the ROC for detecting the onset of the background relative to silence. The respective ROC scores were high (peak value 0.76 ± 0.02; mean ± s.e.m.; reached 100 ms after target onset; **Figure 2E** gray) and significantly above change level ($p < 0.01$). We then calculated the ROC score for detecting the target sounds from background. Importantly, we performed this analysis by pooling responses across SNR conditions, hence mimicking a condition in which a target sound of arbitrary intensity has to be detected. ROC scores were higher for detecting the vocalization (0.75 ± 0.02; peak at 160 ms) than for the noise burst (0.62 ± 0.02; peak at 110 ms; **Figure 2E**). When compared at the same time point (chosen at $t = 125$ ms; defined based on 45 ms average latency and 80 ms target duration), ROC values differed significantly between noise and vocalization targets (paired t-test; $p < 10^{-5}$) and between noise target and background onset ($p < 10^{-8}$). However, they did not differ between vocalization target and background onset ($p = 0.33$). This suggests that claustral neurons could serve to detect changes in an auditory scene flexibly across a range of SNR values, and

they could do so regardless of the specific nature of the target sound.

DISCUSSION

Studying neurons in the claustrum's auditory zone, we found that their response properties point to a role in encoding sound occurrence more than sound category or acoustic qualities. In particular we found that this population of neurons was not sensitive to the overall category of sounds and responded with similar strength and transiently to conspecific vocalizations and other naturalistic sounds. This raises concerns as to a function specifically related to encoding sound type or acoustic detail. However, we found that responses within the same claustral zone could serve well to detect the onset of sounds from silence or the onset of novel sounds within an acoustic background. These results are consistent with previous speculations about a role of the claustrum in novelty or saliency (i.e., critically different from the existing background) (Remedios et al., 2010).

THE CLAUSTRUM AND CHANGE DETECTION

Detecting a change or novel event in the external environment is of paramount importance for survival. An animal may have to respond to a sudden threat, such as an aggressor or predator that may have remained camouflaged until attack, or it may have to attend to the calls of its offspring in need of immediate attention. The claustrum may fulfill such an ethological role by virtue of its widespread anatomical connectivity. It could detect sudden changes in the environment across sensory modalities, possibly relying on the detection in any sensory modality or relying on the detection in multiple modalities. The claustrum could then send out a generalized awareness signal across its connectome to recruit cognitive or attentional mechanisms to respond to the environmental change. Our results are well compatible with the claustrum participating in a general novelty or vigilance network.

For most mammals sudden environmental events are best detected based on acoustic cues. Hearing serves as warning sensory modality regardless of fatigue, sleep and regardless of current gaze direction, and saliency networks hence must critically rely on some auditory sensitive structures. The claustrum's auditory zone may be one such hub in a saliency network. Given claustral projections to structures involved in cognitive and motor control (Pearson et al., 1982; Clascá et al., 1992; Smith and Alloway, 2010; Smith et al., 2012) the claustrum could trigger appropriate behavioral reactions or guide the deployment of additional cognitive resources. Parts of the claustrum are well connected with somatosensory and motor structures and could trigger the rapid and coordinated motor response to a novel sound (Clascá et al., 1992; Smith and Alloway, 2010).

It is important to note that we studied claustral neurons only in the context of acoustic stimuli and our findings hence do not speak about the many other claustral neurons that are sensitive to other modalities (Olson and Graybiel, 1980; Remedios et al., 2010). However, our conclusion is well consistent with findings in the visual zone. Sherk and LeVay recorded neurons in the visual claustrum of the cat and found that these neurons were broadly tuned for orientation, with a trend to large receptive fields concerning the visual periphery, but generally being sensitive to visual motion (LeVay and Sherk, 1981; Sherk and Levay, 1981a,b). These visual neurons are hence ideally suited to detect motion in the visual periphery, the location where predators or other important objects usually appear. It will be interesting for future studies to generally compare the tuning and selectivity of claustral sensory neurons in comparison to their ability to report the simple occurrence of sensory stimuli, in order to quantitatively assess the hypothesis of novelty detector across the different zones of the claustrum.

Additional evidence for a role of the claustrum as novelty detector may be provided by a relation between attentional deficits in Autism spectrum disorders (ASD) and changes in claustral volume in affected individuals. Based on structural imaging it was reported that individuals affected by ASD have a smaller claustral volume compared to control subjects (WB, 2008). The behavioral deficits seen in ASD in turn have been linked to changes in attentional deployment (Klin et al., 2003; Ames and Fletcher-Watson, 2010) and one theory holds that a saliency network prominently involving the insula and possibly neighboring structures is critically involved in ASD (Uddin and Menon, 2009). While not providing direct support for our hypothesis, results such as these are well consistent with the notion of a role of the claustrum in sensory detection.

The hypothesis of a network involved in detecting exogeneous change capitalizes on the claustrum's widespread connectivity with cortical and subcortical structures. Indeed, this structure is ideally placed in order to facilitate the interaction between limbic, sensory and cognitive systems by means of its diverse connectivity, to mediate exchange of sensory or cognitive information or coordinate large-scale activity under challenging circumstances, such as fight or flight situations or mental insight problem solving (Tian et al., 2011; Remedios, 2012; Smythies et al., 2012). Evidence from claustral lesions clearly pinpoint the severe impact of claustral lesions on behavior. Bilateral lesions by herpes encephalitis or mushroom poisoning (Kimura et al., 1994; Nishizawa, 2005) were found to induce severe encephalopathy with disturbance of consciousness, seizures, and psychotic symptoms. In addition, preliminary evidence from targeted claustral lesions in animal models suggest specific behavioral deficits as seen in ASD and large-scale changes in functional brain connectivity (Remedios, 2012). In this context it will also be interesting to understand the relation of the claustrum to neuromodulatory structures. Stimulus novelty also activates the noradrenergic system (Krebs et al., 2013), and relevant structures such as the locus coeruleus interact with limbic structures to facilitate learning during aversive events (Sears et al., 2013). It may well be that the claustrum plays a central role in the formation of memories that facilitate future reactions based on a joint interaction between the claustrum, neuromodulatory systems and the cortex. Further progress towards an improved understanding of the contribution of the claustrum to brain function and cognition hence may benefit from advanced technologies to specifically manipulate activity within this structure or to selectively activate connections between the claustrum and other brain structures (Deisseroth, 2011).

When interpreting the present data it is important to note that the concepts of stimulus novelty or saliency are often used in a loose manner. In particular, in our experiment we did not manipulate stimulus salience independently of stimulus onset or stimulus intensity. While models of acoustic saliency exist (e.g., Kayser et al., 2005), it is generally the case that the onset of a new sound is often the most salient feature in a complex acoustic scene. Hence, any saliency mechanism would also respond strongly to the onset of new sounds. We therefore believe that our findings are well consistent with a role of the claustrum in a more specialized saliency network. Work on the neural underpinnings of visual saliency reported enhanced responses to salient stimuli in those regions potentially implementing the respective saliency map (Constantinidis and Steinmetz, 2005; Arcizet et al., 2011). Interestingly, the neural responses in these areas also scale with the intensity of visual stimuli across a wide range of intensities and exhibit systematically shorter latencies for more salient stimuli (Tanaka et al., 2013). These response properties directly match those observed in the claustrum, where we found stronger and shorter latency responses to more salient (i.e., higher SNR) sounds embedded on a background. Overall it is hence possible that claustral units specifically encode stimulus saliency, but direct tests remain challenging given the difficulty to disentangle saliency and novelty in complex sensory scenes.

To conclude, the role as change or saliency detector provides a data-driven and working hypothesis for future work. It directly suggests experimental paradigms that could be employed in future work to further elucidate this hypothesis and test it in relation to behavior. For example, the detection of salient events by claustral neurons could be probed directed in relation to behavioral detection or to existing algorithmic models of saliency detection in natural scenes (Itti and Koch, 2001; Kayser et al., 2005). Such studies should also test this hypothesis in relation to other sensory modalities, such as the detection of behaviorally or physically salient visual or somatosensory stimuli. A structure with such a widespread connectivity likely has a rather general and amodal (or multisensory) function rather than one pertaining to detailed sensory representations for individual modalities. Hence, any damage of this structure likely results in general brain dysfunction such as seizures, lack of cognitive focus or general psychotic symptoms, which make the interpretation of behavioral deficits following manipulation of claustral activity even more challenging. It will surely remain a challenge to pinpoint the specific function of the claustrum for many coming years, but hypotheses about its putative function are utterly needed to guide future work.

ACKNOWLEDGMENTS

This work was supported by the Max Planck Society and the German Research Foundation (KA 2661/1).

REFERENCES

Ames, C., and Fletcher-Watson, S. (2010). A review of methods in the study of attention in autism. *Dev. Rev.* 30, 52–73. doi: 10.1016/j.dr.2009.12.003

Arcizet, F., Mirpour, K., and Bisley, J. W. (2011). A pure salience response in posterior parietal cortex. *Cereb. Cortex* 21, 2498–2506. doi: 10.1093/cercor/bhr035

Banati, R. B., Goerres, G. W., Tjoa, C., Aggleton, J. P., and Grasby, P. (2000). The functional anatomy of visual-tactile integration in man: a study using positron emission tomography. *Neuropsychologia* 38, 115–124. doi: 10.1016/s0028-3932(99)00074-3

Bogler, C., Bode, S., and Haynes, J. D. (2011). Decoding successive computational stages of saliency processing. *Curr. Biol.* 21, 1667–1671. doi: 10.1016/j.cub.2011.08.039

Clarey, J. C., and Irvine, D. R. (1986). Auditory response properties of neurons in the claustrum and putamen of the cat. *Exp. Brain Res.* 61, 432–437. doi: 10.1007/bf00239531

Clascá, F., Avendaño, C., Roman-Guindo, A., Llamas, A., and Reinoso-Suarez, F. (1992). Innervation from the claustrum of the frontal association and motor areas: axonal transport studies in the cat. *J. Comp. Neurol.* 326, 402–422. doi: 10.1002/cne.903260307

Constantinidis, C., and Steinmetz, M. A. (2005). Posterior parietal cortex automatically encodes the location of salient stimuli. *J. Neurosci.* 25, 233–238. doi: 10.1523/jneurosci.3379-04.2005

Crick, F. C., and Koch, C. (2005). What is the function of the claustrum? *Philos. Trans. R. Soc. Lond. B Biol. Sci.* 360, 1271–1279. doi: 10.1098/rstb.2005.1661

Dahl, C., Logothetis, N., and Kayser, C. (2009). Spatial organization of multisensory responses in temporal association cortex. *J. Neurosci.* 29, 11924–11932. doi: 10.1523/jneurosci.3437-09.2009

Deisseroth, K. (2011). Optogenetics. *Nat. Methods* 8, 26–29. doi: 10.1038/nmeth.f.324

Edelstein, L. R., and Denaro, F. J. (2004). The claustrum: a historical review of its anatomy, physiology, cytochemistry and functional significance. *Cell. Mol. Biol. (Noisy-le-grand)* 50, 675–702. doi: 10.1170/T558

Fernandez-Miranda, J. C., Rhoton, A. L. Jr., Kakizawa, Y., Choi, C., and Alvarez-Linera, J. (2008). The claustrum and its projection system in the human brain: a microsurgical and tractographic anatomical study. *J. Neurosurg.* 108, 764–774. doi: 10.3171/jns/2008/108/4/0764

Hadjikhani, N., and Roland, P. E. (1998). Cross-modal transfer of information between the tactile and the visual representations in the human brain: a positron emission tomographic study. *J. Neurosci.* 18, 1072–1084.

Issa, E. B., and Wang, X. (2008). Sensory responses during sleep in primate primary and secondary auditory cortex. *J. Neurosci.* 28, 14467–14480. doi: 10.1523/jneurosci.3086-08.2008

Itti, L., and Koch, C. (2001). Computational modelling of visual attention. *Nat. Rev. Neurosci.* 2, 194–203. doi: 10.1038/35058500

Kayser, C., and Logothetis, N. K. (2007). Do early sensory cortices integrate cross-modal information? *Brain Struct. Funct.* 212, 121–132. doi: 10.1007/s00429-007-0154-0

Kayser, C., Petkov, C. I., Lippert, M., and Logothetis, N. K. (2005). Mechanisms for allocating auditory attention: an auditory saliency map. *Curr. Biol.* 15, 1943–1947. doi: 10.1016/j.cub.2005.09.040

Kimura, S., Nezu, A., Osaka, H., and Saito, K. (1994). Symmetrical external capsule lesions in a patient with herpes simplex encephalitis. *Neuropediatrics* 25, 162–164. doi: 10.1055/s-2008-1073016

Klin, A., Jones, W., Schultz, R., and Volkmar, F. (2003). The enactive mind, or from actions to cognition: lessons from autism. *Philos. Trans. R. Soc. Lond. B Biol. Sci.* 358, 345–360. doi: 10.1098/rstb.2002.1202

Krebs, R. M., Fias, W., Achten, E., and Boehler, C. N. (2013). Picture novelty attenuates semantic interference and modulates concomitant neural activity in the anterior cingulate cortex and the locus coeruleus. *Neuroimage* 74, 179–187. doi: 10.1016/j.neuroimage.2013.02.027

LeVay, S., and Sherk, H. (1981). The visual claustrum of the cat. II. The visual field map. *J. Neurosci.* 1, 981–992.

Milardi, D., Bramanti, P., Milazzo, C., Finocchio, G., Arrigo, A., Santoro, G., et al. (2013). Cortical and subcortical connections of the human claustrum revealed in vivo by constrained spherical deconvolution tractography. *Cereb. Cortex* doi: 10.1093/cercor/bht231. [Epub ahead of print].

Nishizawa, M. (2005). Acute encephalopathy after ingestion of "sugihiratake" mushroom. *Rinsho Shinkeigaku* 45, 818–820.

Olson, C. R., and Graybiel, A. M. (1980). Sensory maps in the claustrum of the cat. *Nature* 288, 479–481. doi: 10.1038/288479a0

Park, S., Tyszka, J. M., and Allman, J. M. (2012). The claustrum and insula in microcebus murinus: a high resolution diffusion imaging study. *Front. Neuroanat.* 6:21. doi: 10.3389/fnana.2012.00021

Pearson, R. C., Brodal, P., Gatter, K. C., and Powell, T. P. (1982). The organization of the connections between the cortex and the claustrum in the monkey. *Brain Res.* 234, 435–441. doi: 10.1016/0006-8993(82)90883-6

Perrodin, C., Kayser, C., Logothetis, N. K., and Petkov, C. I. (2011). Voice cells in the primate temporal lobe. *Curr. Biol.* 21, 1408–1415. doi: 10.1016/j.cub.2011.07.028

Remedios, R. (2012). The claustrum and th eorchestra of cognitive control. Francis Crick Memorial Conference. Cambridge, UK. Available online at: http://fcmconference.org/#program

Remedios, R., Logothetis, N. K., and Kayser, C. (2009). An auditory region in the primate insular cortex responding preferentially to vocal communication sounds. *J. Neurosci.* 29, 1034–1045. doi: 10.1523/jneurosci.4089-08.2009

Remedios, R., Logothetis, N. K., and Kayser, C. (2010). Unimodal responses prevail within the multisensory claustrum. *J. Neurosci.* 30, 12902–12907. doi: 10.1523/jneurosci.2937-10.2010

Sadowski, M., Morys, J., Jakubowska-Sadowska, K., and Narkiewicz, O. (1997). Rat's claustrum shows two main cortico-related zones. *Brain Res.* 756, 147–152. doi: 10.1016/s0006-8993(97)00135-2

Sears, R. M., Fink, A. E., Wigestrand, M. B., Farb, C. R., De Lecea, L., and Ledoux, J. E. (2013). Orexin/hypocretin system modulates amygdala-dependent threat learning through the locus coeruleus. *Proc. Natl. Acad. Sci. U S A* 110, 20260–20265. doi: 10.1073/pnas.1320325110

Segundo, J. P., and Machne, X. (1956). Unitary responses to afferent volleys in lenticular nucleus and claustrum. *J. Neurophysiol.* 19, 325–339.

Sherk, H. (1986). "The claustrum and the cerebral cortex," in *Cerebral Cortex* (Vol. 5), eds E. G. Jones and A. Peters (New York: Plenum), 467–499.

Sherk, H., and Levay, S. (1981a). The visual claustrum of the cat. III. Receptive field properties. *J. Neurosci.* 1, 993–1002.

Sherk, H., and Levay, S. (1981b). Visual claustrum: topography and receptive field properties in the cat. *Science* 212, 87–89. doi: 10.1126/science.7209525

Smith, J. B., and Alloway, K. D. (2010). Functional specificity of claustrum connections in the rat: interhemispheric communication between specific parts of motor cortex. *J. Neurosci.* 30, 16832–16844. doi: 10.1523/jneurosci.4438-10.2010

Smith, J. B., Radhakrishnan, H., and Alloway, K. D. (2012). Rat claustrum coordinates but does not integrate somatosensory and motor cortical information. *J. Neurosci.* 32, 8583–8588. doi: 10.1523/jneurosci.1524-12.2012

Smythies, J., Edelstein, L., and Ramachandran, V. (2012). Hypotheses relating to the function of the claustrum. *Front. Integr. Neurosci.* 6:53. doi: 10.3389/fnint.2012.00053

Spector, I., Hassmannova, Y., and Albe-Fessard, D. (1970). A macrophysiological study of functional organization of the claustrum. *Exp. Neurol.* 29, 31–51. doi: 10.1016/0014-4886(70)90035-x

Spector, I., Hassmannova, Y., and Albe-Fessard, D. (1974). Sensory properties of single neurons of cat's claustrum. *Brain Res.* 66, 39–65. doi: 10.1016/0006-8993(74)90077-8

Stein, B. E., and Stanford, T. R. (2008). Multisensory integration: current issues from the perspective of the single neuron. *Nat. Rev. Neurosci.* 9, 255–266. doi: 10.1038/nrn2377

Tanaka, T., Nishida, S., Aso, T., and Ogawa, T. (2013). Visual response of neurons in the lateral intraparietal area and saccadic reaction time during a visual detection task. *Eur. J. Neurosci.* 37, 942–956. doi: 10.1111/ejn.12100

Tanné-Gariépy, J., Boussaoud, D., and Rouiller, E. M. (2002). Projections of the claustrum to the primary motor, premotor and prefrontal cortices in the macaque monkey. *J. Comp. Neurol.* 454, 140–157. doi: 10.1002/cne.10425

Tian, F., Tu, S., Qiu, J., Lv, J. Y., Wei, D. T., Su, Y. H., et al. (2011). Neural correlates of mental preparation for successful insight problem solving. *Behav. Brain Res.* 216, 626–630. doi: 10.1016/j.bbr.2010.09.005

Uddin, L. Q., and Menon, V. (2009). The anterior insula in autism: underconnected and under-examined. *Neurosci. Biobehav. Rev.* 33, 1198–1203. doi: 10.1016/j.neubiorev.2009.06.002

WB, D. (2008). *The Claustrum in Autism and Typically Developing Male Children: A Quantitative Mri Study.* Brigham: Young University.

Conflict of Interest Statement: The authors declare that the research was conducted in the absence of any commercial or financial relationships that could be construed as a potential conflict of interest.

Received: 21 January 2014; accepted: 11 March 2014; published online: 04 April 2014.
Citation: Remedios R, Logothetis NK and Kayser C (2014) A role of the claustrum in auditory scene analysis by reflecting sensory change. Front. Syst. Neurosci. ***8****:44. doi: 10.3389/fnsys.2014.00044*
This article was submitted to the journal Frontiers in Systems Neuroscience.